Les informations que la scapula, l'atlas, et l'axis peuvent apporter à la compréhension de la bipédie

Auteur : Van Oostende, Florence
Promoteur(s) : Noiret, Pierre
Faculté : Faculté de Philosophie et Lettres
Diplôme : Master en histoire de l'art et archéologie, orientation archéométrie, à finalité approfondie
Année académique : 2018-2019
URI/URL : http://hdl.handle.net/2268.2/6656

Annexes : corpus d'articles

Mémoire de Van Oostende Florence : *Les informations que l'atlas, l'axis et la scapula peuvent apporter à la compréhension de la bipédie.*

Promoteurs : NOIRET P. (ULiège) et MAUREILLE B. (Université de Bordeaux)

Lectrice : ROTS V. (ULiège)

References and Notes

1. M. A. Norell, X. Xu, *Annu. Rev. Earth Planet. Sci.* **33**, 277 (2005).
2. X. Xu, Y. Guo, *Vertebrat Palasiatica* **47**, 311 (2009).
3. X. Xu, X. Zheng, H. You, *Nature* **464**, 1338 (2010).
4. Z. Zhou, P. M. Barrett, J. Hilton, *Nature* **421**, 807 (2003).
5. Z. Fucheng, Z. Zhonghe, G. Dyke, *Geol. J.* **41**, 395 (2006).
6. X. Xu *et al.*, *Nature* **484**, 92 (2012).
7. D. Hu, L. Hou, L. Zhang, X. Xu, *Nature* **461**, 640 (2009).
8. See the supplementary materials on *Science* Online.
9. Q. Ji, P. J. Currie, M. A. Norell, J. Shu-An, *Nature* **393**, 753 (1998).
10. P. J. Chen, Z. M. Dong, S. N. Zhen, *Nature* **391**, 147 (1998).
11. R. O. Prum, A. H. Brush, *Q. Rev. Biol.* **77**, 261 (2002).
12. R. O. Prum, *J. Exp. Zool.* **285**, 291 (1999).
13. M. H. Schweitzer *et al.*, *J. Exp. Zool.* **285**, 146 (1999).
14. X. Xu, Z. Tang, X. Wang, *Nature* **399**, 350 (1999).
15. C. Dal Sasso, M. Signore, *Nature* **392**, 383 (1998).
16. D. E. G. Briggs, P. R. Wilby, B. P. Pérez-Moreno, J. L. Sanz, M. Fregenal-Martínez, *J. Geol. Soc. London* **154**, 587 (1997).
17. A. W. A. Kellner, *Nature* **379**, 32 (1996).
18. P. G. Davis, D. E. G. Briggs, *Geology* **23**, 783 (1995).
19. A. W. A. Kellner, in *Mesozoic Birds above the Heads of Dinosaurs,* L. M. Chiappe, L. M. Witmer, Eds. (Univ. of California Press, Berkeley, CA, 2002), pp. 389–404.
20. A. M. Lucas, P. R. Stettenheim, *Avian Anatomy. Integument, Part I* (U.S. Government Printing Office, Washington, DC, 1972).
21. R. S. Wray, *Proc. Zool. Soc. London* **55**, 343 (1887).
22. C. Sullivan, D. W. E. Hone, X. Xu, F. Zhang, *Proc. Biol. Sci.* **277**, 2027 (2010).
23. W. J. Bock, *Syst. Zool.* **14**, 272 (1965).
24. X. Xu *et al.*, *Nature* **421**, 335 (2003).
25. D. W. Fowler, E. A. Freedman, J. B. Scannella, R. E. Kambic, *PLoS ONE* **6**, e28964 (2011).
26. J. H. Ostrom, *Q. Rev. Biol.* **49**, 27 (1974).
27. K. P. Dial, *Science* **299**, 402 (2003).
28. A. M. Heers, K. P. Dial, *Trends Ecol. Evol.* **27**, 296 (2012).
29. L. E. Zanno, P. J. Makovicky, *Proc. Natl. Acad. Sci. U.S.A.* **108**, 232 (2011).
30. J. E. Duerden, *Agric. J. Union S. Afr.* **1**, 29 (1911).
31. F. B. Gill, *Ornithology* (W.H. Freeman, New York, ed. 3, 2007).
32. P. Cho, R. Brown, M. Anderson, *Zoo Biol.* **3**, 133 (1984).
33. S. Davies, *Ratites and Tinamous* (Oxford Univ. Press, Oxford, 2002).
34. D. E. Fastovsky, in *The Age of Dinosaurs. Short Courses in Paleontology 2,* S. J. Culver, Ed. (Paleontological Society, Knoxville, TN, 1989), pp. 22–33.
35. A. H. Turner, D. Pol, J. A. Clarke, G. M. Erickson, M. A. Norell, *Science* **317**, 1378 (2007).
36. O. W. M. Rauhut, C. Foth, H. Tischlinger, M. A. Norell, *Proc. Natl. Acad. Sci. U.S.A.* **109**, 11746 (2012).
37. F. Ortega, F. Escaso, J. L. Sanz, *Nature* **467**, 203 (2010).

Acknowledgments: We thank P. Andrew (landowner), D. Brinkman (logistical support), J. Csotonyi (artwork), D. MacLeod (specimen preparation), M. Newbrey (discussions), D. Sloan (technical illustrations), and K. Womble (graphics). Research was funded by the Royal Tyrrell Museum of Palaeontology, a Natural Sciences and Engineering Research Council of Canada Discovery grant (D.K.Z.), the University of Calgary Start-up Fund (D.K.Z.), and an NSF Division of Earth Sciences grant (EAR 0959029) (G.M.E.). TMP 1995.110.1, TMP 2008.70.1, and TMP 2009.110.1 are permanently deposited at the Royal Tyrrell Museum, Drumheller, Alberta, Canada.

Supplementary Materials

www.sciencemag.org/cgi/content/full/338/6106/510/DC1
Supplementary Text
Figs. S1 to S6
Tables S1 and S2
References (*38*–*60*)

30 May 2012; accepted 30 August 2012
10.1126/science.1225376

Australopithecus afarensis Scapular Ontogeny, Function, and the Role of Climbing in Human Evolution

David J. Green[1]* and Zeresenay Alemseged[2]

Scapular morphology is predictive of locomotor adaptations among primates, but this skeletal element is scarce in the hominin fossil record. Notably, both scapulae of the juvenile *Australopithecus afarensis* skeleton from Dikika, Ethiopia, have been recovered. These scapulae display several traits characteristic of suspensory apes, as do the few known fragmentary adult australopith representatives. Many of these traits change significantly throughout modern human ontogeny, but remain stable in apes. Thus, the similarity of juvenile and adult fossil morphologies implies that *A. afarensis* development was apelike. Additionally, changes in other scapular traits throughout African ape development are associated with shifts in locomotor behavior. This affirms the functional relevance of those characteristics, and their presence in australopith fossils supports the hypothesis that their locomotor repertoire included a substantial amount of climbing.

Scapular morphology corresponds closely with locomotor habits, often irrespective of phylogeny (*1*–*7*). However, our understanding of this important element in hominin evolution is limited by the paucity of scapular fossil remains. Upon its discovery, the right scapula associated with the juvenile *Australopithecus afarensis* skeleton from Dikika, Ethiopia (DIK-1-1, "Selam") represented the most complete such fossil known for this well-documented early hominin species (*8*). Furthermore, comparison of this complete juvenile with adult australopith fossils promised to shed light on *A. afarensis* growth and development (*8*, *9*). Continued preparation has since freed both scapulae from the matrix encasing much of the axial skeleton (Fig. 1).

Before DIK-1-1's discovery, the limited number of available fossil scapulae provided only tentative clues that the australopith shoulder was apelike (*10*). In addition, we lack a clear understanding of what the scapular morphology of the last common ancestor (LCA) of *Pan* and *Homo* looked like, making it difficult to determine whether australopiths retained apelike features from the LCA or if these features evolved independently (*11*–*14*). Furthermore, limited information on the postcranial architecture, developmental pathways, and the manner in which behavioral variation contributes to morphological diversity among extant hominoids presents a challenge for reconstructing locomotor patterns in extinct taxa. Here, we describe further the DIK-1-1 scapulae and infer the locomotor behavior of *Australopithecus* through comparisons with other fossil hominins—including the new specimen from Woranso-Mille, Ethiopia (KSD-VP-1/1) (*15*)—and modern apes and humans (*16*). We track the ontogeny of scapular shape among extant hominoids to evaluate how juvenile scapular morphology compares with the adult form. We also evaluate functionally relevant characters throughout development to identify various genetic and epigenetic influences on hard-tissue morphology. These approaches consider how ontogenetic shifts in locomotor behavior (e.g., in *Pan* and *Gorilla*) influence scapular shape, providing context for evaluating the morphology of more fragmentary adult fossils and a more comprehensive view for inferring the locomotor implications of australopith shoulder anatomy.

The original analysis of the right DIK-1-1 scapula showed it to be most similar to that of juvenile *Gorilla* (*8*), but the two principal component axes describing its shape explained only ~7% of variance, drawing criticism (*15*). We performed two canonical variates analyses (CVAs) among juvenile and adult representatives of modern *Homo*, *Pan*, *Gorilla*, and *Pongo*, as well as DIK-1-1 and the immature *H. ergaster* (early *H. erectus*) scapula of the Turkana Boy (KNM-WT 15000) (*17*). In the first CVA, *Homo* and *Pongo* separated from *Pan* and *Gorilla* along the first root axis, which accounted for 70.3% of the variation; *Pongo* and *Pan* separated from *Homo* and *Gorilla*, respectively, along the second root axis (16.0%; Fig. 2A). The DIK-1-1 scapulae did not significantly differ from one another ($P = 0.81$) and were most similar to those of *Gorilla* juveniles (table S6); KNM-WT 15000 fell among the juvenile *Homo* data (Fig. 2A). The second CVA considered fewer variables to include the less complete KSD-VP-1/1,

[1]Department of Anatomy, Midwestern University, Downers Grove, IL 60515, USA. [2]Department of Anthropology, California Academy of Sciences, San Francisco, CA 94118, USA.

*To whom correspondence should be addressed. E-mail: dgreen1@midwestern.edu

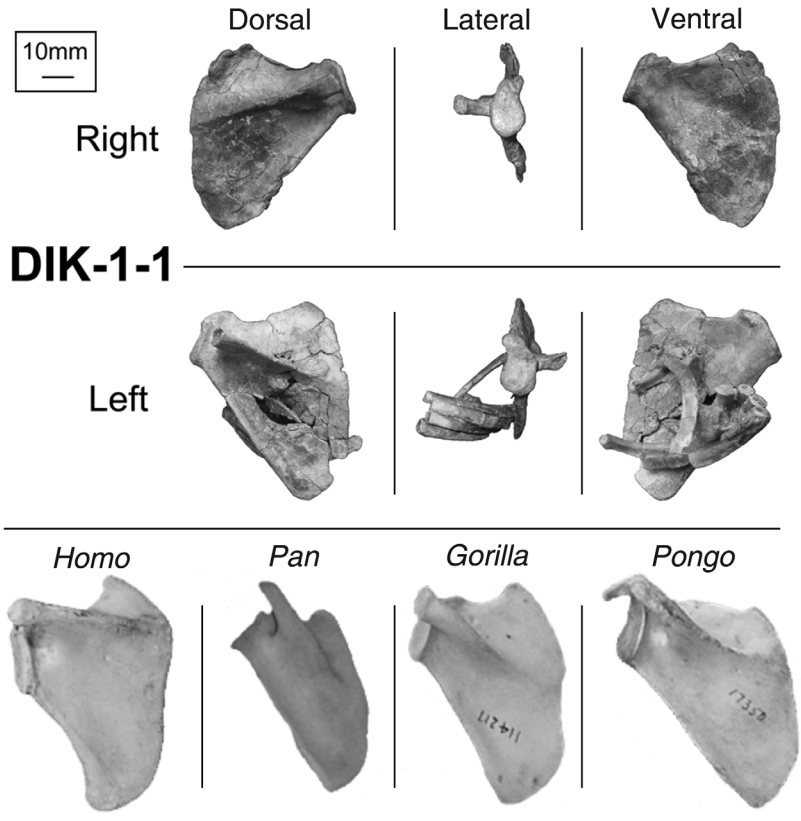

Fig. 1. The DIK-1-1 scapulae; top and middle row images show dorsal, lateral, and ventral views of the recently prepared right and left scapulae, respectively. The left scapula was more recently prepared and some rib and vertebral elements are still adhering to it (this did not impede the measurements presented). Images along the bottom row are scapulae of comparably aged *Homo*, *Pan*, *Gorilla*, and *Pongo* individuals.

but did not distinguish the groups as effectively. *Homo* separated from the African apes along the first root, which explained 84.2% of the variation, and *Pongo* fell between the two groups with considerable overlap (Fig. 2B). The two DIK-1-1 scapulae did not significantly differ (P = 0.42) and fell among the *Pongo* and *Gorilla* data (table S8). KNM-WT 15000 was again most similar to *Homo* juveniles, whereas KSD-VP-1/1 fell near the intersection of adult *Homo* and *Pongo*.

These multivariate analyses confirm that there are two distinct scapular shapes among living and extinct hominoids (tables S5 and S6). The scapulae of the African apes, and to a lesser extent, *Pongo*, differ from those of *Homo* in possessing more cranially oriented glenoid fossae, which may be an adaptation to more effectively distribute strain over the joint capsule during climbing and reaching when the upper limb is loaded (Fig. 3) (*18*). Suspensory great apes also possess obliquely oriented scapular spines (fig. S1) with superoinferiorly narrow infraspinous fossae and relatively broader supraspinous fossae (Fig. 4). The orientation of the scapular spine is associated with the relative size and shape of the dorsal scapular fossae and the corresponding muscles, as a more obliquely oriented spine provides a direct line of action for these muscles in preventing displacement of the humeral head during suspensory behaviors (*19*–*21*).

Other fragmentary *Australopithecus* fossils (*A. afarensis*: A.L. 288-1; *A. africanus*: Sts 7 and Stw 162) were included in bivariate comparisons (table S1). All australopiths possessed more cranially oriented shoulder joints relative to modern humans (Fig. 3) (*17*). Both DIK-1-1 scapulae fell within the *Gorilla* confidence interval (CI), whereas

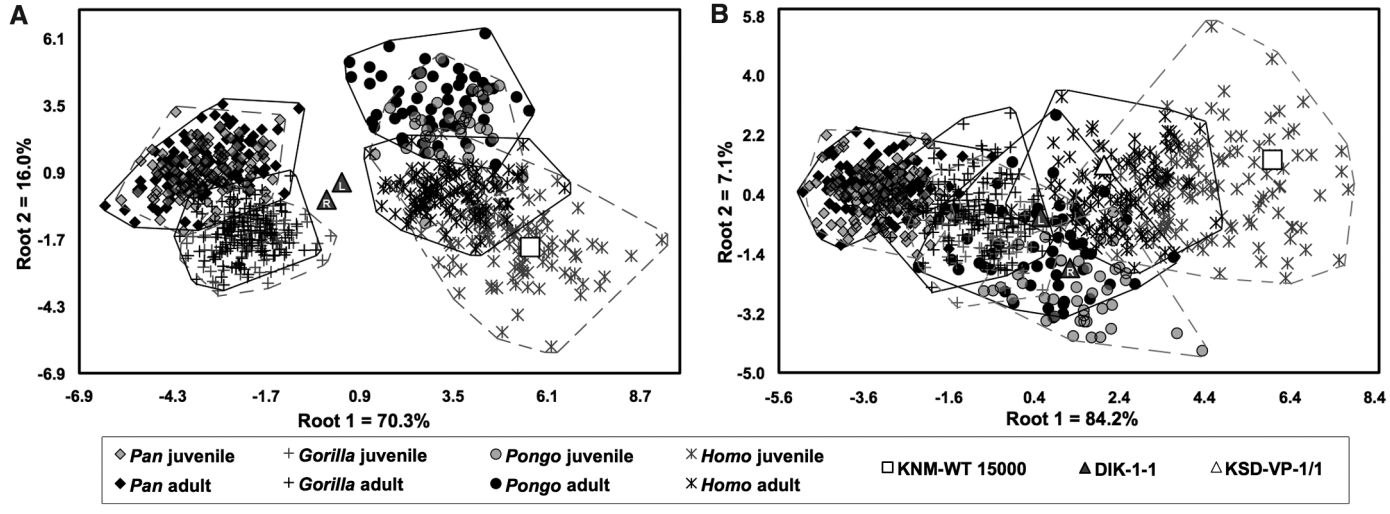

Fig. 2. Canonical variates analysis (CVA) plots. (**A**) The first CVA considered three angular and 10 size-corrected, linear measures (table S5). *Homo*, KNM-WT 15000, and *Pongo* separated from *Pan*, *Gorilla*, and DIK-1-1 positively along the first root. *Homo* could be further distinguished from *Pongo* along the second root, as could *Pan* from *Gorilla*. The DIK-1-1 scapulae were most similar to those of *Gorilla* juveniles, whereas KNM-WT 15000 fell among the juvenile *Homo* data. (**B**) A second CVA considered five angular measures and also the less complete Woranso-Mille specimen, KSD-VP-1/1 (table S7). Although this CVA did not distinguish the extant taxa as effectively as the previous analysis, *Homo* separated from the African apes along the first root and *Pongo* fell intermediately between the two groups. The two DIK-1-1 scapulae did not significantly differ from one another and fell among the *Pongo* and *Gorilla* data. KNM-WT 15000 was most similar to *Homo* juveniles, whereas KSD-VP-1/1 fell near the intersection of adult *Homo* and *Pongo*. See also tables S6 and S8.

KNM-WT 15000's shoulder joint was most similar to that of modern humans (Fig. 3 and table S9). Shoulder joint orientation does not significantly change in *Pan* or *Gorilla* throughout ontogeny, and it becomes slightly more cranially oriented in *Pongo* during the middle ontogenetic stages, but returns to the juvenile configuration in adulthood. In contrast, *Homo* shoulder joints become significantly more cranially oriented throughout ontogeny ($P < 0.001$), but remain more laterally oriented than those of the other hominoids at all stages (Fig. 3, fig. S2, and table S10). Starting from DIK-1-1, a humanlike ontogenetic pattern would imply that adult *A. afarensis* individuals should have more cranially oriented shoulder joints than those displayed by either A.L. 288-1 or KSD-VP-1/1. However, both juvenile and adult *A. afarensis* representatives have comparably oriented shoulder joints, suggesting that this trait remained relatively stable during ontogeny. This implies a developmental pattern for *A. afarensis* similar to that exhibited by the living African apes, but both developmental scenarios point toward a distinctly apelike shoulder joint configuration for *A. afarensis* throughout ontogeny (Fig. 3 and table S9).

It has been debated whether the cranially facing shoulder joint of A.L. 288-1 (Lucy) is an allometric result of the specimen's diminutive size, rather than an indicator of arboreal adaptations (*15*, *22*, *23*). Our results support the functional inference: Both Sts 7 and Stw 162 are larger than A.L. 288-1, yet possess more cranially oriented shoulder joints. Additionally, the Lucy-sized LB6/4 scapula (*H. floresiensis*) has a "hyperhuman," laterally facing shoulder joint (Fig. 3 and table S9) [(*24*), p. 725; (*25*)]. Moreover, the youngest modern humans had the most laterally positioned shoulder joints, further distinguishing them from juvenile great apes and DIK-1-1 (Fig. 3 and table S9). These findings contradict the hypothesis that cranially oriented shoulder joints are a by-product of small size. Thus, we conclude that *A. afarensis* possessed an apelike, cranially oriented scapula, distinct from the configuration seen in modern and fossil *Homo*.

Both DIK-1-1 scapular spines are oriented significantly more obliquely than in *Homo*, with angle values within the *Pongo* CI. In contrast, KNM-WT 15000 has a significantly more transversely oriented spine that even exceeded the modern human range (fig. S1 and table S9). The KSD-VP-1/1 scapula is described as having a more transversely oriented spine (*15*), whereas the spine of A.L. 288-1 is more obliquely oriented, falling just above the *Pongo* CI (table S9). The Sts 7 spine is the most oblique of the australopiths and fell within the *Gorilla* CI (table S9). Scapular spine orientation does not change significantly in the great apes throughout ontogeny, but modern human scapular spines shifted significantly more obliquely ($P < 0.01$; fig. S3 and table S10). As observed for shoulder joint orientation, the relative orientation of juvenile and adult *A. afarensis* scapular spines might be partially explained by a more apelike ontogenetic trajectory than that exhibited by modern humans (figs. S1 and 3 and tables S9 and S10).

Scapular spine orientation is a principal determinant of dorsal scapular fossa shape (*21*). In particular, the infraspinatus muscle has been shown to be primarily involved in shoulder joint stabilization during suspensory activities (*20*). DIK-1-1's infraspinous fossae are narrow relative to glenoid size and most similar to those of *Gorilla* and *Pongo* juveniles, whereas KNM-WT 15000 has an extremely broad fossa (Fig. 4 and tables S1 and S9). Supraspinous breadth generally increases in all taxa throughout ontogeny, whereas infraspinous breadth does not show any significant increase from stage to stage in *Homo* or *Pongo* (table S10). In contrast, infraspinous breadth increases significantly throughout both *Pan* and *Gorilla* ontogeny ($P < 0.03$; fig. S4 and table S10). The ratio of supraspinous:infraspinous breadth (SIB) increases throughout ontogeny in *Homo*, does not significantly change in *Pongo*, but significantly decreases in both *Pan* and *Gorilla*. Given the increase in relative supraspinous breadth in *Pan* and *Gorilla*, the decrease in the SIB ratio similarly

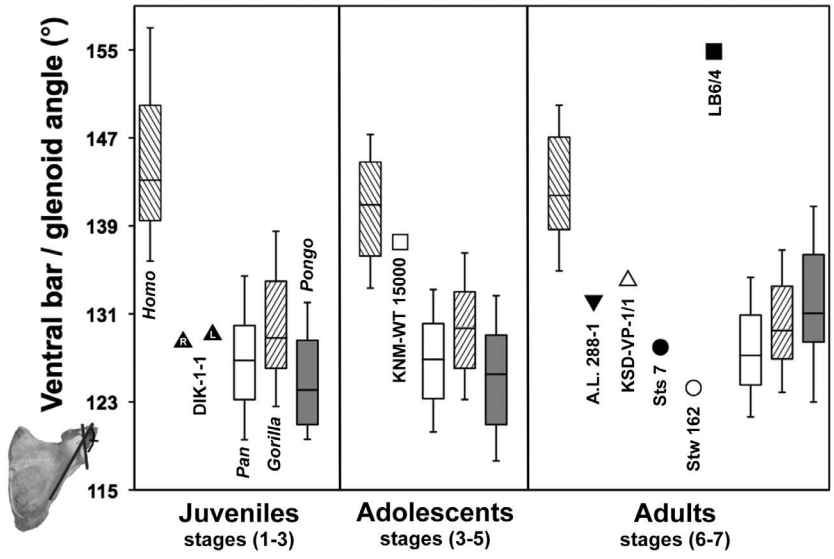

Fig. 3. Box plots of ventral bar/glenoid angle across extant taxa and fossil individuals for juvenile, adolescent, and adult age groups. All of the *Australopithecus* fossils differ significantly from modern human scapulae and are more similar to the suspensory apes with cranially oriented shoulder joints. In contrast, modern humans, KNM-WT 15000, and LB6/4 display more laterally oriented joints.

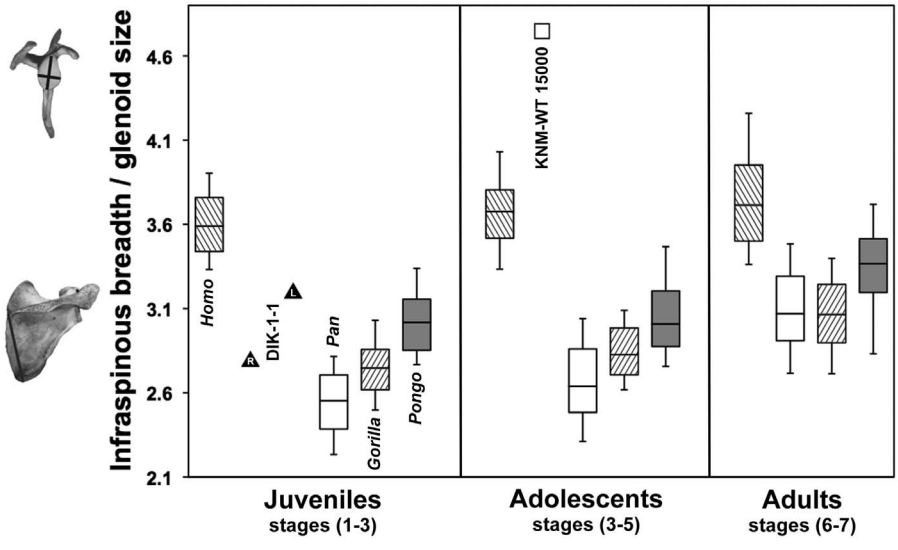

Fig. 4. Box plots of relative infraspinous fossa breadth across extant taxa for juvenile, adolescent, and adult age groups and the DIK-1-1 and KNM-WT 15000 fossils. The two DIK-1-1 scapulae differ from one another, but both possess relatively narrow infraspinous regions that are more similar to those of the suspensory apes, whereas KNM-WT 15000 possesses a very broad infraspinous fossa that exceeded even the modern human range.

highlights the relative increase in infraspinous breadth (table S10).

These developmental patterns further inform the link between shoulder morphology and locomotor behavior. Arboreal hominoids possess narrower infraspinous regions, in contrast to the broad fossae displayed by modern humans (*6*, *19*, *26*). Further, the increase in infraspinous breadth during *Pan* and *Gorilla* ontogeny corresponds with a behavioral shift from a principally arboreal lifestyle at younger ages to an adult locomotor repertoire predominated by terrestrial knuckle-walking (*27*, *28*). The infraspinatus muscle is consistently recruited to stabilize the shoulder joint during both suspensory and knuckle-walking behaviors in chimpanzees (*20*, *29*), so the change in African ape infraspinous fossa shape might represent an adaptive optimization of the scapular blade. A narrow infraspinous region with an obliquely oriented scapular spine is a more effective configuration for infraspinatus' role in stabilizing the shoulder joint during suspensory activities (*19*, *20*). In contrast, an enlarged infraspinous fossa allows the muscle to pass broadly behind the humeral head, which might facilitate joint integrity when the arm is loaded from below as individuals engage more regularly in knuckle-walking activities (*19*).

The change in infraspinous fossa shape during African ape ontogeny may represent a response to the changing loading regimes of a dynamic locomotor repertoire. This interpretation is supported by experimental evidence, where differences in shoulder activity during growth corresponded with significant infraspinous fossa shape changes in mice (*30*). Thus, in addition to a more cranially oriented shoulder joint and an oblique scapular spine, we propose that DIK-1-1's relatively narrow infraspinous region is a functionally meaningful characteristic. This configuration further highlights its overall apelike appearance while also distinguishing it from juvenile modern humans and the considerably more derived KNM-WT 15000 adolescent.

Comparing the DIK-1-1 scapulae to those of adult conspecifics suggests that growth of the *A. afarensis* shoulder may have followed a developmental trajectory more like that of African apes than modern humans. This conclusion is consistent with evidence purporting that *A. afarensis* dental development was also apelike (*31*). Additionally, behavioral changes that occur throughout African ape ontogeny could be linked with morphological shifts, indicating that some scapular blade characteristics track locomotor habits, even during an organism's lifetime. The apelike appearance of the most complete *A. afarensis* scapulae strengthens the hypothesis that these hominins participated in a behavioral strategy that incorporated a considerable amount of arboreal behaviors in addition to bipedal locomotion.

References and Notes

1. E. H. Ashton, C. E. Oxnard, *Proc. Zool. Soc. Lond.* **142**, 49 (1964).
2. V. Inman, J. Saunders, L. Abbott, *J. Bone Joint Surg. Am.* **26**, 1 (1944).
3. C. E. Oxnard, *Am. J. Phys. Anthropol.* **26**, 219 (1967).
4. D. Roberts, Structure and function of the primate scapula, in *Primate Locomotion*, F. A. Jenkins, Ed. (Academic Press, New York, 1974), pp. 171–200.
5. A. Schultz, *Hum. Biol.* **2**, 303 (1930).
6. N. M. Young, thesis, Harvard University (2002).
7. N. M. Young, *Am. J. Phys. Anthropol.* **136**, 247 (2008).
8. Z. Alemseged *et al.*, *Nature* **443**, 296 (2006).
9. C. V. Ward, *Yearb. Phys. Anthropol. S* **35**, 185 (2002).
10. S. G. Larson, *Evol. Anthropol.* **16**, 172 (2007).
11. B. Latimer, in *Origine(s) de la bipédie chez les hominidés,* Y. Coppens, B. Senut, Eds. (CNRS, Paris, 1991), pp. 169–176.
12. C. O. Lovejoy, *Sci. Am.* **259**, 118 (1988).
13. J. T. Stern, *Evol. Anthropol.* **9**, 113 (2000).
14. R. L. Susman, J. T. Stern, in *Origine(s) de la bipédie chez les hominidés*, Y. Coppens, B. Senut, Eds. (CNRS, Paris, 1991), pp. 121–131.
15. Y. Haile-Selassie *et al.*, *Proc. Natl. Acad. Sci. U.S.A.* **107**, 12121 (2010).
16. The new *A. sediba* shoulder blade from Malapa, South Africa (*32*) was not included in the present study, but represents another significant addition to the scapular fossil record.
17. Materials and methods are available as supplementary materials on *Science* Online
18. K. D. Hunt, *Am. J. Phys. Anthropol.* **86**, 521 (1991).
19. S. G. Larson, *Am. J. Phys. Anthropol.* **98**, 13 (1995).
20. S. G. Larson, J. T. Stern Jr., *Am. J. Anat.* **176**, 171 (1986).
21. S. G. Larson, J. T. Stern Jr., W. L. Jungers, *Am. J. Phys. Anthropol.* **85**, 71 (1991).
22. S. E. Inouye, B. T. Shea, *Int. J. Primatol.* **18**, 629 (1997).
23. R. P. Mensforth, B. Latimer, S. Senturia, *Am. J. Phys. Anthropol.* **81**, 267 (1990).
24. S. G. Larson *et al.*, *J. Hum. Evol.* **53**, 718 (2007).
25. M. J. Morwood *et al.*, *Nature* **437**, 1012 (2005).
26. D. J. Green, thesis, The George Washington University (2010).
27. D. M. Doran, *J. Hum. Evol.* **23**, 139 (1992).
28. D. M. Doran, *J. Hum. Evol.* **32**, 323 (1997).
29. S. G. Larson, J. T. Stern Jr., *J. Zool.* **212**, 629 (1987).
30. D. J. Green, B. G. Richmond, S. L. Miran, *J. Exp. Zool. B Mol. Dev. Evol.* (2012).
31. C. Dean *et al.*, *Nature* **414**, 628 (2001).
32. L. R. Berger *et al.*, *Science* **328**, 195 (2010).

Acknowledgments: We thank C. Kiarie and the staff at the National Museum of Ethiopia for help during the preparation of these fragile fossils. We greatly appreciate critical comments offered by B. Richmond, B. Wood, R. Bernstein, M. Hamrick, L.P. Hernandez, and three anonymous reviewers on this manuscript and A. Gordon for analytical assistance. We thank D. Hunt, L. Gordon, E. Westwig, I. Tattersall, G. Garcia, J. Chupasko, M. Omura, Y. Haile-Selassie, L. Jellema, M. Harman, A. Gill, E. Mbua, S. Muteti, M. Yilma, P.V. Tobias, B. Zipfel, S. Potze, and T. Perregil for coordinating museum visits. We also acknowledge the NSF IGERT grant (9987590), NSF Doctoral Dissertation Improvement Grant (BCS-0824552), NSF (BCS-0914687), The Leakey Foundation, the Wenner-Gren Foundation, The George Washington University, Midwestern University, and the California Academy of Sciences for funding support. This paper was written by D.J.G. and Z.A. Fossil data were collected and described by D.J.G. and Z.A. Extant primate data were collected and analyzed by D.J.G. The data reported in this paper are summarized in the supplementary materials; raw data are available on request to D.J.G.

Supplementary Materials

www.sciencemag.org/cgi/content/full/338/6106/514/DC1
Materials and Methods
Supplementary Text
Figs. S1 to S4
Tables S1 to S10
References (*33*–*41*)

9 July 2012; accepted 31 August 2012
10.1126/science.1227123

Status and Solutions for the World's Unassessed Fisheries

Christopher Costello,[1]* Daniel Ovando,[1] Ray Hilborn,[2] Steven D. Gaines,[1] Olivier Deschenes,[3] Sarah E. Lester[1,4]

Recent reports suggest that many well-assessed fisheries in developed countries are moving toward sustainability. We examined whether the same conclusion holds for fisheries lacking formal assessment, which comprise >80% of global catch. We developed a method using species' life-history, catch, and fishery development data to estimate the status of thousands of unassessed fisheries worldwide. We found that small unassessed fisheries are in substantially worse condition than assessed fisheries, but that large unassessed fisheries may be performing nearly as well as their assessed counterparts. Both small and large stocks, however, continue to decline; 64% of unassessed stocks could provide increased sustainable harvest if rebuilt. Our results suggest that global fishery recovery would simultaneously create increases in abundance (56%) and fishery yields (8 to 40%).

When sustainably managed, marine fisheries provide a major source of food and livelihoods for hundreds of millions of people worldwide (*1*). When poorly managed, these benefits to people and ecosystems are severely compromised (*2*). Despite this tremendous global impact, there is considerable debate among conservation and fisheries scientists about the status of global fisheries [e.g., (*3*)]. To date, assessing the biological status of fisheries has relied either on detailed stock assessments, which combine structural population models with data to estimate a species' population size and trajectories under different harvest scenarios, or on local knowledge and less formal analysis (*4*). A recent synthesis of global fisheries with formal assessments

[1]Bren School of Environmental Science and Management, University of California, Santa Barbara, CA 93106, USA. [2]School of Aquatic and Fishery Sciences, University of Washington, Seattle, WA 98195, USA. [3]Department of Economics, University of California, Santa Barbara, CA 93106, USA. [4]Marine Science Institute, University of California, Santa Barbara, CA 93106, USA.

*To whom correspondence should be addressed. E-mail: costello@bren.ucsb.edu

Science

Australopithecus afarensis Scapular Ontogeny, Function, and the Role of Climbing in Human Evolution

David J. Green and Zeresenay Alemseged

Science **338** (6106), 514-517.
DOI: 10.1126/science.1227123

Climbing Like an Ape

Recently, studies of several early human leg and foot fossils have implied that in some early species-–even after humans became bipedal—climbing may have still been important. Shoulder bones, which would provide i mportant complementary information, are scarce, however. One of the few examples is from *Australopithecus afarensis* skeleton (DIK-1-1), which includes both scapula. **Green and Alemseged** (p. 514; see the Perspective of **Larson**) provide an analysis of the fossil's shoulders and show that, unlike modern humans, they retain several traits that are common in climbing apes, which may indicate that *A. afarensis* was an active climber.

Received: 28 April 2016 | Revised: 6 November 2016 | Accepted: 8 December 2016

DOI 10.1002/ajpa.23158

RESEARCH ARTICLE

WILEY American Journal of PHYSICAL ANTHROPOLOGY

Evolution of the hominoid scapula and its implications for earliest hominid locomotion

Michael S. Selby[1] | C. Owen Lovejoy[2]

[1]Department of Biomedical Sciences, Georgia Campus – Philadelphia College of Osteopathic Medicine, Suwanee, Georgia 30024-2937

[2]Department of Anthropology, School of Biomedical Sciences, Kent State University, Kent, Ohio 44242–0001

Correspondence
Michael S. Selby, Department of Biomedical Sciences, Georgia Campus – Philadelphia College of Osteopathic Medicine, 625 Old Peachtree Rd NW, Suwanee, GA 30024-2937.
Email: michaelsel@pcom.edu

Abstract

Objectives: The higher primate scapula has been subject to many explanations of the putative "adaptive value" of its individual traits. However, the shift from the bone's position in above branch quadrupeds to its more posterolateral position in recent hominoids obviously required fundamental changes to its general form. We hypothesize that most features argued to be individually adaptive are more likely secondary consequences of changes in its fundamental bauplan, a view more consistent with modern developmental biology.

Materials and Methods: We tested this hypothesis with scapular metrics and angles from a broad anthropoid sample.

Results: Our results support our hypothesis. Contrary to earlier predictions, vertebral border length differs little relative to body size in anthropoids, inferior angle position primarily reflects mediolateral scapular breadth, and supraspinous and infraspinous fossa sizes largely reflect scapular spine orientation. Suspensory taxa have cranially oriented glenoids, whereas slow clamberers and humans do not. *Australopithecus* most closely resembles the latter.

Discussion: Most scapular features can be explained by only two primary changes: (1) reduction in mediolateral breadth and (2) change in the glenoid position relative to the vertebral border with increased reliance on suspension, which led to a more cranially angled scapular spine. Virtually all other scapular traits appear to be byproducts of these two changes. Based on fossil morphology, hominids[1] were derived from a last common ancestor primarily adapted for clambering and not for suspension. Scapular form in early hominids such as *Australopithecus* is therefore primitive and largely reflects the genus's general clambering heritage.

KEYWORDS
glenoid orientation, scapular spine, serratus anterior, vertebral border

1 | INTRODUCTION

In their influential work on the scapula, [Ashton and Oxnard (1961, 1962, 1963), Oxnard (1963), Ashton and Oxnard (1964), Ashton, Healy, Oxnard, and Spence (1965), and Ashton, Oxnard, and Spence (1965)] assigned anthropoids to several discrete locomotor groups defined by scapular features. They defined adaptations for "brachiators" (in their case meaning hominoid) to include elongated and cranially oriented acromia, more caudally positioned inferior angles, and cranially oriented glenoids, relative to those in taxa considered to be "quadrupeds" (i.e., cercopithecines and most cebines). "Semibrachiators" (i.e., atelines and colobines) were considered to be intermediate between brachiators and quadrupeds (Ashton & Oxnard, 1964; Oxnard, 1967). They argued that these bony features assist muscles associated with arm-raising, as required for brachiation. This inference was based on work by Inman, Saunders, and Abbott (1944), whose electromyographic (EMG) data from humans showed muscle fibers from the cranial portion of the trapezius and the caudal portion of serratus anterior acting as a "force couple" that rotated the scapula cranially.

Ashton and Oxnard (1961) and Oxnard (1963) also found that arm-raising muscles (deltoid, trapezius, and caudal serratus anterior) were larger (and by inference, more powerful) in "brachiators" than in "semibrachiators" and were in turn larger than in their "quadruped" homologues. Furthermore, in brachiators, the superior trapezius fibers

are more cranially oriented due to the angulation of the scapular spine, and more laterally placed than in quadrupeds due to the projection of their acromion (Ashton & Oxnard, 1961; Oxnard, 1963). They further argued that the more caudally positioned inferior angle of the scapula in brachiators elongates the lever arm for caudal serratus anterior fibers (Ashton & Oxnard, 1964). Overall, Ashton and Oxnard concluded that these hominoid scapular features were adaptations for arm-raising because they increase mechanical advantage for the cranial trapezius and caudal serratus anterior. A cranially oriented glenoid was argued to be an adaptation to reduce demand for scapular rotation during arm-raising (Andrews & Groves, 1976; Ashton, Healy, et al., 1965; Ashton & Oxnard, 1964; Hunt, 1991; Tuttle & Basmajian, 1977; Oxnard, 1967). Based on these features, Oxnard (1969) suggested that the human shoulder evolved from an ape most similar to *Pongo* among extant hominoids.

Subsequent EMG studies on non-human primates failed to support some of Ashton and Oxnard's inferences. While Tuttle and Basmajian (1977) found that trapezius and caudal serratus anterior were active during arm-raising in chimpanzee, gorilla, and orangutan subjects, Larson, Stern, and Jungers (1991) later found that in chimpanzees all but the lowest digitations of serratus anterior were active during arm-raising, while cranial trapezius was inactive. Moreover, rather than being most active during arm-raising, cranial trapezius activity was most vigorous during stabilization of and/or turning of the head during suspensory locomotion (Jungers & Stern, 1984; Larson et al., 1991). Furthermore, caudal serratus anterior fibers were most active during the support phase of suspensory locomotion, when they eccentrically control the rate of descent of the trunk relative to the scapula (Jungers & Stern, 1984; Larson et al., 1991; Stern, Wells, Vangor, & Fleagle, 1977). Taken together, these EMG experiments (Larson et al., 1991; Stern et al., 1977; Tuttle & Basmajian, 1977) suggest that only minimal effort is required to raise the arm, questioning the functional interpretations of Ashton and Oxnard.

Another defining feature of "highly suspensory" primates (e.g., hominoids including gibbons, spider monkeys) noted by other observers is a craniocaudally elongated (and mediolaterally narrow) scapula, which is thought to permit greater mobility relative to terrestrial quadrupeds (e.g., baboons) in which the scapula is mediolaterally elongated with shorter vertebral borders (Jolly, 1967; Larson, 1993; Mivart, 1867; Schultz, 1930). In fact, the elongated vertebral border is considered a hominoid synapomorphy by some (Andrews & Martin, 1987; Crompton, Vereecke, & Thorpe, 2008; Harrison, 1987), and as an adaptation for suspensory or orthograde locomotion (Harrison, 1987) by others. An elongated vertebral border has been interpreted as providing mechanical advantage to the rhomboids and/or serratus anterior (Ashton & Oxnard, 1964; Clark, 1959; Miller, 1932), as well as accommodating larger rotator cuff musculature, itself required for increased stability in the face of large kinetic energy transduced through the shoulder joint (Roberts, 1974).

Additional morphological differences in anthropoid scapulae have also been noted, including the long recognized differential proportions of the supraspinous and infraspinous fossae among anthropoids (Mivart, 1867; Schultz, 1930). Roberts (1974) argued that large fossae in suspensory primates were a muscular compensation for joint stability that attended an increased range of motion. Inman et al. (1944) suggested that deltoid and supraspinatus were active in arm-raising, but this hypothesis had limited support from EMG data in chimpanzees (Larson & Stern, 1986; Tuttle & Basmajian, 1978). Larson also argued that large supraspinatus size in hominoids and spider monkeys compensated for the reduced mechanical advantage resulting from the abbreviated height of the humeral tubercles that receive their insertion (Larson, 1993). Roberts argued that the infraspinatus is used to lift and support the body during climbing and suspension (Roberts, 1974), but this was not supported by EMG data in chimpanzees, in which infraspinatus activity was most associated with joint stabilization (Larson & Stern, 1986). Most recently, it has been proposed that scapular spine orientation is related to the line of action of the infraspinatus, and that it helps to stabilize the joint during suspension (Green & Alemseged, 2012; Larson & Stern, 2013).

While the locomotor modes of hominids[1] have long been the subject of debate, only recently have relatively complete scapulae been discovered, allowing for comparisons with living taxa. Two of these fossils have been attributed to *Australopithecus afarensis*: DIK-1-1, a juvenile from about 3.3 million years ago (mya) (Alemseged et al., 2006) and KSD-VP-1/1g, an adult dated to 3.6 mya (Haile-Selassie et al., 2010). An additional find (MH2) has been described for a putative new species, *Au. sediba* from about 2 mya (Berger et al., 2010; Churchill et al., 2013). Both original descriptions for *Au. sediba* and the DIK-1-1 specimen argue that they resemble the scapulae of chimpanzees or gorillas, whereas KSD-VP-1/1g was described as being more similar to humans than African apes (Melillo, 2016). Despite the dissimilarity of these two genera, their morphology has been argued to be evidence for arboreal behavior in these species (Alemseged et al., 2006; Churchill et al., 2013).

1.1 | Scapular development

Although previous functional interpretations of scapular form have relied on a presumption of the independence of these various traits, the scapula has a complex developmental program (Hübler, Molineaux, Keyte, Schecker, & Sears, 2013). Scapular formation requires initial limb patterning, as it does not form in *Tbx5* knockout mice (Rallis et al., 2003). However, further limb outgrowth is not required because *Fgf* murine mutants absent the apical ectodermal ridge (AER), and which therefore lack forelimbs, have fully formed scapulae (Boulet, Moon, Arenkiel, & Capecchi, 2004; Min et al., 1998). Likewise, when *Fgf* signaling is eliminated in chicks, either by experimentally removing the AER or by insertion of an FGF receptor antagonist, the scapula (except the glenoid) forms, whereas the rest of the limb does not, demonstrating partial independence of the limb and scapula (Pröls et al., 2004).

The scapular blade largely derives from lateral plate mesoderm (LPM) in mammals, as does the forelimb, whereas the dermomyotome contributes to its vertebral border (Ehehalt, Wang, Christ, Patel, & Huang, 2004; Valasek et al., 2010), similar to the scapular blade in chicks (Huang, Christ, & Patel, 2006; Huang, Zhi, Patel, Wilting, &

Christ, 2000;). A subset of dermomyotome cells delaminate and migrate to the scapula, where they become fated to be chondrocytes (Fomenou, Scaal, Stockdale, Christ, & Huang, 2005; Huang et al., 2006; Moeller, Swindell, Kispert, & Eichele, 2003; Wang et al., 2010). In addition to these somitic and LPM contributions, there is also evidence that certain muscle attachment sites, such as that for the trapezius, are derived from neural crest (Matsuoka et al., 2005).

The initial condensation of the body of the scapula has been shown to be controlled by *Emx2* and *Pbx1* expression (Capellini et al., 2010). *Emx2* knockout mice lack the scapular blade entirely, but have normal glenoid, acromion, and coracoid structure (Pellegerini, Pantano, Fumi, Lucchini, & Forabosco, 2001), whereas *Pbx1* knockout mice have scapulae with malformations of the glenoid and coracoid (Capellini et al., 2006). After initial patterning, *Alx1*, *Alx4*, *Tbx15*, and *Gli3* regulate the morphological patterning of the scapular blade (Capellini et al., 2010; Kuijper et al., 2005). In *Tbx15* mutants, a foramen forms within the scapular blade, whereas *Tbx15/Gli3* double mutants had severely reduced scapular blades, with no acromion but a normal glenoid (Kuijper et al., 2005). *Alx4* and *Cart1* are required for normal patterning of the superior portion of the blade (Kuijper et al., 2005).

The acromion appears to develop from a condensation of cells that are separate from the rest of the scapula, and under the control of *Pax1* (Timmons, Wallin, Rigby, & Balling, 1994). Indeed, *Pax1* knockout mice lack an acromion on an otherwise normal scapula (Aubin, Lemieux, Moreau, Lapointe, & Jeannotte, 2002; Wilm, Dahl, Peters, Balling, & Imai, 1998). Furthermore, both *Hoxa5* and *Pax1* single and double knockout mice lack much of the scapular spine and the distal acromion (Aubin, Lemieux, Tremblay, Behringer, & Jeannotte, 1998). *Hoxc6* is a marker for glenoid and coracoid formation (Oliver, de Robertis, Wolpert, & Tickle, 1990), and *Hoxa5/Hoxb5/Hoxc5* triple knockout mice have a reduced AP length of the scapula (i.e., a reduced length of the medial border) (Xu et al., 2013).

The above genetic data strongly support potential evolutionary "modularity" of the scapula (Young, 2004). Given that multiple genes contribute to the morphology of a single "trait," convergent phenotypic evolution by altering the expression of different genes among lineages is a strong possibility.

In addition, many earlier studies were based on limited naturalistic behavioral data, in which all great apes were classified simply as "brachiators" (Napier & Napier, 1967), and it was assumed that modern hominoid traits were shared-derived from a single common ancestor (e. g, Keith, 1923; Osborn, 1927; Washburn, 1950).

Current understanding of the locomotor and morphological differences among living and extinct hominoids has led many to suggest extensive homoplasy in hominoid postcranial morphology (Alba, Almécija, Casanovas-Vilar, Méndez, & Moyà-Solà, 2012; Kivell, Barros, & Smaers, 2013; Larson, 1998; Lovejoy, Simpson, White, Asfaw, & Suwa, 2009; Lovejoy, Suwa, Simpson, Matternes, & White, 2009; Moyà-Solà, Köhler, Alba, Casanovas-Vilar, & Galindo, 2004; Reno, 2014; Ward, 2007). Nonetheless, suggestions of homology for hominoid traits continue (Begun, 2007; Benefit & McCrossin, 1995; Harrison, 1987; Harrison & Rook, 1997; Pilbeam, 2002; Young, 2003; Zihlman, McFarland, & Underwood, 2011), as does the hypothesis that humans evolved from a suspensory ancestor (Bello-Hellegouarch, Potau, Arias-Martorell, Pastor, & Pérez-Pérez, 2013; Churchill et al., 2013; Green & Alemseged, 2012) or an African ape-like ancestor (Green, Spiewak, Seitelman, & Gunz, 2016; Young, Capellini, Roach, & Alemseged, 2015), despite substantial data to the contrary as provided by *Ardipithecus ramidus* (Lovejoy, Simpson, et al., 2009; Lovejoy, Suwa, et al., 2009; White, Lovejoy, Asfaw, Carlson, & Suwa, 2015).

Here, we reassess the functional and evolutionary aspects of hominoid scapular morphology, considering how differences in anthropoid scapular shape could potentially arise developmentally and evolutionarily. Specifically, we examine previous predictions of scapular morphology as locomotor and/or ancestral hominoid adaptations, such as relatively long vertebral and axillary borders, a long and cranially oriented acromion, a cranially oriented glenoid, and relatively large supra- and infrascapular fossae. We compare hominoids to a broad sample of anthropoids to determine if the above features are uniformly shared among hominoids, whether there are convergences with other anthropoids, and which features are likely adaptations to locomotor behaviors. We also investigate interactions between scapular features, to determine if putative scapular "adaptations" are more likely evolutionary and/or developmental byproducts of other morphological changes (Gould & Lewontin, 1979). We then compare fossil hominids to extant anthropoids to test the hypothesis that they utilized suspensory locomotor behavior.

2 | MATERIALS AND METHODS

We obtained metric and angular data in a diverse sample of adult anthropoids using standard anatomical landmarks (Tables 1 and 2; Figure 1, see also Supporting Information Table S1). Anatomical sites were chosen to best capture overall scapular shape. Many are taken from Ashton and Oxnard (1964), and were chosen to reflect the relative length and angulation of important muscle attachment sites. Additional angles (GMA, GSA, SMA, SAA) were adopted from those of other authors to allow comparisons with more recent analyses (e. g, Churchill et al., 2013; Green & Alemseged, 2012; Haile-Selassie et al., 2010; Melillo, 2016). Fossil hominid scapulae were measured from published images. Metrics were taken with digital calipers. Angles were measured using Image J version 1.41 from images taken with an Olympus D-560 Zoom digital camera. Principal components, discriminant function, correlation, and linear regression analyses were calculated using SPSS version 22.0. We performed principal components analysis to compare overall scapular form among anthropoids and to identify redundant measurements. We performed stepwise discriminant function analyses of fossil hominids which were not assigned an identity, thus allowing them to be placed in the nearest group. We used a geometric mean (GMEAN) of fore- and hindlimb joint surface metrics (Table 2) to create a ratio with the linear metrics to limit the effect of body size for cross generic and allometric comparisons (Supporting Information Figure S1). Joint surface metrics

TABLE 1 Sample utilized for analysis

	Sex					
	M	F	Total[a]	Locomotion	Museum	Body mass (kg)[b]
Hominoids						
Homo	14	15	29	Bipedal	CM	62.1–72.1
Pan	14	15	29	KW, VC	CM	41.6–46.3
Gorilla	15	15	30	KW, VC	CM	71.5–170.4
Pongo	7	13	20	CL, VC	CM, FM	35.6–77.9
Hylobates	16	6	22	Brach.	CM, FM, SM	5.3–7.8
Symphalangus	1	2	3	Brach.	SM	
Arboreal cercopithecine						
Cercopithecus	0	1	1	ABQ	CM	4–9
Macaca	6	4	10	ABQ	FM, SM	3.6–11.2
Terrestrial cercopithecine						
Chlorocebus	3	3	7	ABQ, TQ	CM, SM	3–5.5
Erythrocebus	1	1	2	TQ	SM	
Baboons						
Papio	10	5	15	TQ	CM, FM, SM	12.1–29.8
Colobine						
Colobus	9	2	11	ABQ	FM, SM	7.9–13.5
Pygathrix	1	0	1	ABQ	FM	
Semnopithecus	1	4	5	ABQ, TQ	FM	6.9–19.2
Trachypithecus	2	3	6	ABQ	CM, FM, SM	5.8–7.9
Ceboid						
Alouatta	7	3	10	CL	FM, SM	6.3–7.8
Ateles	6	8	16	Brach., CL	FM, SM	7.3–9.6
Lagothrix	7	3	11	Brach., CL	CM, FM, SM	7.2–9.3
Cebus	8	2	10	ABQ	FM, SM	2.5–3.7
Saimiri	1	2	3	ABQ	SM	
Total	129	107	241			

Locomotion abbreviations: ABQ = above branch quadrupedism (including frequent leaping between supports); CL = clambering (including climbing/bridging; leaping between supports is rare); KW = knuckle-walking; Brach. = brachiation; TQ= terrestrial quadrupedism; VC = vertical climbing.
Museum abbreviations: CM = Cleveland Museum of Natural History, Cleveland, OH; FM = Field Museum of Natural History, Chicago, IL; SM = Smithsonian Museum of Natural History, Washington, DC.
[a]Totals contain individuals of unknown sex.
[b]Body mass species estimates for males and females, data from Smith and Jungers (1997) (for genera with multiple species sampled, smallest female and largest male means are presented, See also Supporting Information Table S1).

were selected as size correctors as they scale well to body mass (Jungers, 1991). To ensure that phylogenetic relationships did not greatly affect regression analyses, we performed phylogenetic independent contrasts, assuming trees of equal lengths, using the PDAP: PDTREE version 1.15 (Midford, Garland, & Maddison, 2009). Our discussions of selection and development of morphological traits utilize trait types established by Lovejoy, Cohn, and White (1999, 2000) and Lovejoy, Suwa, et al. (2009).

3 | RESULTS

3.1 | Principal components analysis

We performed a principal components analysis (PCA) using size corrected linear metrics and angles (Table 2, Supporting Information Tables S2 and S3) with the goal of identifying potentially redundant or related metrics. This PCA had five significant components, accounting for 91.7% of the variance (Table 3).

TABLE 2 Scapula metrics and angles. Numbers in parentheses refer to the points in Figure 1

Metrics
VERT – AP length of vertebral border from superior angle (1) to inferior angle (2)
AXBORD –Midpoint of glenoid (8) to inferior angle (2)
SPINE – Length of scapular spine from acromion (4) to vertebral border (3)
SPGLN – Breadth of scapula from spine at the vertebral border (3) to glenoid (8)
ACRO – Projection of acromion (SPINE- SPGLN)
SUPRA – Midpoint of spine at vertebral border (3) to superior angle (1)
INFRA – Midpoint of spine at vertebral border (3) to inferior angle (2)
Angles
GLENANG – Angle of glenoid relative to inferior angle. Points- superior border of glenoid (6), inferior border of glenoid (7), inferior angle (2)
GLENSUPANG – Angle of glenoid relative to superior angle. Points- inferior border of glenoid (7), superior border of glenoid (6), superior angle (1)
SPINANG– Angle of scapular spine relative to vertebral border. Points- acromion (4), vertebral border at spine (3), inferior angle (2)
INFANG – Angle of inferior angle from vertebral border at the spine (3) to the inferior angle (2) to inferior border of the glenoid (7).
ACROANG – Angle of acromion relative to scapular spine. Points- vertebral border at spine (3), lateral border of spine on the body (5), acromion (4)
GLENVERTANG – Angle of glenoid compared with vertebral border: 180° – (GLENANG + INFANG)
GMA – Angle from line through inferior (2) and superior angles (1) and line through superior (6) and inferior points of glenoid (7)
SMA – Angle from line through inferior (2) and superior angles (1) and spine from vertebral border (3) to acromion (4)
GSA – The angle formed by the base of the spine (4, 5) and the glenoid height line (6,7)
SAA – Angle of spine from vertebral border (3) to most lateral point (4) compared with line from inferior angle (2) to inferior border of glenoid (7)
BARGLEN – Angle from line of superior and inferior borders of glenoid to line through "ventral bar" on subscapular fossa
Metrics used for size correction
HUMHEDAP– Anteroposterior breadth of the humeral head
HUMHEDPD – Proximodistal length of the humeral head
HUMDISTART – Mediolateral breadth of the distal humerus articular surface
RADHEADML – Mediolateral radial head breadth
RADHEADDP – Dorsopalmar radial head breadth
RADMLCA – Mediolateral breadth of radius from radio-ulnar facet to styloid process
FEMHEAD – Maximum breadth of the femoral head
TIMLART – Mediolateral breadth of the proximal articular surface of the tibia

3.1.1 | Component 1: mediolateral breadth, glenoid and spine orientation

The first component (eigenvalue of 8.46, 47.0% of the variance) has large loadings for several measures of mediolateral breadth (INFANG, SPINE, SPGLN – although the latter two have higher loadings in the second component), glenoid orientation (GLENVERTANG, GMA, GLENANG, GLENSUPANG, BARGLEN), and spine orientation (SPINANG, SMA, SAA) (Table 3). Supraspinous fossa and acromion length have high positive loadings and infraspinous fossa has a negative loading for this component. This component clearly isolates taxa that are more terrestrially quadrupedal (TQs)(*Papio*, *E. patas*, *C. aethiops*) with negative loadings, from more "suspensory" primates (hominoids and *Ateles*) which exhibit positive loadings. Above branch quadrupeds (ABQs, e.g., *Macaca*, colobines, *Cebus*, and *Saimiri*) exhibit intermediate values. Humans overlap with *Alouatta* and *Lagothrix* (Figure 2).

Inferior angle value has a large negative loading for PC 1. Ashton and Oxnard (1964) observed that the inferior angle was relatively more acute in brachiators than in quadrupeds. Our results confirm this, with the most suspensory primates (*Pan*, *Pongo*, and *Ateles*, but not hylobatids, see note in Supporting Information Figure S2) having inferior angle dimensions that are less than 50°, while more terrestrial monkeys have angles greater than 70° (*C. aethiops*, *E. patas*, *Papio*). ABQs fall in between these two extremes. However, this angle may largely reflect differences in ML breadth of the scapula. As hominoids have ML narrower scapulae compared with ABQs and TQs, the reduced distance between the glenoid and vertebral borders renders a more acute

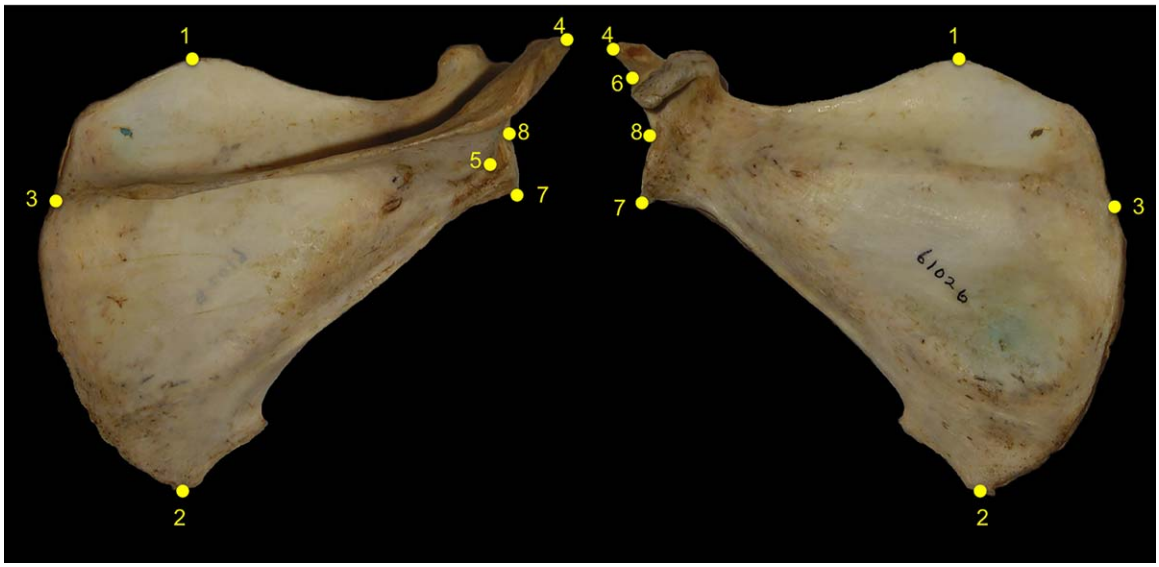

FIGURE 1 Landmarks used for metrics and angles. See Table 2 for definitions

inferior angle. This pattern is seen in anthropoids, in which there is a strong negative correlation of inferior angle with relative ML scapular breadth (−.808, $p < .01$). This is further illustrated in Figure 3, where an image of a macaque scapula has been altered so that the ML breadth is reduced to be equal to, or 2/3rds the length of vertebral border length, changing the inferior angle dimension from 71° to 58°. This suggests that the more acute inferior angle dimension in hominoids is the result of a narrower scapula and not a caudally positioned inferior angle, as has been noted elsewhere (Larson, 2015).

Close inspection of PC1 shows that measures of the scapular spine (SPINE, SPGLN) largely reflect mediolateral breadth of the scapula, and generally discriminate between locomotor groups. When ML breadths (SPGLN) relative to body size are compared (Supporting Information Figure S3), hominoids and atelines have the narrowest scapulae among anthropoids, terrestrial quadrupeds have long scapulae, and ABQs are intermediate.

We quantified the degree of cranial orientation of the glenoid using several methods. GLENANG followed Ashton and Oxnard (Ashton, Healy, et al., 1965; Ashton & Oxnard, 1964; Oxnard, 1963;) by measuring the angle between the glenoid and the inferior angle (Supporting Information Figure S4). Those authors found that this angle separated quadrupeds from "semibrachiators" and "brachiators" (Ashton & Oxnard, 1964). This metric had a relatively high loading for the first component in the study reported here. It is more acute in suspensory anthropoids (hylobatids, *Pan*, *Pongo*, *Ateles*), but shows overlap with less suspensory forms. This angle may not reliably reflect glenoid orientation as it is dependent on the position of the inferior angle, which, as noted above, covaries with mediolateral breadth. Furthermore GLENSUPANG, which compares glenoid orientation to superior angle, had a similarly high loading. However, two measures of glenoid orientation relative to the vertebral border, GMA (following Churchill et al., 2013), and GLENVERTANG, had the highest loadings for this component, whereas bar/glenoid angle (BARGLEN) had a much lower loading. We will discuss glenoid orientation in greater depth below.

Some have argued that a cranially oriented acromion facilitates trapezius action in arm-raising (Ashton & Oxnard, 1964), and has been argued to be an adaptation for brachiation (Andrews & Groves, 1976; Erikson, 1963). The observation that suspensory anthropoids (*Pongo*, hylobatids, *Ateles*, *Pan*) have the most cranially oriented acromia (SPINANG values above 110°, SMA values less than 55°) is supported here, with gorilla values closer to those of ABQs (Figures 4 and 5). ABQs are intermediate (and overlap with humans) but have greater angles compared with TQs. We will also consider scapular spine orientation in greater detail below.

Two metrics that reflect the size of the supraspinous (SUPRA) and infraspinous (INFRA) fossa size have their highest loadings for the first component, with SUPRA having a positive loading, and INFRA having a negative loading, indicating that hominoids and spider monkeys have relatively large supraspinous and small infraspinous fossae. More detail will be provided below.

3.1.2 | Component 2: spine length, and axillary border

The second component has an eigenvalue of 3.16 and accounts for 17.6% of the variance (Figure 2). This component has strong positive loadings for two measures of spine length (SPINE, SPGLN) and for axillary border length (AXBORD). For this component, gibbons, baboons, and TQs had positive loadings, whereas humans and orangutans had negative loadings. African apes and most monkey taxa were intermediate.

Axillary border length shows moderate loading on the second component. When compared with body size across anthropoids, there is slight negative allometry for this metric (slope = .892, 95% CI = .868–.916, Supporting Information Figure S5). To limit the confounding effects of relatedness, we performed phylogenetic

TABLE 3 Principal components analysis: eigenvalues and component values

Eigenvalues			
Component	**Total**	**% of Variance**	**Cumulative %**
1	8.456	46.979	46.979
2	3.163	17.572	64.550
3	1.866	10.364	74.915
4	1.729	9.608	84.522
5	1.286	7.145	91.667

Component matrix					
	Component				
	1	**2**	**3**	**4**	**5**
SAA	**−.675**	−.587	.244	.145	.114
GLENVERTANG	**.903**	−.178	.024	−.336	.097
GMA	**.941**	.077	.061	−.193	.098
ACROANG	.602	.193	−.155	**.628**	−.164
BARGLEN	**−.639**	−.490	.081	.108	−.389
INFANG	**−.695**	.552	−.136	.337	.173
GLENANG	**−.810**	−.312	.111	.211	−.369
GLENSUPANG	**.819**	−.245	.272	.272	.127
SPINANG	**.897**	−.084	−.017	−.336	−.181
GSA	.133	−.228	.261	.229	**.860**
SMA	**−.922**	−.205	−.013	.168	.183
VERT	.286	−.160	**.902**	.087	−.169
AXBORD	−.225	**.628**	.537	−.457	−.058
SPINE	−.503	**.796**	.263	.085	.034
SPGLN	−.646	**.725**	.187	−.081	.057
ACRO	**.627**	.040	.196	.556	−.088
SUPRA	**.665**	.330	.385	.339	−.196
INFRA	**−.642**	−.502	.454	−.268	.070

Bolded values indicate the highest loading for each variable.

independent contrasts (PIC), which confirmed slight negative allometry (least squares [LS] slope = .932). Humans fall below this line. This dimension also shows slight negative allometry among homionids (slope = .933, 95% CI = .881–.985), which is confirmed by PIC analysis (LS = .95). Thus, it seems that hominoids have a relatively shorter axillary border compared with smaller-sized monkeys, but this dimension differs little with body size among hominoids.

3.1.3 | Components 3, 4, and 5: Vertebral border length, acromion length, glenoid/spine angle

The third, fourth, and fifth components have eigenvalues of 1.87, 1.73, and 1.29, respectively, and cumulatively account for 21.7% of the variance. The third component has high loadings for vertebral (VERT) length (Figure 6). Humans and gibbons have low loadings for this component, with great apes intermediate, howler monkeys with a positive loading, with significant overlap with most monkey taxa, despite a long vertebral border being considered a defining hominoid trait (Harrison, 1987). When compared with a body size surrogate based on limb joint surface metrics (GMEAN; see earlier) among all anthropoids, vertebral border length scales with very slight positive allometry (slope = 1.05, 95% CI= 1.022–1.084, Supporting Information Figure S6). PIC analysis comparing anthropoids at the generic level found a similar slope (LS = 1.07), suggesting that phylogeny does not greatly affect the original regression. Acromion angle has its highest loading on the fourth component, although it had a nearly equal loading on the first component. Humans, gibbons, and chimpanzees have a positive loading, whereas orangutans have negative loading, with most other taxa intermediate. The fifth component (Supporting Information Figure S7) has its highest loading for glenoid-spine angle (GSA). There is no obvious taxonomic or locomotor separation for this component.

3.2 | Comparisons with fossil hominids

3.2.1 | Glenoid orientation

Plio-Pleistocene hominids have been hypothesized, based in their forelimb anatomy, to have regularly utilized arboreal suspensory behaviors (Senut, 1980; Stern & Susman, 1983). The traits on which this surmise is based include a cranially oriented glenoid which is argued to be present in *Australopithecus afarensis* (A.L. 288-1). Stern and Susman (1983) compared the orientation of the glenoid to the ventral bar in A.L. 288-1-l, because only the glenoid and part of the axillary border were preserved in this specimen. Their value for A.L. 288-1-l (130°), was closer to the great apes [chimpanzees (126.3°), gorillas (131.6°), and orangutans (127.4°)], than to humans (145°). They considered this to be evidence that *Au. afarensis* was partly arboreal (Stern & Susman, 1983). However, when compared with a broader sample, the value for A.L. 288-1-l overlaps with many non-suspensory forms, including *Alouatta*,

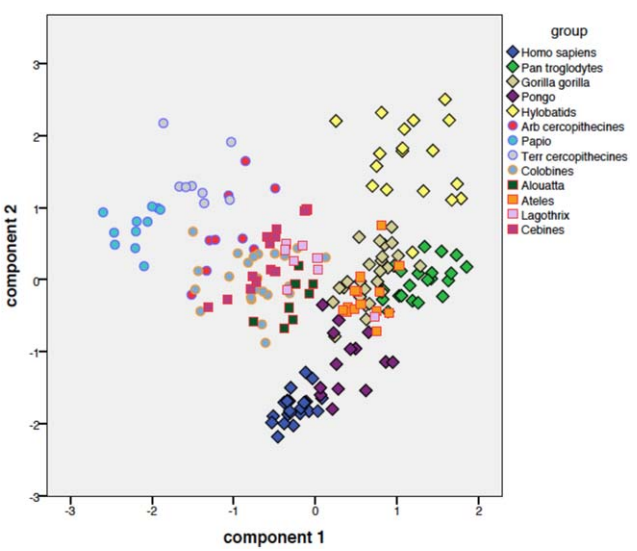

FIGURE 2 Scatter plot for the first and second principal components

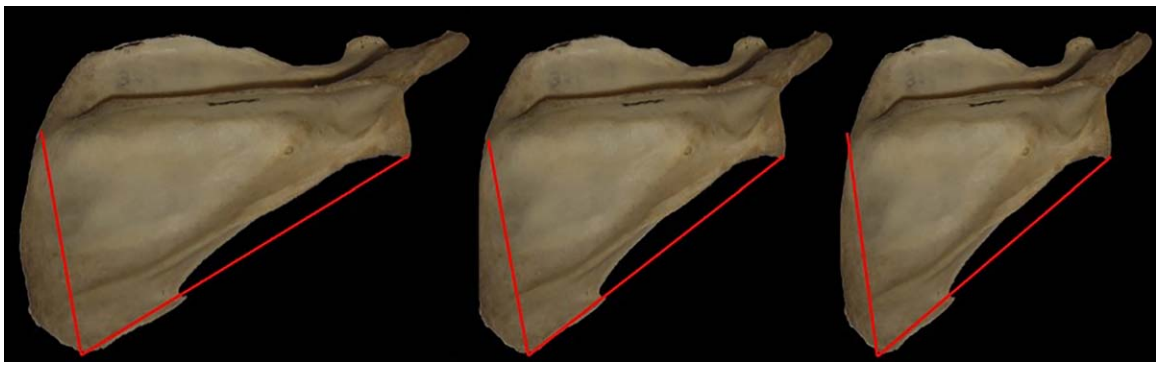

FIGURE 3 Photo of *Macaca* scapula, illustrating the effect of mediolateral scapular breadth on inferior angle dimension. The image on the left is an unmodified specimen with an inferior angle dimension of 71.0°; ML breadth is 0.8 times the length of the vertebral border. The middle image is the same scapula scaled so that ML breadth is equal to vertebral border length; its inferior angle is 63.2°. The image on the right has been scaled so that vertebral border length is 1.5 times ML breadth, with an angle of 57.5°

cebines, and colobines (Figure 7). The value for KSD-VP-1/1g, a more recently discovered *Au. afarensis* scapula, which is far better preserved than that of A.L.288-1-l, is 135° (Haile-Selassie et al., 2010), which is similar to many ABQs. An angle of approximately 129° for DIK-1-1 was suggested to be evidence for ape-like suspensory behavior (Green & Alemseged, 2012), but this again overlaps with many ABQs. The overlapping values of taxa with differing locomotor behaviors suggests that the bar-glenoid angle is not a reliable indicator for determining locomotor behavior, as has been argued previously (Inouye & Shea, 1997; Mensforth et al., 1990).

The functional significance of glenoid orientation is that forelimb load on the shoulder joint is largely counteracted by eccentric contraction of the serratus anterior muscle (see below). To capture this relationship, we measured glenoid orientation as the angle of the glenoid relative to the vertebral border (GLENVERTANG, see Table 2 for definition). Greater positive angles indicate a more cranially oriented glenoid relative to the vertebral border, while angles close to zero indicate a glenoid tangent that nearly parallels the vertebral border. More suspensory anthropoids (hylobatids, *Pan*, *Pongo*, and *Ateles*) have the greatest values (means above 10°), while ABQs, as well as *Homo* and *Gorilla*, have values near zero (Figure 8). TQs all have values of −15° or less, reflecting the greater curvature of the vertebral border, and not necessarily a more caudal orientation of the glenoid. Therefore, it appears that suspensory primates have glenoids that are not parallel to the long axis of the vertebral border, but, as shown by the angle of the glenoid relative to the inferior angle, more perpendicular to the axillary border. We measured this angle in the three fossil hominids with relatively complete scapulae. Their values each fell near zero (MH2: 5.4°, KSD: 4.5°, DIK-1-1: −5.5°). This fails to support an inference of suspensory behavior in the hominid lineage. We also measured glenoid/vertebral border using the Glenoid-Medial Angle (Figure 9) following Churchill et al. (2013) and found that KSD and DIK-1-1 both fall within the ABQ and human range (<20°), whereas the value for MH2 (28.8°, as measured by Churchill et al. (2013)) is similar to that of *Gorilla* (31.5° in Churchill et al.'s sample, 24.5° as measured here) and *Ateles* (29.0°) means.

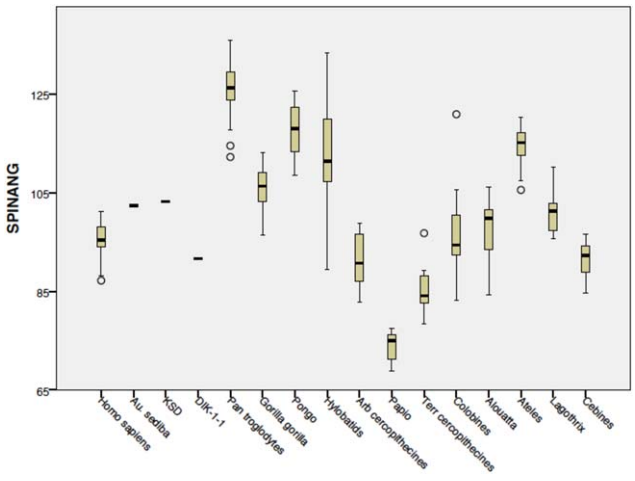

FIGURE 4 Scapular spine angle (SPINANG). For discussion see text

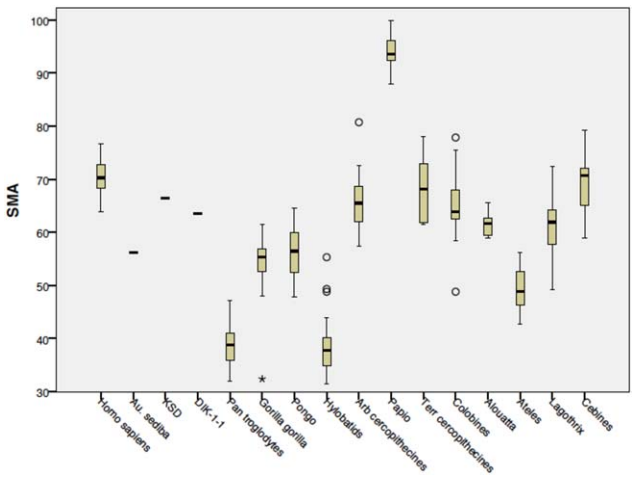

FIGURE 5 SMA based on angle from Churchill et al. (2013)

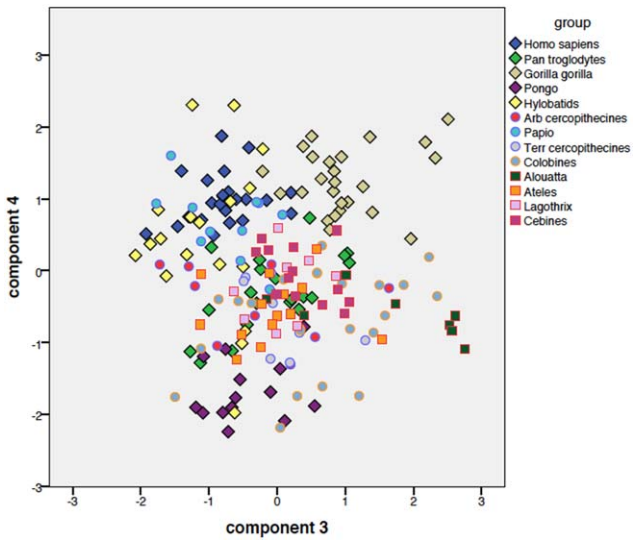

FIGURE 6 Scatter plot for the third and fourth principal components

3.2.2 | Scapular spine angle vs. relative supraspinous/infraspinous fossae size

As noted above, highly suspensory anthropoids have the most cranially oriented scapular spines in our sample. Early hominids (*Au. sediba*, KSD, and DIK-1-1) overlap with the human and/or gorilla range for this variable (SPINANG), but not with those of more suspensory anthropoids.

Churchill and colleagues (2013) measured a similar angle in their description of *Au. sediba*, which compared the angle of the acromion relative to a line through the superior and inferior angles (SMA, Figure 5). For this angle, *Pan* and *Pongo* have the lowest values (means less than 40°), with *Ateles* the next lowest (less than 50°), followed by *Pongo* and *Gorilla* (means of about 55°). Humans overlap with ABQ cercopithecoids and cebines, falling between 60° and 80°. *Papio* is the only taxon with a mean above 80°. Churchill et al. (2013) estimate *Au. sediba* at 56.2°, which is similar to the *Pongo* and *Gorilla* means, while DIK-1-1 and KSD are here estimated to be about 65°, similar to humans. As the points of measurement for this angle and SPINANG include the acromion, superior angle, and inferior angle, which are often absent in fossils, the precision of these angles is somewhat uncertain. Nonetheless, no available fossil hominid overlapped with *Pan* or hylobatids, which had the greatest cranial orientation for both angles. The fossil hominids more often fell within or near the human range, which was close to the arboreal cercopithecine range for both angles. Despite the uncertainty inherent in the measurement of these angles, when viewed from a broader anthropoid sample, the fossil hominids' scapulae do not show acromion angulation like those of more suspensory anthropoids.

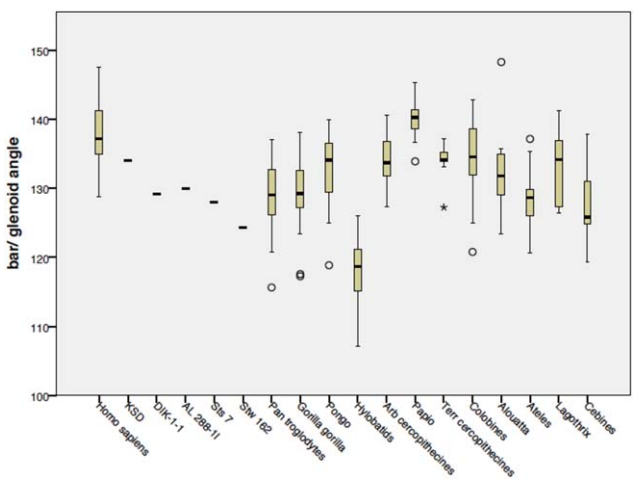

FIGURE 7 Bar/glenoid angle measured as in Stern and Susman (1983). AL 288-1-l angle taken from Stern and Susman (1983). DIK-1-1, STS 7, Stw 162 angles from Green and Alemseged (2012). KSD angle from Haile-Selassie et al. (2010). Note that this angle does not discriminate between anthropoids in terms of locomotor behavior

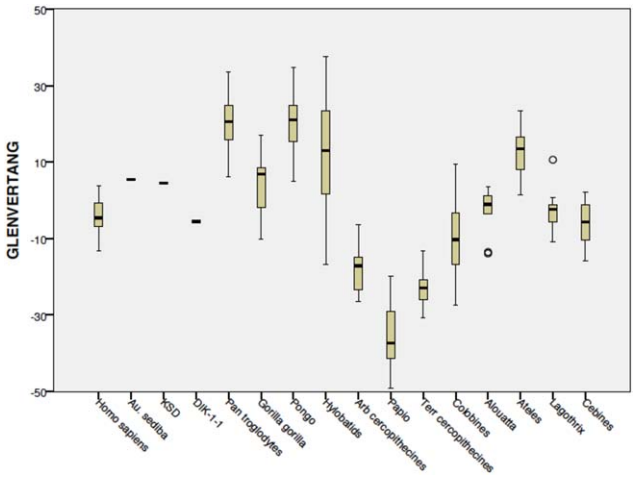

FIGURE 8 The relative orientation of the glenoid compared with the vertebral border as the angle between them. Most ABQs fall within ± 10°. Note that the most suspensory anthropoids, (*Pan*, *Pongo*, hylobatids, *Ateles*) have glenoids that are angled 10° or more above parallel (i.e., 0°). The more terrestrial cercopithecines have angles that indicate a more caudal orientation of the glenoid, however this method does not reflect the curvature of the vertebral border in these taxa

As noted above, there have been many functional explanations for hominoids having a relatively large supraspinous and/or infraspinous fossa, including arm-raising and joint stability. However, when a ratio of supraspinous to infraspinous fossa size is calculated, *Pongo* and hylobatids constitute the two opposite extremes among anthropoids. Schultz (1930) and Ashton, Oxnard, et al. (1965) also found that *Pongo* and *Hylobates* were the two extremes in their anthropoid samples for relative supraspinous/infraspinous fossa size, each using a different method of measurement (Supporting Information Table S4). Considering that *Pongo* and hylobatids are the most suspensory of all modern anthropoids, their extremely divergent values for this ratio suggest that the relative sizes of the supraspinous and infraspinous fossae lack significant selective value. Moreover, there appears to be little correlation between fossa and muscle size (Bello-Hellegouarch et al., 2013; Larson,

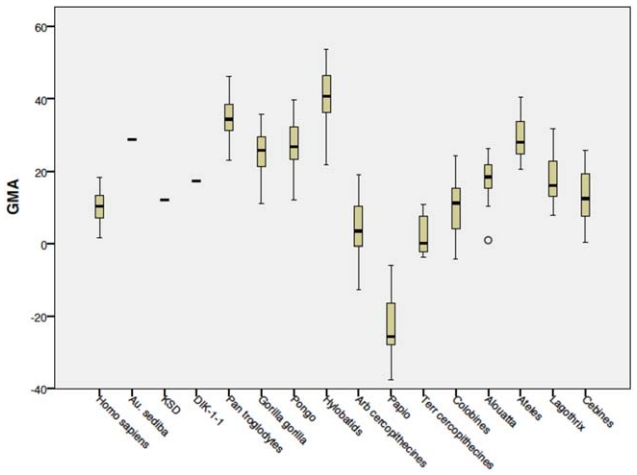

FIGURE 9 GMA based on method from Churchill et al. (2013). Note that most ABQs fall between 0° and 20°, with modern ape, spider monkey and baboon means falling outside this range. Also note that KSD and DIK-1-1 fall between these two values

2015). For example, male gorillas and orangutans were found to have equal ratios of these two muscles (supraspinatus is 38%, infraspinatus is 62% of their combined weight for both taxa (Zihlman et al., 2011)), despite the differences in fossa ratios found here (*Gorilla*: 49%, 51%; *Pongo*: 25%, 75%). Likewise, Larson (2015) found that supraspinatus mass, proportional to rotator cuff muscle mass, is similar in all hominoids. Furthermore, the muscle mass ratio of 42% (supraspinatus) to 58% (infraspinatus) for *Macaca* (Doyle, Siegel, & Kimes, 1980) differs from the fossa ratio here of 34% to 66% (supraspinous/infraspinous fossa). This suggests that muscle function as expressed by force output (i.e., cross sectional area) is easily modified without any underlying change in the muscle's attachment site. If this is the case, care must be assigned with interpretation of relative attachment areas such as the two posterior fossae of the scapula, because relative supraspinous and infraspinous fossae sizes have little direct association with locomotor behavior, although there is a very weak association between the relative size of the supraspinous fossa (compared with overall vertebral border) and scapular spine among anthropoids ($r = .444$, $p < .001$, Supporting Information Figure S8). Both hylobatids and *Pongo* differ the most from this pattern, and when these taxa are removed from the sample, this association increases significantly ($r = .699$, $p < .001$).

Orangutans likely differ from the general anthropoid condition based on the angle of the acromion relative to the scapular spine. In most hominoids, the cranial orientation of the acromion reflects a similar scapular spine orientation. However, for *Pongo*, the acromion is angled cranially away from the scapular spine. For this angle, most hominoids (and *Ateles*) have values above 150°, with hylobatids having extreme values of over 160° (Supporting Information Figure S9). *Pongo*, however, has an angle of ~140°, which is similar to the *Macaca* and *Papio* means. Therefore, it appears that while most hominoids have a cranially oriented scapular spine, which is nearly parallel to the acromion, orangutans have an acromion that angles sharply craniad relative to the scapular spine.

TABLE 4 Stepwise discriminant function analysis with full anthropoid sample

	Function				
	1	2	3	4	5
Structure matrix					
SMA	**.971**	.072	−.126	.174	.070
GMA	**−.725**	−.207	.149	.487	.415
SAA	**.689**	−.585	.413	.091	−.069
INFANG	.447	**.771**	.440	.087	−.064
GSA	.028	−.094	.003	**.947**	−.307
Functions at group centroids					
Homo	2.687	−2.948	.396	.141	−.052
KSD	3.560	−8.331	7.239	−1.520	−1.117
DIK	2.015	−3.183	5.996	0.836	−1.762
MH2	1.048	−7.035	7.479	−0.152	−0.694
Pan	−4.128	−.237	−1.466	−.804	−.315
Gorilla	−.901	−.232	.353	.595	−.514
Pongo	−.769	−2.015	−1.990	.720	.642
Hylobatids	−4.433	3.430	1.159	.735	.215
Arb cerc.	1.766	1.638	.728	−1.572	.339
Papio	6.739	4.579	−2.205	.358	−.254
Terr cerc.	2.358	1.952	1.459	−1.348	.467
Colobines	1.622	−.519	.647	−.585	−.079
Alouatta	.963	−1.750	1.578	.306	−.598
Ateles	−1.853	−1.139	−.125	−.480	.376
Lagothrix	.192	.332	.263	.090	−.149
Cebines	2.245	−.415	.985	.810	.474

Bolded values indicate the highest loading for each variable.
Unstandardized canonical discriminant functions evaluated at group means.

3.2.3 | Discriminant function analysis

We performed two stepwise discriminant function analyses (DFAs) to compare the overall morphology of fossil hominid scapulae (KSD, DIK-1-1, and MH2) to modern anthropoids. One DFA included the entire sample of anthropoids and a second was limited to only hominoids. For both analyses, hominids were not given a prior group classification, allowing the program to "assign" each individual to a group. We utilized angular measurements, which are independent of size, in similar fashion to multivariate analyses of angles performed elsewhere (Churchill et al., 2013; Green & Alemseged, 2012; Haile-Selassie et al., 2010) because reliable body mass estimates or other size correctors are not available. Angles selected for this analysis include those that best reflect scapular shape, based on their loading in our PCA (see above). Although our analysis lacks juvenile anthropoid data (DIK-1-1 is a juvenile), since Alemseged et al. (2006) compared juveniles and adults in their

TABLE 5 Classification results: predicted group membership

Predicted															
Actual	Ho	Pa	Go	Po	Hy	AC	Pp	TC	Co	Al	At	La	Ce	Total	%
Ho	26	0	0	0	0	0	0	0	1	0	0	0	1	28	92.9
Pa	0	26	0	0	0	0	0	0	0	0	3	0	0	29	89.7
Go	0	1	14	2	0	0	0	0	0	4	3	5	0	29	48.3
Po	0	1	0	19	0	0	0	0	0	0	0	0	0	20	95.0
Hy	0	2	0	0	22	0	0	0	0	0	0	0	0	24	91.7
AC	0	0	0	0	0	7	0	3	0	0	0	0	1	11	63.6
Pp	0	0	0	0	0	0	15	0	0	0	0	0	0	15	100.0
TC	0	0	0	0	0	1	0	8	0	0	0	0	0	9	88.9
Co	1	1	0	0	0	1	0	2	8	5	1	3	2	23	34.8
Al	0	0	1	0	0	0	0	0	2	7	0	0	0	10	70.0
At	0	0	3	0	0	0	0	0	0	0	12	1	0	16	75.0
La	0	0	1	0	0	0	0	0	1	0	1	8	0	10	80.0
Ce	2	0	0	0	0	0	0	0	1	1	0	1	9	14	64.3
KSD	1	0	0	0	0	0	0	0	0	0	0	0	0	1	
DIK	0	0	0	0	0	0	0	0	0	1	0	0	0	1	
MH2	0	0	0	0	0	0	0	0	0	1	0	0	0	1	

Ho = *Homo*; Pa = *Pan*; Go = *Gorilla*; Po = *Pongo*; Hy = Hylobatids; AC = Arb Cerc; Pp = *Papio*; TC =Terr Cerc; Co = Colobines; Al = *Alouatta*; At = *Ateles*; La = *Lagothrix*; Ce = Cebines. 76.1% of original grouped cases correctly classified.

multivariate analysis of DIK-1-1, we argue that it is appropriate to also include DIK-1-1 here. Importantly, previous analyses (Alemseged et al., 2006; Churchill et al., 2013; Green & Alemseged, 2012; Haile-Selassie et al., 2010; Melillo, 2016) compared fossil taxa only to extant hominoids, whereas we have included nonhominoid anthropoids in our analysis.

The complete anthropoid sample had a Wilks' lambda for the first five functions of 0.004 (Table 4) and correctly placed 76.1% of the individuals into their taxonomic group (Table 5). The first two functions accounted for 86.9% of the variance. The angles with the highest loadings for the first two functions were those related to glenoid angle (GMA), the angle of the spine (SMA), spine/axillary border angle (SAA), and inferior angle dimension (INFANG). For the first function, *Pan*, hylobatids, and *Ateles* had the strongest negative loadings, whereas baboons, more terrestrial cercopithecines, and humans had the largest positive loadings. All other groups were intermediate for the first function. All three fossils included here had positive loadings for the first function, and negative loadings for the second function, as did humans, colobines, and howler monkeys. KSD was classified as a human, and DIK-1-1 and MH2 were classified as a howler monkey (Table 5).

We ran the second DFA using only hominoids. This analysis had a Wilks' lambda for the first 4 functions of 0.020 (Table 6) and correctly grouped 93.8% of the cases (Table 7). The first two components explained 97.2% of the variance. The highest loadings for the first component were for values related to spine angle (SMA) and spino-axillary angle (SAA), with *Pan* and *Hylobates* having large negative loadings and humans having large positive loadings. The variable with the largest loading for the second component was inferior angle (INFANG). Both *Pan* and *Pongo* exhibited negative loadings, with humans, gorillas, and hylobatids having positive loadings. All three hominid fossils had positive loadings for both the first and second components, and were all grouped with humans (Table 7).

4 | DISCUSSION

Taken as a whole, the results reported here do show that hominoid scapulae are distinct from those of most monkey taxa, but not uniformly so. As predicted, hominoids have relatively narrow scapulae. However, their vertebral border lengths differ little, relative to body size, from other arboreal anthropoids. Atelines have also relatively narrow scapulae, suggesting that a mediolaterally narrow scapula allows for greater mobility, but not necessarily for suspensory behaviors (*contra* Hunt, 1991). The similarity of *Alouatta* to hominoids but not colobines is notable. Both *Alouatta* and *Colobus* are folivores of similar size (*Alouatta* ~4 to 11 kg, *Colobus* ~7 to 14 kg) (Smith & Jungers, 1997). Howler monkeys have scapulae that are significantly narrower than broad, whereas for *Colobus*, these dimensions are nearly equal (Figure 10). Schultz (1930) suggested that a narrow scapula may be an adaptation to increased mobility, which may be reflected in preferred method of crossing gaps in the canopy in these species. Howler monkeys frequently use bridging but rarely leap (Cant, 1986; Fleagle & Mittermeier, 1980; Gebo, 1992; Rosenberger & Strier, 1989), whereas colobus

TABLE 6 Stepwise discriminant function analysis, hominoid sample only

	Function			
	1	2	3	4
Structure matrix				
SAA	**.907**	.253	−.127	.313
SMA	**.768**	.356	.352	−.399
INFANG	−.098	**.906**	−.028	−.411
GSA	−.011	.239	**.573**	.417
GMA	−.499	−.160	.440	**.729**
Functions at group centroids				
Homo	4.902	.705	−.311	.001
KSD	8.518	3.064	−5.489	6.501
DIK-1-1	4.573	4.435	−3.113	3.799
MH2	5.629	3.373	−4.430	7.634
Pan	−2.349	−1.905	−.618	.000
Gorilla	.440	.762	−.171	−.002
Pongo	1.371	−1.478	1.236	.000
Hylobatids	−4.555	1.790	.286	.001

Bolded values indicate the highest loading for each variable.

monkeys leap frequently, and rarely bridge (Gebo & Chapman, 1995; Mittermeier & Fleagle, 1976; Morbeck, 1977). Thus, the narrow scapula seen in hominoids (and atelines) is likely not be related to suspension, but rather to cautious climbing with substantial ABQ locomotion.

More suspensory hominoids (Asian apes and *Pan*) differ from *Homo* and *Gorilla* by having a more cranially oriented glenoid relative to the vertebral border, as well as an inferior angle that is more caudal compared with the glenoid. These differences between *Pan* and *Gorilla* are largely paralleled by those between *Ateles* and *Alouatta* and may be related to the line of action of the serratus anterior (SA). The glenoid plane and vertebral border are nearly parallel in ABQs. This suggests

TABLE 7 Classification results: predicted group membership

Classified							
Actual	Ho	Pa	Go	Po	Hy	Total	%
Ho	28	0	0	0	0	28	100.0
Pa	0	27	1	1	0	29	93.1
Go	0	1	26	1	1	29	89.7
Po	0	1	0	19	0	20	95.0
Hy	0	2	0	0	22	24	91.7
KSD	1	0	0	0	0	1	
DIK	1	0	0	0	0	1	
MH2	1	0	0	0	0	1	

Ho = *Homo*; Pa = *Pan*; Go = *Gorilla*; Po = *Pongo*; Hy = Hylobatids. 93.8% of original grouped cases correctly classified.

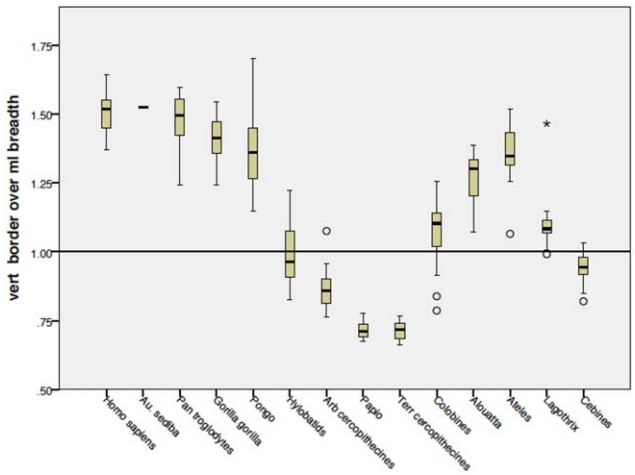

FIGURE 10 Comparison of vertebral border length by ML breadth of scapula. Note that great apes, humans, *Au. sediba*, *Alouatta*, and *Ateles* have individual values or means above 1.25. Hylobatids have a relatively small value for this because of our method of measuring ML breadth of the scapula. This measurement was taken from the glenoid to the vertebral border along the line of the scapular spine. The very obliquely oriented scapular spine of hylobatids increases this dimension. *Au. sediba* value was calculated from data in Churchill et al. (2013)

that the SA is acting mainly in a dorsoventral orientation (Jolly, 1967). At the start of stance phase of quadrupedal locomotion, the scapula moves dorsally relative to the trunk (Boczek-Funcke, Kuhtz-Buschbeck, & Illert, 1996) as the result of forces transmitted through the forelimb. Thus, the dorsoventral orientation of the SA fibers, perpendicular to the glenoid, allows for eccentric contraction of this muscle to dissipate compression by the forelimb during locomotion (Badoux, 1974; Gregory, 1912; Hildebrand, 1959). EMG data support this conclusion, showing that the homologous muscle, serratus ventralis, is active during the support phase in cats (English, 1978), dogs (Carrier, Deban, & Fischbein, 2006), opossums (Jenkins & Weijs, 1979), and vervet monkeys (Whitehead & Larson, 1994). During forelimb suspension, however, the mass of the animal would displace the scapula cranially relative to the thorax, necessitating muscular action to resist this motion. In hominoids and *Ateles*, SA extends to more caudal ribs than in other anthropoids, and these are oriented in a more craniocaudal direction (Stern, Wells, Jungers, & Vangor, 1980). EMG data show that the caudal portion of SA is active during the support phase of suspensory locomotion in gibbons, chimpanzees, and spider monkeys (Jungers & Stern, 1984; Larson et al., 1991; Stern et al., 1977, 1980). Thus, the cranial orientation of the glenoid would align it with the more craniocaudal lower digitations of SA. However, instead of SA crossing the body of the scapula as in quadrupedal locomotion, during suspension the scapula is suspended *above* the SA. This suggests that the action of the muscle's caudal fibers is not to elevate the arm, as has been confirmed by EMG analyses (Larson et al., 1991), but to resist the displacement of the scapula relative to the animal's center of mass during forelimb suspension. Therefore, the orientation of the glenoid relative to the vertebral border may instead be functionally related to the line of action of SA.

Selective hypotheses based on the relative sizes of the scapular fossae and the muscles housed therein have been suggested both for the size of the supraspinatus and the infraspinatus (Roberts, 1974), as well as for the line of action of the infraspinatus relative to the scapular spine (Larson & Stern, 2013). As demonstrated earlier, however, there would appear to be little selective pressure on the size of the fossae with respect to muscle size. Again as noted above, there is little correlation between muscle and fossa size in primates (Bello-Hellegouarch et al., 2013; Kimes, Doyle, & Siegel, 1979; Larson, 2015) and in mice (Green, Hamrick, & Richmond, 2011) (see earlier). Moreover, since the two most suspensory hominoid taxa (*Pongo* and hylobatids) exhibit opposite extremes in terms of relative fossa size, there can be little reliable relationship between fossa size and suspensory locomotor behavior. There appears to be little or no functional difference, as rotator cuff muscle recruitment does not differ between orangutans, chimpanzees, and gibbons (Larson & Stern, 2013).

4.1 | Evolution of the hominoid shoulder girdle from early Miocene to present

Although the independence of hominoid scapular features described above have long been assumed, we have argued here that much of hominoid scapular morphology may, in fact, be attributable to only two relatively simple changes: a ML narrowing of the scapular blade and some degree of cranial rotation of the glenoid and spine. While the selective pressures for these features were likely similar, they nonetheless may have arisen through different developmental mechanisms, which could explain current differences in hominoid scapular morphology.

Although there are few complete hominoid scapulae in the fossil record, inferences about scapular evolution can be made based on the overall postcranial phenotypes of fossil hominoids. Modern hominoids have a mobile shoulder girdle, in large part a function of the dorsal placement of the scapula on the thorax and an elongated clavicle (Chan, 2007, 2014; Erikson, 1963; Schultz, 1950, 1956). A broadened thorax and shortened lumbar spine, both of which are found in modern hominoids and atelines, contrast with the primitive narrow thorax and long lumbar spine seen in extant ABQ and TQ anthropoids (Benton, 1967; Schultz, 1961). Therefore, trunk shape is broadly correlated with locomotor behavior, and the shape of the trunk in Miocene apes can provide a general approximation of scapular morphology.

Extant hominoids likely arose from stem catarrhines, such as *Aegyptopithecus*, that have primitive, ABQ monkey-like postcrania (Fleagle, 1983; Rose, 1997). Early Miocene hominoids share many primitive features consistent with ABQ locomotion, with some features that are suggestive of more advanced, slow-clambering. For example, *Proconsul*, although having been reconstructed as having a clambering type of quadrupedal locomotion based on long grasping fingers and toes and lack of a tail, still retained many primitive characters such as a long lumbar column, narrow thorax, fore- and hindlimbs of similar length, ulnar-carpal contact, and a generalized catarrhine pelvis (Begun, Teaford, & Walker, 1994; Fleagle, 1983; Harrison, 2002; Rose, 1994, 1997; Walker, 1997; Ward, 2007; Ward, Walker, & Teaford, 1991). Although *Proconsul* has limb joint surface features that suggest relatively mobile limbs (Ward, 2007), the long lumbar spine and narrow thorax (Ward, 1993; Ward, Walker, Teaford, & Odhiambo, 1993) suggest that it lacked dorsally-placed scapulae, and thus its locomotor repertoire likely did not resemble those of either modern hominoids or atelines. The small scapular fragments attributed to *Proconsul* have been described as being similar to those of colobines or nonsuspensory NWMs (Harrison, 2002; Rose, 1997). Even if *Proconsul* practiced a predominantly clambering type of locomotion, its scapula would likely be less specialized than those of modern hominoids. Modern hominoids thus likely either share a common ancestor that was an ABQ with an unspecialized scapula, or an incipient clambering anthropoid, with a more generalized ateline scapula, modified from an ABQ ancestor.

Compared with extant monkeys (and fossil apes such as *Proconsul*), modern hominoids have a thorax that is mediolaterally broader than it is deep (Ankel, 1972; Schultz, 1956). This is part of a trunk bauplan shift that includes a broad sternum (Schultz, 1930, 1950) and invagination of the thoracic spine, with a dorsal angulation of the proximal ribs (Kagaya, Ogihara, & Nakatsukasa, 2008). Together, these features result in a more dorsally positioned scapula (Chan, 2007; Schultz, 1950). This has been argued with good reason to be an adaptation for greater shoulder mobility (Cartmill & Milton, 1977; Chan, 2007, 2014; Harrison, 1986). Among primates, the taxa that most closely resemble hominoids for these features are the ateline monkeys, who have a more dorsally placed scapula and broader thorax than do other New World or Old World monkeys (Chan, 2007; Schultz, 1931, 1956). Dorsal positioning would necessitate the scapulae being relatively narrowed mediolaterally, to prevent interference with the vertebral column during locomotion (Roberts, 1974), particularly during clambering or suspensory locomotor behaviors in which the scapula is retracted, thus further accentuating the need for vertebral column invagination.

However, scapular narrowing reduces the SA's ability to dissipate kinetic energy via eccentric contraction. In relatively slow moving/clambering arboreal mammals, forelimb mobility might be of greater selective advantage than energy dissipation. The differences between ABQ scapulae and those of less specialized clamberers or vertical climbers (i.e., *Gorilla*, *Alouatta*) can largely be explained by a mediolateral narrowing of the scapula in these taxa (Figure 11, compare A and B). This would account for the intermediate inferior angle dimension between its acute value seen in highly suspensory forms and the more obtuse one in ABQs. This change in angle is likely directly associated with scapular breadth reduction (type 2).

The second major difference in hominoid scapulae when compared with most other anthropoids is the cranially translated glenoid (i.e., lies relatively nearer the cranial border), especially in highly suspensory forms, a pattern paralleled in atelines. During quadrupedal locomotion in most primates, SA fibers are largely oriented in a dorsoventral pattern, perpendicular to the glenoid, resisting the substrate reaction force (SRF) that forces the scapula to translate dorsally on the trunk (Figure 12A) (Preuschoft et al., 2010). The nearly parallel orientation of the glenoid relative to the vertebral border in ABQs provides a normal orientation of SA function (Preuschoft et al., 2010). The caudal fibers of SA

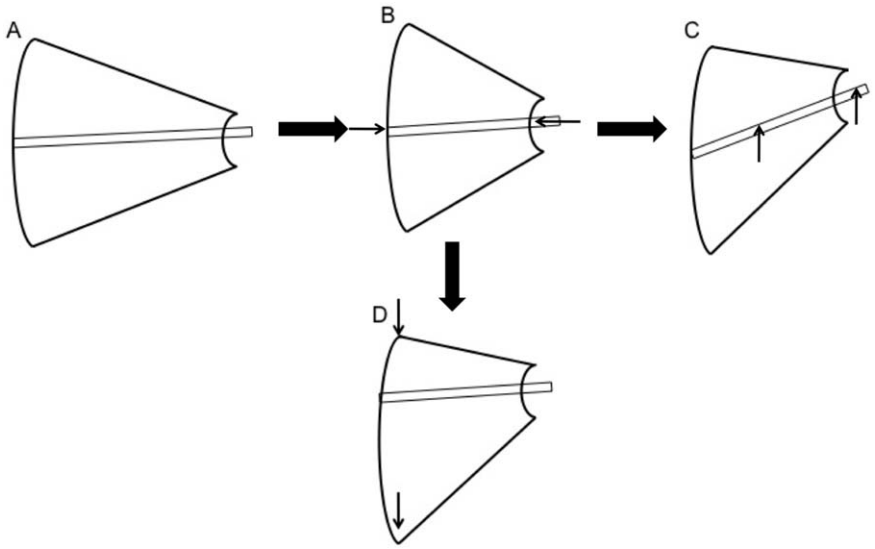

FIGURE 11 Theoretical evolution of the hominoid scapula. The above are schematic diagrams of theoretical stages of hominoid scapula evolution. As an example, the figure shows how modern hominoid scapulae (C and D) could have evolved from an ABQ scapula (A, similar to modern *Macaca*). In A and B, the glenoid and scapular spine at the vertebral border are both centered on the scapula. ABQs have scapulae that are roughly equal in craniocaudal length and mediolateral width (A). Hominoids have a ML narrow scapula, produced by shortening in this dimension (small arrows, B) required with relocation of the scapula posterolaterally and the required (and simultaneous) invagination of the spine and consequent alteration of thoracic shape. In C, the glenoid is moved cranially relative to its position in B. The scapular spine maintains its proximal position relative to the vertebral border with the distal end moving cranially with the glenoid (small arrows). If the acromion retains its position relative to the glenoid, when the glenoid is translated cranially, this would produce a cranially oriented scapular spine, as well as an acute inferior angle dimension. In D, the superior aspect of the vertebral border is reduced and the inferior aspect is increased (small arrows). This also results in a relatively cranial position of the glenoid. This is likely not representative of actual stages of hominoid evolution, but illustrates that relatively simple changes could produce a hominoid-like scapula from a generalized anthropoid one based largely on fundamental changes in positional information rather than targeted selection on numerous individual traits

are aligned with the glenoid due to its cranial translation and orientation. During suspension, the body obviously lies below the substrate, and the SRF would act to translate the scapula cranially relative to the thorax. As suspensory anthropoids have more craniocaudally oriented lower SA fibers (Stern et al., 1980), these would be largely parallel to the cranially transmitted SRF (Figure 12B). The cranially translated glenoid would reduce the rotation necessary to align the glenoid with caudal SA fibers. During suspensory behavior, the force is aligned with the axillary border (Preuschoft et al., 2010). This suggests that the relative position and orientation of the glenoid are, broadly speaking, adaptations to suspensory locomotion.

One potential mechanism that may have produced a cranially translated glenoid is a shift during pattern formation of the initial position of the glenoid relative to the vertebral border. This could account for the morphology seen in *Pan*, *Hylobates* and *Ateles*. The glenoid and vertebral border are derived from separate cell populations: the glenoid from lateral plate mesoderm and the scapular blade from dermomyotome (Valasek et al., 2010). They are also largely under independent genetic control as in many knockout mice, the glenoid is present while much of the scapular blade fails to form (Kuijper et al., 2005; Pellegerini et al., 2001; Wilm et al., 1998). The separate tissue derivatives and the relatively independent gene expression for these two cell populations, suggest that glenoid and blade initial positional information (PI) may be largely independent. However, the glenoid and scapular blade form a functional unit, and thus a change in one must impact the other. Therefore, a cranial shift in the PI of the glenoid would require a concomitant change in the scapular blade, in turn requiring the scapular blade to angle cranially to maintain articulation with the vertebral border (Figure 11C). This would maintain the relative position of the acromion (cranial to the glenoid), while simultaneously angling the scapular spine and further creating a more acute inferior angle (both type 2 changes).

If the glenoid's cranial translation has resulted from shifts in positional information subject to natural selection, then this shift can be classified as a type 1 change or possibly the product of functionally unrelated shift in positional information (type 2). However, cranial glenoid orientation could be the result of differential chondrocyte activity within the growth plate of the glenoid, which could in turn determine the degree of glenoid orientation and thus be classified as a type 4. In children with brachial plexus palsy from birth, the glenoid becomes angled ventrally due to absence of muscle function (Waters, Smith, & Jaramillo, 1998). This type of modeling has also been demonstrated in other skeletal elements in experimental and natural settings (e.g., Karaharju, Ryöppy, & Mäkinen, 1976; Lovejoy, 2007). This suggests that the degree of cranial orientation of the glenoid could be the result of cartilage modeling, in response to ontogenetic stresses on the glenohumeral joint induced by suspensory locomotion. Based on the bar/glenoid angle, there appears to be little change in glenoid throughout ontogeny in nonhuman hominoids or macaques, but the orientation in

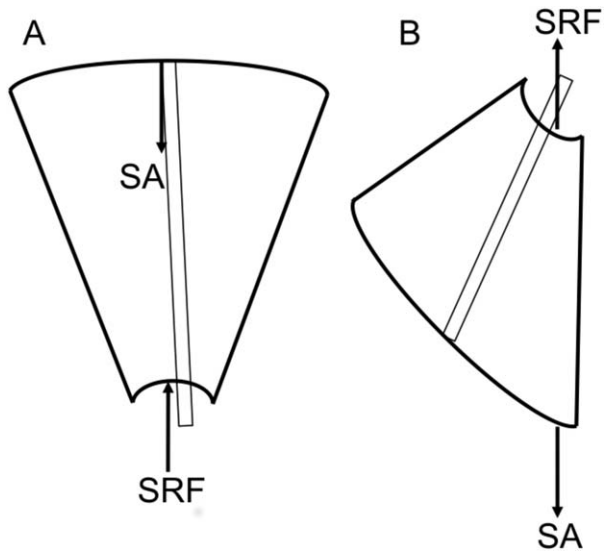

FIGURE 12 Potential locomotor forces in anthropoid scapulae. Above are schematic diagrams of forces about the scapula associated with quadrupedal (A) and suspensory (B) locomotion. In both, the substrate reaction force (SRF) would be transmitted through the forelimb to the glenoid. In quadrupedal locomotion (A), this force would be oriented superiorly, and would translate the glenoid superiorly relative to the trunk. Such potential superior translation would be resisted by an eccentric downward force from the serratus anterior (SA). In contrast, during suspensory locomotion (B) the SRF would translate the scapula cranially relative to the trunk and be resisted by a caudal force from SA fibers that lie more caudally

humans becomes more cranial during ontogeny (Green, 2013; Green & Alemseged, 2012). However, since most hominoids are relatively suspensory throughout ontogeny, it is unclear if these data demonstrate a type 1 or a type 4 change. Both chimpanzees and mountain gorillas practice higher amounts of suspensory locomotion as juveniles than as adults (Doran, 1997), which is, of course, the period of development during which adult morphology is almost entirely determined. Thus, gorilla morphology could easily converge of that of *Pan* depending on pre-adult climbing patterns. In adult gorillas, however, the amount of suspensory locomotion is never as great as in *Pan*, and may curtail at a younger age (Doran, 1997). Therefore, if a threshold strain level is required for ontogenetic glenoid orientation change, gorilla behavior may fall short of such levels.

For *Pongo*, a caudal shift in the PI of the vertebral border would reduce the relative size of the cranial portion of the scapula while simultaneously increasing its caudal portion. This would produce a similar result in this taxon (Figure 11D). As shown above, vertebral border length differs little among anthropoids, and the relative uniformity of this feature suggests that it may be the subject of stabilizing selection (type 1). The craniocaudal length of the scapular blade would likely need to maintain a minimum size for SA insertion and/or origin of the rotator cuff muscles. Therefore, any reduction in the size of the cranial end would require a similar increase in the length of the caudal end. This in turn would simultaneously reduce the size of the supraspinous fossa while increasing the size of the infraspinous fossa, but would not result in angulation of the scapular spine.

Taken together, two major changes in hominoid scapulae – mediolateral shortening of the blade and cranial translation of the glenoid – may account for many of the morphological features observed with other differences being essentially only secondary byproducts of these two primary changes (i.e., type 2) (Gould & Lewontin, 1979). Under this scenario, the selective pressures are for mobility (ML shortening) and reorientation of the resisting forces supplied by SA (glenoid translation/orientation). The ability to simply raise the arm during locomotion does not require excessive power and was therefore likely selectively passive (contra Ashton & Oxnard, 1964; Larson & Stern, 1986; Roberts, 1974). Features which have been argued to enhance simple elevation of the arm such as caudal inferior angle position and acromial angulation are likely only Type 2 byproducts of the first and second changes, respectively (Figure 11B,C).

4.2 | Hominid scapulae do not show adaptations for suspensory locomotion

Results from both DFAs and comparisons of individual angles and ratios reported here show that hominids are not most similar to highly suspensory taxa such as spider monkeys, Asian apes, or even chimpanzees. Instead, hominids are more similar to generally cautious above branch quadrupeds, such as howler monkeys, or even modern humans. As hominids lack the extreme specializations of gibbons or spider monkeys, our data do not support a hypothesis of a suspensory LCA.

Despite the overall differences in scapular morphology among hominoids, the fact that a narrow scapula is found in both hominoids and atelines suggests that a narrow scapula is not associated with suspensory locomotion, but with a more cautious type of above branch locomotion, one that utilizes primarily bridging rather than leaping, in animals of relatively large body size. As humans and gorillas share this more generalized phenotype, it is likely that the LCA for African apes and humans practiced this cautious, clambering type of locomotion, perhaps largely similar to the locomotor behavior of *Alouatta* (Stern, 1975). *Alouatta* differs from ABQ anthropoids that utilize more running and leaping above branch behaviors by having a ML narrower scapula and behaviorally by an increased reliance on bridging gaps in the canopy in place of leaping. The recently described *Ardipithecus ramidus* postcranial material, although lacking a scapula, showed a multiplicity of features that also suggest this cautious type of ABQ locomotion in the LCA (Lovejoy, Simpson, et al., 2009; Lovejoy, Suwa, et al., 2009). Early hominids also appear to have lacked an African ape-like, funnel-shaped thoracic cage (Latimer, Lovejoy, Spurlock, & Haile-Selassie, 2016). The most complete scapulae of *Australopithecus* also show much more affinity with *Homo* (Melillo, 2016) and *Gorilla* than with *Pan*, further suggesting a cautious ABQ hominoid LCA. Taken together, this suggests that the human-African ape LCA was a cautious, clambering ABQ, from which chimpanzees have diverged precipitously to become substantially more suspensory, a likely product of their high canopy ripe fruit feeding strategy.

ACKNOWLEDGMENTS

We would like to thank Yohannes Haile-Selassie and Lymen Jellema of the Cleveland Museum of Natural History, Bruce Patterson and Bill Stanley of the Field Museum of Natural History and Richard W. Thorington and Linda Gordon of the National Museum of Natural History for allowing access to specimens in their care. We also thank two anonymous reviewers, whose comments greatly improved the manuscript.

Notes

[1] Hominid is used here to refer to humans and their ancestors after the lineage split from that leading to chimpanzees.

REFERENCES

Alba, D. M., Almécija, S., Casanovas-Vilar, I., Méndez, J. M., & Moyà-Solà, S. (2012). A partial skeleton of the fossil great ape *Hispanopithecus laietanus* from Can Feu and the mosaic evolution of crown-hominoid positional behaviors. *PLoS One*, *7*, e39617.

Alemseged, Z., Spoor, F., Kimbel, W. H., Bobe, R., Geraads, D., Reed, D., & Wynn, J. G. (2006). A juvenile early hominin skeleton from Dikika, Ethiopia. *Nature*, *443*, 296–301.

Andrews, P., & Groves, C. P. (1976). Gibbons and brachiation. In Rumbaugh, D. M. (Ed.), *Gibbon and siamang* (pp. 167–218). Basel: S. Karger.

Andrews, P., & Martin, L. (1987). Cladistic relationships of extant and fossil hominoids. *Journal of Human Evolution*, *16*, 101–118.

Ankel, F. (1972). Vertebral morphology of fossil and extant primates. In Tuttle, R. H. (Ed.), *The functional and evolutionary biology of primates* (pp. 223–240). Chicago, IL: Aldine.

Ashton, E. H., Healy, M. J. R., Oxnard, C. E., & Spence, T. F. (1965). The combination of locomotor features of the primate shoulder girdle by canonical axis. *Journal of Zoology (London)*, *147*, 406–429.

Ashton, E. H., & Oxnard, C. E. (1961). Muscular variation in the primate shoulder. *Journal of Anatomy*, *95*, 618–619.

Ashton, E. H., & Oxnard, C. E. (1962). Functional variation in the primate shoulder girdle. *Journal of Anatomy*, *96*, 415.

Ashton, E. H., & Oxnard, C. E. (1963). Locomotor patterns in primates. *Proceedings of the Zoological Society of London*, *142*, 1–28.

Ashton, E. H., & Oxnard, C. E. (1964). Functional adaptations in the primate shoulder girdle. *Proceedings of the Zoological Society of London*, *145*, 49–66.

Ashton, E. H., Oxnard, C. E., & Spence, T. F. (1965). Scapular shape and primate classification. *Proceedings of the Zoological Society of London*, *142*, 125–142.

Aubin, J., Lemieux, M., Moreau, J., Lapointe, J., & Jeannotte, L. (2002). Cooperation of *Hoxa5* and *Pax1* genes during formation of the pectoral girdle. *Developmental Biology*, *244*, 96–113.

Aubin, J., Lemieux, M., Tremblay, M., Behringer, R. R., & Jeannotte, L. (1998). Transcriptional interferences at the *Hoxa4/Hoxa5* locus: Importance of correct *Hoxa5* expression for the proper specification of the axial skeleton. *Developmental Dynamics*, *212*, 141–156.

Badoux, D. M. (1974). An introduction to biomechanical principles in primate locomotion and structure. In Jenkins, F.A. (Ed.), *Primate locomotion* (pp. 1–43). New York, NY: Academic Press.

Begun, D. R. (2007). How to identify (as opposed to define) a homoplasy: Examples from fossil and living great apes. *Journal of Human Evolution*, *52*, 559–572.

Begun, D. R., Teaford, M. F., & Walker, A. (1994). Comparative and functional anatomy of *Proconsul* phalanges from the Kaswanga Primate Site, Rusinga Island, Kenya. *Journal of Human Evolution*, *26*, 89–165.

Bello-Hellegouarch, G., Potau, J. M., Arias-Martorell, J., Pastor, J. F., & Pérez-Pérez, A. (2013). A comparison of qualitative and quantitative methodological approaches to characterizing the dorsal side of the scapula in Hominoidea and its relationship to locomotion. *International Journal of Primatology*, *34*, 315–336.

Benefit, B. R., & McCrossin, M. L. (1995). Miocene hominoids and hominid origins. *Annual Review of Anthropology*, *24*, 237–256.

Benton, R. S. (1967). Morphological evidence for adaptations within the expaxial region of the primates. In Vagtbord, H. (Ed.), *The baboon in medical research* (pp. 201–216). Austin: University of Texas Press.

Berger, L. R., de Ruiter, D. J., Churchill, S. E., Schmid, P., Carlson, K. J., Dirks, P. H. G. M., & Kibii, J. M. (2010). *Australopithecus sediba*: A new species of *Homo*-like Australopith from South Africa. *Science*, *328*, 195–204.

Boczek-Funcke, A., Kuhtz-Buschbeck, J. P., & Illert, M. (1996). Kinematic analysis of the cat shoulder girdle during treadmill locomotion: An X-ray study. *European Journal of Neuroscience*, *8*, 261–272.

Boulet, A. M., Moon, A. M., Arenkiel, B. R., & Capecchi, M. R. (2004). The roles of Fgf4 and Fgf8 in limb bud initiation and outgrowth. *Developmental Biology*, *273*, 361–372.

Cant, J. G. H. (1986). Locomotion and feeding postures of spider and howling monkeys: Field study and evolutionary interpretation. *Folia Primatologica*, *46*, 1–14.

Capellini, T. D., Di Giacomo, G., Salsi, V., Brendolan, A., Ferretti, E., Srivastava, D., … Selleri, L. (2006). *Pbx1/Pbx2* requirement for distal limb patterning is mediated by the hierarchical control of Hox gene spatial distribution and Shh expression. *Development*, *133*, 2263–2273.

Capellini, T. D., Vaccari, G., Ferretti, E., Fantini, S., He, M., Pellegrini, M. … Zappavigna V. (2010). Scapula development is governed by genetic interactions of *Pbx1* with its family members and with *Emx2* via their cooperative control of *Alx1*. *Development*, *137*, 2559–2569.

Carrier, D. R., Deban, S. M., & Fischbein, T. (2006). Locomotor function of the pectoral girdle 'muscular sling' in trotting dogs. *Journal of Experimental Biology*, *209*, 2224–2237.

Cartmill, M., & Milton, K. (1977). The lorisiform wrist joint and the evolution of "brachiating" adaptations in the Hominoidea. *American Journal of Physical Anthropology*, *47*, 249–272.

Chan, L. K. (2007). Scapular position in primates. *Folia Primatologica*, *78*, 19–35.

Chan, L. K. (2014). The thoracic shape of hominoids. *Anatomy Research International*, *2014*, 8 pages.

Churchill, S. E., Holliday, T. W., Carlson, K. J., Jashashvili, T., Macias, M. E., Mathews, S., … Berger, L. R. (2013). The Upper Limb of *Australopithecus sediba*. *Science*, *340*, 1233477–1–6.

Clark, W. E. L. G. (1959). *The antecedents of man*. New York, NY: Harper.

Crompton, R. H., Vereecke, E. E., & Thorpe, S. K. S. (2008). Locomotion and posture from the common hominoid ancestor to fully modern hominins, with special reference to the last common ancestor. *Journal of Anatomy*, *212*, 501–543.

Doran, D. M. (1997). Ontogeny of locomotion in mountain gorillas and chimpanzees. *Journal of Human Evolution*, *32*, 323–344.

Doyle, W. J., Siegel, M. I., & Kimes, K. R. (1980). Scapular correlates of muscle morphology in *Macaca mulatta*. *Acta Anatomica*, *106*, 493–501.

Ehehalt, F., Wang, B., Christ, B., Patel, K., & Huang, R. (2004). Intrinsic cartilage-forming potential of dermomyotomal cells requires

ectodermal signals for the development of the scapula blade. *Anatomy and Embryology*, *208*, 431–437.

English, A. W. (1978). Functional analysis of the shoulder girdle of cats during locomotion. *Journal of Morphology*, *156*, 279–292.

Erikson, G. E. (1963). Brachiation in new world monkeys and in anthropoid apes. *Symposium of the Zoological Society of London*, *10*, 135–163.

Fleagle, J. G. (1983). Locomotor adaptations of Oligocene and Miocene hominoids and their phyletic implications. In Ciochon, R. L., & Corruccini, R. S. Eds.), *New interpretations of ape and human ancestry* (pp 301–324). New York, NY: Plenum Press.

Fleagle, J. G., & Mittermeier, R. A. (1980). Locomotor behavior, body size, and comparative ecology of seven Surinam monkeys. *American Journal of Physical Anthropology*, *52*, 301–314.

Fomenou, M. D., Scaal, M., Stockdale, F. E., Christ, B., & Huang, R. (2005). Cells of all somitic compartments are determined with respect to segmental identity. *Developmental Dynamics*, *233*, 1386–1393.

Gebo, D. L. (1992). Locomotor and postural behavior in *Alouatta palliata* and *Cebus capucinus*. *American Journal of Primatology*, *26*, 277–290.

Gebo, D. L., & Chapman, C. A. (1995). Positional behavior in five sympatric old world monkeys. *American Journal of Physical Anthropology*, *97*, 49–76.

Gould, S. J., & Lewontin, R. C. (1979). The spandrels of San Marco and the Panglossian paradigm: A critique of the adaptationist programme. *Proceedings of the Royal Society of London Series B*, *205*, 581–598.

Green, D. J. (2013). Ontogeny of the hominoid scapula: The influence of locomotion on morphology. *American Journal of Physical Anthropology*, *152*, 239–260.

Green, D. J., & Alemseged, Z. (2012). *Australopithecus afarensis* scapular ontogeny, function, and the role of climbing in human evolution. *Science*, *338*, 514–517.

Green, D. J., Hamrick, M. W., & Richmond, B. G. (2011). The effects of hypermuscularity on shoulder morphology in myostatin-deficient mice. *Journal of Anatomy*, *218*, 544–557.

Green, D. J., Spiewak, T. A., Seitelman, B., & Gunz, P. (2016). Scapular shape of extant hominoids and the African ape/modern human last common ancestor. *Journal of Human Evolution*, *94*, 1–12.

Gregory, W. K. (1912). Notes on the principles of quadrupedal locomotion and on the mechanism of the limbs in hoofed animals. *Annals of the New York Academy of Sciences*, *22*, 267–294.

Haile-Selassie, Y., Latimer, B. M., Alene, M., Deino, A. L., Gibert, L., Melillo, S. M., … Lovejoy, C. O. (2010). An early *Australopithecus afarensis* postcranium from Woranso-Mille, Ethiopia. *Proceedings of the National Academy of Sciences of the United States of America*, *107*, 12121–12126.

Harrison, T. (1986). A reassessment of the phylogenetic relationships of *Oreopithecus bambolii* Gervais. *Journal of Human Evolution*, *15*, 541–583.

Harrison, T. (1987). The phylogenetic relationships of the early catarrhine primates: A review of the current evidence. *Journal of Human Evolution*, *16*, 41–80.

Harrison, T. (2002). Late Oligocene to middle Miocene catarrhines from Afro-Arabia. In Hartwig, W. C. (Ed.), *The primate fossil record* (pp. 311–338). Cambridge: Cambridge University Press.

Harrison, T., & Rook, L. (1997). Enigmatic anthropoid or misunderstood ape? In Begun, D. R., Ward, C. V., & Rose, M. D. (Eds.), *Function, phylogeny, and fossils: Miocene hominoid evolution and adaptations* (pp. 327–362). New York, NY: Plenum Press.

Hildebrand, M. (1959). Motions of the running cheetah and horse. *Journal of Mammology*, *40*, 481–495.

Huang, R., Christ, B., & Patel, K. (2006). Regulation of scapula development. *Anatomy and Embryology 221*, S65–S71.

Huang, R., Zhi, Q., Patel, K., Wilting, J., & Christ, B. (2000). Dual origin and segmental organisation of the avian scapula. *Development*, *127*, 3789–3794.

Hübler, M., Molineaux, A. C., Keyte, A., Schecker, T., & Sears, K. E. (2013). Development of the marsupial shoulder girdle complex: A case study in *Monodelphis domestica*. *Evolution & Development*, *15*, 18–27.

Hunt, K. D. (1991). Mechanical implications of chimpanzee positional behavior. *American Journal of Physical Anthropology*, *86*, 521–536.

Inman, V. T., Saunders, J. B. D. M., & Abbott, L. C. (1944). Observations on the function of the shoulder joint. *Journal of Bone & Joint Surgery*, *26*, 1–30.

Inouye, S. E., & Shea, B. T. (1997). What's your angle? Size correction and bar-glenoid orientation in "Lucy" (A.L. 288-1). *International Journal of Primatology*, *18*, 629–650.

Jenkins, F. A., & Weijs, W. A. (1979). The functional anatomy of the shoulder in the *Virginia opossum* (*Didelphis virginiana*). *Journal of Zoology (London)*, *188*, 379–410.

Jolly, C. J. (1967). The evolution of the baboons. In Vagtborg, H. (Ed.), *The baboon in medical research* (pp. 23–50) Austin: University of Texas Press.

Jungers, W. L. (1991). Scaling of postcranial joint size in hominoid primates. *Human Evolution*, *6*, 391–399.

Jungers, W. L., & Stern, J. T. (1984). Kinesiological aspects of brachiation in lar gibbons. In Preuschoft, H., Chivers, D. J., Brockelman, W. Y., & Creel, N. (Eds.), *The lesser apes* (pp. 119–134). Edinburgh: Edinburgh University Press.

Kagaya, M., Ogihara, N., & Nakatsukasa, M. (2008). Morphological study of the anthropoid thoracic cage: Scaling of thoracic width and an analysis of rib curvature. *Primates*, *49*, 89–99.

Karaharju, E. O., Ryöppy, S. A., & Mäkinen, R. J. (1976). Remodelling by asymmetrical epiphysial growth. *Journal of Bone & Joint Surgery*, *58*, 122–126.

Keith, A. (1923). Man's posture: Its evolution and disorders. *British Medical Journal*, *1*, 451–454, 499–502, 545–548, 587–590, 624–626, 669–672.

Kimes, K. R., Doyle, W. J., & Siegel, M. I. (1979). Scapular correlates of muscle morphology in *Papio cynocephalus*. *Acta Anatomica*, *104*, 414–420.

Kivell, T. L., Barros, A., & Smaers, J. (2013). Different evolutionary pathways underlie the morphology of wrist bones in hominoids. *BMC Evolutionary Biology*, *13*, 229.

Kuijper, S., Beverdam, A., Kroon, C., Brouwer, A., Candille, S., Barsh, G., & Meijlink, F. (2005). Genetics of shoulder girdle formation: Roles of Tbx15 and aristaless-like genes. *Development*, *132*, 1601–1610.

Larson, S. G. (1993). Functional morphology of the shoulder in primates. In Gebo, D. L. (Ed.), *Postcranial adaptation in nonhuman primates* (pp. 45–69). DeKalb: Northern Illinois University Press.

Larson, S. G. (1998). Parallel evolution in the hominoid trunk and forelimb. *Evolutionary Anthropology*, *6*, 87–99.

Larson, S. G. (2015). Rotator cuff muscle size and the interpretation of scapular shape in primates. *Journal of Human Evolution*, *80*, 96–106.

Larson, S. G., & Stern, J. T. (1986). EMG of scapulohumeral muscles in the chimpanzee during reaching and "arboreal" locomotion. *American Journal of Anatomy*, *176*, 171–190.

Larson, S. G., & Stern, J. T. (2013). Rotator cuff muscle function and its relation to scapular morphology in apes. *Journal of Human Evolution*, *65*, 391–403.

Larson, S. G., Stern, J. T., & Jungers, W. L. (1991). EMG of serratus anterior and trapezius in the chimpanzee: Scapular rotators revisited. *American Journal of Physical Anthropology*, *85*, 71–84.

Latimer, B. M., Lovejoy, C. O., Spurlock, L., & Haile-Selassie, Y. (2016). The thoracic cage of KSD-VP-1/1. In Haile-Selassie, Y. & Su, F. D., (Eds.), *The postcranial anatomy of Australopithecus afarensis: New insights from KSD-VP-1/1* (pp. 143–153). Dordrecht: Springer Netherlands.

Lovejoy, C. O. (2007). The natural history of human gait and posture. Part 3: The knee. *Gait & Posture*, *25*, 325–341.

Lovejoy, C. O., Cohn, M. J., & White, T. D. (1999). Morphological analysis of the mammalian postcranium: A developmental perspective. *Proceedings of the National Academy of Sciences of the United States of America*, *96*, 13247–13252.

Lovejoy, C. O., Cohn, M. J., & White, T. D. (2000). The evolution of mammalian morphology: A developmental perspective. In O'Higgins, P., & Cohn, M. J., (Eds.), *Development, growth and evolution* (pp. 41–55). San Diego, CA: Academic Press.

Lovejoy, C. O., Simpson, S. W., White, T. D., Asfaw, B., & Suwa, G. (2009). Careful climbing in the Miocene: The forelimbs of *Ardipithecus ramidus* and humans are primitive. *Science*, *326*, 70.

Lovejoy, C. O., Suwa, G., Simpson, S. W., Matternes, J. H., & White, T. D. (2009). The great divides: *Ardipithecus ramidus* reveals the postcranium of our last common ancestor with African apes. *Science*, *326*, 100–106.

Matsuoka, T., Ahlberg, P. E., Kessaris, N., Iannarelli, P., Dennehy, U., Richardson, W. D., … Koentges, G. (2005). Neural crest origins of the neck and shoulder. *Nature*, *436*, 347–355.

Melillo, S. M. (2016). The shoulder girdle of KSD-VP-1/1. In Haile-Selassie, Y., & Su, F. D. (Eds.), *The postcranial anatomy of Australopithecus afarensis: New insights from KSD-VP-1/1* (pp. 113–141) Dordrecht: Springer Netherlands.

Mensforth, R. P., Latimer, B., & Senturian, S. (1990). A review of the functional significance of the A.L. 288 axilloglenoid angle. *American Journal of Physical Anthropology*, *81*, 267–268.

Midford, P. E., Garland, T., & Maddison, W. P. (2009). PDAP:PDTREE package for Mesquite, version 1.15. http://mesquiteproject.org/pdap_mesquite/

Miller, R. A. (1932). Evolution of the pectoral girdle and forelimb in the primates. *American Journal of Physical Anthropology*, *17*, 1–56.

Min, H., Danilenko, D. M., Scully, S. A., Bolon, B., Ring, B. D., Tarpley, J. E., … Simonet, W. S. (1998). *Fgf-10* is required for both limb and lung development and exhibits striking functional similarity to *Drosophila branchless*. *Genes & Development*, *12*, 3156–3161.

Mittermeier, R. A., & Fleagle, J. G. (1976). The locomotor and postural repertoires of *Ateles geoffroyi* and *Colobus guereza*, and a reevaluation of the locomotor category semibrachiation. *American Journal of Physical Anthropology*, *45*, 235–256.

Mivart, S. G. (1867). On the appendicular skeleton of the primates. *Philosophical Transactions of the Royal Society (London)*, *157*, 299–429.

Moeller, C., Swindell, E. C., Kispert, A., & Eichele, G. (2003). Carboxypeptidase Z (CPZ) modulates Wnt signaling and regulates the development of skeletal elements in the chicken. *Development*, *130*, 5103–5111.

Morbeck, M. E. (1977). Positional behavior, selective use of habitat substrate and associated non-positional behavior in free-ranging *Colobus guereza* (Rüppel, 1835). *Primates*, *18*, 35–58.

Moyà-Solà, S., Köhler, M., Alba, D. M., Casanovas-Vilar, I., & Galindo, J. (2004). *Pierolapithecus catalaunicus*, a new Middle Miocene great ape from Spain. *Science*, *306*, 1339–1344.

Napier, J. R., & Napier, P. H. (1967). *A handbook of living primates*. London: Academic Press.

Oliver, G., de Robertis, E., Wolpert, L., & Tickle, C. (1990). Expression of a homeobox gene in the chick wing bud following application of retinoic acid and grafts of polarizing region tissue. *EMBO Journal*, *9*, 3093–3099.

Osborn, H. F. (1927). Recent discoveries relating to the origin and antiquity of man. *Science*, *65*, 481–488.

Oxnard, C. E. (1963). Locomotor adaptations in the primate forelimb. *Symposium of the Zoological Society of London*, *10*, 165–182.

Oxnard, C. E. (1967). The functional morphology of the primate shoulder as revealed by comparative anatomical, osteometric and discriminant function techniques. *American Journal of Physical Anthropology*, *26*, 219–240.

Oxnard, C. E. (1969). Evolution of the human shoulder: Some possible pathways. *American Journal of Physical Anthropology*, *30*, 319–332.

Pellegerini, M., Pantano, S., Fumi, M. P., Lucchini, F., & Forabosco, A. (2001). Agenesis of the scapula in *Emx2* homozygous mutants. *Developmental Biology*, *232*, 149–156.

Pilbeam, D. (2002). Perspectives on the Miocene Hominoidea. In Hartwig, W. C. (Ed.), *The primate fossil record* (pp. 303–310). Cambridge: Cambridge University Pression.

Preuschoft, H., Hohn, B., Scherf, H., Schmidt, M., Krause, C., & Witzel, U. (2010). Functional analysis of the primate shoulder. *International Journal of Primatology*, *31*, 301–320.

Pröls, F., Ehehalt, F., Rodriguez-Niedenführ, M., He, L., Huang, R., & Christ, B. (2004). The role of *Emx2* during scapula formation. *Developmental Biology*, *275*, 315–324.

Rallis, C., Bruneau, B. G., Del Buono, J., Seidman, C. E., Seideman, J. G., Nissim, S., … Logan, M. P. O. (2003). *Tbx5* is required for forelimb bud formation and continued outgrowth. *Development*, *130*, 2741–2751.

Reno, P. L. (2014). Genetic and developmental basis for parallel evolution and its significance for hominoid evolution. *Evolutionary Anthropology*, *23*, 188–200.

Roberts, D. (1974). Structure and function of the primate scapula. In Jenkins, F. A. (Ed.), *Primate locomotion* (pp. 171–200). New York, NY: Academic Press.

Rose, M. D. (1994). Quadrupedalism in some Miocene catarrhines. *Journal of Human Evolution*, *26*, 387–411.

Rose, M. D. (1997). Functional and phylogenetic features of the forelimb in Miocene hominoids. In Begun, D. R., Ward, C. V., & Rose, M. D. (Eds.), *Function, phylogeny, and fossils* (pp. 79–100). New York, NY: Plenum Press.

Rosenberger, A. L., & Strier, K. B. (1989). Adaptive radiation of the ateline primates. *Journal of Human Evolution*, *18*, 717–750.

Schultz, A. H. (1930). The skeleton of the trunk and limbs of higher primates. *Human Biology*, *2*, 303–438.

Schultz, A. H. (1931). Man as a primate. *Scientific Monthly*, *33*, 385–412.

Schultz, A. H. (1950). The specializations of man and his place among the catarrhine primates. *Cold Spring Harbor Symposia on Quantitative Biology*, *15*, 37–53.

Schultz, A. H. (1956). Postembryonic age changes. *Primatologia*, *1*, 887–964.

Schultz, A. H. (1961). Vertebral column and thorax. *Primatologia*, *5*, 1–66.

Senut, B. (1980). New data on the humerus and its joints in Plio-Pleistocene hominids. *Collegium Antropologicum*, *4*, 87–93.

Smith, R. J., & Jungers, W. L. (1997). Body mass in comparative primatology. *Journal of Human Evolution*, *32*, 523–559.

Stern, J. T. (1975). Before bipedality. *Yearbook of Physical Anthropology*, *19*, 59–68.

Stern, J. T., & Susman, R. L. (1983). The locomotor anatomy of *Australopithecus afarensis*. *American Journal of Physical Anthropology*, *60*, 279–317.

Stern, J. T., Wells, J. P., Jungers, W. L., & Vangor, A. K. (1980). An electromyographic study of serratus anterior in Atelines and *Alouatta*: Implications for hominoid evolution. *American Journal of Physical Anthropology*, *52*, 323–334.

Stern, J. T., Wells, J. P., Vangor, A. K., & Fleagle, J. G. (1977). Electromyography of some muscles of the upper limb in *Ateles* and *Lagothrix*. *Yearbook of Physical Anthropology*, *20*, 498–507.

Timmons, P. M., Wallin, J., Rigby, P. W. J., & Balling, R. (1994). Expression and function of *Pax1* during development of the pectoral girdle. *Development*, *120*, 2773–2785.

Tuttle, R. H., & Basmajian, J. V. (1977). Electromyography of pongid shoulder muscles and hominoid evolution I: Retractors of the humerus and rotators of the scapula. *Yearbook of Physical Anthropology*, *20*, 491–497.

Tuttle, R. H., & Basmajian, J. V. (1978). Electromyography of pongid shoulder muscles II: Deltoid, rhomboid, and "rotator cuff". *American Journal of Physical Anthropology*, *49*, 47–56.

Valasek, P., Theis, S., Krejci, E., Grim, M., Maina, F., Shwartz, Y., … Patel, K. (2010). Somitic origin of the medial border of the mammalian scapula and its homology to the avian scapula blade. *Journal of Anatomy*, *216*, 482–488.

Walker, A. (1997). *Proconsul* function and phylogeny. In Begun, D. R., Ward, C. V., & Rose, M. D. (Eds.), *Function, phylogeny, and fossils* (pp. 209–224) New York, NY: Plenum Press.

Wang, B., Pu, Q., De, R., Patel, K., Christ, B., Wilting, J., & Huang, R. (2010). Commitment of chondrogenic precursors of the avian scapula takes place after epithelial-mesenchymal transition of the dermomyotome. *BMC Developmental Biology*, *10*, 91.

Ward, C. V. (1993). Torso morphology and locomotion in *Proconsul nyanzae*. *American Journal of Physical Anthropology*, *92*, 291–328.

Ward, C. V. (2007). Postcranial and locomotor adaptations of hominoids. In Henke, W., & Tattersall, I., (Eds.), *Handbook of paleoanthropology* (pp. 1011–1030). Berlin: Springer.

Ward, C. V., Walker, A., & Teaford, M. F. (1991). *Proconsul* did not have a tail. *Journal of Human Evolution*, *21*, 215–220.

Ward, C. V., Walker, A., Teaford, M. F., & Odhiambo, I. (1993). Partial skeleton of *Proconsul nyanzae* from Mfangano Island, Kenya. *American Journal of Physical Anthropology*, *90*, 77–111.

Washburn, S. L. (1950). The analysis of primate evolution with particular reference to the origin of man. *Cold Spring Harbor Symposia on Quantitative Biology*, *15*, 67–78.

Waters, P. M., Smith, G. R., & Jaramillo, D. (1998). Glenohumeral deformity secondary to brachial plexus birth palsy. *Journal of Bone & Joint Surgery*, *80*, 668–677.

White, T. D., Lovejoy, C. O., Asfaw, B., Carlson, J. P., & Suwa, G. (2015). Neither chimpanzee nor human, *Ardipithecus* reveals the surprising ancestry of both. *Proceedings of the National Academy of Sciences of the United States*, *112*, 4877–4884.

Whitehead, P. F., & Larson, S. G. (1994). Shoulder motion during quadrupedal walking in *Cercopithecus aethiops*: Integration of cineradiographic and electromyographic data. *Journal of Human Evolution*, *26*, 525–544.

Wilm, B., Dahl, E., Peters, H., Balling, R., & Imai, K. (1998). Targeted disruption of *Pax1* defines its null phenotype and proves haploinsufficiency. *Proceedings of the National Academy of Sciences of the United States*, *95*, 8692–8697.

Xu, B., Hrycaj, S. M., McIntyre, D. C., Baker, N. E., Takeuchi, J. K., Jeannotte, L., … Wellik, D. M. (2013). *Hox5* interacts with *Plzf* to restrict *Shh* expression in the developing forelimb. *Development*, *110*, 19438–19443.

Young, N. M. (2003). A reassessment of living hominoid postcranial variability: implications for ape evolution. *Journal of Human Evolution*, *43*, 441–464.

Young, N. M. (2004). Modularity and integration in the hominoid scapula. *Journal of Experimental Zoology Part B: Molecular and Developmental Evolution*, *302B*, 226–240.

Young, N. M., Capellini, T. D., Roach, N. T., & Alemseged, Z. (2015). Fossil hominin shoulders support an African ape-like last common ancestor of humans and chimpanzees. *Proceedings of the National Academy of Sciences of the United States*, *112*, 11829–11834.

Zihlman, A. L., McFarland, R. K., & Underwood, C. E. (2011). Functional anatomy and adaptation of male gorillas (*Gorilla gorilla gorilla*) with comparison to male orangutans (*Pongo pygmaeus*). *Anatomical Record*, *294*, 1842–1855.

SUPPORTING INFORMATION

Additional Supporting Information may be found in the online version of this article.

How to cite this article: Selby MS, and Lovejoy CO. Evolution of the hominoid scapula and its implications for earliest hominid locomotion. *Am J Phys Anthropol.* 2017;162:682–700. doi:10.1002/ajpa.23158.

Evolutionary Anthropology 16:172–187 (2007)

Evolutionary Transformation of the Hominin Shoulder

SUSAN G. LARSON

Despite the fact that the shoulder is one of the most extensively studied regions in comparative primate and human anatomy, two recent fossil hominin discoveries have revealed quite unexpected morphology. The first is a humerus of the diminutive fossil hominin from the island of Flores, *Homo floresiensis* (LB1/50), which displays a very low degree of humeral torsion[1,2] (Fig. 1; see Box 1). Modern humans have a high degree of torsion and, since this is commonly viewed as a derived feature shared with hominoids,[3–6] one would expect all fossil hominins to display high humeral torsion. The second is the recently discovered *Australopithecus afarensis* juvenile scapula DIK-1-1 from Dikika, Ethiopia, which seems to most closely resemble those of gorillas.[7] This specimen is the first nearly complete scapula known for an early hominin and, given the close phylogenetic relationship between humans and chimpanzees suggested by molecular studies,[8–13] one would have expected more similarity to chimpanzees among extant hominoids.

These fossils do not fit into current perspectives that view evolution of the human pectoral girdle and shoulder as a more or less direct transformation from an essentially ape-like hominid common ancestral condition through an early hominin transitional stage consisting of a mixture of primitive and derived features that was replaced by an essentially modern human configuration with the appearance of early *Homo*. If these fossils indicate that this was not the sequence of events, then what was the course of evolutionary transformation of the hominin shoulder? To address this question, I present the following overview of what is known about fossil hominin pectoral girdle and shoulder morphology, and suggest that rather than undergoing a direct change from the primitive hominid condition to that of modern humans, the hominin shoulder passed through unexpected intermediate stages, and that the configuration seen in modern humans is actually relatively recent.

EARLY HOMININS

Although several fossil clavicular specimens are known for early hominins (Table 1), most are only small segments and attempts to interpret them have been limited. The most complete specimen is A.L. 333x-6/9,[14] attributed to *A. afarensis*, which is mainly missing a portion of its sternal end (Fig. 2). Ohman[15] observed that A.L. 333x-6/9 is distinct from other hominoids in the orientation of its lateral end (on frontal view) and in the position of the deltoid attachment area, features which he interpreted as evidence of descent of the hominin shoulder by three to four million years ago. However, in his analysis of clavicular shape in primates, Voisin[16] reports that the uniquely low shoulder position in humans is indicated, on dorsal view, by a distinctive curvature of the medial rather than the lateral end of the human clavicle. Although A.L. 333x-6/9 was not included in his analysis, the fact that it apparently does not display this distinctive morphology of the medial end suggests that *A. afarensis* maintained a high shoulder position. More recently, Partridge and coworkers[17] have described a partial clavicle from Jacovec Cavern at Sterkfontein (StW 606) attributed to *Australopithecus* sp that displays a pronounced conoid tubercle like chimpanzee clavicles and unlike those of other hominins, including modern humans. This suggests that there may be some diversity in clavicular morphology among early hominins. In general, however, these clavicular fossils have received limited attention and have contributed correspondingly little to our understanding of pectoral girdle or shoulder form and function in early hominins.

Most interpretations of early hominin shoulder morphology have been based on two scapular fossil fragments, Sts 7[18] attributed to *A. africanus,* and A.L. 288-11[19] attributed to *A. afarensis* (Fig. 3). The feature that has received the most attention in functional analyses of these fossils is the orientation of the glenoid fossa. In hominoid primates the glenoid faces cranially, reflecting the importance of overhead limb postures, while in modern humans the fossa faces more laterally, reflecting the typical lowered position of the upper limb. Several workers have measured the axillo-glenoid angle of Sts 7,[20–23] and while the reported values vary, ranging between 103° and 125°, all agree that the glenoid faced more cranially than in modern humans,

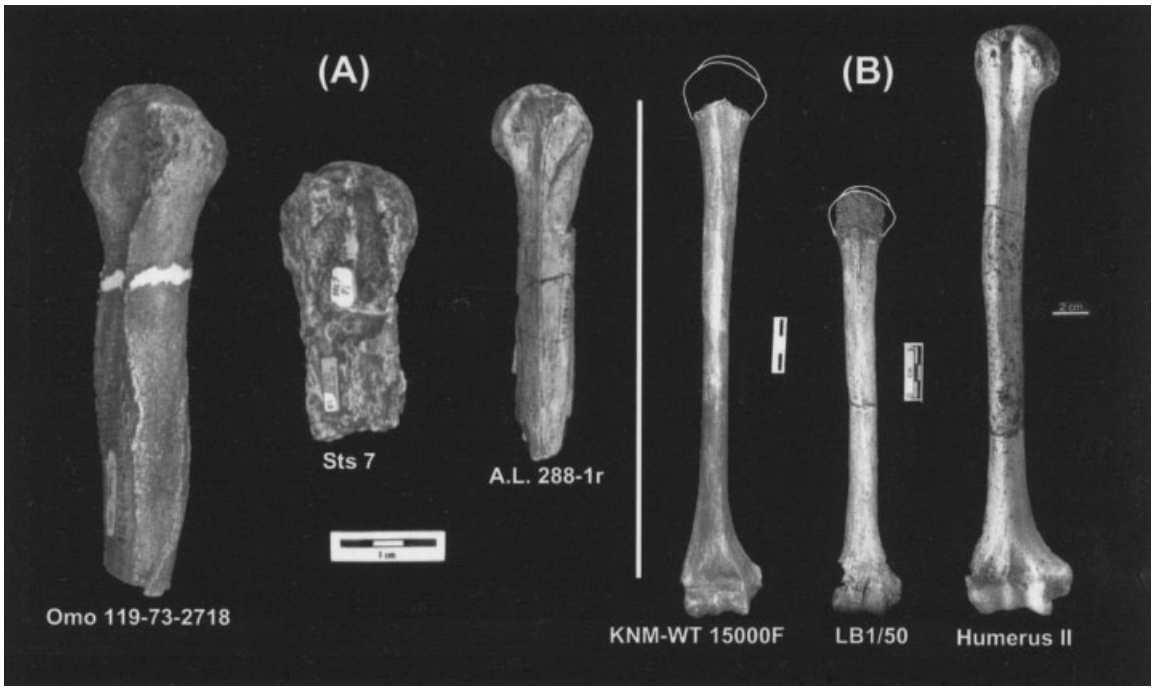

Figure 1. Anterior views of hominin fossil humeri. (A) Casts of early hominin proximal humeri Omo 119-73-2718 (left side), Sts 7 (right side), and A.L. 288-1r (left side). (B) KNM-WT 15000F (*H. erectus*), LB1/50 (*H. floresiensis*), and humerus II (*H. heidelbergensis*), all right sides. Photos of KNM-WT 15000F (cast) and LB1/50 (original material) were taken by the author. Image of humerus II is from Carretero, Arsuaga, and Lorenzo[58] and is used with permission of the author. (A) and (B) are of very different scales; the three images in (B) are only approximately to the same scale. White outlines have been added to KNM-WT 15000F and LB1/50 as rough indications of missing portions of proximal epiphyses.

suggesting retention of some arboreal adaptations in this early hominin. Stern and Susman[24] attempted to assess the orientation of the glenoid fossa of A.L. 288-11 relative to the ventral bar, a scapular buttress lying medial to the axillary border, since little of the axillary border is preserved in this specimen. They concluded that the glenoid of this scapular fragment also faced more cranially than in modern humans (Fig. 4). Although Inouye and Shea[25] argued that the cranial orientation of the glenoid of A.L. 288-11 is due to its small size, they based their analysis on ontogenetic scaling of the bar-glenoid angle in African apes and modern humans, thus confounding age-related changes with possible size effects. The *A. afarensis* juvenile scapula DIK-1-1 also has a cranially directed glenoid fossa.[7]

The size and shape of the coracoid process is another feature of the Sts 7 scapula that has received attention in the literature.[20–23,26,27] The coracoid is frequently described as displaying a large area of attachment for the short head of the biceps brachii, which has been interpreted as reflecting a brachiating adaptation. However, Vrba[23] reported that part of the coracoid origin for the short head of the biceps is missing from Sts 7. Vrba speculated that the source of this misconception about the coracoid attachment area for biceps brachii comes from a mis-

TABLE 1. Early Hominin Pectoral Girdle Material

	Ardipithecus	*A. afarensis*	*A. africanus*	*Australopithecus* sp.	*Homo habilis*
Clavicle	STD-VP-2/893	A.L. 333x-6/9 A.L. 333-94 A.L. 288-lbz A.L. 438-lv L.H. 21P	StW 431 StW 582	StW 606	O.H. 48 KNM-ER 3735
Scapula		A.L. 288-11 DIK-1-1	Sts 7 StW 366 StW 431		
Proximal humerus	ARA-VP-7/2	A.L. 288-1r A.L. 333-87 A.L. 333-107 KNM-BC 1745	Sts 7 StW 328 StW 517	Omo 119-73-2718 KNM-ER 1473	

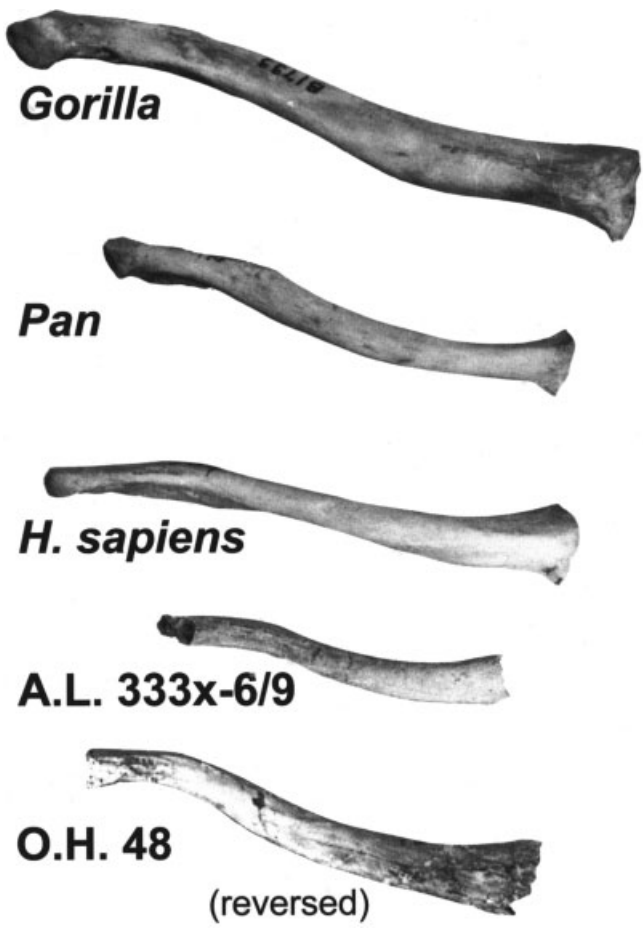

Figure 2. Anterior views of right clavicles. Image has been modified from Ohman,[15] and is used with permission of the author.

reading or misquotation of Broom, Robinson, and Schepers,[18] who described a well-developed attachment area for biceps, but meant the long head from the supraglenoid tubercle. Vrba[23] noted that the coracoid of Sts 7 displays a prominent dorsolateral tubercle placed somewhat more laterally than in modern humans, features which she interpreted as reflecting a scapula positioned high on a funnel-shaped thorax with an oblique clavicle, as in modern great apes.

Larson[28] described several new functional features of primate scapulae, including a few that could be measured on fossils, and reported that while the angle between the base of the scapular spine and the axillary border did not sort locomotor groups well, it did distinguish humans from most other taxa. As shown in Figure 5, both Sts 7 and A.L. 288-11 again group with apes, not modern humans. According to Alemseged and coworkers,[7] the scapular spine of DIK-1-1 is also oblique.

The proximal humeri known from early hominins have received comparatively less attention (Fig. 1). To the degree that it can be determined, the humeral heads of all known early hominin humeri are elliptical like those of humans rather than spherical as in modern apes. In addition, their intertubercular grooves are somewhat shallow rather than deep and tunnel-like, although the latter feature is actually characteristic only of the African apes. Broom, Robinson, and Schepers[18] describe the Sts 7 proximal humerus as basically humanlike, although the tubercles are somewhat distinct, with a more prominent lesser tubercle than typically is seen in modern humans or great apes. The Chemeron proximal humeral fragment KNM-BC 1945 and the A.L. 288-1r proximal humerus are also described as displaying relatively large lesser tubercles.[19,29]

Larson[28] measured the width and length of the subscapular insertion facet on the lesser tubercle of primates and found that hominoids were distinct in displaying relatively long and narrow facets, which she related to greater functional differentiation within subscapularis, implying more versatility in controlling glenohumeral motion. As shown in Figure 6, the human subscapular facet is not quite as long as that in apes. The human mean is significantly different from those of either African ape, with $p < 0.001$, and Sts 7 is once again more similar to apes than to humans (different from humans with $p < 0.05$). Robinson[22] noted that, unlike most modern humans, Sts 7 displays a prominent ridge on the greater tubercle separating the facets for attachment of supraspinatus and infraspinatus. Although the area of attachment for supraspinatus is not preserved in A.L. 288-1r, there is a ridge that would have separated it from the clearly defined ovoid depression for the attachment of infraspinatus.[19] Lovejoy, Johanson, and Coppens[14] described similar separation of the facets for attachment of the dorsal rotator cuff muscles on the greater tubercle of A.L. 333-107.

Humeral torsion refers to the orientation of the head relative to the distal end of the humerus. Modern humans display a high degree a torsion,[30,31] which is commonly viewed as a derived feature shared with other hominoids.[3–6] Since all known early hominin humeri are incomplete, direct measurement of their degree of torsion has been impossible, although "eyeball" estimates have sometimes been offered, for example by Pickford and coworkers.[29] However, Larson[32] developed methodologies for estimating the degree of humeral torsion on incomplete humeri using regression analysis and a set of alternative references axes. Contrary to expectations based on the view that a high degree of torsion is a shared derived

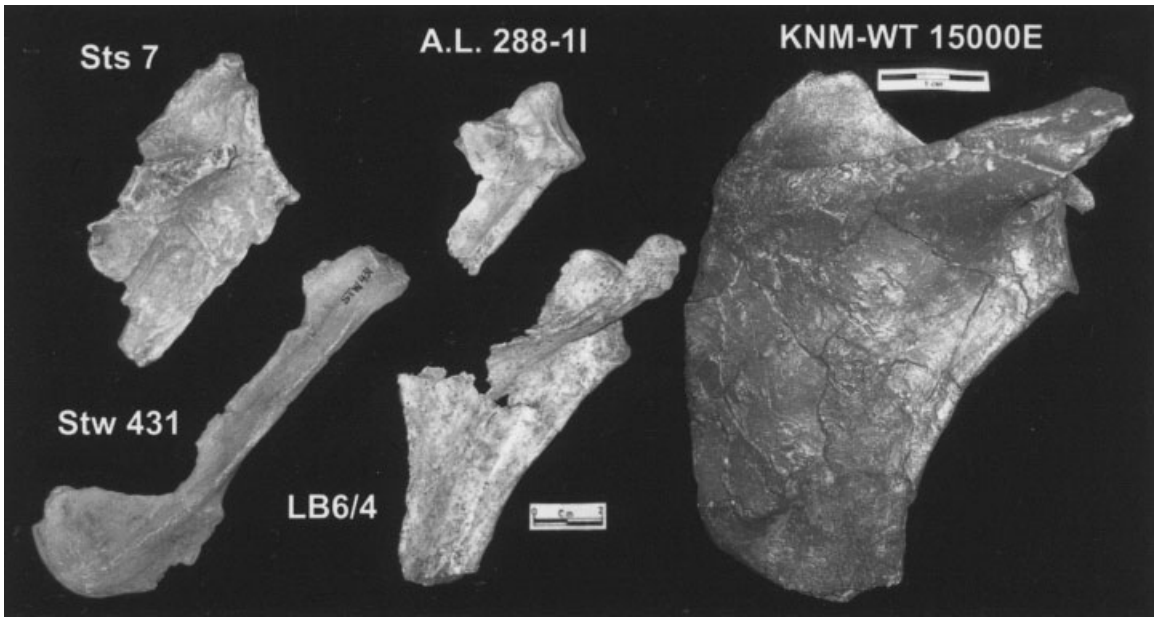

Figure 3. Dorsal views of fossil hominin scapulae. All are casts except LB6/4 (*H. floresiensis*). All photos were taken by the author. KNM-WT15000E is only approximately to the same scale as the other scapulae. The scapulae are positioned to have roughly parallel axillary borders. The glenoid fossae of the early hominin scapulae (Sts 7 and A.L. 288-11) are more cranially directed than are those of the later fossil hominins (see Fig. 4).

feature of humans and apes, she reported modest to low levels of torsion for the A.L. 288-1r, Sts 7, Omo 119-73-2718, and KNM-ER 739 humeri (Fig. 7). Larson[32] concluded that the high torsion of modern humans is therefore a more recently acquired characteristic, and that its similarity to other hominoids is due to convergence. In fact, among hominoids, only African apes display as high a degree of torsion as do modern humans, which Larson[32,33] related to the necessity of having a sagittally oriented elbow joint during quadrupedal postures.

Overall, the pectoral girdle and shoulder of early hominins appears to have retained many features of the presumed ancestral condition. Judging from Vrba's[23] interpretation of the coracoid of Sts 7, the scapula was positioned high on a funnel-shaped thorax (see also Schmid[34]), the clavicle was oriented obliquely, and the glenoid fossa was cranially directed.[20–24] However, the intertubercular groove was relatively shallow, the humeral head was elliptical, and the humerus displayed only modest torsion. This is admittedly a very grade-like rather than cladistic view of early hominin fossil material, but because of their limited number and fragmentary nature, these fossils do not lend themselves to a more fine-grained analysis. Putting aside any implications that this morphology may have with regard to reconstructing the life of early hominins, this configuration can be taken as the starting point from which the shoulder of early *Homo* was derived.

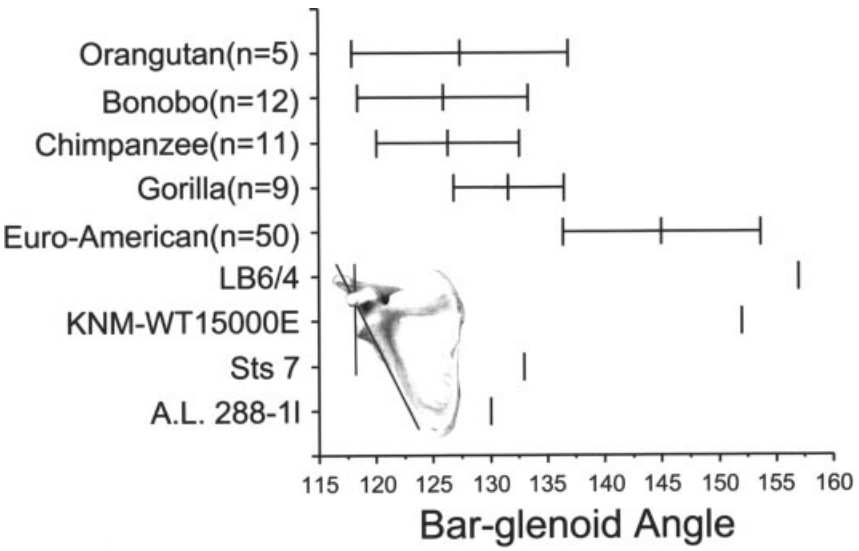

Figure 4. Bar-glenoid angles for comparative samples and fossils. The comparative data are from Stern and Susman,[24] who reported means and standard deviations for each sample. Using their data, 95% confidence intervals for each sample were calculated and are represented by the bars around each mean. The glenoid fossae of early hominins Sts 7 and A.L. 288-11 face cranially, as in extant apes, while both LB6/4 (*H. floresiensis*) and KNM-WT 15000E (*H. erectus*) are ''hyperhuman'' in having very large bar-glenoid angles.

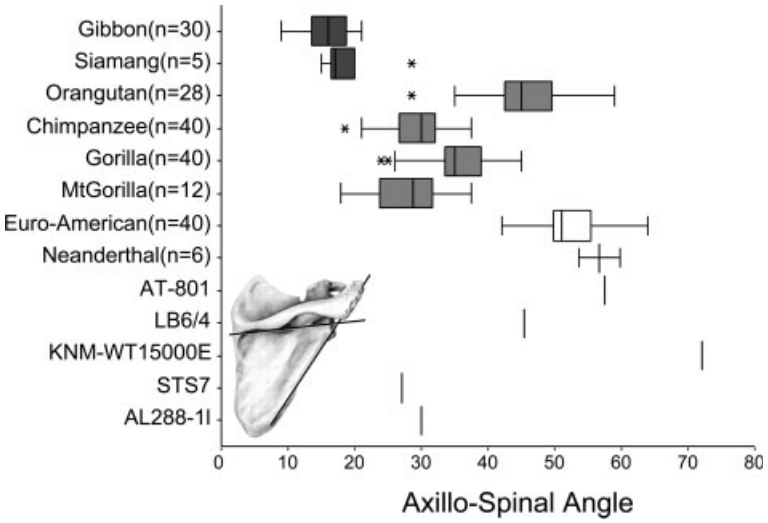

Figure 5. Box and whisker plots for axillo-spinal angles of comparative samples and fossils. Comparative data for extant taxa are from Larson.[28] Data for *H. heidelbergensis* specimen AT-801 and Neanderthals (mean value with calculated 95% confidence interval for sample) is from Carretero and coworkers.[58] Axillo-spinal angles for other fossils were measured by the author. Neanderthals, AT-801, LB6/4 (*H. floresiensis*), and KNM-WT 15000E (*H. erectus*) are like modern humans in having scapular spines that are oriented horizontally, whereas earlier hominins have oblique scapular spines, as do all apes except orangutans.

HOMO HABILIS

Unfortunately, little shoulder material is known for *H. habilis* (Table 1). O.H. 48 is a nearly complete clavicle (Fig. 2), which Napier[35] described as basically human-like except for the cross-sectional shape of the medial end. Based on the orientation of the long axis of this cross-section, he concluded that the clavicle would have been rotated slightly around its longitudinal axis and the shoulder positioned higher than in modern humans to sit on a thorax with a steep inlet. However, he felt that the range of motion of such a shoulder girdle would nonetheless be comparable to that of modern humans. Oxnard[36] reported a significantly higher degree of torsion in the O.H. 48 clavicle than in modern humans, and concurred that it would have been twisted cranially and the shoulder positioned more superiorly, which he interpreted as reflecting some ability for upper limb suspension. In response to Oxnard,[36] Day[37] argued that the missing ends of the specimen make any measure of torsion unreliable, and emphasized the basically human appearance of the fossil. This view was echoed by Ohman.[15] However, on the basis of differences in clavicular curvature, Voisin[38] returned to earlier views that O.H. 48 does not display the distinctive morphology of modern humans, concluding that the scapula of early *Homo* was situated higher on the thorax than in modern humans. The only other shoulder remains attributed to *H. habilis* are the lateral portion of a clavicle and a small piece of scapula from the KNM-ER 3735 partial skeleton. Noting the thickness of the preserved scapular spine along with the large size of other forelimb features of KNM-ER 3735, Leakey and coworkers,[39] suggested that *H. habilis* may have displayed substantial climbing ability. In sum, although little can be said with certainty based on this limited sample, the fossil evidence suggests that earliest *Homo* continued to possess a largely primitive shoulder configuration like that of earlier hominins.

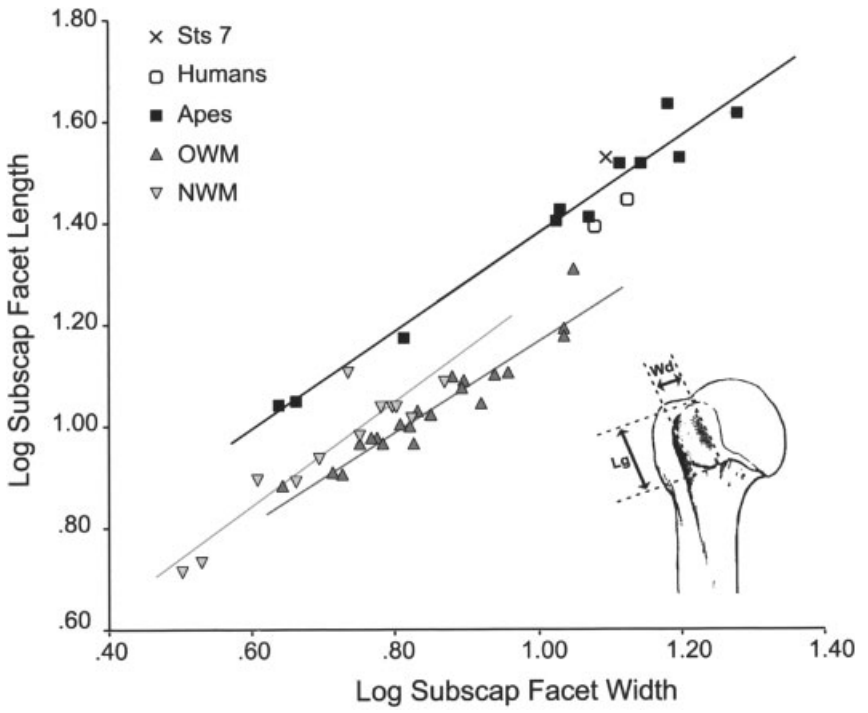

Figure 6. Shape of the subscapularis insertion facet in primates. Comparative data are from Larson.[28] Slopes of lines for apes, New World monkeys (NWM), and Old World monkeys (OWM), are not significantly different and all approximate isometry. However, the ape line is shifted above those for monkeys indicating that apes have significantly longer subscapularis insertion facets and, consequently, more versatility within subscapularis to control the position of the humeral head of a mobile shoulder joint.[28] Sts 7 is similar to the extant apes and significantly different from modern humans, who fall slightly below the line for apes.

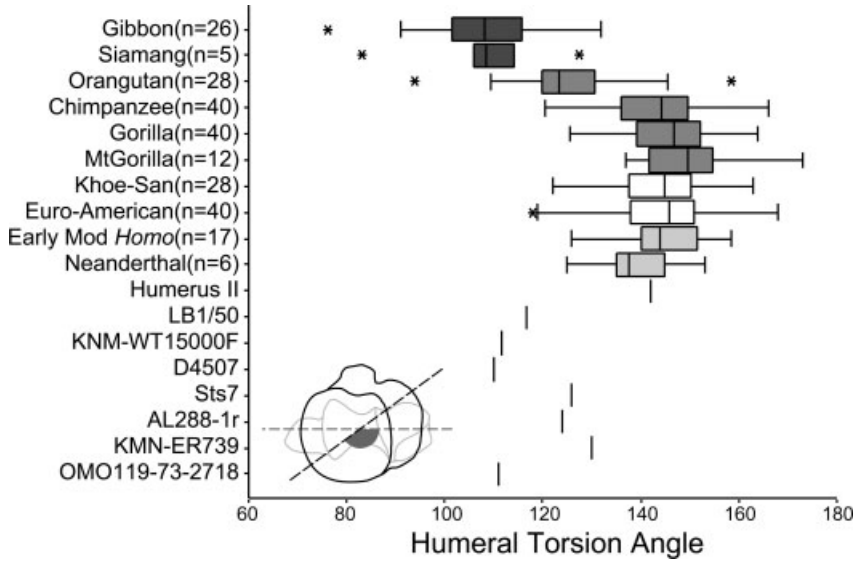

Figure 7. Box and whisker plots of humeral torsion for comparative samples of apes, modern humans, and fossils. Comparative extant data (except the Khoe-San sample) and early hominin fossil torsion estimates are from Larson.[32] Fred Grine and Louise Jacqui Friedling collected the African Khoe-San humeral data. Torsion data for Neanderthals (Lezetxiki 1, Régourdou 1, Neanderthal 1, La Chapelle 1, Tabun C1, Kebara 2) and Early Modern *Homo* (Skhul IV, Qafzeh 9, and humeri from fifteen Early Upper Paleolithic sites) are from Churchill.[64] The Humerus II (*H. heidelbergensis*) torsion value is from Carretero and colleagues.[58] Humeral torsion for large adult from Dmanisi (D4507) is from Lordkipanidze and colleagures.[115] The lesser apes have a fairly low degree of humeral torsion, while orangutans display an intermediate amount of torsion and the African apes have the highest torsion values among hominoids. Modern human samples also display a high degree of torsion. In samples of early modern *Homo,* Neanderthals, and *H. heidelbergensis,* humeral tension is slightly lower than that of modern humans. However, estimated torsion for LB1/50 (*H. floresiensis*), KNM-WT 15000F (*H. erectus*), and early hominins are much lower than modern human values.

EARLY *HOMO ERECTUS*

Unlike the situation with earlier hominins, early *H. erectus* is known from a nearly complete skeleton, KNM-WT 15000. Although in a meetings presentation Latimer and Ohman[40] suggested that this skeleton displays pathologies, particularly in the vertebral column, no published documentation of such skeletal dysplasia yet exists, and previous detailed analyses of the axial[41,42] and appendicular skeletons[43] do not indicate the presence of any abnormalities. The pectoral girdle and shoulder elements include both clavicles, one nearly complete and one partial scapula (Fig. 3), and a humerus missing only its proximal epiphysis and part of the medial epicondyle (Fig. 1). According to Walker and Leakey,[43] the clavicles display the typical S-shape seen in humans and African apes. The acromial ends are flattened superiorly and somewhat concave inferiorly. Along the anterior edge of the lateral curve is a shallow groove for attachment of the anterior deltoid, medial to which the body of the bone twists by about 30° and becomes more rounded in contour. The sternal end is ovoid; on the inferior surface there is a low, blunt conoid tubercle approximately one quarter of the way from the lateral end.

Despite their unremarkable shape, the KNM-WT 15000 clavicles are unusual in their length. Using the claviculohumeral ratio to express relative clavicular length, since the humerus displays a conservative scaling relationship to body size,[44] Larson[45] has shown that relative clavicular length in the Nariokotome boy is low compared to those of modern human groups, as well as later fossil hominins (Fig. 8). This difference in relative length is not simply due to the immaturity of the KNM-WT 15000 skeleton. Jungers and Hartman[46] reported that humeral length displays isometric growth allometry in great apes and slight positive growth allometry in humans, while clavicular length displays negative growth allometry in all taxa. Therefore, whether KNM-WT 15000 followed a great ape or human growth trajectory, these scaling patterns would have resulted in an even shorter relative clavicular length if the Nariokotome boy had reached adulthood, and the 40.9 claviculohumeral ratio reported in Figure 8 is likely to be an *underestimate*. Since all extant apes except orangutans also display low claviculohumeral ratios, Larson[45] argues that a relatively short clavicle is probably the primitive condition for hominoids, which is retained in early *H. erectus*. The recently described short clavicles of early *H. erectus* from Dmanisi[115] lend support to this view.

Walker and Leakey[43] reported that the right scapula, though reconstructed from fragments, is the more complete of the pair (Fig. 3). The juvenile age of the Nariokotome boy is evident in the missing regions of the superior and inferior angles, and though the coracoid was found, it was not fused to the main part of the bone at the time of death. The surface of the glenoid fossa, which would have been largely cartilaginous, is missing, though it is possible to measure its maximum diameters and orientation. According to measurements on a cast, the axillo-glenoid angle is 147°; the glenoid-ventral bar angle is 152°. By either measure, therefore, the glenoid no longer faced cranially as it did in earlier hominins. Lordkipanidze and colleagues[115] report a slightly more cranial orientation to the glenoid of the scapular fragment from Dmanisi, with an axillo-glenoid angle of approximately 133° (estimated from a photograph). As in modern humans, the supraspinous fossa of KNM-WT 15000 is small relative to the infraspinous fossa[43] and the scapular spine is not oblique. In fact, its angle with the axillary border exceeds that in modern Euro-Americans (Fig. 5).

Since the humerus is missing its proximal epiphysis, it is not possible to determine the condition of the articular surface or tubercles. The

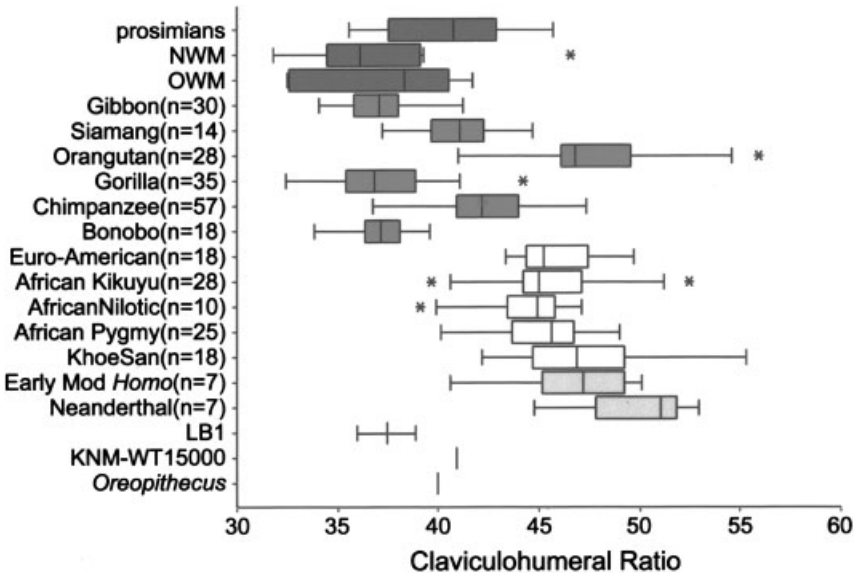

Figure 8. Box and whisker plots of claviculohumeral length ratios for comparative samples and fossils. Prosimian, New World monkey, and Old World monkey samples were constructed from the mean values for clavicular and humeral length from Mivart.[110] Comparative ape, African pygmy, and Euro-American data were provided by William Jungers. Fred Grine and Louise Jacqui Friedling collected clavicular and humeral data for a sample of African Khoe-San. African Kikuyu and Nilotic data were provided by Chris Ruff. The early modern *Homo* sample includes Abri Pataud 5,[64] Jebel Sahaba, Wadi Kubbaniya,[111] Doni Věstonice 13 and 15,[112] and Skhul IV and V.[113] The Neanderthal sample includes Kebara 2,[64] Shanidar 1 and 3, Régourdou 1, Tabūn C1, La Ferrassie 1,[60] and Neanderthal.[113] Error bars around the claviculohumeral ratio for LB1 (*H. floresiensis*) refer to prediction error associated with the reconstruction of clavicular length for this specimen (see Larson and coworkers[2]). The samples of modern humans vary in average stature, yet all have similar claviculohumeral ratios, which are consistently higher than those in apes other than orangutans. The relative clavicular lengths for KNM-WT 15000 and LB1 are more similar to those in apes than in modern humans. Neanderthals appear to have, on average, the longest clavicles among hominins. The claviculohumeral ratio for *Oreopithecus* is included to offer an indication of relative clavicular length in Miocene hominoids. (The humeral length for *Oreopithecus* is from Harrison[114]; an estimate of clavicular length was provided by Terry Harrison).

intertubercular groove is wide and shallow, and the shaft is straight and slender with only light muscle markings.[43] Although the proximal epiphysis is missing, it is possible to estimate the degree of humeral torsion using either a bisector of the intertubercular groove as a surrogate for head position[32] or a posteriorly positioned buttress for the humeral head that is aligned with the humeral head axis. Both methods yield a value of 111.5°,[2] which is well below mean values published for modern humans (for example, Evans and Krahl[30]), but not out of line with earlier hominins (Fig. 7). Although the Nariokotome boy is believed to be a juvenile, it is unlikely that his adult torsion value would have been much higher. According to the human growth trajectory chart presented by Krahl,[31] by the age of 10 years an average human child already displays approximately 92% of the average of adult torsion, and torsion increase ends by about 20 years of age. Therefore, maximum adult humeral torsion for KNM-WT 15000F would have been only about 120°, still well below modern human mean values (Fig. 7). According to Lordkipanidze and colleagues,[115] the humeri from Dmanisi also display low humeral torsion (Fig. 7).

Contrary to expectations of an essentially modern human shoulder configuration with the appearance of *Homo*, the shoulder region of the early *H. erectus* as represented by the KNM-WT 15000 skeleton presents an unanticipated combination of features, including relatively short clavicles and very low humeral torsion, which likely are retained primitive conditions. However, this skeleton has a fairly modern-looking scapula, with a glenoid that did not face cranially, sitting on a barrel-shaped rib cage.[47] How might such a combination of primitive and derived features functioned? An abnormality found occasionally in modern humans known as short or hypoplastic clavicle syndrome[48–51] suggests an answer. In this syndrome, there typically is significant anterior displacement of the shoulder joints and the vertebral borders of the scapulae are often prominent posteriorly and widely separated. Thus, in individuals with this syndrome, the short clavicles have caused the scapulae to be shifted forward so that they are positioned more laterally on the rib cage, which in turn results in more anteriorly directed glenoids. The clavicles, except for their diminished length, are normal in appearance and, in most cases, there are no other abnormalities or upper extremity dysfunctions. The chief complaint is abnormal posture. Unfortunately, no study describing short clavicle syndrome has attempted to quantify clavicular length nor to report the degree of humeral torsion in patients with this condition, although Guidera and colleagues[49] noted that the humeri are located anteriorly on CT scans. However, given that humeral torsion is somewhat plastic developmentally,[31,52,53] it is plausible that these individuals have reduced humeral torsion to accommodate the anterior orientation of their glenoid fossae.

If the relatively short clavicle in KNM-WT 15000 is indeed the retention of a primitive characteristic, this in itself should not alter the configuration of the pectoral girdle or shoulder. However, the scapula has also undergone modification in relation to reduction of the cranial orientation of the glenoid. Along with this change in scapular morphology there probably was also a change in position from a high "shrugged" shoulder, likely to characterize early hominins, to something nearer to the human condition. I suggest that these changes were constrained to a degree by a relatively short clavicle so that the scapula moved anteriorly as well as inferiorly,

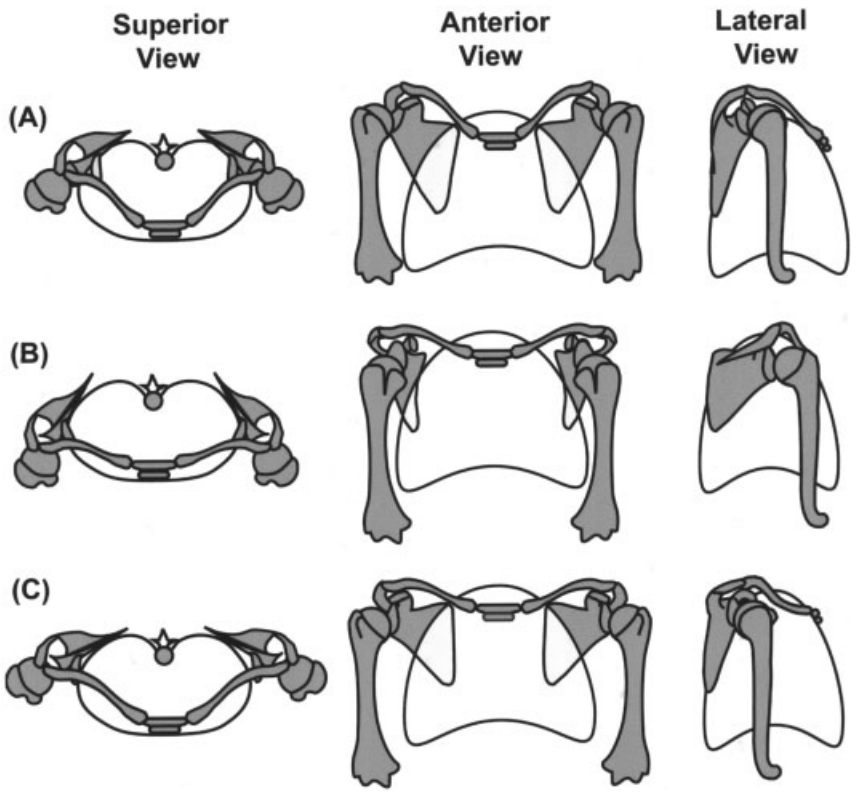

Figure 9. Proposed course of evolution of the hominin pectoral girdle. (A) Superior, anterior, and lateral schematic views of a torso showing the pectoral girdle and shoulder of the presumed ancestral hominin condition. Scapulae are dorsally positioned with cranially facing glenoids. Clavicles are short and oriented obliquely, resulting in a ``shrugged-shoulder'' appearance. The humerus displays low to modest torsion. (B) Proposed configuration for the pectoral girdle in *H. erectus* and *H. floresiensis*. The change from a scapula positioned high on the thorax with a cranially oriented glenoid fossa has been brought about by both a downward shift in position and a morphological change analogous to a glenoid-down rotation of the scapula, constrained by a relatively short clavicle. The result is a more laterally positioned scapula with a glenoid fossa that faces anteriorly. Sagittal functioning of the elbow joint is maintained without a major increase (but possibly a decrease) in humeral torsion. (C) Pectoral girdle and shoulder of a modern human with elongated clavicles, dorsally positioned scapulae, and laterally facing glenoid fossae. The humerus displays marked torsion to maintain a sagittal plane for elbow function.

and thus came to occupy a more lateral position on the rib cage (Fig. 9B). The result of this shift in scapular position and morphological change in glenoid orientation were anteriorly facing glenoid fossae, as in people with hypoplastic clavicle syndrome. A humerus with a posteriorly direct head (that is, with very low torsion) was therefore appropriate to maintain a sagittally functioning elbow and the ability to use the hands for manipulation. Picturing glenohumeral range of motion as a wide cone with its apex at the glenoid fossa, such a shoulder configuration would have had a somewhat limited range of motion (Fig. 10A). Elevation at the shoulder would be mainly via flexion, and true abduction (humeral elevation in a coronal plane) may not have been possible. However, the loss of the cranial orientation to the glenoid fossa indicates that reliance on use of the forelimb in overhead supporting postures had decreased along with the frequency of arboreality. Apparently, such a loss of in range of motion at the shoulder was not deleterious.

Given the pronounced similarity between individuals displaying short clavicle syndrome and the shoulder configuration suggested here for the KNM-WT 15000, a potential alternative interpretation is that the Nariokotome boy simply had this syndrome. However, corroboration that this represents a stable functional configuration comes from a surprising source, *H. floresiensis* (Box 1). The humerus from the relatively recent LB1 skeleton also displays very low torsion[1] as well as a relatively short clavicle[2] (Figs. 7, 8).

Although there is no scapula associated with the LB1 partial skeleton, a nearly complete scapula from a different individual (LB6/4) displays a high bar-glenoid angle, putting to rest the proposal by Inouye and Shea[25] that a high angle in *A. afarensis* is due to its small size. LB6/4 also has a large axillo-spinal angle (Fig. 5), just as does KNM-WT 15000E.[2] The fact that both *H. floresiensis* and the Nariokotome skeleton display this unexpected combination of features despite being from very different times, places, and evolutionary histories suggests that these features are neither pathologies nor chance similarities, but part of a functional complex that characterized early *H. erectus* and was retained in *H. floresiensis*. Although the status of *H. floresiensis* is still controversial (Box 1), the short clavicle and low humeral torsion reported for the early *H. erectus* postcranial material from Dmanisi[115] also offer corroboration of this hypothesized transitional stage in evolution of the pectoral girdle and shoulder.

HOMO ANTECESSOR

If the proposal put forward here that early *H. erectus* is characterized by a relatively short clavicle, low humeral torsion, and a more protracted scapula position, is verified by future discoveries, when might the clavicular elongation, dorsal repositioning of the scapula, and concomitant increase in humeral torsion leading to the shoulder configuration of more recent hominins first occurred? The lower Pleistocene site of Gran Dolina, Sierra de Atapuerca, Spain has yielded a variety of postcranial remains attributed to *H. antecessor*,[56] including a complete adult clavicle (ATD6-50), as well as one complete and one partial subadult clavicle. Although no humeri are

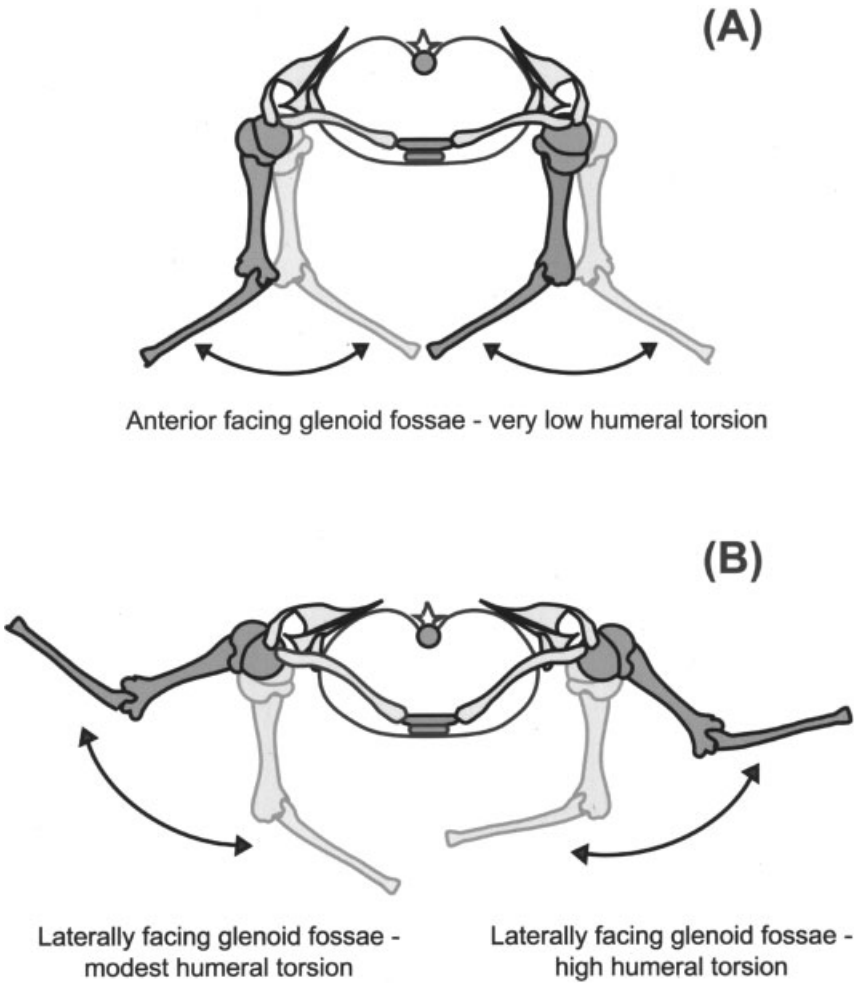

Figure 10. Effect of scapula position and degree of humeral torsion on range of motion at the shoulder. (A) Schematic superior view of a hominin torso with laterally positioned scapulae and low humeral torsion. Elevation of the arm would be mainly confined to forward flexion. Dark and ``ghosted'' limb images, which have been offset slightly for clarity, show suggested ranges of motion due to humeral rotation at the shoulder. (B) Schematic superior view of a hominin torso with dorsally positioned scapulae. The dorsal scapular position reorients the glenoid fossa so that it faces laterally, which permits true abduction and horizontal extension at the shoulder, thus dramatically increasing glenohumeral mobility. However, the particular range of motion possible at the shoulder can vary depending on the degree of humeral torsion. The humerus of the right shoulder has a modest amount of humeral torsion; the one on the left has a higher degree of torsion. Although the humeral heads are in the same position relative to the glenoid on both right and left sides, the right arm, with less torsion, has a somewhat greater range of external rotation but less internal rotation, while the arm on the left, with its greater amount of humeral torsion, can achieve a higher degree of internal rotation but less external rotation. Such differences in range of motion associated with differences in degree of torsion have been documented in the human sports literature.[69–72]

known from the site with which to calculate a claviculohumeral index, the adult clavicle ATD6-50 is absolutely quite long, falling at the upper fringes of size ranges for modern human samples.[56] It is possible, therefore, that *H. antecessor*, which has been proposed to represent the last common ancestor of *H. sapiens* and *H. neanderthalensis*,[57] exhibits the clavicular elongation that is seen in both later taxa. If a humerus is ever recovered from Gran Dolina, it should display a greater degree of humeral torsion than is seen in KNM-WT 15000F, although not necessarily a degree as high as that in modern humans.

HOMO HEIDELBERGENSIS

A total of fifteen clavicular fragments, seventeen scapular fragments, and thirty-three humeral fragments are known from the middle Pleistocene site of Sima de los Huesos, Sierra de Atapuerca, Spain.[58] Unfortunately, only one of these specimens from the shoulder region of *H. heidelbergensis* is complete: Humerus II (Fig. 1). This humerus is very long, falling well above mean values for both Neanderthals and modern human samples.[58] The humeral head is wider than it is long, like that in later Neanderthals and unlike that in modern humans. Carretero, Arsuaga, and Lorenzo[58] reported a humeral torsion value of 142°, which is considered somewhat low for modern humans, but again similar to Neanderthals (Fig. 7). The Sima de los Huesos proximal humeri display very large lesser tubercles, again like Neanderthals[59] and in contrast to a smaller lesser tubercle in modern humans. Although Carretero, Arsuaga, and Lorenzo[58] viewed this as another shared derived trait of *H. heidelbergensis* and Neanderthals, an enlarged lesser tubercle is reminiscent of the condition in early hominin proximal humeri Sts 7, KNM-BC 1945, and A.L. 288-1r.[18,19,29] In this case, it may represent a retention of the primitive condition for hominins.

Although none of the Sima de los Huesos scapular fragments are complete, Carretero, Arsuaga, and Lorenzo[58] estimated the axillo-glenoid angle on one adult specimen (AT-320, 140°) and one subadult (AT-801, 144°). These values fall toward the high end of modern human variation, but are similar to Neanderthal mean values.[58] Similarly, the AT-801 scapular fragment displays a scapular spine-axillary border angle that is somewhat high for modern humans but like that of Neanderthals[58] (Fig. 5).

Overall, the morphology of the shoulder region in *H. heidelbergensis* appears to be most similar to that of later Neanderthals. In fact, many of these shoulder features are viewed as evidence that *H. heidelbergensis* is ancestral to *H. neanderthalensis*.[58,60] If the clavicle also displays the relative elongation seen in Neanderthals com-

Box 1. *Homo floresiensis*: New hominin species or pathological human?

Since the 2004 announcement of the discovery of diminutive hominins with tiny brains living until 12,000 years ago on the island of Flores,[91] there has been controversy regarding the correct interpretation of this material. Although initial claims that the LB1 partial skeleton was an isolated pathological individual have been countered by the recovery of remains from another eight individuals,[1] skeptics remain.[92–96] Most debate regarding the validity of *H. floresiensis* as a new species has focused on brain size and configuration.[92,94,95,97–100] However, three recent reviews of the LB1 skeleton have concluded that it was not a member of a distinct species of hominin, but rather was an atypical modern human. According to Jacob and coworkers,[93] LB1 was derived from an Australomelanesian *H. sapiens* population and manifested microcephaly accompanied by other developmental abnormalities. In particular they report that the postcranial elements of LB1 display evidence of weakened muscles, thin cortical bone, enlarged medullary cavities, and marked right and left asymmetries. However, their contention that LB1 had weak muscles is based on muscle markings. Several studies have shown that muscularity cannot be reliably deduced from muscle scars (see Zumwalt[101]). In addition, Larson and colleagues[102] report that cortical bone thickness in LB1 is perfectly normal and well within modern ranges, as are degrees of left-right asymmetry.

Richards[96] argues that Flores hominins represent an *H. sapiens* group that became dwarfed in an island environment through changes in genes controlling the growth hormone, insulin-like growth factor I axis. According to Richards' scenario, disruptions to the normal developmental pathways are responsible for the distinctive features of LB1, noting that "Morphological features of the skeleton (wide pelvis, long arms relative to legs, tibial cross-sectional shape, etc.) that are said to link *H. floresiensis* with early hominids are also found in modern human pygmy populations." However, Jungers and coworkers[103] and Larson and coworkers[102] report that both limb proportions and stature reconstruction for LB1 are completely outside ranges ever observed in modern humans, including the smallest "pygmoids."

Herskhovitz and colleagues[104] also argue that the unique morphology of LB1 can be explained by a growth-hormone-related syndrome, Laron syndrome (LS), a genetic disease resulting in growth hormone insensitivity. They claim that patients with LS have relatively short and shallow clavicles and humeri that are thick for their length and display limited torsion. (Elsewhere in the paper, however, they describe the long bones of patients with LS as slender in appearance). Like Jacob and coworkers,[93] these investigators interpret the weak muscle markings on the humerus as evidence of muscle weakness, also a characteristic of LS. Unfortunately, they offer no actual data to substantiate these claims, nor are these features documented in the literature of LS, making it difficult to assess just how similar they are to LB1. It can be said with certainty, however, that one feature of patients with LS, namely very small hands and feet,[105] is definitely not characteristic of LB1.[106]

In contrast, Argue and co-workers[107] have recently analyzed the cranial and postcranial morphology of LB1, including comparisons to individuals with microcephaly and short stature. These authors conclude that LB1 is unlikely to be a microcephalic human and that it is distinct from any known hominin species. Similarly, Tocheri and colleagues,[108] have shown that the distinctive morphology of the carpal bones of LB1, which are more similar to those of early hominins than those of modern humans, cannot be explained by disruptions in development. Papers such as these, which look beyond brain size, have observed unexpected and interesting morphology that defies simple explanations. As Gundling[109] has noted, attributing unprecedented fossil hominin morphology such as that in LB1 to pathology is not new in paleoanthropology. However, the controversy surrounding *H. floresiensis* will probably continue until additional fossils, especially new cranial material, are found.

pared to modern humans (Fig. 8), then a complete clavicle from the same individual as the Humerus II specimen should be approximately 170 mm long.

NEANDERTHALS

The shoulder of Neanderthals is characterized by a relatively long clavicle[59,61] (Fig. 8), a scapula that displays distinctive axillary border morphology, a horizontal scapular spine, and a tall, narrow glenoid fossa.[61–63] The humerus has a prominent lesser tubercle and a head that is wider than long. There also is a modest level of humeral torsion[59,64,65] (Fig. 7). Vandermeersch and Trinkaus[59] and Churchill[65] related the modest level of humeral torsion in Neanderthals to their cold climate adaptation of an enlarged chest, suggesting that their scapulae were positioned more laterally, with the result that their glenoid fossae were directed more anteriorly. Thus, a humeral head that was directed more posteriorly (that is, had low humeral torsion) was needed to maintain a sagittally functioning elbow joint. It would follow that the relatively long clavicles of Neanderthals were also products of large chest size, needed to bridge the longer distance from the sternum to the acromion.

Such a configuration in many ways resembles what I am suggesting here for early *H. erectus* and could, therefore, be viewed as retention of the primitive condition with the addition of increased chest size. This would imply that the last common ancestor of Neanderthals and modern humans also retained the primitive pectoral girdle and shoulder configuration. But if *H. antecessor* does indeed represent this ancestral condition, the very long clavicle ATD6-50 may indicate that clavicular elongation had already occurred before the appearance of Neanderthals. However, *H. antecessor* is unlikely to have had the cold climate adaptation of an enlarged chest as do later Neanderthals, since analysis of the ungulates from unit 6 of Gran Dolina in the Sierra de Atapuerca indicates a virtual absence of cold-adapted taxa from the Spanish lower and middle Pleistocene.[66] Therefore, if the long absolute length of ATD6-50 also indicates a long relative length, initial clavicular elongation in lower Pleistocene hominins was unassociated with chest size increase; other factors were responsible for this elongation. In addition, while humeral torsion in Neanderthals, as well as *H. heidelbergensis*, is low compared to what is commonly seen in modern humans, it does not even approach that of the Nariokotome boy (Fig. 7).

A possible alternative interpretation of the course of pectoral girdle and shoulder evolution is based on the implications of hypoplastic clavicle syndrome. The dramatic shift in scapular position due to shorted clavicle length in individuals with this syndrome indicates that clavicular length and scapula position are strongly linked. I suggest that the clavicular elongation that occurred in the human lineage subsequent to early *H. erectus* was most directly related to dorsal repositioning of the scapula, and that this shift in scapular position occurred in order to increase the range of motion of the upper limb. If we again imagine possible motion at the glenohumeral joint as a wide cone, moving the scapula onto the dorsum of the rib cage positions the apex of that cone, the glenoid fossa, lateral to the torso, which dramatically increases the potential range of motion (Fig. 10B). True abduction of the humerus is now possible, as well as horizontal abduction (that is, extension of the abducted arm). According to this interpretation, the common ancestor of *H. sapiens* and Neanderthals had a derived pectoral girdle configuration, which included longer clavicles, dorsally positioned scapulae, and laterally facing glenoid fossae. The only major modification in Neanderthals was an additional increase in clavicle length over something that was perhaps more similar to modern humans (Fig. 8), which was necessary to keep the scapula dorsally positioned with an enlarged chest.

But if Neanderthals did display the derived condition of a dorsally positioned scapula, why are they characterized by only modest humeral torsion as compared to modern humans? It is well known that there is considerable variation in humeral torsion values both within and between modern human populations.[52,64,67,68] One of the correlates of reduced humeral torsion that has been documented in the human clinical and sports literature is overhand throwing,[69–72] which entails a high degree of external rotation of the abducted and extended arm during the cocking phase.[73–75] Individuals who have lower torsion values have been demonstrated to have greater ranges of external rotation.[76] Those who throw habitually have both significantly lower torsion and a greater range of external rotation on their throwing side[69–72] (Fig. 10B). However, while it is tempting to attribute the reduced torsion in Neanderthals to enhanced throwing ability, attempts to use this relationship to account directly for variation in the degree of humeral torsion in ancient modern populations has met with only limited success.[77] In addition, it should be pointed out that the amount of reduction in torsion that has been observed in association with an increase in range of external rotation at the shoulder in humans is relatively small, on the order of 10–15°, and is therefore unlikely to explain the very low torsion values observed in KNM-WT 15000F or LB1 (Fig. 7). It also presumes a lateral orientation for the glenoid fossa. If Neanderthals actually did have a more laterally positioned scapula, one would expect their degree of humeral torsion to be much lower, nearer to that of KNM-WT 15000F. The resulting anteriorly facing glenoid fossa would have posed limits on shoulder mobility (Fig. 10A), negatively affecting overhand throwing ability.

It is possible that the modest degree of humeral torsion observed in Neanderthals needs no explanation. Since earlier hominin taxa such as *H. heidelbergensis* also had a modest amount of humeral torsion, perhaps the very high degree of torsion of modern humans is a more recently derived condition. In other words, what needs to be explained is why modern humans have developed

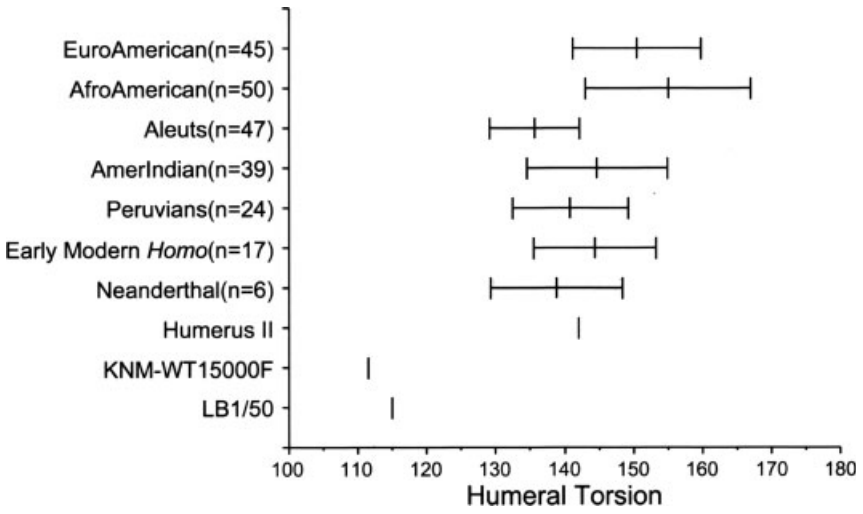

Figure 11. Comparison of humeral torsion among modern humans groups (means ±1 sd). Since small differences in methods used to measure humeral torsion can produce subtle differences in torsion values (see Larson and coworkers[2]), comparative data for modern human populations as well as for samples of early modern *Homo* and Neanderthals have been taken from a single investigator (Churchill[64]) to minimize this effect. The torsion value for humerus II (*H. heidelbergensis*) is from Carretero and colleagues.[58] Although few of the differences between modern human samples are statistically significant, the mean torsion values for non-Western populations are all lower than those of the Euro- or Afro-American samples. If the degree of torsion in non-Western populations is taken as representative for modern humans, then the humeral torsion in Neanderthals or *H. heidelbergensis* does not seem unusual.

greater humeral torsion than our recent ancestors, not why our ancestors had less torsion than we do. Although this runs counter to traditional views about which aspects of shoulder morphology have been inherited and which are unique to modern humans, this perspective is more in line with the fossil evidence of humeral torsion evolution among hominins, as well as with our understanding of the factors influencing the development of humeral torsion.

HOMO SAPIENS

Modern humans have dorsally positioned scapulae with laterally facing glenoids, relatively long clavicles (Fig. 8), and a high degree of humeral torsion (Fig. 7). Relative clavicular elongation is another trait said to distinguish apes and humans from other primates,[3–6,78] and therefore has been assumed to characterize all hominins. This view may stem from the use of trunk length to express relative clavicular length.[78–81] Since hominoids typically have relatively short trunks, this inflates relative clavicular length. Humerus length has a more conservative scaling relationship to body size in apes and humans[44] and, when used to express relative clavicular length, as in Figure 8, modern humans as well as early modern *Homo* and Neanderthals display a derived condition of relative clavicular elongation compared to the retained primitive condition in African and lesser apes.

As mentioned earlier, because high humeral torsion was thought to be a shared derived feature of apes and humans, it was presumed to be characteristic of all hominins. However, the evidence summarized here for earlier hominins indicates that they had low to modest torsion, supporting the view that the high degree of torsion in modern humans and apes has been independently acquired.[32]

Reported variation in the degree of humeral torsion within modern humans includes differences between dominant and nondominant sides, between males and females of a population, and between different populations (for example, Krahl and Evans[30] and Edelson[52]). Although this variation is generally assumed to be related to differences in habitual behaviors and activity levels, other than the documented relationship between overhand throwing and reduced humeral torsion mentioned earlier, there is little hard data linking specific behaviors to degree of torsion. Historically, variation in humeral torsion has been viewed somewhat as a *scala naturæ* starting with low values for monkeys and increasing for apes, leading to so-called "primitive" races of humans until reaching the highest values in "civilized" groups (for example, Martin[68]). However, if we remove the racial overtones of this perspective, a case can be made that much of the variation between modern human groups is due to a contrast between Western with non-Western populations. Figure 11 presents humeral torsion data for several human populations derived from a single researcher (Churchill[64]), since subtle differences in measuring methods can influence results (see Larson and coworkers[2]). Although few of the differences are statistically significant, the two samples of Western populations (Euro-Americans and Afro-Americans) display higher average humeral torsion than do any of the non-Western populations. Edelson[52] has also examined variation in humeral head orientation in modern humans by documenting retroversion angles, which constitute the supplement of torsion angles. Edelson similarly found lower retroversion angles (that is, higher torsion angles) for his Euro- and Afro-American samples than for his samples of Aleut, Amerindian, or Northern Chinese humeri, although values for Negev Desert Bedouins were similar. It is also the case that there is no difference between the torsion values for samples

What needs to be explained is why modern humans have developed greater humeral torsion than our recent ancestors, not why our ancestors had less torsion than we do.

of Khoe-San and Afro-American humeri reported in Figure 7.

Studies such as these are based on skeletal collections that for non-Western peoples are typically drawn from prehistoric or pre-Western-contact populations, whereas skeletal samples of Europeans or Americans are often cadaver-based material. Therefore, more often than not, the Western samples are derived from individuals living in industrialized societies, whereas non-Western samples are from preindustrialized societies in which it was likely that activity levels were generally higher throughout the lifetime of an individual. Since humeral torsion increases during development in humans,[31,52] which Krahl[31] suggested is caused in part by the influence of muscular forces on the humerus, it is therefore possible to imagine that there will be different endpoints to this developmental process depending on the degree and nature of muscular forces acting on the upper limb throughout ontogeny. I suggest that the lower degree of humeral torsion often observed in non-Western or prehistoric human samples is related to the influence of muscular forces and/or the demands for a particular range of motion associated with typically higher activity levels. While associating differences in torsion with activity levels is not new (for example, Rhodes[77]), instead of trying to relate *lower* humeral torsion to particular behaviors such as overhand throwing, I believe that it is the *high* degree of torsion in Western samples that needs to be explained. In other words, the more moderate degree of humeral torsion in non-Western and prehistoric populations is what should be viewed as characterizing modern humans in comparisons to other hominin taxa, while the high levels of torsion in groups such as Europeans or Americans constitute a very recent phenomenon related to reduced physical demands on the upper limb associated with industrialized culture. Viewed in this way, the levels of humeral torsion in early modern *Homo,* Neanderthals, and even *H. heidelbergensis* are not low, but actually quite similar to those of modern humans if non-Western human groups, rather than Euro- or Afro-American samples, are taken as typical (Fig. 7).

Support for the proposal that higher torsion is associated with reduced activity levels in modern humans can be found in the pattern of variation in torsion within groups. As Edelson[52] demonstrated, within a population sample torsion is typically higher in females than in males. This is not to say that women are inactive, but that men usually do the most physically demanding activities. In addition, torsion is usually higher for left humeri, typically the nondominant side, than for right humeri, the dominant side for most people.[52] Although Krahl[31] attributed such differences in degree of humeral torsion to the balance of muscular forces, I suggest that selection for particular ranges of motion may also play a role, and may explain why some non-Western populations display a comparable level of torsion to Western groups (for example, Khoe-San and Afro-Americans, Fig. 7).

Although this proposal glosses over many differences in habitual behaviors between modern human groups, I suggest it is a better perspective in which to evaluate the evolution of humeral torsion in hominins. Since, from this standpoint, torsion is not particularly low in Neanderthals, perhaps their elongated clavicles were largely able to compensate for their enlarged chest size, making it unnecessary to posit a more anterior scapular position. The smaller relative clavicular length in early modern *Homo* and in modern humans (Fig. 8) would in turn reflect the fact that they had smaller chests than did Neanderthals. However, once again, I should emphasize that the differences in degree of torsion between Western and non-Western groups are relatively small, making it unlikely that balance of muscular forces or range of motion can account for the dramatically lower degree of torsion seen in KNM-WT 15000F, LB1, or the humeri from Dmanisi.

CONCLUSIONS

This survey of hominin fossil material indicates that early hominins generally retained much of the presumed primitive condition for pectoral girdle and shoulder morphology (short clavicle, dorsal scapula, cranially directed glenoid, low to modest humeral torsion). The implications of this condition for reconstructing the way of life of early hominins is a matter of continuing debate, with some researchers viewing these primitive features as phylogenetic "baggage" retained because of no selective force against them and others considering the persistence of features an indication of continuing function (for a recent review, see Stern[82]). The first major transformation of the hominin shoulder appears with early *H. erectus,* when the scapula takes on a more modern appearance. Larger brain size and more sophisticated tool technology, both implying greater dependence on manipulatory abilities in *H. erectus*, may account for these changes. However, it is also possible that these changes reflect the final abandonment of habitual use of trees for resources or refuge. Despite the changes in scapular morphology, *H. erectus* still retained a short clavicle and low humeral torsion. Evidence that this combination of features formed a stable functional system is found in the fact that *H. floresiensis,* which is distant in time and space, also displays a relatively short clavicle and low humeral torsion in combination with a relatively modern-looking scapula.

Following early *H. erectus*, clavicular elongation formed the basis for a second major transformation in the hominin shoulder, possibly occurring as early as the lower Pleistocene, judging from the very long clavicle known for *H. antecessor*. I suggest that this clavicular elongation pushed the scapula to a more dorsal position so that the glenoid fossa faced laterally, which concomitantly required an increase in humeral torsion. Such a shift in scapular position would have dramatically increased the range of upper limb motion, particularly in the posterior direction. It is interesting to speculate about the selective factors that may have brought about this change. One potential selective force favoring

such an increase in shoulder mobility is throwing, which entails a significant component of posterior motion of the abducted arm during the cocking phase.[73–75] As long as people have been attempting to explain the origins of upright posture and bipedalism, the throwing of objects for self-defense and hunting has been included as a significant factor contributing to the survival and success of the human lineage.[83–86] Unfortunately, there is little physical evidence of when and where throwing skill might have evolved. Preuschoft[87] recently noted, in reference to the potential influence of throwing in hominin evolution, that "at present, the claims reach further than the facts." However, the discovery of 400,000-year-old throwing spears[88] suggests that it had developed by at least the middle Pleistocene. The anterior position of the shoulder postulated here for early *H. erectus* would not have permitted the abducted arm posture that is an integral component of the form of overhand throwing we are familiar with today. It is interesting, in this context, to note that one incidental complaint of people with short clavicle syndrome is that they cannot throw well.[48,49] Effective throwing, therefore, could have been an important selective influence in transforming the pectoral girdle/shoulder complex from the condition in *H. erectus* to that resembling modern humans.

A second potential selective force for clavicular elongation is running, which requires shoulder and upper body rotation to counteract the destabilizing torque created by the oppositely moving lower limbs. Although running ability to achieve higher speeds has obvious advantages, Carrier[89] and, more recently, Bramble and Lieberman[90] have argued that endurance running in particular has been instrumental in shaping hominin evolution, possibly contributing to the origins of the genus *Homo*. However, for the pectoral girdle to contribute to an effective upper body counter-rotation mechanism, the shoulders should be widely separated. The analysis of the course of change in shoulder morphology presented here suggests that early *H. erectus* did not have particularly wide shoulders and, by inference, neither did earlier members of the genus. Although this would not have made running impossible for early *Homo*, the fact that their shoulders were narrow suggests that an effective upper body counter-rotation mechanism was not yet an important selective factor. As Bramble and Lieberman[90] note, several of the changes in lower limb morphology in early *Homo* could alternatively be explained as adaptations to long-distance walking. However, running, whether for speed or endurance, could well have been an impetus for clavicular elongation at a somewhat later stage of human evolution to spread the shoulders apart in order to enhance the upper body counter-rotation mechanism.

This overview of the course of change of the hominin pectoral girdle/shoulder configuration has been painted with a somewhat broad brush, many other subtle changes that took place along the way have been ignored. Although the timing of events remains uncertain, it appears that features such as scapular position have changed multiple times. Therefore, rather than being a simple change from primitive to modern, evolution of the hominin shoulder has proceeded in a mosaic fashion.

ACKNOWLEDGMENTS

I thank Alan Walker for the loan of casts of the KNM-WT 15000 forelimb bones, Bill Jungers for comparative data on extant apes, Chris Ruff for the use of his metric data on African Nilotic and Kikuyu peoples, Terry Harrison for an estimate of clavicular length in *Oreopithecus*, and Fred Grine and Louise Jacqui Friedling for measuring Khoe-San clavicles and humeri. Thanks also to Tony Djubiantono, Director of the Indonesian Centre for Archaeology (ARKENAS), for permission to examine the Flores hominin fossils, and to Mike Morwood for insisting I actually come and see the material. Steve Churchill, Ossie Pearson, and Brian Richmond provided helpful comments on a different version of this manuscript, although this does not mean they necessarily endorse my interpretations of the material. Financial support for the project came in part from NSF grant BCS-0509190, and from a grant to Mike Morwood from the Australian Research Council.

REFERENCES

1 Morwood MJ, Brown P, Jatmiko, Sutikna T, Wahuy Saptomo E, Westaway KE, Awe Due R, Roberts RG, Maeda T, Wasisto S, Djubiantono T. 2005. Further evidence for small-bodied hominins from the Late Pleistocene of Flores, Indonesia. Nature 437:1012–1017.

2 Larson SG, Jungers WL, Morwood M, Sutikna T, Jatmiko, Saptomo EW, Due RA, Djubiantono T. n.d. *Homo floresiensis* and the evolution of the hominin shoulder. J Hum Evol. In press.

3 Le Gros Clark WE. 1959. The antecedents of man. Edinburgh: Edinburgh University Press.

4 Andrews P. 1985. Family group systematics and evolution among catarrhine primates. In: Delson E, editor. Ancestors: the hard evidence. New York: Alan R. Liss. p 14–22.

5 Martin L. 1986. Relationships among extant and extinct great apes and humans. In: Wood B, Martin L, Andrews P, editors. Major topics in primate and human evolution. Cambridge: Cambridge University Press. p 161–187.

6 Harrison T. 1987. The phylogenetic relationships of the early catarrhine primates: a review of the current evidence. J Hum Evol 16:41–80.

7 Alemseged A, Spoor F, Kimbel WH, Bobe R, Geraads D, Reed D, Wynn JG. 2006. A juvenile early hominin skeleton from Dikika, Ethiopia. Nature 443:296–301.

8 Caccone A, Powell JR. 1989. DNA divergence among hominoids. Evolution 43:925–942.

9 Goodman M, Tagle DA, Fitch DHA, Bailey W, Czelusniak J, Koop BF, Benson P, Slightom JL. 1990. Primate evolution at the DNA level and a classification of hominoids. J Mol Evol 30:260–266.

10 Horai S, Satta Y, Hayasaka K, Kondo R, Inoue T, Ishida T, Hayashi S. 1992. Man's place in Hominoidea revealed by mitochondrial DNA geneology. J Mol Evol 35:32–43.

11 Ruvolo M. 1994. Molecular evolutionary processes and conflicting gene trees: the hominoid case. Am J Phys Anthropol 94:89–113.

12 Li W-H, Saunders MA. 2005. The chimpanzee and us. Nature 437:50–51.

13 Patterson N, Richter DJ, Gnerre S, Lander ES, Reich D. 2006. Genetic evidence for complex speciation of humans and chimpanzees. Nature 441:1103–1108.

14 Lovejoy CO, Johanson DC, Coppens Y. 1982. Hominid upper limb bones recovered from the Hadar formation: 1974–1977 collections. Am J Phys Anthropol 57:637–649.

15 Ohman JC. 1986. The first rib of hominoids. Am J Phys Anthropol 70:209–229.

16 Voisin J-L. 2006. Clavicle, a neglected bone: morphology and relation to arm movements and shoulder architecture in primates. Anat Rec 288A:944–953.

17 Partridge TC, Granger DE, Caffee MW, Clarke RJ. 2003. Lower Pliocene hominid remains from Sterkfontein. Science 300:607–612.

18 Broom R, Robinson JT, Schepers GWH. 1950. Sterkfontein ape-men *Plesianthropus*.

Transvaal Mus Mem No. 4.

19 Johanson DC, Lovejoy CO, Kimbel WH, White TD, Ward SC, Bush ME, Latimer BM, Coppens Y. 1982. Morphology of the Pliocene partial hominid skeleton (A.L. 288-1) from the Hadar Formation, Ethiopia. Am J Phys Anthropol 57:403–451.

20 Campbell BG. 1966. Human evolution. London: Heinemann.

21 Oxnard CE. 1968. A note on the fragmentary Sterkfontein scapula. Am J Phys Anthropol 28:213–217.

22 Robinson JT. 1972. Early hominid posture and locomotion. Chicago: University of Chicago Press.

23 Vrba ES. 1979. A new study of the scapula of *Australopithecus africanus* from Sterkfontein. Am J Phys Anthropol 51:117–130.

24 Stern JT Jr, Susman RL. 1983. The locomotor anatomy of *Australopithecus afarensis*. Am J Phys Anthropol 60:279–317.

25 Inouye SE, Shea BT. 1997. What's your angle? Size correction and bar-glenoid orientation in "Lucy" (A.L. 288-1). Int J Primatol 18:629–650.

26 Roberts D. 1974. Structure and function of the primate scapula. In: Jenkins FA, editor. Primate locomotion. New York: Academic Press. p 171–200.

27 Ciochon RL, Corruccini RS. 1976. Shoulder joint of Sterkfontein *Australopithecus*. S Afr J Sci 72:80–82.

28 Larson SG. 1995. New characters for the functional interpretation of primate scapulae and proximal humeri. Am J Phys Anthropol 98:13–35.

29 Pickford M, Johanson DC, Lovejoy CO, White TD, Aronson JL. 1983. A hominoid humeral fragment from the Pliocene of Kenya. Am J Phys Anthropol 60:337–346.

30 Evans FG, Krahl VE. 1945. The torsion of the humerus: a phylogenetic study from fish to man. Am J Anat 76:303–337.

31 Krahl VE. 1947. The torsion of the humerus: its localization, cause and duration in man. Am J Anat 80:275–319.

32 Larson SG. 1996. Estimating humeral torsion on incomplete fossil anthropoid humeri. J Hum Evol 31:239–257.

33 Larson SG. 1988. Subscapularis function in gibbons and chimpanzees: implications for interpretation of humeral head torsion in hominoids. Am J Phys Anthropol 76:449–462.

34 Schmid P. 1983. Eine Rekonstruktion des Skelettes von A.L. 288-1 (Hadar) und deren Konsequenzen. Folia Primatol 40:283–306.

35 Napier JR. 1965. Comment on "new discoveries in Tanganyika: their bearing on hominid evolution" by PV Tobias. Curr Anthropol 5:402–403.

36 Oxnard CE. 1969. A note on the Olduvai clavicular fragment. Am J Phys Anthropol 29:429–432.

37 Day M. 1978. Hominid postcranial material from Bed I, Olduvai Gorge. In: Isaac GL, McCown ER, editors. Human origins: Louis Leakey and the East African evidence. Menlo Park: WA Benjamin. p 363–374.

38 Voisin J-L. 2001. Évolution de la morphologie claviculaire au sein du genre *Homo*. conséquences architecturales et fonctionnells sur la ceinture scapulaire. L'Anthropol 105:449–468.

39 Leakey RE, Walker A, Ward CV, Grausz HM. 1989. A partial skeleton of a gracile hominid from the upper Burgi member of the Koobi Fora formation, East Lake Turkana, Kenya. In: Giacobini G, editor. Hominidae. Proceedings of the 2nd International Congress of Human Paleontology. Milano: Jaka Books. p 167–173.

40 Latimer B, Ohman JC. 2001. Axial dysplasia in *Homo erectus*. Abstracts of Paleoanthropology Society meeting. p 9.

41 Latimer B, Ward CV. 1993. The thoracic and lumbar vertebrae. In: Leakey R, Walker A, editors. The Nariokotome *Homo erectus* skeleton. Cambridge: Harvard University Press. p 266–293.

42 MacLarnon A. 1993. The vertebral canal. In: Leakey R, Walker A, editors. The Nariokotome *Homo erectus* skeleton. Cambridge: Harvard University Press. p 359–390.

43 Walker A, Leakey RE. 1993. The postcranial bones. In: Leakey R, Walker A, editors. The Nariokotome *Homo erectus* skeleton. Cambridge: Harvard University Press. p 95–160.

44 Jungers WL. 1994. Ape and hominid limb length. Nature 369:194.

45 Larson SG. n.d. Evolution of the hominin shoulder: early Homo. In: Grine FE, Leakey RE, editors. The first humans: origins of the genus Homo. Vertebrate Paleobiology and Paleoanthropology Series. New York: Springer.

46 Jungers WL, Hartman SE. 1988. Relative growth of the locomotor skeleton in orangutans and other large-bodied hominoids. In: Schwartz JE, editor. Orang-utan biology. Oxford: Oxford University Press. p 347–359.

47 Jellema LM, Latimer B, Walker A. 1993. The rib cage. In: Leakey R, Walker A, editors. The Nariokotome *Homo erectus* skeleton. Cambridge: Harvard University Press. p 294–325.

48 Milgram JE. 1942. Congenital forward shoulders (quadrupedal type): treatment by clavicular osteotomy. Bull Hosp Joint Dis 3:93–96.

49 Guidera KJ, Grogan DP, Pugh L, Ogden JA. 1991. Hypoplastic clavicles and lateral scapular redirection. J Pediatr Orthop 11:523–526.

50 Beals RK. 2000. The short clavicle syndrome. J Pediatr Orthop 30:389–391.

51 Beals RK, Sauser DD. 2006. Nontraumatic disorders of the clavicle. J Am Acad Orthop Surg 14:205–214.

52 Edelson G. 1999. Variations in the retroversion of the humeral head. J Shoulder Elbow Surg 8:142–145.

53 Edelson G. 2000. The development of humeral head retroversion. J Shoulder Elbow Surg 9:316–318.

54 Fischman J. 2005. Family ties. Natl Geogr 207:16–27.

55 Rightmire GP, Lordkipanidze D, Vekua A. 2006. Anatomical descriptions, comparative studies and evolutionary significance of the hominin skulls from Dmanisi, Republic of Georgia. J Hum Evol 50:115–141.

56 Carretero JM, Larenzo D, and Arsuaga JL. 1999. Axial and appendicular skeleton of *Homo antecessor*. J Hum Evol 37:459–499.

57 Bermúdez de Castro JM, Arsuaga JL, Carbonell E, Rosas A, Martinez I, Mosquera M. 1997. A hominid from the lower Pleistocene of Atapuerca, Spain: possible ancestor to Neandertals and modern humans. Science 276:1392–1395.

58 Carretero JM, Arsuaga JL, Lorenzo C. 1997. Clavicles, scapulae and humeri from the Sima de los Huesos site (Sierra de Atapuerca, Spain). J Hum Evol 33:357–408.

59 Arsuaga JL, Martinez I, Garcia A, Lorenzo C. 1997. The Sima de los Huersos crania (Sierra de Atapuerca, Spain): a comparative study. J Hum Evol 33:219–281.

60 Trinkaus E. 1983. The Shanidar Neandertals. New York: Academic Press.

61 Vandermeersch B, Trinkaus E. 1995. The postcranial remains of the Régourdou 1 Neandertal: the shoulder and arm remains. J Hum Evol 28:439–476.

62 Trinkaus E. 1977. A functional interpretation of the axillary border of the Neandertal scapula. J Hum Evol 6:231–234.

63 Churchill SE, Trinkaus E. 1990. Neandertal scapular glenoid morphology. Am J Phys Anthropol 83:147–160.

64 Churchill SE. 1994. Human upper body evolution in the Eurasian later Pleistocene. Ph.D. dissertation. University of New Mexico.

65 Churchill SE. 1996. Particulate versus integrated evolution of the upper body in Late Pleistocene humans: a test of two models. Am J Phys Anthropol 100:559–583.

66 van der Made J. 1999. Ungulates from Atapuerca TD6. J Hum Evol 37:389–413.

67 Krahl VE, Evans FG. 1945. Humeral torsion in man. Am J Phys Anthropol 3:229–252.

68 Martin CP. 1933. The cause of torsion of the humerus and the notch of the anterior edge of the glenoid cavity of the scapula. J Anat 67:573–582.

69 Pieper H-P. 1998. Humeral torsion in the throwing arm of handball players. Am J Sports Med 26:247–253.

70 Crockett HG, Gross LB, Wilk KE, Schwartz ML, Reed J, O'Mara J, Reilly MT, Dugas JR, Meister K, Lyman S, Andrews JR. 2002. Osseous adaptation and range of motion at the glenohumeral joint in professional baseball pitchers. Am J Sports Med 30:20–26.

71 Reagan KM, Meister K, Horodyski MB, Werner DW, Carruthers C, Wilk K. 2002. Humeral retroversion and its relationship to glenohumeral rotation in the shoulder of college baseball players. Am J Sports Med 30:354–360.

72 Osbahr DC, Cannon DL, Peer KP. 2002. Retroversion of the humerus in the throwing shoulder of college baseball pitchers. Am J Sports Med 30:347–353.

73 Tullos HS, King JW. 1973. Throwing mechanisms in sports. Orthop Clin North America 4:709–720.

74 Atwater AE. 1979. Biomechanics of overarm throwing movements and of throwing injuries. Exercise Sport Sci Rev 7:43–85.

75 Perry J. 1983. Anatomy and biomechanics of the shoulder in throwing, swimming, gymnastics, and tennis. Clin Sports Med 2:247–270.

76 Kronberg M, Broström L-Å, Söderlung V. 1990. Retroversion of the humeral head in the normal shoulder and its relationship to the normal range of motion. Clin Orthop Related Res 253:113–117.

77 Rhodes JA. 2006. Adaptations to humeral torsion in medieval Britain. Am J Phys Anthropol 130:160–166.

78 Ciochon RL. 1983. Hominoid cladistics and the ancestry of modern apes and humans. In: Corruccini RS, Ciochon RL, editors. New interpretations of ape and human ancestry. New York: Academic Press. p 783–843.

79 Napier JR, Napier PH. 1967. A handbook of living primates. New York: Academic Press.

80 Schultz AH. 1968. The recent hominoid primates. In: Washburn SL, Jay PC, editors. Perspectives on human evolution. New York: Holt, Rinehard, and Winston. p 122–195.

81 Andrews P, Groves CP. 1976. Gibbons and brachiation. In: Rumbaugh DM, editor. Gibbon and Siamang, vol 4. Basel: Karger. p 167–218.

82 Stern JT Jr. 2000. Climbing to the top: a personal memoir of *Australopithecus afarensis*. Evol Anthropol 9:113–133.

83 Darlington PJ. 1975. Group selection, altruism, reinforcement, and throwing in human evolution. Proc Nat Acad Sci 72:3748–3752.

84 Calvin WH. 1983. A stone's throw and its launch window: timing and precision and its implications for language and hominid brains. J Theor Biol 104:121–135.

85 Bingham PM. 1999. Human uniqueness: a general theory. Q Rev Biol 74:133–169.

86 Dunsworth H, Challis JH, Walker A. 2003. Throwing and bipedalism: a new look at an old idea. Cour Forsch-Inst Senckenberg 243:105–110.

87 Preuschoft H. 2004. Mechanisms for the acquisition of habitual bipedality: are there biomechanical reasons for the acquisition of upright bipedal posture. J Anat 204: 363–384.

88 Thieme H. 1997. Lower Palaeolithic hunting spears from Germany. Nature 385:807–810.

89 Carrier DR. 1984. The energetic paradox of human running and hominid evolution. Curr Anthropol 25:483–495.

90 Bramble DM, Lieberman DE. 2004. Endurance running and the evolution of *Homo*. Nature 432:345–352.

91 Brown P, Sutikna T, Morwood MJ, Soejono RP, Jatmiko, Wayhu Saptomo E, Awe Due R. 2004. A new small-bodied hominin from the Late Pleistocene of Flores, Indonesia. Nature 431:1055–1061.

92 Weber J, Czarnetzki A, Pusch CM. 2005. Comment on "The brain of LB1, *Homo floresiensis*." Science 310:236b.

93 Jacob T, Indriati E, Soejono RP, Hsü K, Frayer DW, Eckhardt RB, Kuperavage AJ, Thorne A, Henneberg M. 2006. Pygmoid Australomelanesian *Homo sapiens* skeletal remains from Liang Bua, Flores: population affinities and pathological abnormalities. Proc Nat Acad Sci USA 103:13421–13426.

94 Martin RD, MacLarnon AM, Phillips JL, Dussubieux L, Williams PR, Dobyns WB. 2006. Comment on "The brain of LB1, *Homo floresiensis*." Science 312:999b (full text at www.sciencemag.org/cgi/content/full/312/5776/999b).

95 Martin RD, MacLarnon AM, Phillips JL, Dobyns WB. 2006. Flores hominid: new species or microcephalic dwarf? Anat Rec 288A:1123–1145.

96 Richards GD. 2006. Genetic, physiologic and ecogeographic factors contributing to variation in *Homo sapiens: Homo floresiensis* reconsidered. J Evol Biol 19:1744–1767.

97 Falk D, Hildebolt C, Smith K, Morwood MJ, Sutikna T, Brown P, Jatmiko, Saptomo EW, Brunsden B, Prior F. 2005. The brain of LB1, *Homo floresiensis*. Science 308:242–245.

98 Falk D, Hildebolt C, Smith K, Morwood MJ, Sutikna T, Jatmiko, Saptomo EW, Brunsden B, Prior F. 2005. Response to comment on "The brain of LB1, *Homo floresiensis*." Science 310:236c.

99 Falk D, Hildebolt C, Smith K, Morwood MJ, Sutikna T, Jatmiko, Saptomo EW, Brunsden B, Prior F. 2006. Response to comment on "The brain of LB1, *Homo floresiensis*." Science 312:999c (full text: www.sciencemag.org/cgi/content/full/312/5776/999c).

100 Falk D, Hildebolt C, Smith K, Morwood MJ, Sutikna T, Jatmiko, Saptomo EW, Imhof H, Seidler H, Prior F. 2007. Brain shape in human microcephalics and *Homo floresiensis*. Proc Nat Acad Sci USA 104:2513–2518.

101 Zumwalt A. 2006. The effect of endurance exercise on the morphology of muscle attachment sites. J Exp Biol 209:444–454.

102 Larson SG, Jungers WL, Morwood MJ, Sutikna T, Jatmiko, Saptomo EW, Due RA, Djubiantono T. 2007. Misconceptions about the postcranial skeleton of *Homo floresiensis*. Am J Phys Anthropol S44:151.

103 Jungers WL, Sutikna T, Jatmiko, Saptomo EW, Awe Due R, Djubiantono T, Morwood M. 2006. Body size and shape in *Homo floresiensis* and pygmy humans. African genesis: a symposium on hominid evolution in Africa. p 14.

104 Hershkovitz I, Kornreich L, Laron Z. 2007. Comparative skeletal features between *Homo floresiensis* and patients with primary growth hormone insensitivity (Laron Syndrome). Am J Phys Anthropol 134:198–208.

105 Laron Z. 2004. Laron syndrome (primary growth hormone resistance or insensitivity): the personal experience 1958–2003. J Clin Endocrin Metab 89:1031–1044.

106 Jungers WL, Larson SG, Harcourt-Smith W, Morwood MJ, Sutikna T, Due RA, Djubiantono T. n.d. Descriptions of the lower limb skeleton of *Homo floresiensis*. J Hum Evol. Submitted.

107 Argue D, Donlon D, Groves C, Wright R. 2006. *Homo floresiensis*: microcephalic, pygmoid, *Australopithecus*, or *Homo*? J Hum Evol 51:360–374.

108 Tocheri MW, Orr CM, Larson SG, Sutikna T, Jatmiko, Saptomo EW, Due RA, Djubiantono T, Morwood MJ, Jungers WL. 2007. The primitive wrist of *Homo floresiensis* and its implications for hominin evolution. Science. 317:1743–1745.

109 Gundling T. 2007. The taxonomy of the Flores hominin: an historical perspective. Am J Phys Anthropol 44(suppl):122.

110 Mivart St G. 1868. On the appendicular skeleton of the primates. Philos Trans R Soc London 157:299–426.

111 Angel JL, Kelley JO. 1986. Description and comparison of the skeleton. In: Wendorf F, Schild, R, editors. The Wadi Kubbaniya skeleton: a late Paleolithic burial from Southern Egypt. Dallas: Southern Methodist University Press. p 53–70.

112 Sládek V, Trinkuas E, Hillson SW, Holliday TW. 2000. The people of the Pavlovian: skeletal catalogue and osteometrics of the Gravettian fossil hominids from Dolní Věstonice and Pavlov. Brno: Academy of Sciences of the Czech Republic.

113 McCown TD, Keith A. 1939. The Stone Age of Mount Carmel: the fossil human remains from the Levalloiso-Mousterian. Oxford: Clarendon Press.

114 Harrison T. 1986. A reassessment of the phylogenetic relationships of *Oreopithecus bambolii* Gervais. J Hum Evol 15:541–583.

115 Lordkipanidze D, Jashashvili T, Vekua A, Ponce de Leon MS, Zollikofer CPE, Rightmire GP, Pontzer H, Ferring R, Oms O, Tappen M, Bukhsianidze M, Agusti J, Kahlke R, Kiladze G, Martinez-Navarro B, Mouskhelishvilli A, Nioradze M, Rook L. 2007. Postcranial evidence from early *Homo* from Dmanisi, Georgia. Nature 449:305–309.

Available online at www.sciencedirect.com
ScienceDirect
Journal of Human Evolution 53 (2007) 6–25

Metric and morphological study of the upper cervical spine from the Sima de los Huesos site (Sierra de Atapuerca, Burgos, Spain)

Asier Gómez-Olivencia [a,b,*], José Miguel Carretero [a,b], Juan Luis Arsuaga [b,c], Laura Rodríguez-García [a,b], Rebeca García-González [a,b], Ignacio Martínez [b,d]

[a] *Laboratorio de Evolución Humana. Dpto. de Ciencias Históricas y Geografía. Universidad de Burgos. Edificio I+D+i. Plaza Misael de Bañuelos s/n. 09001 Burgos, Spain*
[b] *Centro UCM-ISCIII de Investigación sobre Evolución y Comportamiento Humanos, c/Sinesio Delgado, 4 (Pabellón 14), 28029 Madrid, Spain*
[c] *Departamento de Paleontología, Facultad de Ciencias Geológicas, Universidad Complutense de Madrid, Ciudad Universitaria s/n, 28040 Madrid, Spain*
[d] *Departamento de Geología, Universidad de Alcalá, Edificio de Ciencias, Campus Universitario, 28871 Alcalá de Henares, Spain*

Received 22 February 2006; accepted 21 December 2006

Abstract

In this article, the upper cervical spine remains recovered from the Sima de los Huesos (SH) middle Pleistocene site in the Sierra de Atapuerca (Burgos, Spain) are described and analyzed. To date, this site has yielded more than 5000 human fossils belonging to a minimum of 28 individuals of the species *Homo heidelbergensis*. At least eleven individuals are represented by the upper cervical (C1 and C2) specimens: six adults and five subadults, one of which could represent an adolescent individual. The most complete adult vertebrae (three atlases and three axes) are described, measured, and compared with other fossil hominins and modern humans. These six specimens are associated with one another and represent three individuals. In addition, one of these sets of cervical vertebrae is associated with Cranium 5 (Individual XXI) from the site. The metric analysis demonstrates that the Sima de los Huesos atlases and axes are metrically more similar to Neandertals than to our modern human comparative sample. The SH atlases share with Neandertals a sagittally elongated canal. The most remarkable feature of the SH (and Neandertal) axes is that they are craniocaudally low and mediolaterally wide compared to our modern male sample. Morphologically, the SH sample shares with Neandertals a higher frequency of caudally projected anterior atlas arch, which could reflect greater development of the longus colli muscle. In other features, such as the frequency of weakly developed tubercles for the attachment of the transverse ligament of the atlas, the Sima de los Huesos fossils show intermediate frequencies between our modern comparative samples and the Neandertals, which could represent the primitive condition. Our results are consistent with the previous phylogenetic interpretation of *H. heidelbergensis* as an exclusively European species, ancestral only to *H. neanderthalensis*.

Keywords: Atlas; Axis; Cervical vertebrae; Middle Pleistocene; Sima de los Huesos

Introduction

The Sima de los Huesos (SH) site is approximately 0.5 km from the Cueva Mayor entrance, well inside the Cueva Mayor–Cueva del Silo cave system in the Sierra de Atapuerca in northern Spain (Arsuaga et al., 1997b). To date, more than 5000 fossil human remains have been recovered from the site (Arsuaga and Martínez, 2004) in the excavations directed by one of us (JLA). Based on dental evidence, these remains belong to a minimum number of 28 individuals (Bermúdez de Castro et al., 2004) of both sexes and diverse ages. In addition, thousands of carnivore bones have been recovered mixed with and stratigraphically above the human fossils (García et al., 1997; García, 2002). All anatomical parts of the skeleton are represented among the human remains, suggesting that

* Corresponding author. Laboratorio de Evolución Humana, Dpto. de Ciencias Históricas y Geografía, Universidad de Burgos, Edificio I+D+I, Plaza Misael de Bañuelos s/n, 09001 Burgos, Spain. Tel.: +34 947 25 93 24.
E-mail address: agolivencia@ubu.es (A. Gómez-Olivencia).

0047-2484/$ - see front matter © 2007 Elsevier Ltd. All rights reserved.
doi:10.1016/j.jhevol.2006.12.006

complete corpses were accumulated at this site. The age-at-death distribution suggests that a nonattritional demographic event affected this living population (Bocquet-Appel and Arsuaga, 1999; Bermúdez de Castro et al., 2004). The origin of the human accumulation is most likely to be anthropogenic (Arsuaga et al., 1997b). A recently discovered handaxe has been interpreted as evidence of symbolic behavior in these early humans (Carbonell et al., 2003).

A recently found in situ speleothem (SRA-3), which seals the human-fossil-bearing sediments throughout the site, has been dated. There is a hiatus in the speleothem growth at about 4 cm below the top. This upper portion shows a linear growth rate of about 1 cm per 32,000 years. Ten dates have been obtained in the lower 10 cm of speleothem below the hiatus, all of which indicate a minimum age of 350 ka, although this thickness could represent a significant amount of time beyond this date. Thus, a range of 400–500 ka has been proposed for the human remains (Bischoff et al., 2003). These dates are compatible with both the micro- and macromammalian assemblages (Cuenca-Bescós et al., 1997; García et al., 1997; García, 2002). Bischoff et al. (2006) recently published a reanalysis of six samples of SRA-3 using inductively coupled plasma-multicollector mass-spectrometry (ICP-MS), which yielded new dates that cluster around 600 ka, with an estimated minimum age of the speleothem, and thus of the underlying human fossils, of 530 ka.

The human remains from this site have been assigned to *Homo heidelbergensis*. This species, in our view, is exclusively European, and is ancestral only to the later Neandertals (Arsuaga et al., 1991, 1997c; Carretero et al., 1997; Martínez and Arsuaga, 1997).

The record of the upper cervical vertebral column is relatively abundant for *Homo neanderthalensis* and late Pleistocene *Homo sapiens*, but with respect to the rest of the genus *Homo*, it is scarce or nonexistent.[1] The virtual absence of a fossil record of the upper cervical spine for the middle Pleistocene underscores the importance of the SH specimens described and analyzed here.

Regarding the Neandertals, the most conspicuous traits described for the atlas vertebra (C1) are (1) weakly developed tubercles for the insertion of the transverse ligament and (2) a caudal projection of the anterior tubercle (Boule, 1911–1913; Martin, 1923; Heim, 1976; Arensburg, 1991); for the Neandertal axis (C2) no trait or pattern has been highlighted except its great morphological variability (Piveteau, 1966). In his study of the cervical spine of the Kebara 2 Neandertal individual, Arensburg (1991) concluded that, except for the horizontal spinous process of the C6 and C7, the cervical column seemed to be within the range of variation of modern human populations. Nevertheless, the study of the middle Pleistocene SH upper cervical vertebrae (C1 and C2) may reveal some previously undocumented morphological features and/or patterns of variation within the Neandertal evolutionary lineage.

The first part of the study comprises the inventory of all the atlases and axes, with the determination (if possible) of the age at death (Tables 3 and 4) and the minimum number of individuals represented among the remains. A brief description of the most complete adult vertebrae is also provided. In the second part, we perform a metrical analysis of the adult vertebrae and compare the anatomical features present in the SH specimens with those found in other samples of *Homo*, especially *H. neanderthalensis* and *H. sapiens*.

Materials

The SH vertebral sample comprises 455 fossils that represent at least 180 vertebrae. The cervical sample consists of 116 fossils (Gómez-Olivencia, 2005), including 22 first cervical vertebrae (atlas) and 16 second cervical vertebrae (axis). The present study includes the atlas (C1) and axis (C2) remains recovered up through the 2004 field season. An inventory and photographic documentation of all the fossil material, as well as short descriptions and metrical data of the most complete adult vertebrae, are provided.

Descriptions of a few of the cervical vertebrae [including the atlas VC3 (AT-1554) and a general description of the SH cervical vertebrae] have been published previously (Carretero et al., 1999; Gómez et al., 2005). The present study provides a detailed analysis of the SH upper cervical spine. Appendix 1 provides information on the labeling of the SH vertebrae.

For comparative purposes we have studied a large sample of modern human skeletons and fossil hominin specimens from the following species: *H. antecessor*, *H. neanderthalensis*, and late Pleistocene *H. sapiens* (Table 1). Although remains of the atlas and axis are also known from the Mousterian site of Qafzeh (Vandermeersch, 1981), their fragmentary nature makes comparison with these specimens difficult. Data for the following specimens have been taken from the literature: Kebara 2 (Arensburg et al., 1990; Arensburg, 1991), Régourdou 1 (Piveteau, 1966), Shanidar 2 and 4 (Stewart, 1962; Trinkaus, 1983), Subalyuk (Pap et al., 1996), and Dolní Věstonice 14 (Sládek et al., 2000).

Methods

We used standard anthropometric techniques and instruments to take all measurements. The metric variables are illustrated in Fig. 1. Following Meyer (2005), the areas of vertebral canals were measured on scaled digital images and cross-checked for accuracy by comparing imaged linear measurements to physical dimensions measured with digital calipers. This method avoids the considerable error of area estimation by simply multiplying the dorsoventral and transverse diameters of the neural canal (Meyer, 2005). Vertebral-canal areas were measured on cranial (atlas) and caudal (axis) photographs using CAD software and cross-checked using the canal's maximum transverse diameter (M11). For the atlas, the photograph was taken in superior view.

[1] The exceptions are the specimens from Dmanisi (Meyer, 2005), Gran Dolina (Carretero et al., 1999), and Koobi Fora (KNM-ER 1808; Walker et al., 1982; Leakey and Walker, 1985) for the early Pleistocene and, for the middle Pleistocene, the atlas from the Zhoukoudian I1 individual (Boaz et al., 2004).

Table 1
Comparative specimens and samples of atlases and axes measured by the authors

Specimen/sample	Species	Sex	Original/cast	Location
ATD6-90 (C1)	*H. antecessor*	Female	Original	Museo de Burgos, Burgos (Spain)
Krapina (C1, $n = 3$; C2, $n = 3$)	*H. neanderthalensis*	?	Original	Croatian Natural History Museum, Zagreb (Croatia)
La Chapelle-aux-Saints (C1 and C2)	*H. neanderthalensis*	Male	Original	Musée de l'Homme, Paris (France)
La Ferrassie 1 (C1 and C2)	*H. neanderthalensis*	Male	Original	Musée de l'Homme, Paris (France)
Shanidar 2 (C1 and C2)	*H. neanderthalensis*	Male	Cast	Musée de l'Homme, Paris (France)
Skhul V (C1 and C2)	*H. sapiens*	Male	Original	Peabody Museum of Archaeology and Ethnology, Cambridge (MA, USA)
Arcy-sur-Cure, Grotte des Fées (C1 and C2)	*H. sapiens* (?)[1]	?	Original (C1) Cast (C2)	Musée de l'Homme, Paris (France) (C1) Institut de Paléontologie Humaine, Paris (France) (C2)
Cro-Magnon (C1)	*H. sapiens*	Male	Original	Musée de l'Homme, Paris (France)
Carolingian[2] (C2, $n = 4$)	*H. sapiens*	?	Original	Musée de l'Homme, Paris (France)
Neolithic[3] (C2, $n = 2$)	*H. sapiens*	?	Original	Musée de l'Homme, Paris (France)
Afalou-Bou-Rhummel[4] (C1, $n = 12$; C2, $n = 10$)	*H. sapiens*	?	Original	Institut de Paléontologie Humaine, Paris (France)
Taforalt[5] (C1, $n = 8$; C2, $n = 9$)	*H. sapiens*	?	Original	Institut de Paléontologie Humaine, Paris (France)
Burgos[6] ($n = 40$)	*H. sapiens*	Males	Original	Laboratorio de Evolución Humana-University of Burgos, Burgos (Spain)
Hamman-Todd[7] ($n = 101$)	*H. sapiens*	50 males/51 females	Original	Cleveland Museum of Natural History, Cleveland (OH, USA)

[1] The Arcy-sur-Cure atlas was found in 1860 in the lower level of the Grotte des Fées, (Yonne, France). The axis was found in 1898 in the clearings of older excavations (Leroi-Gourhan, 1958). Leroi-Gourhan (1958) identified both specimens as Neandertal. In the case of the axis, the taxonomic assignment was based on the surface color of the fossil; Leroi-Gourhan pointed out that this specimen is within the modern human range of variation but that it resembles Neandertals in its weak cervical curvature. In the case of the atlas, he did not find any trait to distinguish it from modern humans. Due to the problematic provenience of both specimens and the fact that these fossils are morphologically more similar to our modern human comparative samples than to Neandertals, they should be cautiously considered as representing *H. sapiens*.

[2] The Carolingian sample comes from the Saint-Germain-des-Prés cementery (Paris, France).

[3] The Neolithic sample comes from a cave site in the Petit Morin Valley (France).

[4] The Afalou-Bou-Rhummel sample was recovered from the homonymous rock-shelter in Algeria. This sample and the Taforalt sample are dated to >10,000 BP (see Irish, 2000, and references therein).

[5] The Taforalt sample was recovered from the homonymous cave site in Morocco.

[6] The Burgos sample comprises 40 contemporary adult (estimated age at death is 20–45 years) male individuals from Burgos, Spain.

[7] The Hamann-Todd sample comprises 100 North American adults (50 Euro-Americans and 50 Afro-Americans, with equal sexual representation) from the Hamann-Todd Osteological Collection.

Univariate comparative analysis was performed on all of the variables measured in the atlases and axes. Bivariate analysis was performed on the vertebral-canal variables (M10 and M11) in both C1 and C2, and the M1a and STrD measurements in the axes. We used nonparametric methods in cases where one or more of the groups had a sample size of $n < 10$. For the univariate analysis, we performed a Kruskal–Wallis test to compare the differences between the SH, Neandertal, and Burgos modern human samples. When a significant difference ($p < 0.05$) was found in a variable, we performed a Mann–Whitney test between all possible pairs of samples to determine which ones were significantly different. We adjusted the *p*-values for these comparisons using the Bonferroni method and have reported all the cases in which $p < 0.10$.

Inventory

Here we provide an inventory of all the atlas and axis remains. These fossils are listed in Tables 2 and 3 and depicted in Figs. 2–5. The SH upper cervical sample comprises 22 atlas specimens and 16 axis specimens.

Age at death

The age at death has been estimated for the SH cervical vertebrae (Tables 2 and 3) based on modern human patterns of maturation (i.e., fusion of the principal centers of ossification, presence/absence of the epiphyseal rings, and degree of obliteration of the metaphyseal scars). However, since the SH hominins had a shorter period of dental growth (Ramírez Rozzi and Bermúdez de Castro, 2004), the ages at death might be overestimated if tooth formation is correlated with somatic development, as proposed by Smith (1991).

Given the difficulty of assigning a precise age at death based on the ossification patterns of the atlas (except in limited circumstances), these specimens are classified as adult or subadult. The atlas's principal centers of ossification are fused by the sixth year of life (Scheuer and Black, 2000). Additional attention was given to the surface of the articular facets for the determination of the age at death, since immature individuals show a more porous surface. In the Atapuerca sample, the VC3 atlas shows a partially obliterated metaphyseal scar on its transverse processes. This feature is consistent with the

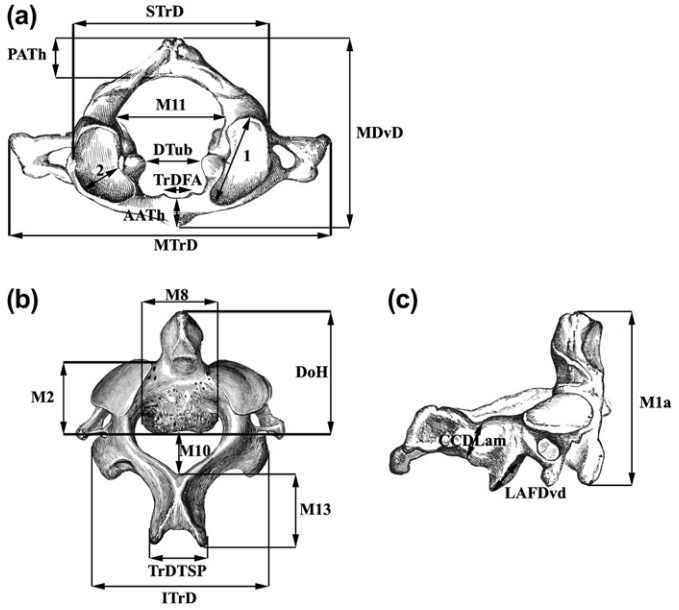

Fig. 1. Some of the dimensions used in the osteometric analysis, as defined in the text: (a) atlas (C1) in cranial view; (b) axis (C2) in craniodorsal view; (c) axis (C2) in lateral view. Drawings modified from Gray (1959). (1) Diameters in major axis of upper articular facets (UAFMAD) (right-left); (2) diameter at a right angle to the major axis of upper articular facets (UAFTrD) (right-left); anterior arch thickness at the level of the anterior tubercle (AATh); craniocaudal diameter of laminae (CCDLam) (right-left); total vertebral dorsal height (DoH); distance between the tubercles for the attachment of the transverse ligament (DTub); inferior transverse diameter (ITrD); lower articular facet dorsoventral diameter (LAFDvD) (right-left); total vertebral ventral height (M1a); body craniocaudal dorsal diameter (M2); body inferior transverse diameter (M8); canal dorsoventral maximum diameter (M10); canal transverse maximum diameter (M11); spine length (M13); maximum dorsoventral diameter (MDvD); maximum transverse diameter (MTrD); posterior arch thickness at the level of the posterior tubercle (PATh); superior transverse diameter (STrD); transverse diameter of the facet for the axis (TrDFA); maximum transverse diameter of the tip of the spinous process (TrDTSP). The following variables have not been drawn: body inferior anteroposterior diameter (M5), taken perpendicular to M8; upper articular facet dorsoventral diameter of the axis (UAFDvD) (right-left); upper articular facet transverse diameter of the axis (UAFTrD) (right-left); lower articular facet transverse diameter (LAFTrD) (right-left), taken perpendicular to LAFDvD; thickness of the laminae (ThLam), taken perpendicular to CCDLam; anterior arch height at the level of the anterior tubercle (AAH), taken perpendicular to AATh; maximum height of lateral masses (right-left) (MHLM), taken at the lateral edges of the lateral masses of the atlas; posterior arch height at the level of the posterior tubercle (PAH), taken perpendicular to PATh; height of the posterior arch in the groove for the vertebral artery (HPAG) (right-left). M# refers to the Martin number (Bräuer, 1988) and variable definition. In the axes, M10 has been measured on the caudal aspect of the vertebral foramen.

age at death estimated (21–25 years) for the associated vertebra VC4(C2). The left mass AT-2078 exhibits the immature appearance on the surface of both articular facets, while VC17 only exhibits this appearance in the upper articular facet.

In contrast to the atlas, the complex ossification pattern of the axis allows for more precise age-at-death estimates. The axis ossifies from five primary centers: one for the body, one for each half of the dens, and one for each half of the neural arch. The halves that form the dens are already fused at birth, whereas the neural arch is fused by the third or fourth year and the body is joined to the other elements by the fifth or sixth year of life. The axis has five secondary centers of ossification: two for the transverse processes; the *ossiculum terminale*, which fuses at the end of the dens by the twelfth year; one for the spine; and an inferior epiphyseal ring, which fuses to the caudal part of the body (Scheuer and Black, 2000). Buikstra et al. (1984) reported that the fusion of the inferior epiphyseal ring commences by 17–19 years and is completed by the twenty-fifth year in their female sample from the Terry Collection. Both VC4 and VC28 show a partial fusion of the caudal epiphyseal ring. Nevertheless, VC4 shows a more advanced state of fusion, so it could belong to an individual who was older than VC28.

Minimum number of individuals

A minimum of 28 individuals, based on the dental remains, have been identified among the SH human fossils (Bermúdez de Castro et al., 2004). Regarding the atlas, a minimum of 10 individuals are represented, based on the repetition of the left mass. In addition, AT-3985 (a right lateral mass) represents another individual due to its incompatibility with any of the left lateral masses. These 11 individuals represent six adults (one of them less than 25 years of age, represented by VC3) and five subadults, one of them possibly an adolescent, represented by VC17 (Table 2). Among the axes, based on the repetition of the most common element (the dens of the axis), at least 10 individuals are recognizable: four adults (one of them less than 25 years of age), one late adolescent or young adult, one immature individual between 12 and 16 years of age, and four individuals older than 12 years. All these ages at death are fully compatible with those based on dental (Bermúdez de Castro et al., 2004), cranial (Arsuaga et al., 1997c), and postcranial evidence (Carretero et al., 1997).

Sex determination

Sex determination of the three most complete SH atlases and axes, which represent three individuals, was attempted based on multiple regression equations and discriminant functions (Marino, 1995; Wescott, 2000). The results suggest that these three sets of upper cervical vertebrae all represent male individuals.

Additionally, a discriminant function was generated from data taken from atlas specimens in the Hamann-Todd Osteological Collection, and we calculated the a posteriori probability of the most complete SH atlases (VC3 and VC7) being classified as belonging to male individuals (Table 4). These two SH atlases show a posteriori probabilities of being from male individuals higher than 0.80. Due to the incompleteness of VC16, it was not possible to apply the discriminant function, but using an additional discriminant function in which only ITrD is used, VC16 is classified as being from a male with an a posteriori probability of 0.79.

Marino's (1995), Wescott's (2000), and our formulae were used to estimate the sex of several additional fossil atlases and axes. The results agree with the sex determinations based on other postcranial features with one exception: the Régourdou 1 individual is classified as being from a male using the

Table 2
Inventory of the atlas (C1) remains from the SH site (as of the 2004 field season)

Specimen number	Year	Preservation	Age at death	Figure
VC3[1]	1995	Complete vertebra	Adult	2a,b,c
VC7[2]	2000	Complete vertebra	Adult	2d,e,f
VC16[3]	1994, 1997	Masses and posterior arch	Adult	2g,h
VC17[4]	1995, 2000	Anterior arch and left mass	Adolescent (?)	3a
AT-269	1989	Left mass	Subadult	3b
AT-326	1990	Left mass		3c
AT-1818	1996	Left mass	Adult	3d
AT-2078	1997	Left mass	Subadult	3e
AT-2130	1997	Anterior arch		3l
AT-2264	1997	Posterior arch	>5 years	3p
AT-2584	1998	Left mass, posterior arch		3f
AT-2852	1998	Anterior arch		3m
AT-3003	1999	Left mass		3g
AT-3013	1999	Right mass, posterior arch fragment	Adult	3h
AT-3687	2000	Posterior arch	Subadult (?)	3q
AT-3691	2000	Posterior arch	Subadult (?)	3r
AT-3693	2000	Anterior arch		3n
AT-3694	2000	Right mass	Subadult	3i
AT-3971	1994	Right mass	Subadult	3j
AT-3985	?	Right mass	Adult	3k
AT-3992	1992	Posterior arch		3s
AT-4037	2000	Anterior arch fragment		3o

[1] VC3 = AT-1554.
[2] VC7 = AT-3339 + AT-3340 + AT-3341 + AT-3688.
[3] VC16 = AT-1140 + AT-2201.
[4] VC17 = AT-3374 + AT-3973 + AT-3991.

Table 3
Inventory of the axis (C2) remains from the SH site (as of the 2004 field season)

Specimen number	Year	Preservation	Age at death	Figure
VC2[1]	1998	Complete vertebra	>25	4a,b,c
VC4[2]	1995	Complete vertebra	17–25 (21–25)?	4d,e,f
VC8[3]	2000, 2001	Complete vertebra	>25	4g,h,i
VC28[4]	2003	Complete except right transverse process	17–25 (17–20)?	5a
AT-150	1988	Right lamina, spinous process	>25	5d
AT-1573	1995	Dens, body, right art. facet, frag. upper left art. facet	12–16	5b
AT-2289	1997	Dens, frag. body, frag. upper right facet	12–16	5c
AT-2883	1998	Dens	>12	5f
AT-3696	2000	Dens	>12	5g
AT-3741	2000	Left superior art. facet	>6	5k
AT-3979	1998	Dens	>12	5h
AT-4046	1994	Frag. laminae, spinous process	4-25	5j
AT-4051	1998	Frag. right lamina, right lower art. facet	>4	5l
AT-4187	2003	Frag. body, right upper art. facet	6–16	5m
AT-4314	2003	Dens	>12	5i
AT-4662	1995	Tip of the spinous process	<25 (16–25)?	5e

[1] VC2 = AT-2465.
[2] VC4 = AT-1555.
[3] VC8 = AT-3680 + AT-3840.
[4] VC28 = AT-4634 + AT-4643.

axis, while its sex has been regarded as indeterminate by Vandermeersch and Trinkaus (1995). On the other hand, Krapina 98 and 104, of unknown sex, were classified as belonging to females. The classification of the Gran Dolina ATD6-90 still agrees with the previous sex determination by Carretero et al. (1999), but the result should be interpreted more cautiously due to its low a posteriori probability (0.67).

The results of the sex determination of the VC7 atlas and VC8 axis are also congruent with the sex assignment of Cranium 5 based on the associated mandible AT-888 (Rosas et al., 2002; Bermúdez de Castro et al., 2004). Although Cranium 5 appears to be a small male or a female when the cranial measurements are compared with other middle Pleistocene fossils and Neandertals, the facial skeleton is large and thus likely that of a male (Arsuaga et al., 1997c).

Brief description of the most complete atlases and axes

Atlases

The most complete adult atlases are shown in Fig. 2.

Specimen VC3(C1) is the most complete nonmodern atlas of a fossil hominin yet found. It preserves the transverse processes, which show an incompletely obliterated metaphyseal line. This vertebra was found in anatomical connection with the VC4 axis. The anterior bar of the left transverse process is not fused to the posterior bar, and this specimen exhibits subtle tubercles for the attachment of the transverse ligament. The transverse processes show a triangular cross section, making the dorsal surface quite vertical.

Specimen VC7(C1) is slightly larger and more robust than VC3. It lacks the transverse processes. The sulcus for the right vertebral artery is covered by a bony arch, while that on the left side is only partially covered. Such foramina are not unusual and have been reported in the atlas of the Shanidar 2 Neandertal (Stewart, 1962; Trinkaus, 1983). Like VC3, this specimen exhibits subtle tubercles for the attachment of the transverse ligament.

Specimen VC16(C1) lacks the anterior arch and the transverse processes. It exhibits severe postmortem erosion to the superior articular facets and inferior left articular facet. It is smaller than the VC3 and VC7 atlases, although the size of its posterior arch falls between that of VC3 and VC7. It also

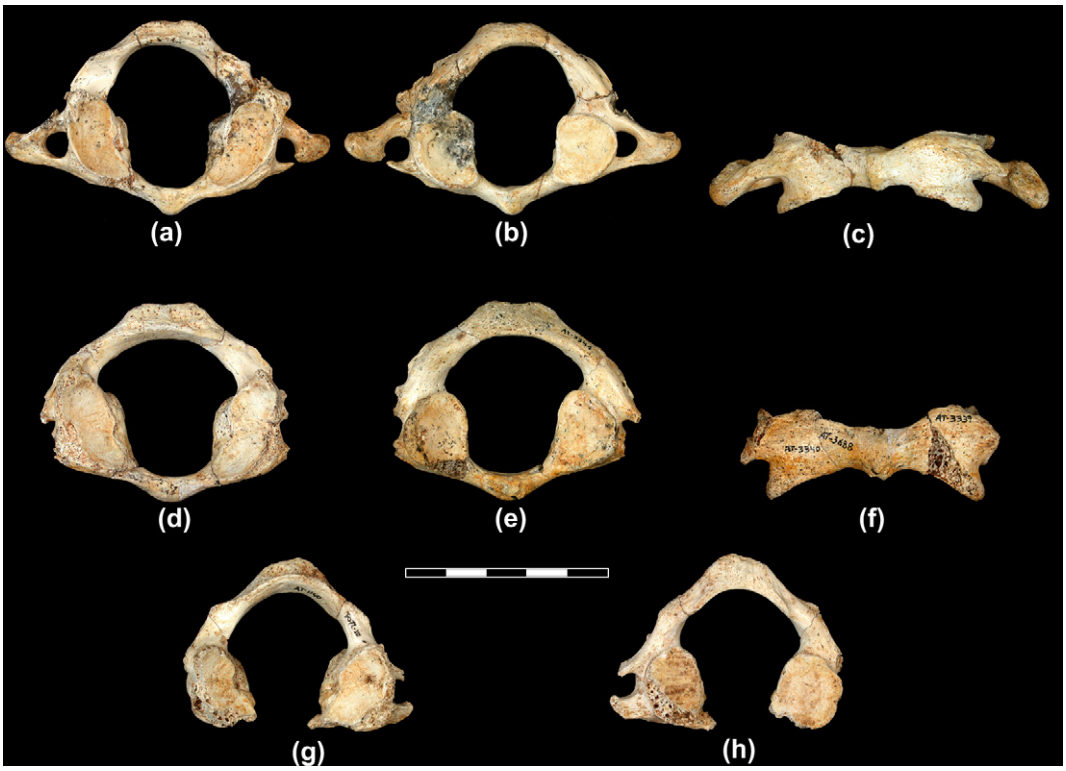

Fig. 2. Complete or nearly complete atlases from Sima de los Huesos. VC3 atlas in cranial (a), caudal (b), and ventral (c) views. VC7 atlas in cranial (d), caudal (e), and ventral (f) views. VC16 atlas in cranial (g), caudal (h), and ventral views. Scale bar = 5 cm.

exhibits more strongly developed tubercles for the attachment of the transverse ligament.

All of the SH atlases possess straight medial edges of the inferior articular facets, a feature that is also found in the Neandertal specimens from La Chapelle-aux-Saints and La Ferrassie 1, while most atlases in our modern human comparative sample from Burgos possess rounded edges. We cannot evaluate this trait in other fossil hominins because this anatomical region suffers erosion [e.g., the Gran Dolina ATD6-90 and KNM-ER 1808 atlases (see Leakey and Walker, 1985)].

Axes

The most complete adult axes are shown in Fig. 4.

Specimen VC2(C2) is a nearly complete axis that lacks only the transverse processes and is eroded at the dorsoinferior (posteroinferior) part of the vertebral body, at both lateral ends of the superior articular surfaces, and at the spinous process. It is attributed to a fully adult individual, as the inferior epiphyseal ring is completely fused. Its size is intermediate between the large axes (VC4 and VC8) and the small axis VC28.

Specimen VC4(C2) is a complete axis that is only slightly eroded on the dorsoinferior (posteroinferior) part of the body, at the tip of the spine, and at the lateral ends of the transverse processes and inferior articular facets. The secondary center of ossification of the spinous process is still unfused, and the inferior epiphyseal ring is in a more advanced state of fusion than VC28. This specimen was found in anatomical connection in the excavation with the VC3 atlas.

Specimen VC8(C2) lacks the transverse processes and bone chips from the vertebral body at the base of the dens, from the tip of the spinous process, and from the ventralmost part of the right superior articular facet. It is slightly worn at the dorsoinferior (posteroinferior) part of the body. It is similar in size to VC4, albeit slightly more robust. The spinous process is clearly bifid.

All of the spinous processes of the SH axes are robust. The axis specimens in the modern human samples that we have studied (Burgos and Hamann-Todd) possess spinous processes with a triangular shape in dorsal view and crowned with a narrow ridge at the cranial end. On the other hand, all the spinous processes of the SH axes possess more vertically oriented lateral walls, and therefore the whole spinous process has a ‘‘trapezoidal’’ and massive appearance. Neandertals that preserve this region show the same pattern [e.g., La Ferrassie 1 (Gómez-Olivencia, personal observation) and Krapina 104 (see Figure 177 in Radovcic et al., 1988: 72)], as do some late Pleistocene modern humans [e.g., Taforalt III (Gómez-Olivencia, personal observation) and Dolní Věstonice 15 (see Figure 14.4 in Holliday, 2006: 244)]. This pattern could be related to strong development of the nuchal muscles *M. rectus capitis posterior major* and *M. obliquus capitis inferior*.

Associations of vertebrae

Among the atlas and axis remains from the SH site, it has been possible to recognize three associated sets of vertebrae

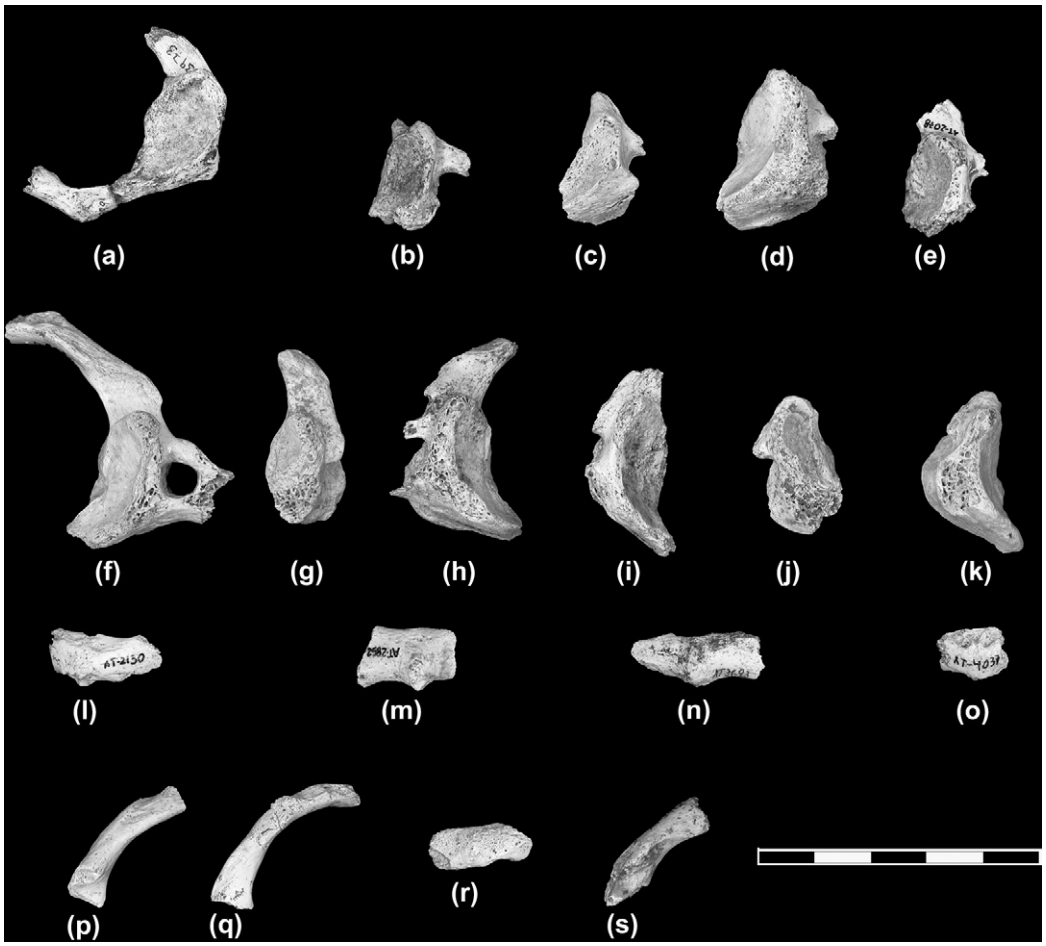

Fig. 3. Sima de los Huesos fragmentary atlases. Cranial view of (a) VC17, (b) AT-269, (c) AT-326, (d) AT-1818, (e) AT-2078, (f) AT-2584, (g) AT-3003, (h) AT-3013, (i) AT-3694, (j) AT-3971, (k) AT-3985. Dorsal view of (l) AT-2130, (m) AT-2852, (n) AT-3693, (o) AT-4037. Cranial view of (p) AT-2264, (q) AT-3687, (r) AT-3691, (s) AT-3992. Scale bar = 5 cm.

based on age at death, size, and anatomical compatibility (articular congruence). These sets are listed below:

- VC3(C1) and VC4(C2): These specimens are the first two cervical vertebrae of a young adult individual of about 21–25 years of age at death based on the degree of fusion of the epiphyses. The atlas was found articulated with the axis.
- VC7(C1) and VC8(C2): These vertebrae belong to an adult individual older than 25 years of age at death based on the complete fusion of the inferior epiphyseal ring. In addition, VC7 (and hence VC8) has been associated with Cranium 5 (Individual XXI; see Bermúdez de Castro et al., 2004) based on size, articular congruence and similar degree of osteophytosis (see below). This association is the first between cranial and postcranial remains from this site.
- VC16(C1) and VC2(C2): These vertebrae belong to an adult individual of more than 25 years of age at death based on the complete fusion of the inferior epiphyseal ring. They exhibit a comparable degree of ossification of the insertion of the articular capsules between C1 and C2.

Morphology and metrics of the atlas

Metrics

The metric dimensions and indices of the SH atlases and comparative data from Neandertal and modern human samples are provided in Tables 5–7. Results of the Kruskal–Wallis test and Mann–Whitney *U*-test are presented in Table 5.

The SH atlases are metrically closer to Neandertals than to our modern human comparative samples; they show a sagittally elongated canal, sagittally expanded inferior articular facets, and a broader inferior transverse diameter. In Neandertals, the sagittal elongation of the atlas is more extreme than in the SH vertebrae. The significantly broader inferior transverse diameter of the SH atlases (ITrD) (compared with both modern human samples) has its counterpart in the significantly broader superior transverse diameter (STrD) of the SH axes (see below).

All the SH indices are well within the ranges of variation of our modern human comparative samples (Table 7). In contrast, Neandertals show a high shape index due to their significantly larger maximum dorsoventral diameter.

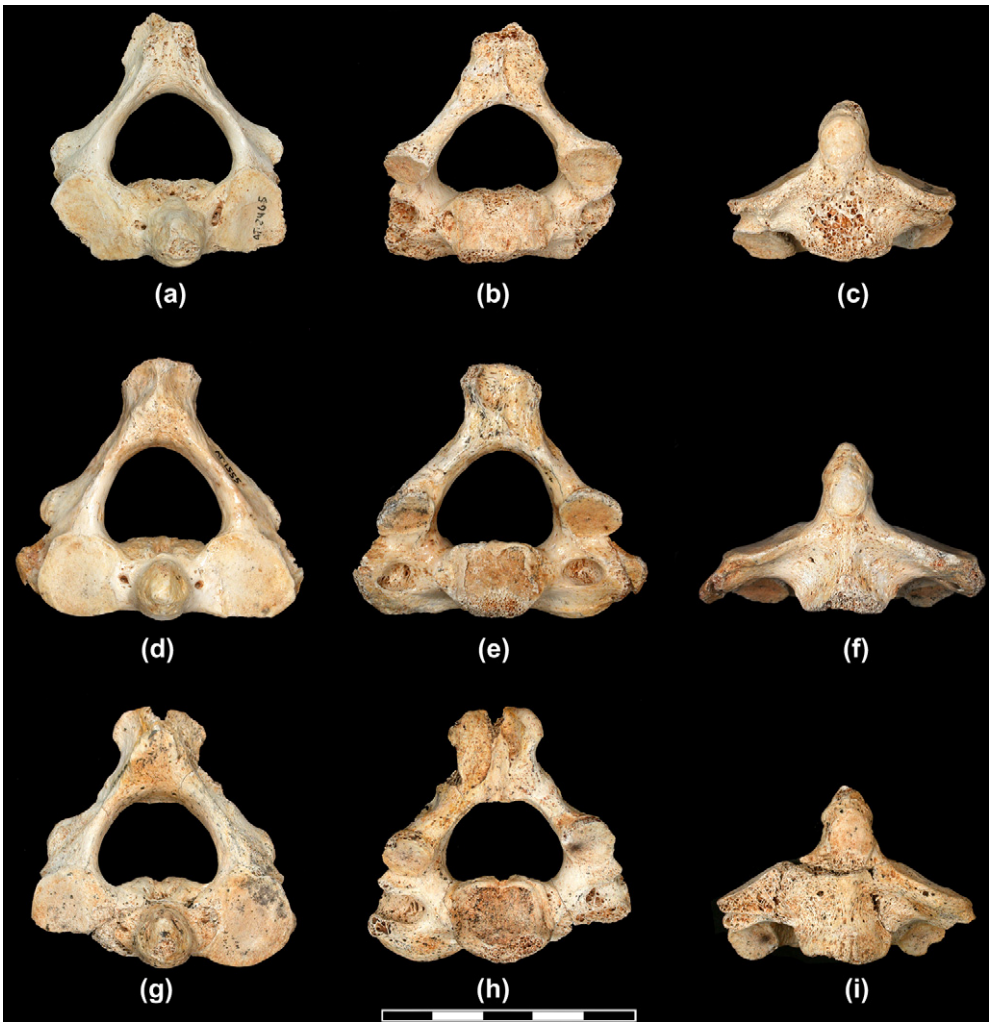

Fig. 4. Sima de los Huesos complete adult axes. VC2 axis in cranial (a), caudal (b), and ventral (c) views. VC4 axis in cranial (d), caudal (e), and ventral (f) views. VC8 axis in cranial (g), caudal (h), and ventral (i) views. Scale bar = 5 cm.

Size and shape of the vertebral foramen

The vertebral foramen of the atlas does not accurately reflect the size of the spinal cord (this trait will be discussed in the axis section and in the discussion below) because the ventral half is occupied by the dens of the axis. A Mann–Whitney *U*-test indicates that the SH sample has a significantly larger dorsoventral canal diameter (M10) than the Burgos modern human sample. The Neandertals have a larger canal, in both dorsoventral (M10) and transverse (M11) diameters, than the Burgos modern human sample. This larger dorsoventral diameter results in a high canal-shape index in Neandertals (Table 7), which could be related to the dorsoventral elongation of the foramen magnum, a proposed Neandertal autapomorphy (Rak et al., 1994, 1996; but see Creed-Miles et al., 1996). It appears that the length, rather than the shape of the foramen magnum, is primarily responsible for distinguishing Neandertals from modern humans (Rak et al., 1996).

The values for the dorsoventral diameter of the foramen magnum (M7) of SH crania are similar to those of Neandertals, and both of these values are significantly larger than those for our human male comparative samples (Table 8). Unfortunately, the number of associated fossil atlases and cranial bases is small. Figure 6 compares the dorsoventral diameter of the atlas with that of the foramen magnum in the VC7 atlas (associated with Cranium 5), La Ferrassie 1, Skhul V, Dolní Věstonice 14, Cro-Magnon, and two recent human samples. The SH specimen is well above the means for the modern human sample, but it is still inside their ranges. The fossil *H. sapiens* specimens from Skhul V and Cro-Magnon are just within the limits of the 95% equiprobability ellipse of the recent human samples. In contrast, the La Ferrassie 1 Neandertal and the Dolní Věstonice 14 modern human exhibit much larger values in both dimensions and are clearly outliers. When the variables are considered separately (Tables 6 and 8), the SH and Neandertal specimens lie between the recent human sample and the extreme La Ferrassie 1 individual.

The canal-shape index calculated for all the SH atlases is well within the recent human range of variation (Table 7). In contrast, the Neandertal mean canal-shape index is above the range of variation of the Burgos male sample, but it is still encompassed within the Hamann-Todd range of variation. When

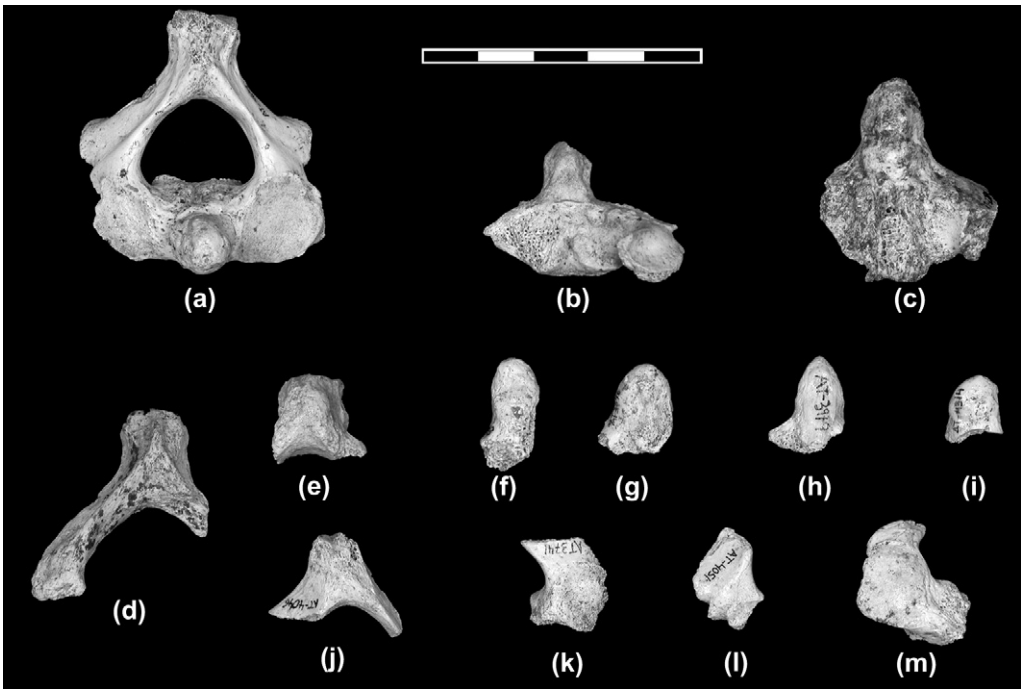

Fig. 5. Sima de los Huesos fragmentary and/or immature axes. (a) Cranial view of VC28. Dorsal views of (b) AT-1573 and (c) AT-2289. Cranial views of (d) AT-150 and (e) AT-4662. Ventral views of (f) AT-2883, (g) AT-3696, (h) AT-3979, and (i) AT-4314. Cranial views of (j) AT-4046, (k) AT-3741, (l) AT-4051, and (m) AT-4187. Scale bar = 5 cm.

Table 4
Sex assignments for Atapuerca (SH) and other fossil atlases and axes

	Sex assignment of individual	Atlas		Axis
		Sex using Marino's (1995) formulae[1]	Discriminant analysis[2] (sex; posterior probability)	Sex using Wescott's (2000) formulae[3]
VC3(C1), VC4(C2)		M (14)	M; 0.81	M (5/4)
VC7(C1), VC8(C2)		M (14)	M; 0.90	M (5/3)
VC16(C1), VC2(C2)		M (4)		M (5/5)
ATD6-90 (Gran Dolina)	F*	F (14)	F; 0.67	
Kebara 2	M†	M (8)		
Krapina 98		F (6)		
Krapina 104				F (1/1)
La Chapelle	M#	M(6)		
La Ferrassie 1	M**	M(14)	M; 0.78	M (5/5)
Régourdou 1	?			M (5/4)
Shanidar 2	M§	M (14)	M; 0.95	M (1/1)
Subalyuk 1	F¶	F (6)		
Percentage correct classification	—	75–85%	72.3%	81.7–83.4%

* Sex assignment is from Carretero et al. (1999).
† Sex assignment is from Rak and Arensburg (1987).
# Sex assignment is from Boule (1911–1913).
** Sex assignment is from Heim (1976).
? The sex of the Régourdou 1 specimen was undetermined by Vandermeersch and Trinkaus (1995), but discriminant analysis performed by Carretero (1994) on the clavicle sexed this individual as a male with a probability of 99%, and Churchill and Formicola (1997) considered it to be from a male in their analysis.
§ Sex assignment is from Trinkaus (1983).
¶ Sex assignment is from Pap et al. (1996).
[1] Marino (1995) proposed 14 different formulae (7 multiple regression equations and 7 discriminant functions). The number of these formulae that we have used is in parentheses. The formulae used different measurements, so the number of formulae used was contingent on the preservation of the fossil and/or the number of measurements available from the literature. All of the results were consistent with each other.
[2] Five variables were entered into the forward stepwise discriminant analysis (MDvD, STrD, ITrD, M10, M11); the variables used to calculate the discriminant function are: MDvD, STrD, ITrD.
[3] Wescott proposed five different discriminant equations. The number of formulae that we used and how many of them resulted in the proposed sex are in parentheses. Two equations in the case of VC8 and one in the case of VC4 and Régourdou 1 classified these specimens as females but with a result close to the sectioning point. In contrast, three of the formulae classified all of the SH specimens, La Ferrassie 1, and Régourdou 1 as males with a value well-above the mean for the male sample used by Wescott (2000).

Table 5
Raw dimensions (in mm) of the Sima de los Huesos atlases and results of the Mann–Whitney *U*-test for differences between sample means in SH, Neandertals, and recent humans

Variable	VC3	VC7	VC16	SH-N-BU	SH-BU		SH-N	BU-N	
				K-W	M-W	M-W (B)	M-W	M-W	M-W (B)
Maximum dorsoventral diameter (MDvD)#	47.4	48.1		*				*	†
Maximum transverse diameter (MTrD)	80.0								
Superior transverse diameter (STrD) §	49.7	51.5	(47.5)						
Inferior transverse diameter (ITrD) §	48.6	50.4	(48.3)	*	*	*			
Canal dorsoventral maximum diameter (M10)	34.8	33.3	(32.5)	**	*	†		**	*
Canal transverse maximum diameter (M11)	30.1	33.7	29.2						
Distance between the tubercles for the attachment of the transverse ligament (DTub)	18.6	20.3	16.5						
Anterior arch height at the level of the anterior tubercle (AAH)	10.5	12.2							
Anterior arch thickness at the level of the anterior tubercle (AATh)	6.6	6.3							
Transverse diameter of the facet for the axis (TrDFA)	11.8	11.8		**				*	*
Maximum height of lateral masses (MHLM)	19.5/20.0	22.6/22.6							
Posterior arch height at the level of the posterior tubercle (PAH)	8.5	9.3	9.5						
Posterior arch thickness at the level of the posterior tubercle (PATh)	5.9	7.6	7.6	*				*	†
Height of the posterior arch in the groove for the vertebral artery (HPAG)	4.1/5.5	—/5.3	4.3/4.9	X/**	/**	/*		/*	
Diameters in major axis of upper articular facets (UAFMAD)	22.7/22.1	(23.1)/24.7							
Diameters in right angle to major axis of upper articular facets (UAFTrD)	11.4/11.5	11.9/11.5		**/				*/	*/
Lower articular facet dorsoventral diameter (LAFDvD)	18.9/(18.0)	19.1/18.4	17.7/—	**/**	*/*	*/		**/**	*/*
Lower articular facet transverse diameter (LAFTrD)	15.9/15.4	16.0-16.5	16.1/—						

Values in parentheses are estimated. Cells that contain two entries are for the right and left sides (right/left).
Maximum anteroposterior diameter along the sagittal plane (McCown and Keith, 1939).
§ Maximum transverse diameter measured to the lateral margins of the superior or inferior articular facets (Trinkaus, 1983).
Abbreviations are as follows: SH = Sima de los Huesos; BU = Burgos males; N = Neandertals; HT = Hamann-Todd males; K-W refers to the Kruskal–Wallis test performed on SH, BU, and N samples; M-W refers to the Mann–Whitney *U*-test performed on different pairs of samples; M-W (B) refers to the Mann–Whitney *U*-test adjusted using the Bonferroni method; * $p < 0.05$; ** $p < 0.01$; † $0.05 < p < 0.10$; X = the analysis was not performed because one of the samples is of size $n = 0$ (K-W) or $n < 2$ (M-W).

Table 6
Comparison of linear atlas measurements (mm) between the SH specimens, Neandertals, and fossil and recent *H. sapiens*

	Sima de los Huesos			Neandertals[1]			Burgos males			H-T males	
	n	Mean	SD	*n*	Mean	SD	*n*	Mean	SD	Mean	SD
MDvD	2	47.8	0.5	2	50.9	3.3	35	44.8	2.8	46.6	3.3
MTRD	1	80.0					32	78.3	3.9	78.1	5.3
STrD	3	49.6	2.0	5	49.1	2.6	35	48.6	2.4	50.0	3.6
ITrD	3	49.1	1.1	5	47.5	2.0	36	45.5	2.5	46.4	2.7
M10	3	33.5	1.2	3	35.2	1.6	35	30.2	1.9	31.5	2.4
M11	3	31.0	2.4	5	30.1	2.2	36	29.0	2.1	28.5	2.4
DTub	3	18.5	1.9	2	17.3	1.5	36	16.0	2.0		
AAH	2	11.4	1.2	3	11.0	1.9	37	11.0	1.1	11.1	8.5
AATh	2	6.4	0.2	5	5.7	1.8	38	6.3	0.8	10.1	6.6
TrDFA	2	11.8	0.0	3	13.0	1.2	38	10.1	1.4		
MHLM	2/2	21.1/21.3	2.2/1.8	1/2	19.3/20.5	—/1.5	38/36	21.5/21.6	1.9/1.8		
PAH	3	9.1	0.5	2	8.2	2.5	35	9.9	2.0		
PATh	3	7.0	1.0	2	3.6	0.6	35	7.8	2.1		
HPAG	2/3	4.2/5.2	0.1/0.3	0/2	—/5.2	—/0.1	35/33	4.2/4.0	0.9/0.6		
UAFMAD	2/2	22.9/23.4	0.3/1.8	6/6	23.6/24.1	2.2/2.2	37/36	23.7/23.5	1.8/1.7		
UAFTrD	2/2	11.6/11.5	0.4/0.0	6/5	12.2/11.4	1.4/0.7	38/37	10.4/10.5	1.2/1.0		
LAFDvD	3/2	18.6/18.2	0.8/0.3	5/5	18.1/18.2	0.9/1.4	37/37	16.3/16.2	1.3/1.2		
LAFTrD	3/2	16.0/16.0	0.1/0.8	4/5	14.3/15.6	1.2/1.6	37/38	15.5/15.8	1.0/1.2		

Cells that contain two entries are for the right and left sides (right/left).
[1] Neandertal sample ($n = 9$; MNI = 8) includes: Kebara 2 (Arensburg, 1991); Krapina 98, 99, and 100; La Chapelle-aux-Saints; La Ferrassie 1; Shanidar 2; Subalyuk 1 (Pap et al., 1996); and Tabun C1 (McCown and Keith, 1939).

Table 7
Comparison of the indices of the atlas in the SH sample, Neandertals, and fossil and living *H. sapiens*

Specimen/sample	Shape index[1]	Canal-shape index[2]	Articular-facet superposition[3]
VC3	95.4	115.6	102.3
VC7	93.4	98.8	102.1
VC16	—	(111.3)	(98.3)
ATD6-90	89.1	111.1	102.0
Neandertals[4]	107.6 ± 1.4 (106.2–109.0) ($n = 2$)	118.4 ± 7.1 (106.0–127.4) ($n = 3$)	103.7 ± 6.1 (91.0–112.3) ($n = 5$)
Skhul V	96.6	98.4	99.8
Burgos (males)	92.3 ± 6.9 (77.9–107.5) ($n = 34$)	104.7 ± 7.8* (90.5–118.2) ($n = 35$)	107.1 ± 6.6 (93.3–121.4) ($n = 35$)
Hamann-Todd			
Males ($n = 50$)	93.6 ± 8.6 (74.6–117.6)	111.2 ± 9.0 (88.9–130.0)	107.8 ± 6.4 (92.2–121.9)
Females ($n = 51$)	92.7 ± 8.5 (75.0–116.0)	110.4 ± 9.4 (87.1–131.0)	108.0 ± 6.6 (96.9–127.2)
Total ($n = 101$)	93.2 ± 8.6 (74.6–117.6)	110.8 ± 9.2 (87.1–131.0)	107.9 ± 6.5 (92.2–127.2)

* Significantly different from Hamann-Todd sample ($p < 0.01$; Student's *t*-test).
[1] Shape-index = MDvD/STrD × 100.
[2] Canal-shape index = M10/M11 × 100.
[3] Articular-facet superposition = STrD/ITrD × 100.
[4] Neandertal sample includes: Kebara 2 (Arensburg, 1991), Krapina 98, La Ferrassie 1, Shanidar 2, and Subalyuk 1 (Pap et al., 1996).

the dorsoventral diameter of the canal is plotted against the transverse diameter (Fig. 7), the estimated values for Shanidar 2 fall out of the 95% equiprobability ellipse of the Hamann-Todd females and Burgos sample due to its extreme values. The three complete atlases from SH fall well within the 95% equiprobability ellipse of the Hamann-Todd male and Burgos male samples. Specimen VC7 falls outside the Hamann-Todd female subsample due to its large maximum transverse diameter of the canal (M11). Specimen ATD6-90 from Gran Dolina possesses small canal diameters, but it is still well-within our modern human samples' 95% equiprobability ellipses.

The area of the vertebral foramen of the most complete SH atlases is significantly larger ($p < 0.05$, Mann–Whitney *U*-test) than that of the Burgos male sample, regardless of the method used to estimate the area (Table 9). However, as noted above, this does not reflect the actual size of the spinal cord.

Tubercles for the insertion of the transverse ligament

The tubercles for the insertion of the transverse atlantal ligament are located just below the medial margin of each superior facet in the atlas (Gray, 1959). Tubbs et al. (2002) found that 14.7% of the tubercles in his sample ($n = 50$ individuals) "did not protrude from the lateral masses into the vertebral foramen and were merely smooth surfaces" (p. 345). Thus, we can recognize two different morphologies in the insertion of the transverse atlantal ligament: (1) a tubercle that protrudes into the vertebral foramen and (2) a flat surface or a tubercle significantly reduced in size that does not protrude into the vertebral foramen (Fig. 8). We will refer to the former morphology as "projected tubercle" or "large tubercle" and to the latter one as "weakly developed tubercle" or "small tubercle." We have classified the SH, Neandertal, and comparative samples into these two categories in Table 10. In the literature, the tubercles for the transverse ligament in Neandertals have been described as "slightly prominent" ("peu saillant"; Boule, 1911–1913: 92; Heim, 1976: 311), "small, poorly developed" (Arensburg, 1991:114), or even "replaced by a rough surface" ("remplacé par une surface rugueuse"; Martin, 1923: 214). These descriptions are fully consistent with the "small tubercle" morphology.

The first cervical vertebra ATD6-90 from Gran Dolina possesses a large tubercle for the attachment of the transverse ligament (Carretero et al., 1999; Gómez-Olivencia, 2005). We lack information about this trait for the left mass of the female *H. ergaster* specimen KNM-ER 1808 (Walker et al., 1982; Leakey and Walker, 1985) and for the left mass KNM-ER 1825, found at a locality where robust australopith fossils

Table 8
Comparison of the dorsoventral diameter of the foramen magnum in the SH sample, Neandertals, and recent humans[1]

Sample	Foramen magnum DV diameter (M7)	Reference
SH[2] ($n = 3$)	41.3 ± 3.1	Arsuaga et al., 1997c; Martínez, 1995
Neandertal pooled sex[3] ($n = 7$)	40.7 ± 4.7	Arsuaga et al., 1997c; Martínez, 1995; McCown and Keith, 1939; Present study
Burgos males ($n = 10$)	34.8 ± 1.7	Present study
Hamann-Todd males ($n = 22$)	36.3 ± 2.4	Present study
Coimbra males ($n = 78$)	36.8 ± 2.8	Martínez, 1995
Coimbra females ($n = 75$)	35.7 ± 2.6	Martínez, 1995

[1] The results of the Mann–Whitney *U*-test showed no significant difference between the SH and Neandertal samples, but both are significantly ($p < 0.05$ and $p < 0.01$, respectively) larger than the Burgos sample. The Coimbra males are significantly ($p < 0.05$) larger than the Coimbra females (Martínez, 1995).
[2] SH sample is composed of Crania 4, 5, and 6, all of which are assigned to male individuals.
[3] Neandertal sample includes: Gibraltar 1, La Chapelle-aux-Saints, La Ferrassie 1, Engis 2, Saccopastore 1, Shanidar 1, and Tabun C1.

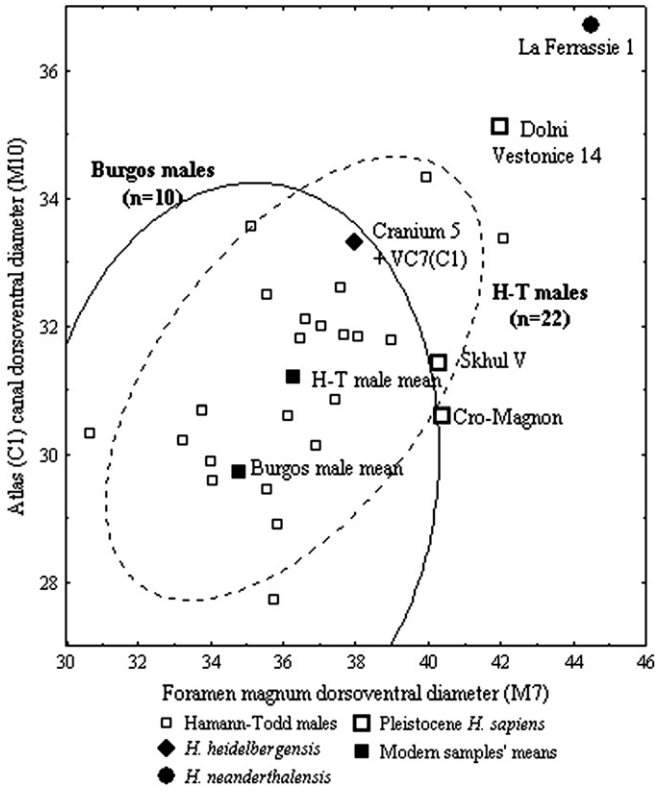

Fig. 6. Dorsoventral diameter of the foramen magnum versus the dorsoventral diameter of the atlas in several fossil specimens and recent humans. The 95% equiprobability ellipses for the Burgos male and the Hamann-Todd samples are shown.

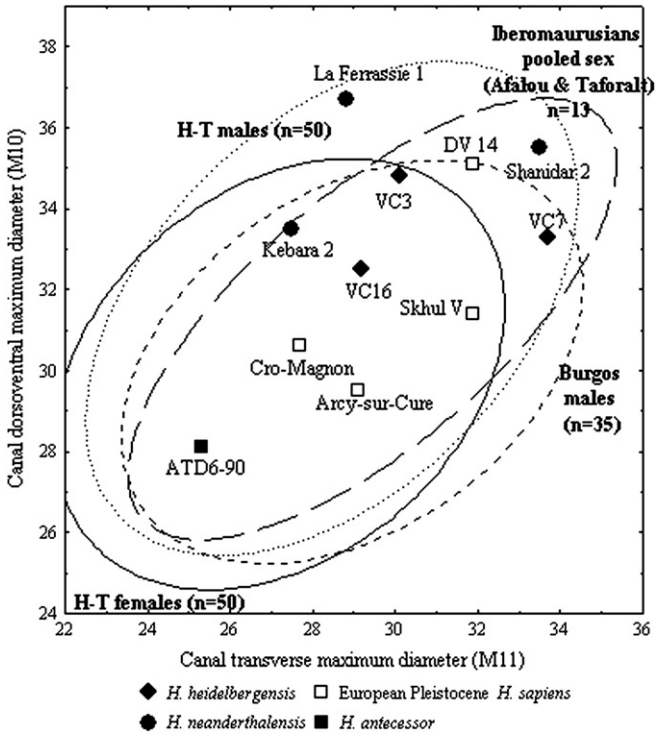

Fig. 7. Dorsoventral diameter of the canal vs. the maximum transverse diameter of the canal in the atlas in several fossil specimens, the terminal Pleistocene sample from the sites of Afalou and Taforalt, and several recent human samples. The 95% equiprobability ellipses are given for the Afalou/Taforalt and recent human samples. DV 14 refers to Dolní Věstonice 14.

have been collected (Leakey and Walker, 1985). The area in which the tubercles should be present has suffered mild damage to the left articular process of the *Australopithecus afarensis* atlas A.L. 333-83 (Lovejoy et al., 1982).

The atlases from the Sima de los Huesos site show higher frequencies of small tubercles than do our two modern human comparative samples, but lower frequencies than are observed in Neandertals. Although we cannot completely rule out the possibility that the condition is a general reflection of robusticity, the tubercle for the insertion of the transverse ligament does not appear to be remodeled by physical stress and thus the degree of development could be epigenetic (Tubbs et al., 2002), which implies that this trait could be useful as a phylogenetic character. Moreover, the percentages of small tubercles in the two modern human populations (Burgos and Afalou) are similar, despite their different chronology, geography, and lifestyles. The presence of large tubercles in the ATD6-90 atlas from Gran Dolina suggests that high frequencies of well-developed tubercles could be the primitive condition within the genus *Homo*, which has been preserved in late Pleistocene *H. sapiens*, as represented in the atlases SAM-AP 6268 from Klasies River Mouth (Grine et al., 1998) and Skhul V, and in the modern human samples (see above). In contrast, high frequencies of weakly developed tubercles would be the derived condition of *H. neanderthalensis*, and the middle Pleistocene European populations of *H. heidelbergensis* would represent an intermediate stage. Alternatively, we could hypothesize a polymorphic primitive condition that led to high frequencies of small tubercles in the European *H. heidelbergensis–H. neanderthalensis* lineage and to high frequencies of large tubercles in *H. sapiens*.

Table 9
Comparison of the vertebral-foramen area (mm^2) the SH and recent human atlases

Specimen/sample	Vertebral-foramen area 1*	Vertebral-foramen area 2**
VC3	726.7	697.3
VC7	781.6	749.7
VC16	(697.3)	(626.8)
Burgos[1] (males)	603.5 ± 63.2 (478.2–735.2) ($n = 30$)	594.6 ± 67.5 (458.7–723.9) ($n = 30$)

* Imaged area measures.
** Cross-checked for accuracy by comparing imaged linear measures to physical dimensions measured with digital calipers.
[1] The two mean values of the vertebral-foramen area in the Burgos sample are not statistically different.

Anterior tubercle of the anterior arch of the atlas

In the Sima de los Huesos atlases, all of the anterior arches ($n = 7$), regardless of their age at death, display a projecting anterior tubercle. The anterior tubercle of the anterior arch of the atlas (Fig. 9) projects caudally in 48.6% of the individuals in the modern human male comparative sample from Burgos

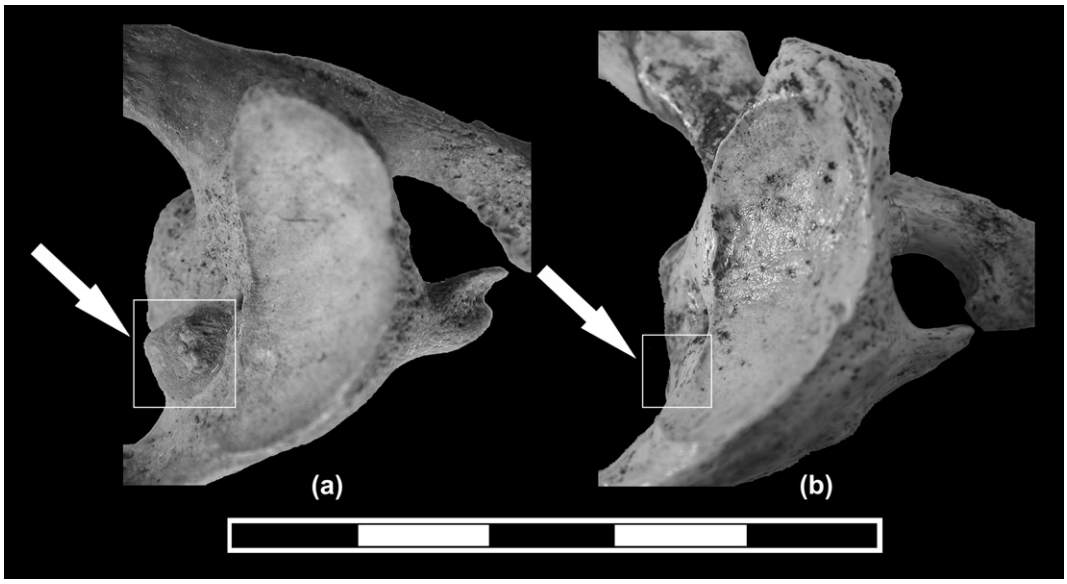

Fig. 8. Cranial view of the left mass of the atlas. (a) Modern human from the Burgos sample, showing a well-developed tubercle for the insertion of the atlantal transverse ligament, which protrudes medially into the vertebral foramen. (b) VC3 from SH showing a flat surface instead of a tubercle for the insertion of the atlantal transverse ligament.

($n = 37$). Among Neandertals, all of the atlases that preserve the anterior arch ($n = 5$) have anterior tubercles that clearly project caudally: La Quina (Martin, 1923), Kebara 2 (Arensburg, 1991), La Chapelle-aux-Saints (Boule, 1911–1913), La Ferrassie 1 (Heim, 1976), and Krapina 98 (Gorjanovic-Kramberger, in Boule, 1911–1913). A caudally projecting anterior tubercle of the atlas is also present in the Gran Dolina atlas ATD6-90 and the Klasies River Mouth atlas SAM-AP 6268 (Grine et al., 1998). In contrast, Skhul V does not possess this morphological pattern (McCown and Keith, 1939).

A caudally projecting anterior tubercle is not related to a thickened anterior arch in the SH sample. Moreover, the thickness of the anterior tubercle of VC3 and VC7 are similar to the mean value of our modern male comparative sample. The anterior tubercle is the insertion point of the longus colli muscle, which flexes the neck, so high frequencies of a caudal projection of the anterior tubercle could be related to the hypertrophy of this muscle.

Table 10
Comparison of the frequencies of weakly developed tubercles in the atlas of the SH specimens, Neandertals, and recent humans

Sample	Sex	Large tubercle	Asymmetry[1]	Small tubercle
SH[2] ($n = 6$)	Male ($n = 3$); unknown sex ($n = 3$)	33.3%	0%	66.7%
Neandertals[3] ($n = 6$)	Pooled sex	0%	16.7%	83.3%
Burgos ($n = 39$)	Male	74.4%	10.2%	15.4%
Afalou ($n = 12$)	Pooled sex	83.3%	0%	16.7%

[1] Asymmetry refers to the presence of a large tubercle in one of the lateral masses and a small tubercle in the other lateral mass of the atlas.

[2] Among the adult atlases from SH, the tubercles are large in VC16 and AT-3985 (MNI = 2) and are small in VC3, VC7, AT-1818, AT-2584, and AT-3013 (MNI = 4).

[3] Among Neandertals, the tubercles are weakly developed in La Ferrassie 1 (Heim, 1976; present study), La Chapelle (Boule, 1911–1913; present study), Kebara 2 (Arensburg, 1991), La Quina H5 (Martin, 1923), and Krapina 100 (present study). Shanidar 2 shows a large tubercle on the left side but a small one on the right side.

Posterior tubercle of the posterior arch of the atlas

The posterior tubercle of the posterior arch of the atlas is the insertion area for *M. rectus capitis posterior minor*, which extends (bilaterally) and rotates (unilaterally) the atlanto-occipital joint (Gray, 1959). In the three most complete individuals from SH, especially VC7, the posterior tubercle is big, and may be related to muscular hypertrophy.

Morphology and metrics of the axis

Metrics

The metric dimensions and indices of the SH axes and comparative data from Neandertal and modern samples are provided in Tables 11–13. Results of the Kruskal–Wallis test and Mann–Whitney *U*-test are given in Table 11; Table 12 compares Neandertal and modern samples to the SH sample.

The most remarkable feature of the SH axes is that they are relatively low (low value of M1a and DCCDA) and wide (high values of STrD) compared to our modern male samples (both recent and late Pleistocene), which are higher and narrower, as shown in Fig. 10. These differences result in lower shape and axis height/breadth indexes in the SH specimens. The SH axes clearly group with the Neandertals, but Skhul V also exhibits the same morphology, and so we cannot evaluate this trait phylogenetically. More fossils are needed to clarify this pattern.

Fig. 9. (a) A modern atlas from the Burgos sample that lacks the anterior tubercle caudal projection. (b) Ventral view of VC7, showing the caudal projection of the anterior arch tubercle (arrow).

Size and shape of the vertebral foramen

The SH axes have canal-size dimensions and canal-shape indices that are well within our modern human sample range of variation (Tables 11–13; Fig. 11). Moreover, the area of the vertebral foramen calculated for the SH specimens is close to the mean of our Burgos male sample (Table 14). Among Neandertals, the remarkably large transverse diameter of the canal (M11) in Shanidar 2 and the large dorsoventral diameter of the canal (M10) in Krapina 105 place these vertebrae out of the 95% equiprobability ellipse of the modern human comparative sample from Burgos (Fig. 11).

Finally, we have compared the vertebral-canal surface area of the axes to their articular surface areas (as a proxy for size). The SH specimens' mean falls close to that of the Burgos human sample (Burgos mean $= 97.9 \pm 18.8$, $n = 29$; SH mean $= 99.6 \pm 19.5$, $n = 3$). Moreover, within the Burgos male sample, there is no evidence of a correlation between these two variables.

Pathological lesions

Pathology in the vertebral column has been described in several hominins (Cook et al., 1983; Dawson and Trinkaus, 1997; Trinkaus, 1985; Ogilvie et al., 1998), including some of the SH hominins (Pérez, 2003). We have found two kinds of pathology in the SH upper cervical vertebrae: a developmental defect and degenerative pathology.

In the VC3 atlas, the anterior bar of the transverse process remains unfused to the posterior bar of the transverse process, and thus the *foramen transversarium* is not completely delimited. The fusion of the anterior bar to the posterior bar of

Table 11
Raw dimensions (in mm) of the SH axes and results of the Mann–Whitney *U*-test for differences between sample means in SH, Neandertals, and recent humans

Variable	VC2	VC4	VC8	SH-N-BU	SH-BU		SH-N	BU-N	
				K-W	M-W	M-W(B)	M-W	M-W	M-W(B)
Maximum dorsoventral diameter (MDvD) #	(50.0)	50.1	48.9						
Maximum transverse diameter (MTrD) §		(60.0)							
Superior transverse diameter (STrD) §	(48.0)	50.5	51.1	**	**	*			
Inferior transverse diameter (ITrD)	46.0	(49.6)	45.4						
Canal dorsoventral maximum diameter (M10)	17.4	18.3	15.5						
Canal transverse maximum diameter (M11)	23.7	22.9	23.9	*				*	†
Body craniocaudal dorsal diameter (M2)	19.0	17.1	18.0	*				*	*
Total vertebral ventral height (M1a)	(34.5)	(36.2)	(36.0)	**	*			**	**
Total vertebral dorsal height (DoH)	31.5	32.2	31.9	*	*			*	
Body inferior anteroposterior diameter (M5)		(15.5)	(16.1)						
Body inferior transverse diameter (M8)	18.4	16.4	18.4						
Cranial articular facet dorsoventral diameter (UAFDvD)	17.0/17.7	16.1/17.0	—/18.2						
Cranial articular facet transverse diameter (UAFTrD)	19.2/—	15.9/15.1	—/19.6	/X					
Caudal articular facet dorsoventral diameter (LAFDvD)	10.4/—	10.0/—	11.9/10.9	/X					
Caudal articular facet transverse diameter (LAFTrD)	12.6/—	12.3/—	10.2/10.1	/X					
Laminae: craniocaudal diameter (CCDLam)	12.0/11.2	10.8/11.7	11.8/11.6	*/*				**/*	*/*
Laminae: thickness (ThLam)	4.9/4.5	5.8/6.6	5.2/7.0						
Spine length (M13)	(16.5)	17.0	18.4						
Maximum transverse diameter of the tip of the spinous process (TrDTSP)	12.8	(16.3)	18.5						

Values in parentheses are estimated. Cells that contain two entries are for the right and left sides (right/left).
Maximum anteroposterior diameter along the sagittal plane (McCown and Keith, 1939).
§ Maximum transverse diameter measured to the lateral margins of the superior or inferior articular facets (Trinkaus, 1983).
Abbreviations are as follows: SH = Sima de los Huesos; BU = Burgos males; N = Neandertals; HT = Hamann-Todd males; K-W refers to the Kruskal–Wallis test performed on SH, BU, and N samples; M-W refers to the Mann–Whitney *U*-test performed on different pairs of samples; M-W (B) refers to the Mann–Whitney *U*-test adjusted using the Bonferroni method; * $p < 0.05$; ** $p < 0.01$; † $0.05 < p < 0.10$; X = the analysis was not performed because one of the samples is of size $n = 0$ (K-W) or $n < 2$ (M-W).

Table 12
Comparison of linear axis measurements (mm) in the SH specimens, Neandertals, and fossil and recent *H. sapiens*

	Sima de los Huesos			Neandertals[1]			Burgos males			H-T males ($n = 50$)	
	n	Mean	SD	*n*	mean	SD	*n*	Mean	S.D	Mean	S.D
MDvD	3	49.7	0.7	4	51.2	4.0	35	49.6	2.3	51.6	2.8
MTRD	1	60.0	—	2	51.8	0.4	35	54.7	4.4	55.2	4.0
STrD	3	49.9	1.6	8	47.8	2.7	39	45.2	2.3		
ITrD	3	47.0	2.3	2	51.8	3.9	38	47.2	2.4	47.8	2.9
M10	3	17.1	1.4	6	18.0	1.6	39	16.5	1.5		
M11	3	23.5	0.5	8	24.5	1.3	39	23.1	1.3	23.4	1.9
M2	3	18.0	1.0	6	16.2	2.7	37	19.0	1.5		
M1a	3	35.6	0.9	9	34.3	2.8	38	37.9	2.3	38.9	2.6
DCCDA	3	31.9	0.4	5	30.7	3.2	38	34.0	2.1		
M5	2	15.8	0.4	7	16.2	2.1	39	15.1	1.1	16.7	1.6
M8	3	17.7	1.1	8	19.3	1.6	35	18.1	1.4	19.8	2.3
UAFDvD	2/3	16.6/17.6	0.6/0.6	3/2	17.9/18.3	1.1/3.0	37/39	17.7/18.1	1.2/1.4		
UAFTrD	2/2	17.6/17.3	2.3/3.1	1/0	15.0/—	—/—	36/39	16.4/16.3	1.3/1.4		
LAFDvD	3/1	10.8/10.9	1.0/—	2/0	11.8/—	0.6/—	36/35	10.1/10.1	1.4/1.4		
LAFTrD	3/1	11.7/10.1	1.3/—	2/0	12.4/—	0.2/—	35/34	11.2/11.2	1.2/1.5		
CCDLam	3/3	11.5/11.5	0.6/0.3	7/6	10.4/10.5	1.1/1.1	39	11.9/11.8	1.1/1.1		
ThLam	3/3	5.3/6.0	0.4/1.3	7/5	5.5/5.3	0.1/0.6	39	5.7/5.6	1.3/1.0		
M13	3	17.3	1.0	4	17.3	1.8	36	18.9	2.7		
TrDTSP	3	15.9	2.9	1	14.2	—	32	14.1	4.0		

Cells that contain two entries are for the right and left sides (right/left).

[1] The Neandertal sample ($n = 11$) comprises the following individuals: Kebara 2 (Arensburg et al., 1990; Arensburg, 1991), Krapina 103, Krapina 104, Krapina 105, La Chapelle-aux-Saints, La Ferrassie 1, La Quina H5 (Martin, 1923), Régourdou 1 (Piveteau, 1966), Shanidar 2, Shanidar 4 (Stewart, 1962; Trinkaus, 1983), and Tabun C1 (McCown and Keith, 1939).

the transverse process in modern humans occurs at about 3–4 years of age (Scheuer and Black, 2000).

The VC7 atlas shows a slight osteophytosis along the edges of its superior articular facets. This very slight osteophytosis finds its counterpart in the occipital condyles of Cranium 5, with which it is associated. Cranium 5's age at death has been estimated to be in excess of 35 years based on tooth wear, and thus it represents one of the oldest individuals in the SH sample, consistent with the appearance of this pathology. The VC16 atlas shows porosity in the middle-dorsal part of its superior articular facets. It exhibits abnormal proliferation of bone on the edge of the lower articular facet, which is congruent with the abnormal porous bone present on the associated VC2 axis at the edge of the superior articular facet. Moreover, the VC2 axis shows osteophytosis along the ventral edges of the superior articular facet (the only part of the facet that is preserved) and on the inferior articular facets. This would be consistent with early stages of degenerative joint disease (DJD). Finally, even if it cannot be considered technically pathological, the axis AT-2289 shows a rugosity on the craniolateral end of the dens on the alar ligament's insertion points. This condition could be related to a slight ossification of the ligamentous attachment point (enthesophyte).

In general, the level of DJD present in the SH upper cervical sample is not very severe, with the VC16-VC2 association being the most strongly affected. Degenerative joint disease is

Table 13
Comparison of the indices of the axis in the SH sample, Neandertals, and fossil and living *H. sapiens*

Specimen/sample	Shape index[2]	Canal-shape index[3]	Articular-facet superposition[4]	Axis height/width index[5]
VC2	(104.2)	73.4	(104.3)	(71.9)*
VC4	92.2*	79.9	(101.8)	(71.7)*
VC8	95.7*	64.9	112.6*	(70.5)*
Neandertals[1]	109.5 ± 11.3	73.8 ± 9.5	93.0 ± 1.9	$71.1^* \pm 8.3$
	(100.0–125.8) ($n = 4$)	(65.2–91.3) ($n = 6$)	(91.6–94.3) ($n = 2$)	(57.1–83.5) ($n = 8$)
Skhul V	107.0	69.3	—	67.6*
Burgos (males)	110.4 ± 5.6	70.9 ± 4.8	95.5 ± 4.5	84.1 ± 4.7
	(99.7–122.0) ($n = 35$)	(61.1–81.4) ($n = 36$)	(87.3–104.8) ($n = 37$)	(75.2–94.3) ($n = 38$)

Values in parentheses are estimated.

* Value is out of the Burgos recent human sample range.

[1] The Neandertal sample ($n = 8$) includes the following specimens: Kebara 2 (Arensburg et al., 1990; Arensburg, 1991), Krapina 103, Krapina 104, Krapina 105, La Chapelle-aux-Saints, La Ferrassie 1, Régourdou 1 (Piveteau, 1966), and Shanidar 2.

[2] Shape index = MDvD/STrD × 100.

[3] Canal-shape index = M10/M11 × 100.

[4] Articular-facet superposition = STrD/ITrD × 100.

[5] Axis height/width index = M1a/STrD.

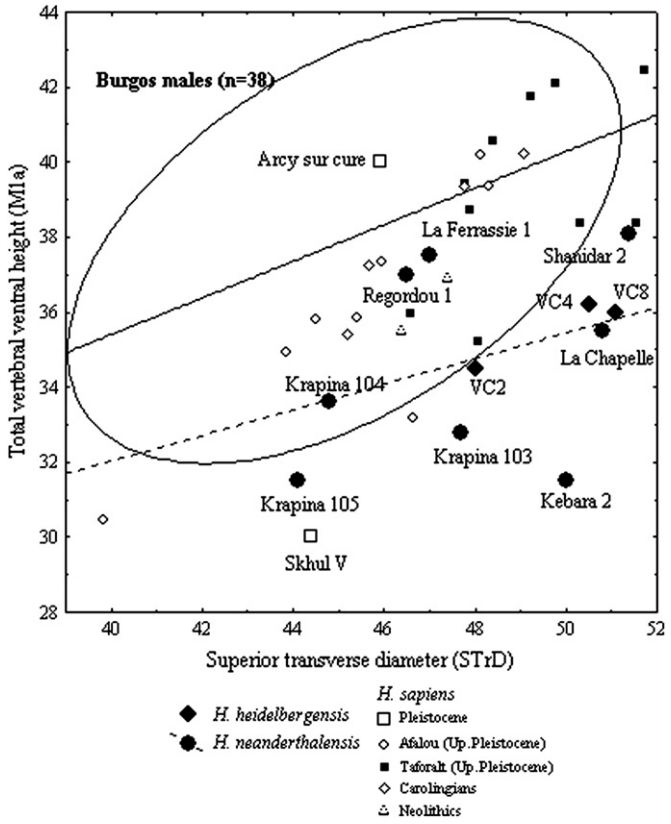

Fig. 10. Axis total vertebral height (y) vs. superior transverse diameter in the Burgos sample and several fossil atlases. The 95% equiprobability ellipse for the Burgos male sample and the regression line for the Burgos sample (solid line) and the Neandertals (dotted line) are shown. For the Burgos modern male sample, $y = 0.4879x + 15.8829$ ($n = 38$). For the Neandertal sample, $y = 0.3415x + 18.369$ ($n = 8$). The extremely low value for the total vertebral height in the Kebara 2 axis could be due to an underestimation of this measurement by Arensburg et al. (1990). On the other hand, McCown and Keith (1939) underscore the smallness of Skhul V axis.

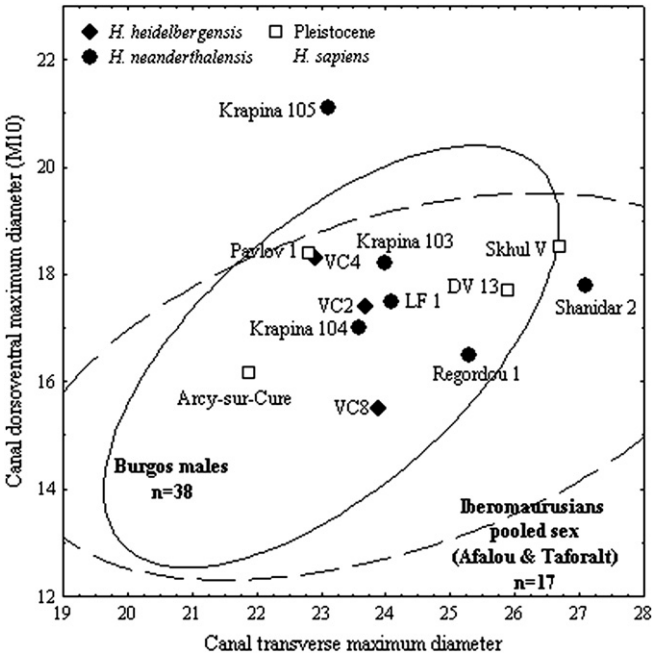

Fig. 11. Axis canal dorsoventral diameter (y) vs. canal transverse maximum diameter in the Burgos sample and several fossil atlases. The 95% equiprobability ellipses for the Burgos male sample and for the Iberomaurusian pooled sex sample are given. DV 13 refers to Dolní Věstonice 13. LF1 refers to La Ferrassie 1. The value of M10 reported by McCown and Keith (1939) for the Skhul V axis is 24.6 mm, 0.1 mm above the value reported by Stewart (1962), which is 6 mm above our value. This extraordinary difference could be due to differences in measurement method (see Fig. 1).

age-progressive (Aufderheide and Rodríguez-Martín, 1998). In 80% of the cases, no cause is evident, and in other cases, the cause may be physical, infectious, or metabolic, among other factors.

Bocquet-Appel and Arsuaga (1999) demonstrated that there is a dearth of mature adult individuals at the SH site. Based on the study of dental wear, Bermúdez de Castro et al. (2004) found only three individuals who were older than 35 years (one male and two of indeterminate sex). Of these three individuals, one could also be represented by Pelvis 1 (older than 35) and another, represented by the isolated pubis AT-2500, could be more than 45 years.

Bermúdez de Castro and Pérez (1995) studied the enamel hypoplasia in the SH sample to determine the level of biological stress that affected the development of these hominins. They found that this population probably suffered a lower level of biological stress than did Neandertal populations (see also Cunha et al., 2004).

In summary, the appearance of different degrees of DJD in two SH adult individuals represented by the upper cervical vertebrae could indicate that these vertebrae belong to some of the older individuals represented by the dental material. In one case, this is confirmed by the association of VC7(C1) and VC8(C2) with Cranium 5 (age at death ≥ 35; Bermúdez de Castro et al., 2004).

Discussion

Phylogenetic evidence suggests that the SH sample and all European middle Pleistocene hominins represent populations that were ancestral to the Neandertal populations, as they are characterized by a mixture of shared primitive features and Neandertal apomorphies (Arsuaga et al., 1997c; Carretero

Table 14
Comparison of the vertebral-foramen area (mm^2) of the SH and recent human axes

Specimen/sample	Vertebral-foramen area 1*	Vertebral-foramen area 2**
VC2	(306.3)	(302.0)
VC4	329.1	331.4
VC8	295.4	314.0
Burgos[1] (males)	301.9 ± 43.1 (234.5–401.2) ($n = 30$)	302.9 ± 47.5 (233.8–415.2) ($n = 30$)

Values in parentheses are estimated.
* Imaged linear measures.
** Cross-checked for accuracy by comparing imaged linear measures to physical dimensions measured with digital calipers.
[1] The two mean values of the vertebral-foramen area in the Burgos sample are not statistically different.

et al., 1997; Martínez and Arsuaga, 1997). In the SH upper cervical vertebral sample, we have found some features that could be of phylogenetic significance but whose polarity is difficult to ascertain due to the scarcity of hominin vertebrae. Within this group we can mention: (1) the development of the tubercle for the attachment of the transverse ligament of the atlas and (2) the height/breadth index of the axis. We should note that the SH specimens are metrically more similar to Neandertals than to our modern human comparative samples. Moreover, we have found that (1) the atlases from the Sima de los Huesos site exhibit a percentage of weakly developed tubercles for the attachment of the transverse ligament that is intermediate between modern human populations and Neandertals, and (2) the SH axes exhibit a height/breadth index similar to that of the Neandertals. These findings are fully compatible with the phylogenetic position proposed for these hominins (i.e., that *H. heidelbergensis* is an exclusively European species, ancestral only to *H. neanderthalensis*; Arsuaga et al., 1997c; Carretero et al., 1997; Martínez and Arsuaga, 1997).

Biomechanics

The atlanto-occipital articulation allows only for flexion and extension (Bogduk and Mercer, 2000). It acts as a first-class lever in which the occipital condyles act as the fulcrum, lying between the nuchal muscles and the mass of the head (Escuredo et al., 2002). In all other respects, the head and atlas move essentially as a single unit. Few muscles act directly on the atlas and, in fact, its movements are governed by the muscles that act on the head (Bogduk and Mercer, 2000). The SH hominins show a degree of prognathism (as measured by basion–prosthion length) that is similar to that of the Neandertals (Arsuaga et al., 1997c) and well-above the prognathism of modern humans (Martínez, 1995). The SH atlases show enlarged insertion areas for *M. rectus capitis posterior minor* and the SH axes have robust spinous processes that could relate to development of *M. obliquus capitis inferior* and *M. rectus capitis posterior major*. While these features could indicate muscular force acting at the atlanto-occipital joint to counter the aforementioned prognathism, we should recall that other muscles also act to extend the head (e.g., the *M. semispinalis capitis*), which could also play an important biomechanical role in this joint. Alternatively, these enlarged muscular-attachment areas could simply reflect a generally robust body build and/or high activity levels, factors that could produce increased caudal projection of the anterior tubercle, which would agree with the high body mass calculated for these hominins (Arsuaga et al., 1999; Carretero et al., 2004).

The upper cervical spine of the SH hominins is characterized by a mediolaterally expanded atlantoaxial joint, represented by the ITrD of the atlas and the STrD of the axis, and a short craniocaudal dimension of the axis. During lateral inclination of the head, there is no movement in the atlantoaxial joint (Kapandji, 1998) and we hypothesize that a mediolateral expansion would further stabilize this joint. The close relationship between neck biomechanics and head movement and the fact that the head is the final link in an open kinematic chain that includes the cervical and the upper thoracic vertebrae (Winters and Peles, 1990) make it necessary, if we want to fully assess the biomechanics of this anatomical region, to take into account both the upper and lower cervical vertebrae and cranial morphology, which we plan to do in a future publication.

Size of the vertebral canal and its implications

Much attention has been devoted to vertebral-canal size and its relationship to spoken language. One factor in the evolution of human language that would be reflected in vertebral-canal morphology is increased breath control (MacLarnon, 1993; MacLarnon and Hewitt, 1999, 2004). Modern humans have an enlarged thoracic vertebral canal, reflecting a larger amount of gray matter. Based on the morphology of the KNM-WT 15000 individual, a narrower thoracic canal has been proposed for *Homo ergaster*, indicating that this species may only have been capable of short, unmodulated utterances, such as those used by extant nonhuman primates (MacLarnon and Hewitt, 1999). However, significant abnormalities have been found in the KNM-WT 15000 individual (Latimer and Ohman, 2001), which could indicate some form of axial dysplasia, and so the small canal may be a reflection of a neural-canal stenosis associated with the pathology. In contrast, Schiess et al. (2006) argued that the diagnosis of a congenital dysplasia is not supported, indicating that the pathological lesions in the KNM-WT 15000 individual may not be as severe as previously reported. Moreover, the Dmanisi vertebrae (Meyer, 2005; Meyer et al., 2006), which are the oldest known for the genus *Homo*, follow the modern human pattern in all regions, as the raw and relative sizes of the vertebral canals fall well within the human range, indicating that these hominins may have had fine control of the respiratory muscles involved in spoken language (Meyer, 2005; Meyer et al., 2006).

Arsuaga et al. (1997a) showed that the mean cranial capacity of SH's three most complete crania (1245 cm^3) (Arsuaga et al., 1993, 1997c) is slightly less than that of two comparative samples from the Hamann-Todd Osteological Collection. However, given the large body-weight estimates for these hominins, their encephalization quotients are below both modern human or Neandertal values (Arsuaga et al., 1999). In Neandertals, higher encephalization quotients are reached by expansion of the cranial capacity, while in modern humans it is mainly achieved by a reduction in body mass (Arsuaga et al., 1999; Carretero et al., 2004). In addition to the parallel trends in encephalization in these two lineages, the absolute size of the bony vertebral canal in the upper cervical spine reached modern human values by the middle Pleistocene. Preliminary studies (Carretero et al., 1999; Gómez et al., 2004; Gómez-Olivencia, 2005) have shown that the SH lower cervical spine's canal had a similar size compared to modern humans, but a full assessment of this anatomical region will not be possible until larger sets of cervical and thoracic vertebrae are associated. In any case, as demonstrated by Martínez et al. (2004), the SH hominins had the skeletal characteristics of the outer and middle ear that support the perception of spoken language.

Summary and conclusions

Study of the SH upper cervical spine leads us to identify a minimum of 11 individuals represented by these fossils: 6 adults and 5 subadults. Three sets of associated atlases and axes, probably belonging to male individuals, have been identified: two older adults (one of them associated with Cranium 5) and one young adult. Metrical and morphological attributes reveal that SH atlases and axes are more similar to Neandertal homologues than to our modern male comparative samples. The SH upper cervical spine is characterized by: (1) a large maximum dorsoventral diameter of the atlas's canal, which may be related to the large dorsoventral diameter of the foramen magnum; (2) dorsoventrally large lower facets of the atlas; (3) a mediolaterally expanded atlantoaxial joint; (4) a craniocaudally short axis; (5) a caudally projecting anterior tubercle of the anterior arch of the atlas; and (6) lateral masses of the atlas that possess weakly developed tubercles for the attachment of the transverse ligament at frequencies that lie between those of modern humans and Neandertals. Future associations of more cervical elements from SH will clarify the anatomy of this region and will improve our understanding of the biology of these humans.

Acknowledgements

Special thanks go to our colleagues and friends A. Gracia, C. Lorenzo, N. García, R. Quam, and A. Esquivel for their great work at the Sima de los Huesos site. M.C. Ortega restored the fossils for us. We are grateful to Jakov Radovcic (Croatian Natural History Museum), Bruce Latimer and Yohannes Haile-Selassie (Cleveland Natural History Museum), Philippe Mennecier (Musée de l'Homme), Dominique Grimaud-Hervé (Département de Préhistoire—Muséum national d'Histoire naturelle), José María Bermúdez de Castro (Centro de Investigación de Evolución Humana), Belen Castillo (Museo de Burgos), and Michele Morgan (Peabody Museum of Archaeology and Ethnology) for providing access to the skeletal collections in their care. We are also indebted to Aurélie Fort, Lyman Jellema, Stéphanie Renault, and Olivia Herschensohn for curatorial assistance. Further thanks go to our colleagues at the Laboratorio de Evolución Humana (LEH) of the Universidad de Burgos and at the Centro UCM-ISCIII de Investigación sobre Evolución y Comportamiento Humanos. Special thanks go to Aimara for her help in the determination of the vertebral-canal area, with the figures, and all her comments, which greatly improved this manuscript. Luis Cabo provided helpful advice regarding statistics. Antoine Balzeau, Isabelle de Groote, J.E. González Urquijo, and Jeremiah Scott provided helpful comments on different parts of the manuscript. We are indebted to Marc R. Meyer discussing ideas dealing with vertebrae. We are grateful to Rolf Quam and Ciarán Brewster (P.D.), who helped with the English translation. Angelica Torres kindly revised the English in an earlier version of the manuscript. Rolf Quam also provided helpful comments that greatly improved this paper. We are indebted to William H. Kimbel for his thorough edit of the manuscript and his helpful comments, as well as those provided by the associate editor and three anonymous referees, which greatly improved the manuscript.

The first author is supported by a grant from the Ministerio de Educación y Ciencia. Laura Rodríguez is supported by a grant from the Fundación Siglo para las Artes en Castilla y León. This research was supported by the Ministerio de Ciencia y Tecnología, Proyecto BOS2003-08938-C03-01. Funding for the fieldwork came from the Junta de Castilla y León and Fundación Atapuerca. Help in the field from the Grupo Espeleológico Edelweiss was essential.

Appendix 1. Labeling of the SH vertebrae

Every human fossil from this site is identified by the field label "AT-" followed by the inventory number. For example, AT-333 is a distal epiphysis of a left adult humerus (see Carretero et al., 1997) and AT-121 is a frontal bone (Arsuaga et al., 1991). The fossils that consist of several fragments and labels have a second identification number with the initial letter of the bone and a Roman numeral. For example, H-I is Humerus I, a distal epiphysis of an immature individual composed of AT-741 and AT-791 (Carretero et al., 1997). In the case of anatomical parts that consist of different bones, like crania, a third inventory number is used. When significant parts of the calvaria (including different bones) are represented (with or without the face), the term "cranium" is used to label it, followed by an Arabic number. For example, Cranium 1 comprises AT-40, AT-63a-b, AT-65, AT-86, AT-122, AT-177a-e, AT-206, AT-216, AT-223, AT-472, and AT-937 (Arsuaga et al., 1997c), which includes Occipital III [described as an isolated cranial bone by Arsuaga et al. (1991)]. Finally, based on dental evidence, 28 individuals have been identified (Bermúdez de Castro et al., 2004) and are labeled with Roman numerals. For example, the individual XXI includes Cranium 5 and the mandible AT-888.

We present a somewhat different way of labeling the SH vertebrae from that used for other bones in the same collection due to the large number of vertebral elements within each spine and the difficulty in assessing the exact anatomical position of vertebrae in some cases. The most complete vertebrae are also labeled with a "V" (for vertebra) and the initial letter of the vertebral region to which they belong ("C" for cervical, "T" for thoracic, and "L" for lumbar). Arabic numbers indicate the "inventory" number within each vertebral region. For example, VC16 is formed by AT-1140 and AT-2201, and among the most complete cervical vertebrae, it is the sixteenth labeled element (Table 2). Specimen VC15 is formed only by AT-2582, but this vertebra is complete enough to warrant a VC label, and among the most complete cervical vertebrae, it is the fifteenth labeled element. To make the discussion in the text easier to follow, the anatomical position within the region is indicated in parentheses. For example, VC1(C7) (formerly known as C7-I in Carretero et al., 1999) is formed by AT-321, AT-1556, AT-1569, and AT-1609, and it is the first labeled cervical of the sample (Table 2); the specimen is a seventh

cervical vertebra. Specimen VT27(T4-8) is formed by AT-1135 and AT-4008 and is the twenty-seventh thoracic element labeled, and its anatomical position lies between the fourth and the eighth thoracic vertebrae. For other elements, even if the anatomical determination can be made with complete accuracy we use the ''AT-'' field label due to the incompleteness of the fossil. For example, AT-2883 is the dens of an axis (C2) (Table 3). Future reconstructions of ''AT-'' labeled fragments will yield new complete VC specimens.

References

Arensburg, B., 1991. The vertebral column, thoracic cage and hyoid bone. In: Bar-Yosef, O., Vandermeersch, B. (Eds.), Le squelette moustérien de Kébara 2. Éditions du CNRS, Paris, pp. 113–147.

Arensburg, B., Schepartz, L.A., Tillier, A.M., Vandermeersch, B., Rak, Y., 1990. A reappraisal of the anatomical basis for speech in Middle Palaeolithic hominids. Am. J. Phys. Anthropol. 83, 137–146.

Arsuaga, J.L., Carretero, J.M., Lorenzo, C., Gracia, A., Martínez, I., Bermúdez de Castro, J.M., Carbonell, E., 1997a. Size variation in middle Pleistocene humans. Science 277, 1086–1088.

Arsuaga, J.L., Martínez, I., Gracia, A., Carretero, J.M., Lorenzo, C., Garcia, N., Ortega, A.I., 1997b. Sima de los Huesos (Sierra de Atapuerca, Spain). The site. J. Hum. Evol. 33, 109–127.

Arsuaga, J.L., Martínez, I., Gracia, A., Lorenzo, C., 1997c. The Sima de los Huesos crania (Sierra de Atapuerca, Spain). A comparative study. J. Hum. Evol. 33, 219–281.

Arsuaga, J.L., Carretero, J.M., Martínez, I., Gracia, A., 1991. Cranial remains and long bones from Atapuerca/Ibeas (Spain). J. Hum. Evol. 20, 191–230.

Arsuaga, J.L., Lorenzo, C., Carretero, J.M., Gracia, A., Martínez, I., García, N., Bermúdez de Castro, J.M., Carbonell, E., 1999. A complete human pelvis from the middle Pleistocene of Spain. Nature 399, 255–258.

Arsuaga, J.L., Martínez, I., 2004. Atapuerca y la Evolución Humana. Fundació Caixa Catalunya, Barcelona.

Arsuaga, J.L., Martínez, I., Gracia, A., Carretero, J.M., Carbonell, E., 1993. Three new human skulls from the Sima de los Huesos middle Pleistocene site in Sierra de Atapuerca, Spain. Nature 362, 534–537.

Aufderheide, A.C., Rodríguez-Martín, C., 1998. The Cambridge Encyclopedia of Human Paleopathology. Cambridge University Press, Cambridge.

Bermúdez de Castro, J.M., Pérez, P.J., 1995. Enamel hypoplasia in the middle Pleistocene hominids from Atapuerca (Spain). Am. J. Phys. Anthropol. 96, 301–314.

Bermúdez de Castro, J.M., Martinón-Torres, M., Lozano, M., Sarmiento, S., Muela, A., 2004. Paleodemography of the Atapuerca–Sima de los Huesos hominin sample: a revision and new approaches to the paleodemography of the European middle Pleistocene population. J. Anthropol. Res. 60, 5–26.

Bischoff, J.L., Shamp, D.D., Aramburu, A., Arsuaga, J.L., Carbonell, E., Bermúdez de Castro, J.M., 2003. The Sima de los Huesos hominids date to beyond U/Th equilibrium (>350 kyr) and perhaps to 400–500 kyr: new radiometric dates. J. Archaeol. Sci. 30, 275–280.

Bischoff, J.L., Williams, R.W., Rosenbauer, R.J., Aramburu, A., Arsuaga, J.L., García, N., Cuenca-Bescós, G., 2006. High-resolution U-series dates from the Sima de los Huesos hominids yields 600 $+\infty/-66$ kyrs: implications for the evolution of the early Neanderthal lineage. J. Archaeol. Sci. 34, 763–770.

Boaz, N.T., Ciochon, R.L., Xu, Q., Liu, J., 2004. Mapping and taphonomic analysis of the *Homo erectus* loci at Locality 1 Zhoukoudian, China. J. Hum. Evol. 46, 519–549.

Bocquet-Appel, J.P., Arsuaga, J.L., 1999. Age distributions of hominid samples at Atapuerca (SH) and Krapina could indicate accumulation by catastrophe. J. Archaeol. Sci. 26, 327–338.

Bogduk, N., Mercer, S., 2000. Biomechanics of the cervical spine. I: Normal kinematics. Clin. Biomech. 15, 633–648.

Boule, M., 1911–1913. L'homme fossile de la Chapelle-aux-Saints. Ann. Paléontol. 6, 111–172. 7, 21–56, 85–192; 8, 1–70.

Bräuer, G., 1988. Osteometrie. In: Knussmann, R. (Ed.), Anthropologie. Handbuch der vergleichenden Biologie des Menschen. Gustav Fischer, Stuttgart, pp. 160–232.

Buikstra, J.E., Gordon, C.C., St. Hoyme, L., 1984. The case of severed skulls. Individuation in forensic anthropology. In: Rathbun, T., Buikstra, J.E. (Eds.), Human Identification: Case Studies in Forensic Anthropology. Charles C. Thomas Pub. Ltd., pp. 121–135.

Carbonell, E., Mosquera, M., Ollé, A., Rodríguez, X.P., Sala, R., Vergés, J.M., Arsuaga, J.L., Bermúdez de Castro, J.M., 2003. Les premiers comportements funéraires auraient-ils pris place à Atapuerca, il y a 350 000 ans? L'Anthropologie 107, 1–14.

Carretero, J.M., 1994. Estudio del esqueleto de las dos cinturas y el miembro superior de los homínidos de la Sima de los Huesos, Sierra de Atapuerca, Burgos. Ph.D. Dissertation, Universidad Complutense de Madrid.

Carretero, J.M., Arsuaga, J.L., Lorenzo, C., 1997. Clavicles, scapulae and humeri from the Sima de los Huesos Site (Sierra de Atapuerca, Spain). J. Hum. Evol. 33, 357–408.

Carretero, J.M., Arsuaga, J.L., Martínez, I., Quam, R., Lorenzo, C., Gracia, A., Ortega, A.I., 2004. Los humanos de la Sima de los Huesos (Sierra de Atapuerca) y la evolución del cuerpo en el género *Homo*. In: Baquedano, E., Rubio, S. (Eds.), Miscelánea en Homenaje a Emiliano Aguirre. Volumen III. Paleoantropología. Museo Arqueológico Regional, Alcalá de Henares, pp. 120–135.

Carretero, J.M., Lorenzo, C., Arsuaga, J.L., 1999. Axial and appendicular skeleton of *Homo antecessor*. J. Hum. Evol. 37, 459–499.

Churchill, S.E., Formicola, V., 1997. A case of marked bilateral asymmetry in the upper limbs of an Upper Palaeolithic male from Barma Grande (Liguria), Italy. Int. J. Osteoarchaeol. 7, 18–38.

Cook, D.C., Buikstra, J.E., DeRousseau, C.J., Johanson, D.C., 1983. Vertebral pathology in the Afar australopithecines. Am. J. Phys. Anthropol. 60, 83–102.

Creed-Miles, M., Rosas, A., Kruszynski, R., 1996. Issues in the identification of Neandertal derivative traits at early post-natal stages. J. Hum. Evol. 30, 147–153.

Cuenca-Bescós, G., Laplana, C., Canudo, J.I., Arsuaga, J.L., 1997. Small mammals from Sima de los Huesos. J. Hum. Evol. 33, 175–190.

Cunha, E., Ramirez Rozzi, F.V., Bermudez de Castro, J.M., Martinón-Torres, M., Wasterlain, S.N., Sarmiento, S., 2004. Enamel hypoplasias and physiological stress in the Sima de los Huesos middle Pleistocene hominins. Am. J. Phys. Anthropol. 125, 220–231.

Dawson, J.E., Trinkaus, E., 1997. Vertebral osteoarthritis of the La Chapelle-aux-Saints 1 Neanderthal. J. Archaeol. Sci. 24, 1015–1021.

Escuredo, B., Sánchez, J.M., Borrás, F.X., Serrat, J., 2002. Estructura y función del cuerpo humano. McGraw-Hill, Interamericana, Madrid.

García, N., 2002. Los carnívoros de los yacimientos Pleistocenos de la Sierra de Atapuerca. Ph.D. Dissertation, Universidad Complutense de Madrid.

García, N., Arsuaga, J.L., Torres, T., 1997. The carnivore remains from the Sima de los Huesos middle Pleistocene site (Sierra de Atapuerca, Spain). J. Hum. Evol. 33, 155–174.

Gómez, A., Carretero, J.M., Arsuaga, J.L., Martínez, I., Quam, R., Lorenzo, C., Gracia, A., García, N., Ortega, A.I., Rodríguez, L., 2004. El raquis de los humanos del yacimiento de la Sima de los Huesos (Sierra de Atapuerca, Burgos). In: Egocheaga, J.E. (Ed.), Biología de Poblaciones Humanas: Diversidad, Tiempo, Espacio. Dpto. de Biología de Organismos y Sistemas, Antropología Física, Universidad de Oviedo, Oviedo, pp. 283–293.

Gómez, A., Carretero, J.M., Rodríguez, L., García, R., Arsuaga, J.L., 2005. The cervical vertebrae from the Sima de los Huesos site (Sierra de Atapuerca, Burgos, Spain). Am. J. Phys. Anthropol. 40 (Suppl.), 107.

Gómez-Olivencia, A., 2005. Estudio de la columna cervical de los humanos de la Sima de los Huesos (Sierra de Atapuerca, Burgos). Master's Thesis, Universidad Complutense de Madrid.

Gray, H., 1959. Anatomy of the Human Body. Lea and Febiger, Philadelphia.

Grine, F.E., Pearson, O.M., Klein, R.G., Rightmire, G.P., 1998. Additional human fossils from Klasies River Mouth, South Africa. J. Hum. Evol. 35, 95–107.

Heim, J.-L., 1976. Les Hommes fossiles de la Ferrassie. I. Le Gisement. Les Squelettes Adultes (Crâne et Squelette du Tronc). Masson, Paris.

Holliday, T.W., 2006. The vertebral columns. In: Trinkaus, E., Svoboda, J. (Eds.), Early Modern Human Evolution in Central Europe. Oxford University Press, Oxford, pp. 242–294.

Irish, J.D., 2000. The Iberomaurusian enigma: North African progenitor or dead end? J. Hum. Evol. 39, 393–410.

Kapandji, A.I., 1998. Fisiología Articular. 3. Tronco y Raquis. Editorial Médica Panamericana. Maloine, Madrid.

Latimer, B., Ohman, J.C., 2001. Axial dysplasia in *Homo erectus*. J. Hum. Evol. 40, A12.

Leakey, R.E.F., Walker, A.C., 1985. Further hominids from the Plio-Pleistocene of Koobi Fora, Kenya. Am. J. Phys. Anthropol. 67, 135–163.

Leroi-Gourhan, A., 1958. Étude des restes humains fossiles provenant des grottes d'Arcy-sur-Cure. Ann. Paléontol. 44, 87–148.

Lovejoy, C.O., Johanson, D.C., Coppens, Y., 1982. Elements of the axial skeleton recovered from the Hadar formation: 1974–1977 collections. Am. J. Phys. Anthropol. 57, 631–635.

MacLarnon, A.M., 1993. The vertebral canal. In: Walker, A., Leakey, R.E.F. (Eds.), The Nariokotome *Homo erectus* Skeleton. Springer-Verlag, Berlin, pp. 359–390.

MacLarnon, A.M., Hewitt, G.P., 1999. The evolution of human speech: The role of enhanced breathing control. Am. J. Phys. Anthropol. 109, 341–363.

MacLarnon, A.M., Hewitt, G.P., 2004. Increased breathing control: another factor in the evolution of human language. Evol. Anthropol. 13, 181–197.

Marino, E.A., 1995. Sex estimation using the first cervical vertebra. Am. J. Phys. Anthropol. 97, 127–133.

Martin, H., 1923. L'Homme fossile de la Quina. Librairie Octave Doin, Paris.

Martínez, I., 1995. La base del cráneo y el hueso temporal en la evolución de los homínidos, con especial referencia a los fósiles de la Sierra de Atapuerca (Burgos). Ph.D. Dissertation, Universidad Complutense de Madrid.

Martínez, I., Arsuaga, J.L., 1997. The temporal bones from Sima de los Huesos middle Pleistocene site (Sierra de Atapuerca, Spain). A phylogenetic approach. J. Hum. Evol. 33, 283–318.

Martínez, I., Rosa, M., Arsuaga, J.L., Jarabo, P., Quam, R., Lorenzo, C., Gracia, A., Carretero, J.M., Bermúdez de Castro, J.M., Carbonell, E., 2004. Auditory capacities in middle Pleistocene humans from the Sierra de Atapuerca in Spain. Proc. Natl. Acad. Sci. U.S.A. 101, 9976–9981.

McCown, T.D., Keith, A., 1939. The Stone Age of Mount Carmel. The Fossil Human Remains from the Levalloiso-Mousterian. Clarendon Press, Oxford.

Meyer, M.R., 2005. Functional biology of the *Homo erectus* axial skeleton from Dmanisi, Georgia. Ph.D. Dissertation, University of Pennsylvania.

Meyer, M.R., Lordkipanitze, D., Vekua, 2006. Evidence for the anatomical capacity for spoken language in *Homo erectus*. Am. J. Phys. Anthropol. 42 (Suppl.), 130.

Ogilvie, M.D., Hilton, C.E., Ogilvie, C.D., 1998. Lumbar anomalies in the Shanidar 3 Neandertal. J. Hum. Evol. 35, 597–610.

Pap, I., Tillier, A.-M., Arensburg, B., Chech, M., 1996. The Subalyuk Neanderthal remains (Hungary): a re-examination. Annales Historico-Naturales Musei Nationalis Hungarici 88, 233–270.

Pérez, P.-J., 2003. Recopilación de diagnósticos paleopatológicos en fósiles humanos, con casos relativos a homínidos de Atapuerca. In: Isidro, A., Malgosa, A. (Eds.), Paleopatología. La Enfermedad no Escrita. Masson, Barcelona.

Piveteau, J., 1966. La Grotte de Regourdou (Dordogne). Paléontologie humaine. Ann. Paléontol. 52, 163–194.

Radovcic, J., Smith, F.H., Trinkaus, E., Wolpoff, M.H., 1988. The Krapina Hominids. An Illustrated Catalog of Skeletal Collection. Mladost, Croatian Natural History Museum, Zagreb.

Rak, Y., Arensburg, B., 1987. Kebara 2 Neanderthal pelvis: first look at a complete inlet. Am. J. Phys. Anthropol. 73, 227–231.

Rak, Y., Kimbel, W.H., Hovers, E., 1994. A Neandertal infant from Amud Cave, Israel. J. Hum. Evol. 26, 313–324.

Rak, Y., Kimbel, W.H., Hovers, E., 1996. On Neandertal autapomorphies discernible in Neandertal infants: a response to Creed-Miles *et al*. J. Hum. Evol. 30, 155–158.

Ramírez Rozzi, F.V., Bermúdez de Castro, J.M., 2004. Surprisingly rapid growth in Neanderthals. Nature 428, 936–939.

Rosas, A., Bastir, M., Martínez-Maza, C., Bermudez de Castro, J.M., 2002. Sexual dimorphism in the Atapuerca-SH hominids: the evidence from the mandibles. J. Hum. Evol. 42, 451–474.

Scheuer, L., Black, S., 2000. Developmental Juvenile Osteology. Academic Press, San Diego.

Schiess, R., Haeusler, M., Langenegger, E., 2006. How pathological is the Nariokotome boy KNM-WT 15000 (*Homo erectus*)? Am. J. Phys. Anthropol. 42 (Suppl.), 159.

Sládek, V., Trinkaus, E., Hillson, S.W., Holliday, T.W., 2000. The People of the Pavlovian. Skeletal Catalogue of the Gravettian Fossil Hominids from Dolní Věstonice and Pavlov. Academy of Sciences of the Czech Republic, Institute of Archaeology in Brno, Brno.

Smith, B.H., 1991. Dental development and the evolution of life history in Hominidae. Am. J. Phys. Anthropol. 86, 157–174.

Stewart, T.D., 1962. Neanderthal cervical vertebrae with special attention to the Shanidar Neanderthals from Iraq. Bibl. Primatol. 1, 130–154.

Trinkaus, E., 1983. The Shanidar Neandertals. Academic Press, New York.

Trinkaus, E., 1985. Pathology and the posture of the La Chapelle-aux-Saints Neandertal. Am. J. Phys. Anthropol. 67, 19–41.

Tubbs, R.S., Wellons, J.C., Banks, J., Blount, J.P., Oakes, W.J., 2002. Quantitative anatomy of the transverse ligament tubercles. J. Neurosurg. Spine 97, 343–345.

Vandermeersch, B., 1981. Les hommes fossiles de Qafzeh (Israël). CNRS, Paris.

Vandermeersch, B., Trinkaus, E., 1995. The postcranial remains of the Régourdou 1 Neandertal: the shoulder and arm remains. J. Hum. Evol. 28, 439–476.

Walker, A., Zimmerman, M.R., Leakey, R.E.F., 1982. A possible case of hypervitaminosis A in *Homo erectus*. Nature 296, 248–250.

Wescott, D.J., 2000. Sex variation in the second cervical vertebra. J. Forensic Sci. 45, 462–466.

Winters, J.M., Peles, J.D., 1990. Neck muscle activity and 3-D head kinematics during quasi-static and dynamic tracking movements. In: Winters, J.M., Woo, S.L.-Y. (Eds.), Multiple Muscle Systems. Biomechanics and Movement Organization. Springer-Verlag, New York, pp. 461–480.

AMERICAN JOURNAL OF PHYSICAL ANTHROPOLOGY 159:325–341 (2016)

Standing on the Shoulders of Apes: Analyzing the Form and Function of the Hominoid Scapula Using Geometric Morphometrics and Finite Element Analysis

Thomas A. Püschel* and William I. Sellers

Computational and Evolutionary Biology Group, Faculty of Life Sciences, University of Manchester, Manchester, M13 9PT, UK

KEY WORDS shape; biomechanical performance; scapulae; hominoidea

ABSTRACT

Objective: The aim was to analyze the relationship between scapular form and function in hominoids by using geometric morphometrics (GM) and finite element analysis (FEA).

Methods: FEA was used to analyze the biomechanical performance of different hominoid scapulae by simulating static postural scenarios. GM was used to quantify scapular shape differences and the relationship between form and function was analyzed by applying both multivariate-multiple regressions and phylogenetic generalized least-squares regressions (PGLS).

Results: Although it has been suggested that primate scapular morphology is mainly a product of function rather than phylogeny, our results showed that shape has a significant phylogenetic signal. There was a significant relationship between scapular shape and its biomechanical performance; hence at least part of the scapular shape variation is due to non-phylogenetic factors, probably related to functional demands.

Discussion: This study has shown that a combined approach using GM and FEA was able to cast some light regarding the functional and phylogenetic contributions in hominoid scapular morphology, thus contributing to a better insight of the association between scapular form and function. Am J Phys Anthropol 159:325–341, 2016.

Primates live in diverse environments, mastering both life in trees and in terrestrial locations (Fleagle, 1998). Because of the variable requirements of these diverse ecological niches, primate movements are consequently complex, exhibiting an impressively large locomotor repertoire. This locomotor complexity relies on the strong hind limbs and mobile forelimbs. The overall mobility of the forelimb depends on the structure and function of the shoulder region (Larson, 1995; Chan, 2007). Consequently, the evolution of shoulder mobility is one of the important evolutionary processes generating the locomotor diversity of primates. The latter is especially relevant among hominoids because within Hominoidea five divergent locomotion modes and associated body plans have evolved (Preuschoft, 2004): arm-swinging in gibbons; forelimb-dominated slow climbing in orangutans; quadrupedalism with climbing in the African apes; mixed bipedal climbing for australopithecines; and bipedal walking in humans. Although the anatomy of the upper limb of apes has been suggested to be adapted for suspensory behaviors (Aiello and Dean, 1990; Larson, 1993; Rose, 1993), some significant differences in limb morphology have also been described that could correspond to differences in locomotion. Even though the locomotor repertoires of non-human apes overlap to a certain extent, the proportions of the different locomotor behaviors and their related kinematics differ between species and hence it is logical to expect that these differences will be reflected in their shoulder morphology. One of the main behavioral dissimilarities is the amount of time that each species spends in arboreal locations. For instance, orangutans and gibbons are predominantly arboreal spending the majority of their time in the canopy (Rodman, 1984), while on the other hand African apes are primarily terrestrial using knuckle-walking when travelling (Hunt, 2004), spending time in the forest canopy to almost exclusively sleep and feed (Hunt, 1992).

The shoulder is a region that in primates functions in rather dissimilar ways in different groups (Oxnard, 1967). It is a pivotal component of the locomotor system as it links the upper limb with the trunk and participates in several ways during different locomotion behaviors (e.g., grasping, climbing, brachiation, among others). Primates exhibit some specific morphological features in their shoulders that distinguish them with respect to other mammals, such as a well-developed clavicle, a dorsally shifted scapula with a prominent acromion and robust spine, and a relatively straight humerus with a globular head (Schultz, 1930, 1961). These traits have usually been related to the high mobility of the arm, and the wide

Additional Supporting Information may be found in the online version of this article.

Grant sponsor: Becas Chile Scholarship Program, CONICYT, Chile.

*Correspondence to: Thomas A. Püschel, Faculty of Life Sciences, University of Manchester, Michael Smith Building, Oxford Road, Manchester, M13 9PT, United Kingdom.
E-mail: thomas.puschel@postgrad.manchester.ac.uk

Received 9 December 2014; revised 2 September 2015; accepted 1 October 2015

DOI: 10.1002/ajpa.22882
Published online 16 October 2015 in Wiley Online Library (wileyonlinelibrary.com).

excursions of the forelimb. Earlier studies (Oxnard and Ashton, 1962; Ashton and Oxnard, 1963, 1964a,b) showed that forelimb function was related to the degree to which the limb is subject to tensile or compressive forces, being consequently classified based on these results: a) quadrupeds (shoulder subject to mainly compressive forces), b) brachiators (shoulder subject to mostly tensile forces), and c) semi-brachiators (shoulder intermittingly subject to both forces) (Oxnard, 1967, 1968, 1973; Feldesman, 1976; Corruccini and Ciochon, 1978). Following this trend, several authors attempted to relate the observed variability in the primate scapula and associate it with a priori defined locomotor categories by using morphometrics (Miller, 1932; Inman et al., 1944; Davis, 1949; Smith and Savage, 1956; Ashton and Oxnard, 1963, 1964a; Müller, 1967; Oxnard, 1973; Roberts, 1974; Corruccini and Ciochon, 1976; Fleagle, 1977; Kimes et al., 1981; Shea, 1986; Taylor, 1997; Young, 2004, 2006, 2008). These studies have shown that the primate scapular morphology mainly reflects its function; however these analyses do not provide any understanding about the underlying processes relating the scapular form with its function. Although valuable, most of the research about the shoulder girdle have been restricted to morphological comparisons and infrequently aimed to elucidate function from a biomechanical perspective (Preuschoft et al., 2010).

The scapula is anatomically and biomechanically involved in shoulder function and the movement of the arm (Kibler and McMullen, 2003). During daily activities, the shoulder and arm movements required to produce a change in the glenohumeral position are linked. Scapula, shoulder, and arm are either moved into or stabilize in a certain position in order to generate, absorb, and transfer forces that allow movement. Nonetheless, the specific biomechanical function of the shoulder is poorly known when compared to other anatomical locations (Preuschoft et al., 2010). Some classical studies have focused on estimating the force equilibrium for the glenoid cavity of chimpanzees (Preuschoft, 1973), defining basic conditions (Badoux, 1974; Roberts, 1974) and analyzing the functional loadings of the scapula by modeling it as a framework (Müller, 1967). In spite of the practical difficulties involved in observing the movements of the shoulder, some primate taxa have been analyzed (Schmidt and Fischer, 2000; Schmidt, 2005, 2008; Schmidt and Krause, 2011), complementing the observations made earlier by several authors (Stern and Oxnard, 1973; Rose, 1974, 1979; Larson, 1993; Whitehead and Larson, 1994). Preuschoft et al., (2010) applied both armchair biomechanics and 2D finite element models in order to understand the basic functional conditions that occur in the shoulder joint and shoulder girdle of primates. The stress distributions in their hypothetical scapula under the conditions of terrestrial versus suspensory behavior showed that during quadrupedalism the scapula concentrates stress along the cranial margin whereas during suspension generates higher stresses along the axillary border. This would mean that quadrupedal locomotion involves joint forces and muscle activities that would require a long scapula with axillar and cranial margins of a relatively similar length. On the other hand, suspensory behaviors would need a more extended axillary border and a relatively shorter cranial margin in order to provide longer lever arms to the active muscles. Based on their results, they suggested that the forces exerted on the scapula generate, at least partially, its shape (Preuschoft et al., 2010). Indeed, arboreal monkeys seem to have concordant morphological features such as the reinforcement of the axillary border of the scapula and the extension of the infraspinatous fossa (Larson, 1993). This is coherent with all the evidence supporting the idea that bone is functionally adapted to the mechanical demands that are imposed during life (Wolff, 1892; Pearson and Lieberman, 2004).

Nevertheless, other lines of evidence regarding shoulder form and function have found that this relationship is not as clear or straightforward as initially thought (Taylor, 1997; Young, 2003, 2008; Larson and Stern, 2013). It has been found that locomotion differences are not well reflected at an intraspecific level in gorilla scapulae (Taylor, 1997) and that despite locomotion similarities, the scapulae of hylobatids are most similar to those of panids, rather than to those of orangutans (Young, 2008). Furthermore, comparative electromyography data recorded from different apes have shown that there are few differences in patterns of muscle activity among them, consequently suggesting that perhaps hominoids in general use basically similar shoulder mechanisms during locomotion (Larson and Stern, 2013). Unfortunately, there is no clear perspective about the relationship between scapular morphology and its function, in spite of its growing relevance due to recent finding of several hominin scapulae such as *Australopithecus afarensis* (Alemseged et al., 2006; Haile-Selassie et al., 2010; Green and Alemseged, 2012) or *Australopithecus sediba* (Berger et al., 2010; Churchill et al., 2013). In fact, the analyses of these fossils have shown that they tend to resemble the scapula of juvenile gorillas (Green and Alemseged, 2012) or orangutans (Churchill et al., 2013), instead of those of our closest phylogenetic relatives (i.e., panids). Because scapular form has been widely regarded to be primarily a product of shoulder function, it has been a central element in the interpretation of the primate fossil record (Larson, 2007). Understanding how scapular morphology is related to biomechanical performance is important in order to reconstruct the possible locomotor repertoires of extinct species and to appreciate the locomotor diversity observed in extant hominoids.

Nowadays it is possible to produce scientifically accurate virtual reconstructions of primates (Zollikofer and Leon, 2005; Sellers et al., 2010; Ogihara et al., 2011; Weber and Bookstein, 2011). Technological advances in 3D imaging allow the generation of virtual models based on skeletal morphology and comparative soft tissue data obtained from the literature. This is highly useful since the study of primate biomechanics is challenging because traditional experimental techniques are not easily applicable due to practical, conservation, and ethical reasons (Sellers et al., 2010; D'Août and Vereecke, 2011). Computer-based biomechanics comprise 3D quantitate image analysis and simulation techniques applied to musculo-skeletal systems such as finite element analysis (FEA) and multibody dynamics (Sellers and Crompton, 2004; Kupczik, 2008; O'Higgins et al., 2012). FEA is a technique that reconstructs stress, strain, and deformation in material structures and has its origin in mathematical and engineering problems, although it is been increasingly used in biological fields (Rayfield, 2007). This technique is a numerical analysis that acts by dividing a system into a finite number of discrete elements with well-known properties (e.g., triangles, tetrahedrons, or cubes) (Ross, 2005). Strain and stress can be solved by finding analytical solutions if the geometry of the object is simple enough. However, more complex forms may be difficult or even impossible to solve using analytical means, especially if the loading regimens and/or material

properties are complex (Beaupré and Carter, 1992). This situation is the most common when dealing with realistic representations of biological structures. FEA offers an alternative approach, approximating the solution by subdividing complex geometries into multiple finite elements of simple geometry. In a structural analysis, typical mechanical parameters of interest are strain, which is the deformation within a structure (Δlength/length; unitless) and stress, the applied force per unit area (Nm^{-2}), which are obtainable as result of FEA (Kupczik, 2008). FEA studies of the scapula have been mostly restricted to orthopedic studies focusing principally on the generation of models of the implanted glenoid (e.g., Friedman et al., 1992; Lacroix et al., 2000; Gupta and van der Helm, 2004; Gupta et al., 2004; Yongpravat et al., 2013; Campoli et al., 2014; Hermida et al., 2014). Even though other FEA studies have been used in comparative primatology and paleoanthropology, they have been predominantly devoted to the analysis of the craniofacial system during mastication (Kupczik et al., 2007; Wroe et al., 2007, 2010; Strait et al., 2009; Curtis et al., 2011; Dumont et al., 2011; O'Higgins et al., 2011; Fitton et al., 2012; Kupczik and Lev-Tov Chattah, 2014). There have been fewer attempts applying FEA to analyze different primate scapulae (Ogihara et al., 2003), so the present study probably represents one of the first analyses of this anatomical structure using an explicit comparative framework.

Morphometrics can be understood as the quantitative analysis of form (i.e., shape and size) and how it covaries with regard to other factors (e.g., biomechanics, development, ecology, genetics, etc.) (O'Higgins, 2000; Adams et al., 2004, 2013). More specifically, geometric morphometrics (GM) refers to the application of morphometrics to coordinate data (i.e., 2D or 3D Cartesian coordinates), normally defined as discrete anatomical loci that are homologous among all the individuals under analysis (Bookstein, 1991; Slice, 2007). GM allows the analysis of the association between morphometric and biomechanical data, which is really useful when studying the relationship between shape and function. There are many available methods to study the connection between morphological and biomechanical variables (e.g., canonical correlation, regression analysis, Mantel test, principal coordinate analysis, and partial least squares, among others). Recent developments in the study of geometric shape and biomechanical modeling have proposed that using both GM and FEA could provide a better understanding of the existing relationship between the shape of skeletal elements and their mechanical performance (Pierce et al., 2008; Piras et al., 2012, 2013; Tseng, 2013). Even though there has been some controversy regarding how to properly combine FEA and GM data (Bookstein, 2013), there is relative agreement that bridging these two techniques could provide interesting insights about the relationship between form and function (O'Higgins et al., 2011; Parr et al., 2012). Because of this reason, different approaches have been proposed to combine FEA and GM data, such as landmark-based analysis in the size-and-shape space of the deformations obtained as result of FEA (Cox et al., 2011; Gröning et al., 2011; O'Higgins et al., 2011; Milne and O'Higgins, 2012; O'Higgins and Milne, 2013), the analysis of finite element models based on warped and target surface meshes (Parr et al., 2012), and the construction of regressions for strain energy density on the largest-scale relative warps (Bookstein, 2013). Besides the issues of how to properly analyze both GM and FEA data, another problem arises when carrying out any biological study containing several species, due to the phylogenetic structure of the data (i.e., non-independence problem). Some approaches have been proposed to take into account phylogeny such as the application of phylogenetic generalized least squares models (PGLS) to fit regressions between matrices of functional/ecological variables and shape variables (Rüber and Adams, 2001; Clabaut et al., 2007; Meloro et al., 2008; Nogueira et al., 2009; Raia et al., 2010; Piras et al., 2013), the use of phylogenetic-independent contrasts estimated for each shape variable before associating them with contrasts derived from functional/ecological variables applying either partial least squares (Klingenberg and Ekau, 1996) or multivariate regressions (Figueirido et al., 2010) and the correlation between morphometric, functional/ecological, and phylogenetic matrices (Harmon et al., 2005; Young et al., 2007; Astúa, 2009; Monteiro and Nogueira, 2010). In the present study, PGLS was preferred because this method is considered more informative and powerful than other methods (e.g., distance matrix correlation) (Peres-Neto and Jackson, 2001).

In this work, FEA was used to analyze the biomechanical performance of different hominoid scapulae by simulating two basic static scenarios: a) quadrupedal standing and b) bimanual suspension. It is expected that scapular mechanical performances will vary depending on the principal locomotion mode of each species. Hence, it is expected that those species that are mostly quadrupedal (i.e., chimpanzees, bonobos, and gorillas) will better withstand the forces generated during quadrupedal standing, while more arboreal species (i.e., orangutans and gibbons) will better bear the forces generated during suspension, as previously proposed (Oxnard and Ashton, 1962; Ashton and Oxnard, 1964a; Roberts, 1974; Preuschoft et al., 2010). On the other hand, GM was used to quantify shape differences, thus comparing different scapular morphologies in relation to their known locomotion regimes. Based on preceding studies (Oxnard and Ashton, 1962; Ashton and Oxnard, 1964a; Young, 2008), scapular shape is expected to reflect mostly functional demands instead of phylogenetic relationships. Finally both FEA and GM were used to study the relationship between form and function by applying both multiple multivariate regressions and PGLS regressions. Our results are expected to contribute to a better insight of the association between hominoid scapular morphology and its biomechanical performance.

MATERIALS AND METHODS

Sample

CT-scan stacks of 11 different hominoid individuals obtained from online databases and two zoos were analyzed (Table 1; Fig. 1) (for further details about the sample see Supporting Information 1). The included species were *Hylobates lar, Pongo abelii*, *Pongo pygmaeus, Gorilla gorilla, Pan paniscus*, *Pan troglodytes*, and *Homo sapiens*. All the specimens were adult with no evident or reported pathologies associated with their shoulder girdles. Only left scapulae were modeled, although due to some CT artifacts, some right scapulae were reflected to be used in the subsequent analyses.

Finite element modeling

Segmentation. The first step to build a model from a CT stack is to carry out image segmentation. This procedure basically consists in extracting the material of

TABLE 1. Sample

Species	Common name	Accession number	Origin	Sex	Number of elements
Pan paniscus	Bonobo	Desmond	The Royal Zoological Society of Antwerp	Male	953156
Gorilla gorilla	Gorilla	Willie (GAIN 23)	Digital Morphology Museum (KUPRI)	Male	931087
Pan troglodytes	Chimpanzee	9266	Digital Morphology Museum (KUPRI)	Male	936693
Pan troglodytes	Chimpanzee	9783	Digital Morphology Museum (KUPRI)	Female	952156
Pan troglodytes	Chimpanzee	10048	Digital Morphology Museum (KUPRI)	Female	950295
Pongo pygmaeus	Bornean Orangutan	Satsuki (GAIN 37)	Digital Morphology Museum (KUPRI)	Female	996480
Pongo abelii	Sumatran Orangutan	9653	Digital Morphology Museum (KUPRI)	Male	935358
Homo sapiens	Human	Visible human female	The Visible Human Project	Female	962225
Homo sapiens	Human	Visible human male	The Visible Human Project	Male	985562
Hylobates lar	White-handed Gibbon	3308	National Museum of Scotland	Male	940973
Hylobates lar	White-handed Gibbon	3508	National Museum of Scotland	Female	939611

interest (in this case bone) out of the surrounding background and tissues where it is embedded. The CT-scans of the different hominoid species were segmented; DICOM files were imported into Seg3D v. 2.1 (CIBC, USA) where each specimen was segmented by applying a combination of case-specific thresholding values and manual painting techniques. Scapulae can be complicated to segment because their blade is extremely thin at certain areas. As a result all the models were dilated one extra voxel, to avoid possible holes in the mesh that could affect the FEA results. After performing this procedure and manually checking the results, the extra voxel layer was removed by using an erode function in the same software. The scapulae were modeled as solid parts composed only by cortical bone. Surfaces were then generated and exported as .STL files into Geomagic Studio v. 12 (Geomagic, USA). Using this software, possible errors in the polygon mesh were detected and corrected in order to remove protruding vertices and localized holes. The models had dissimilar number of elements derived from the differences in the original scan resolution; therefore they were decimated to a number of elements ranging from 20,000 to 25,000 mesh triangles. All the models were globally remeshed to simplify their element geometry, keeping the number of mesh triangles in a similar number range (i.e., 20,000–25,000). The remeshing process was applied to generate a more homogenous mesh in terms of the shape of the triangles, their distribution on the surface, and their connectivity. In addition, one individual was selected as a reference to perform a best-fit alignment using the same software in order to align all the models with respect to a common reference plane. This procedure was carried out prior to FEA to align all the models, so that loads could be applied in the same axis and to allow easier interpretation of stress results. Basically, the procedure consisted in fitting two scapula models at each time by measuring from point to point and adjusting the location of the target model to the stationary reference specimen until the average deviation was as low as possible using an iterative process (sample size: 10,000). The sums of squares of the distances between the sample pairs were minimized over all the rigid motions that could realign the two models to achieve the best-fit alignment of them. This procedure was repeated for each one of the analyzed specimens. The models were then exported as .OBJ files into Autodesk 3ds Max 2012 (AutoDesk, USA), where they were converted into .SAT files. The models were then imported into Abaqus v. 6.13 (Simulia, USA) as closed manifold solid parts in order to carry out an implicit static FEA. Finite element validation analyses have shown that both four-node and eight-node tetrahedral, and mixed four-node tetrahedral and eight-node hexahedral meshes perform well when compared with experimental data (Panagiotopoulou et al., 2011). Likewise, it has been shown that meshes composed by more than 200,000 elements show negligible stress differences between models with four- or ten-node tetrahedra elements (Brassey et al., 2013). Because ten-node tetrahedra are computationally more expensive than those composed by four nodes, the surfaces were meshed using four-node tetrahedral elements (C3D4) by applying a built-in Delaunay meshing algorithm in Abaqus v. 6.13. FE meshes were verified in the same software to find poor-meshed areas or low quality elements (i.e. aspect ratio >10). When found, those areas were re-meshed to improve mesh quality.

Material properties and boundary conditions. Many researchers are currently trying to produce more accurate finite element models by incorporating more detailed information such as muscle activation data, anisotropic material properties, several different tissues with dissimilar material attributes, etc. (Ross et al., 2005; Strait et al., 2005; Kupczik et al., 2007; Gröning et al., 2011; Rayfield, 2011). These kinds of analyses have shown that when this type of information is included, the correlation between simulations and experimental data is usually increased. Nevertheless, in this work FEA was used in a comparative fashion rather than being used to validate the models. Because of the fact that hominoid scapulae are relatively uncommon (belonging most of the time to museum specimens), destructive experimental mechanical approaches are

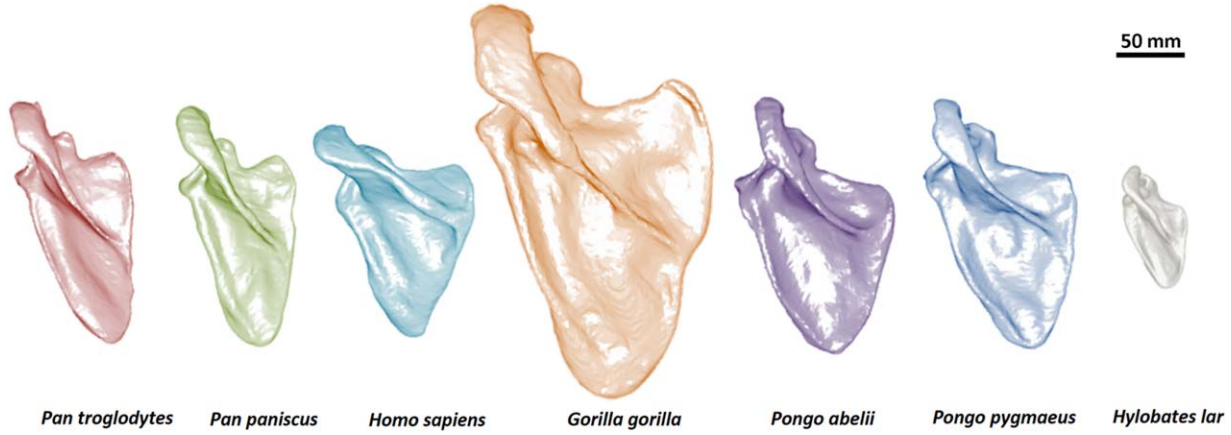

Fig. 1. Three-dimensional volumetric models of the hominoid scapulae considered in this study. [Color figure can be viewed in the online issue, which is available at wileyonlinelibrary.com.]

typically difficult or impossible to perform. The present study therefore applied FEA as a structural comparative technique rather than trying to specifically recreate how the hominoid is loaded during life; the idea was to compare a general measure of mechanical performance taking into account phylogenetic relationships. Furthermore, living specimens would probably withstand the tensile strain and stresses experienced during locomotion mostly on their shoulder soft tissues such as muscles, ligaments, and tendons rather than directly on their scapulae. Even though shoulder muscle origin and insertions for hominoids are known (Diogo et al., 2010,2012,2013a,2013b; Diogo and Wood, 2012) and physiological cross-sectional areas of some the muscles are available for some of the analyzed species (Veeger et al., 1991; Keating et al., 1993; Thorpe et al., 1999; Cheng and Scott, 2000; Carlson, 2006; Oishi et al., 2008, 2009; Michilsens et al., 2009; Peterson and Rayan, 2011; Myatt et al., 2012), the specific activation patterns are unknown for the majority of the species when performing the analyzed postures. These reasons ratified the decision of carrying out simpler comparative structural analyses instead of simulating in detail loading scenarios based on unknown or uncertain information. This means that the current work can be better understood as an analysis of how the mechanical behavior of the hominoid scapula is related to its shape, rather than being a highly-realistic simulation of how the scapula is loaded in vivo.

After the construction of the finite element mesh, it was necessary to specify the mechanical properties of the elements composing the specimens. Even though several material properties for primate cortical and trabecular bone have been published especially for humans (e.g., Currey and Butler, 1975; Williams and Lewis, 1982; Currey, 1988; Dechow et al., 1993; Ding et al., 1998; Zysset et al., 1999; Margulies and Thibault, 2000; Phelps et al., 2000; Dechow and Hylander, 2000; Peterson and Dechow, 2003; Havill et al., 2003; Bayraktar et al., 2004; Kaneko et al., 2004; Wang et al., 2006a,b; van Eijden et al., 2006; Hofmann et al., 2006; Kupczik et al., 2007; Daegling et al., 2009), there is almost a total absence of material property values for the analyzed hominoid scapulae. We used rough average values for mammalian-longitudinal cortical bone samples (Currey, 2002) (Young's modulus: 18 GPa; Poisson's ratio 0.3). The scapulae were modeled as solid models composed only of cortical bone in order to simplify the analyses, as well as to limit the number of assumptions. In fact, recent evidence has shown that FEA applied to specimens with unknown internal architecture can produce reliable results, even when the internal bone architecture cannot be modeled in detail (Fitton et al., 2015). In addition, scapulae do not exhibit high internal complexity in comparison with other bones, because most of the scapular blade consists of only a thin layer of compact tissue (i.e., cortical bone). Although bone generally behaves anisotropically, it was modeled as a linear elastic and isotropic material due to the same reasons outlined above. Besides, it has been shown that isotropic modeling seems to have little effect compared to anisotropic modeling on the pattern of stress (Chen and Povirk, 1996; Strait et al., 2005). Apart from assigning material properties, it was necessary to define boundary conditions (Bhatti, 2005). Two essential boundary conditions were specified; one recreating the action the rhomboideus, and another simulating the constraint imposed by the serratus anterior, as shown in Figure 2a. It was decided to constrain these areas because in both quadrupedal and suspensory situations the forces applied to the shoulder region seem to be predominantly supported by the muscles attached to the vertebral border of the scapula (Badoux, 1974). In these areas the displacements were only constrained in the z-direction in both cases because the forces were applied only in that direction. These boundary conditions were defined to prevent rigid body motions of the geometry and counteract residual moments (from errors when applying the loadings), but without over-constraining the models.

Loading scenarios. The scapula is one of the most complex bones of the primate skeleton due to its particular shape and because it is subjected to a great variety of forces from attached muscles during its movement (Roberts, 1974; Aiello and Dean, 1990). This bone is subject to a number of muscle, ligament, and joint reaction forces during elevation of the arm, that are difficult to quantify (Bagg and Forrest, 1986; Johnson et al., 1996; Kibler and McMullen, 2003; Fayad et al., 2006; Amadi et al., 2008; Bello-Hellegouarch et al., 2013). Quantitative and qualitative estimates of all the muscles, ligaments, and joint reaction forces acting on the human scapula during humeral abduction have shown that the scapula is relatively loaded all over its structure during abduction (van der Helm,

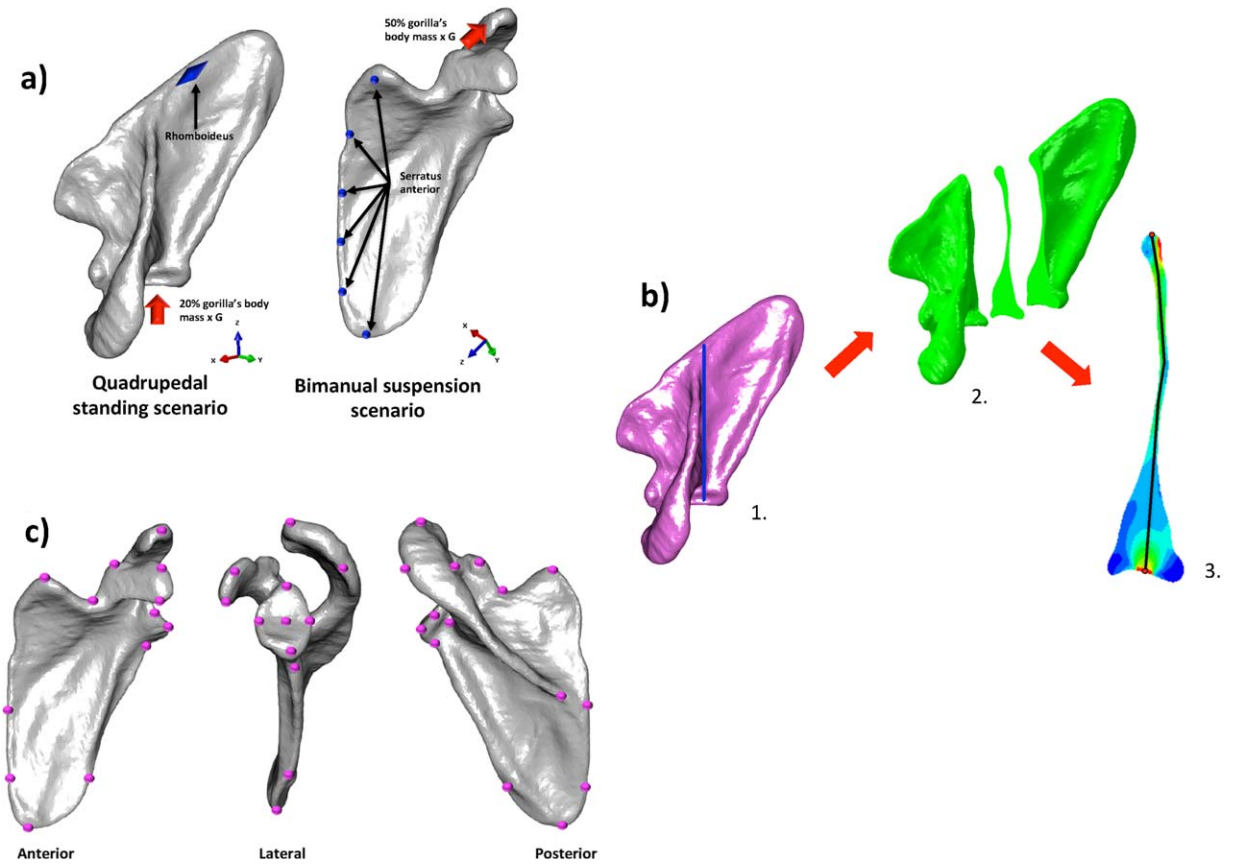

Fig. 2. *Pan paniscus* scapula used to depict **a**) FEA loading scenarios: the red arrows represent the force vectors and their direction, while the blue shapes represent the applied constraints. The constraints representing the action of serratus anterior and rhomboideus muscles were applied in both the quadrupedal standing and bimanual suspension scenarios by limiting displacement in the *z*-axis; **b**) Extraction method of the stress values: 1) At the center of the glenoid cavity a slice on the *x*-axis was defined (blue line), 2) this slice was separated and 3) two coordinates at each extreme of the slice (red dots) were used to define a path (black line) divided in 101 equidistant points used to extract von Mises stress values; **c**) 3D landmarks used to perform GM analyses. [Color figure can be viewed in the online issue, which is available at wileyonlinelibrary.com.]

1994; Gupta and van der Helm, 2004). It is therefore extremely difficult to define realistic loading scenarios and necessary to simplify the load cases in order to avoid excessive assumptions.

One important consideration to take into account when analyzing different individuals using FEA is how to make the obtained results comparable. Strain energy is proportional to the square of the load and to volume (Dumont et al., 2009), hence it is important to account for size differences when performing strain energy comparisons. Several solutions have been proposed to compare total strain between different specimens. Suggestions include scaling the loads to yield similar force:surface area ratio or scaling them to a relevant biological measurement (e.g., bite force, moment arm, animal weight) (Fitton et al., 2012; Parr et al., 2012; Brassey et al., 2013). Another possibility is to scale the models to achieve the same surface area or same volume, or to simply scale the obtained results from the analysis with respect to a sensible measure (Dumont et al., 2009). In the present work, it was decided to normalize scapular size by volume while applying the same forces to all the individuals during the FEA. This decision was based on the fact that this approach seems more suitable to evaluate how scapular shape affects mechanical strength. All the scapulae were scaled to have the same volume as the gorilla specimen (i.e., 387810.84 mm^3) in Geomagic Studio v. 12 (Geomagic, USA), and depending on the specific loading scenarios, different percentages of the reported body weight of the gorilla specimen (i.e., 176 kg) were applied to simulate the mechanical loadings. The biomechanical performance of different hominoid scapulae was tested in two basic static scenarios (Fig. 2a).

Quadrupedal standing: African apes predominantly use knuckle-walking when travelling. According to Hunt (2004), terrestrial quadrupedalism represents 96% of the locomotor behavior in mountain gorillas, 64.4% in lowland gorillas, and 35.3% in bonobos, but only 9.9% in chimpanzees. African ape scapular morphology is therefore expected to show clearer adaptations to terrestrial quadrupedalism. It is important to take in to account that chimpanzees and other primates support most of their body mass on their hind limbs during quadrupedalism rather than on their forelimbs (Reynolds, 1985; Kimura, 1992; Demes et al., 1994; Li et al., 2004; Raichlen et al., 2009). Nonetheless, due to the greater use of terrestrial locomotion modes in the African apes than in orangutans or gibbons, it is reasonable to expect that their forelimbs would be less specialized for arboreal behaviors. Even though African apes do use suspensory behaviors as a static postural activity, it is likely their scapulae are not as specialized for more recurrent suspensory behaviors such as those observed in gibbons and orangutans.

Although adult humans do not use their forelimbs for quadrupedal locomotion, the same loading scenario was applied for comparative purposes. Hominoid forelimbs support about 40% of the body weight during terrestrial quadrupedalism (Reynolds, 1985; Kimura, 1992; Demes et al., 1994; Li et al., 2004; Raichlen et al., 2009). Hence, the total applied load was calculated as 20% of the gorilla's body mass Mb; kg) multiplied by gravitational acceleration (G: 9.81 m s^{-2}), because only one scapula was analyzed per individual. This yielded a total force vector of 345.31 N., which was directed towards the center of the glenoid cavity in the *z*-axis, and applied in 24 nodes (total force/24 nodes). In addition, two models (one gibbon and the gorilla) were selected to carry out additional simulations to the test the sensitivity of the results to small differences in the application angle of the load vector, so it was changed in 5°. The results were extracted according to the procedure described in Figure 2b and a correlation was estimated to assess the level of concordance between the original stress values and those obtained after changing the load vector (Gibbon: R^2: 0.981, *P* value: <0.001; Gorilla: R^2: 0.969, *P* value: <0.001) . Therefore, the results seem to be robust to at least small changes in load direction.

Bimanual suspension: Arm-hanging is probably the only common ape posture requiring complete abduction of the arm (Hunt, 1991a,b,1992,2004). It has been suggested that the cranially oriented glenoid fossa observed among apes may be adaptive to distribute strains more evenly over the glenohumeral joint capsule during arm-hanging (Hunt, 1991b,). The long and narrow scapular shape exhibited by apes has been hypothesized to increase the mechanical advantage of the trapezius and serratus anterior during the scapular rotation necessary for arm-raising (Ashton and Oxnard, 1963, 1964b; Oxnard, 1967). However some hominoid species probably use this locomotor behavior more often than others. For instance, the highly arboreal gibbons and orangutans are expected to better cope with strains derived from this posture than the more quadrupedal species.

Even though earlier studies (Roberts, 1974; Tuttle and Basmajian, 1978) suggested that no scapulohumeral muscle was activated during bimanual or unimanual hanging assuming that joint integrity was kept solely by osseoligamentous structures, new evidence have proved the contrary. Opposed to the common idea that no muscle activation is required while the body is suspended beneath the hand (likely causing transarticular tensile stress at the glenoid cavity), hominoid electromyography data during bimanual hanging has shown that there is a continuous activity in the infraspinatous, posterior deltoid, and teres minor muscles (Larson and Stern, 1986; Larson and Stern, 2013). It has been pointed out that when climbing or hanging, primates activate the levator scapulae and trapezius muscles to prevent the caudal movement of the scapula (Larson and Stern, 1986). The resulting dorsal rotation of the caudal angle of the scapula is counteracted by the action of the caudal portion of the serratus anterior (Larson and Stern, 2013). This implies that the scapula seems to achieve its equilibrium during suspension by the coordinated action of levator scapulae and cranial trapezius, as well as the caudal serratus (Larson and Stern, 1986). In addition, to avoid the pulling of the scapula in a ventral direction, the activity of the caudal portion of the trapezius is required (Larson et al., 1991). In fact it has been observed that this muscular portion is prominently developed in apes (Aiello and Dean, 1990). It has been also mentioned that some of the forces applied to the shoulder region during suspension are supported by the muscles attached to the vertebral border of the scapula (i.e., serratus anterior and rhomboideus) (Badoux, 1974). The models were loaded in a simpler scenario by applying total load estimated as 50% of the gorilla's body mass Mb; kg) multiplied by gravitational acceleration (G: 9.81 m s^{-2}), because the total animal weight was supported by the two shoulders, thus yielding a total force vector of 863.28 N. This tensile force vector was directed away from the acromion in the *z* axis and it was also applied on 24 nodes (total force/24 nodes).

Solution. After defining the material properties and establishing the boundary conditions, the models were submitted into the Abaqus implicit solver. Each specimen was subjected to two different simulations: a) quadrupedal standing and b) bimanual suspension. Stress values were obtained and exported as .CSV files.

Statistical analyses of FEA results. von Mises stress values were obtained from 101 locations extracted along a path as described in Figure 2b. Starting from the center of the glenoid a slice on the *x*-axis was selected. Two points were defined at each opposite extremes of the slice and between these two coordinates a path was established where 101 equidistant points were positioned to extract stress values. These values were imported into R v.3.1.3 (http://www.R-project.org/) to carry out statistical analyses. The average values per species were calculated for each one of the locations. To visualize these results, a UPGMA clustering was estimated by calculating the Euclidean distances between species using the hclust() function of the package "stats." In addition a Principal Components Analysis (PCA) was performed using the princomp() function of the same package in order to reduce the number variables of this high dimensional dataset, and to subsequently perform the multivariate multiple regressions and the PGLS regressions. Because of the fact that the obtained stress could have values that differ in orders of magnitude between anatomical loci, the PCA was carried out based on the correlation matrix to standardize these possible scale differences. The number of PCs used in the successive analyses was selected to account for ca. 95% of the total variance of the sample.

Geometric morphometrics

The 3D surface models were imported into the R package "geomorph" where 20 homologous landmarks were collected on each one of the analyzed specimens using the digit.fixed() function (Adams and Otárola-Castillo, 2013) (Fig. 2c). All the GM analyses were carried out in the same package. A generalized procrustes analysis was applied to extract the shape variables from the raw landmark data, by removing all the differences due to translation, rotation and scale (Bookstein, 1991). The average shape and biomechanical performance was estimated for each species and used in the subsequent analyses. A PCA of the procrustes coordinates was performed in order to find the orthogonal axes of maximal variation, thus allowing the visualization of scapular shape variation. A consensus phylogeny (described below) was projected onto the space identified by the first two PCs obtained from the covariance matrix of the average shapes of the analyzed taxa. Using this consensus phylogeny, both morphological (i.e., shape variables) and biomechanical (i.e., stress values)

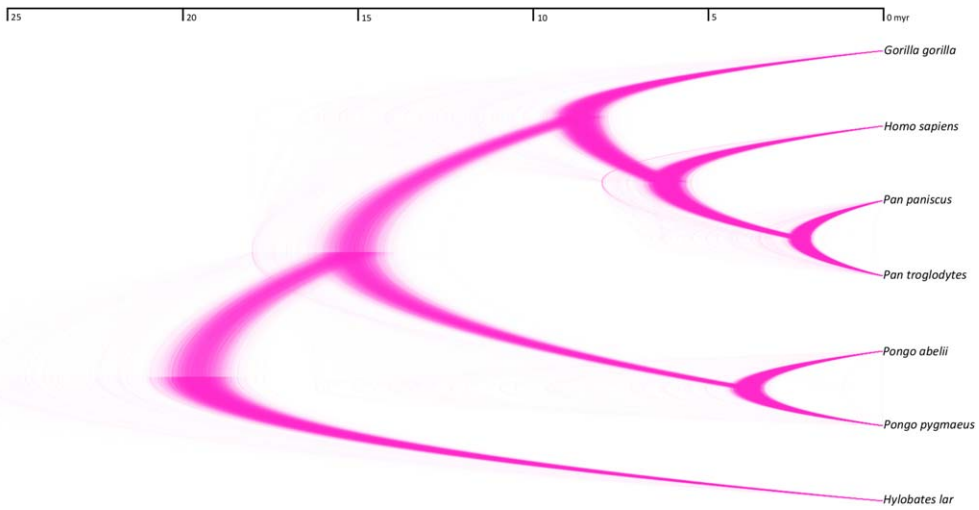

Fig. 3. 10,000 molecular phylogenetic trees plotted to overlap on top of each other in order to represent the evolutionary relationships of the analyzed taxa. The high density of the main branches is indicative of a high consistency between trees. The consensus tree was estimated and used in the subsequent comparative analyses. The plot was generated using DensiTree 2.01 (Bouckaert, 2010) and the phylogenies were obtained from the 10KTrees website (http://10ktrees.fas.harvard.edu/Primates/index.html). [Color figure can be viewed in the online issue, which is available at wileyonlinelibrary.com.]

phylogenetic signal were estimated using a generalization of the Kappa statistic suitable for highly multivariate data using the physignal() function (Blomberg et al., 2003; Adams, 2014). This method, denominated as Kmult, is based on the equivalency between statistical methods based on covariance matrices and those based on distance matrices, thus allowing a convenient way to assess phylogenetic signal in high-dimensional multivariate traits, such as those analyzed here (Adams, 2014). The K-statistic varies between 0 (no phylogenetic signal in the data, for instance with a star phylogeny) to 1 or more (data fit a Brownian motion model of evolution) (Blomberg et al., 2003). To analyze the relationship between shape and function a multiple multivariate regression of shape variables and stress PC scores was performed using the procD.lm() function. Subsequently, in order to examine the relationship between morphology and biomechanical performance taking into account the phylogenetic structure of the data a PGLS regression of shape variables and stress PC scores was performed using the procD.pgls() function. The idea in both cases was to evaluate the amount of shape explained by functional demands (Piras et al., 2013). The PGLS regressions were carried out using the procD.pgls() function. It is important to consider that the phylogenetic covariance matrix is just a 7×7 matrix, which is a limitation. In previous methodological papers (e.g., Blomberg and Garland, 2002; Blomberg et al., 2003), it has been suggested that about 15–20 OTUs are the minimum to have an acceptable statistical power, hence the obtained results have to be cautiously considered. All the aforementioned analyses were carried out in R v. 3.0.3. (http://www.R-project.org/).

Phylogeny

Using the 10kTrees Website (http://10ktrees.fas.harvard.edu/Primates/index.html), 10,000 phylogenies of the analyzed hominoid species were downloaded using the third version of this dataset (Arnold et al., 2010) (Fig. 3). These phylogenies were sampled from a Bayesian phylogenetic analysis of molecular data for eleven mitochondrial and six autosomal genes that were available in GenBank (Arnold et al., 2010). The advantage of using the 10kTrees dataset that it allows the generation of a set of phylogenetic trees suitable for comparative research that actually reflects uncertainty levels in the understanding of phylogenetic relationships, as well as providing a robust way to test phylogenetic relationships. The consensus tree of these 10,000 phylogenies was estimated and used in the subsequent comparative analyses.

RESULTS

FEA

All the analyzed individuals showed a stress widely distributed on the scapular blade, although it was logically higher in the locations where the constraints were placed (Fig. 4) (the stress values used in the analyses are available in the Supporting Information 2). The suspension scenario logically showed greater stress values (mostly on the acromion) than the quadrupedal standing simulation, due to the fact that higher loads were applied. *Hylobates lar* experienced the lowest stress for both loading scenarios when compared with rest of the hominoids, while the gorilla specimen showed the highest stress values. Interestingly, the pongids showed relatively high stress values for the standing scenario, while exhibiting relatively similar values to the gibbons during the suspension scenario. Biomechanical performance measured as von Mises stress also showed significant phylogenetic signal (quadrupedal standing, Kmult: 0.73; *P* value: 0.022; 10,000 perm. and bimanual suspension, Kmult: 0.67; *P* value: 0.042; 10,000 perm.). The UPGMA clustering of the standing scenario partially followed the hominoid phylogeny, although the gibbon and the gorilla were in reverse positions. On the other hand, UPGMA clustering of the suspension scenario showed that the suspensory species grouped together with lower stress values as compared with the rest of specimens.

GM

Phylogenetic signal was found for shape (Kmult: 0.74; *P* value: 0.007; 10,000 perm.) but not for centroid size (Kmult: 1.09; *P* value: 0.07; 10,000 perm.). Regarding shape

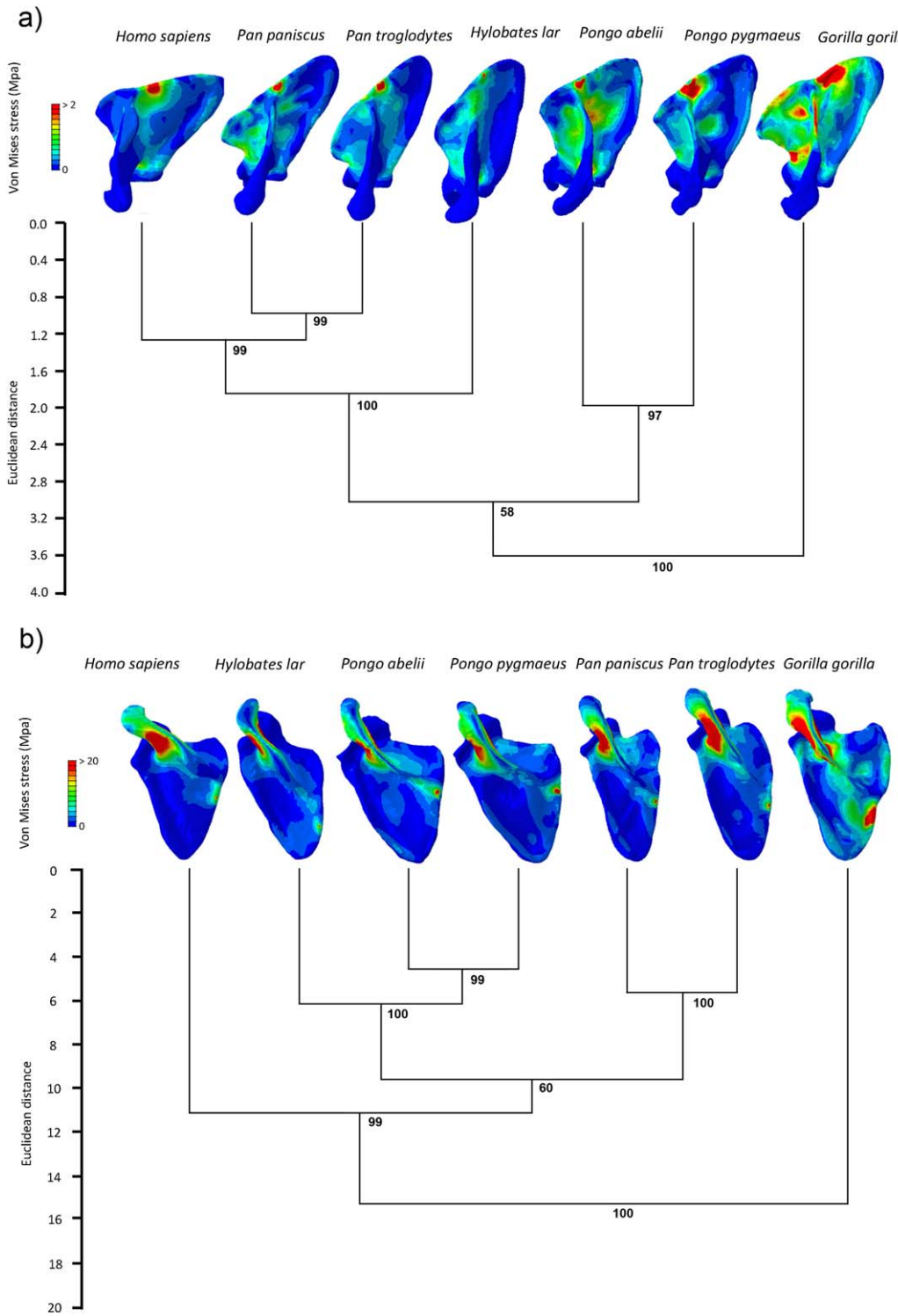

Fig. 4. UPGMA dendrogram of the von Mises stress values extracted from the different scapulae: **a**) quadrupedal standing and **b**) bimanual suspension. Bootstrap values at nodes were calculated after 10,000 permutations. Above each dendrogram the finite element models were drawn to depict the distributions of von Mises stress observed in the different hominoid scapulae. [Color figure can be viewed in the online issue, which is available at wileyonlinelibrary.com.]

(Fig. 5), the lack of overlapping branches of the phylogeny projected onto the shape space seems to imply that there is little evidence to support convergent evolution in the hominoid scapular shape, although further tests are required. The variation along PC1 could be described as more slender shapes at the positive side (e.g., *Hylobates lar*; *Pan troglodytes*) while the scapular morphologies occupying the negative side were relatively wider (e.g., *Homo sapiens*). Interestingly, *Homo* and *Pongo* morphology seem to be the most divergent compared to the other nonhuman

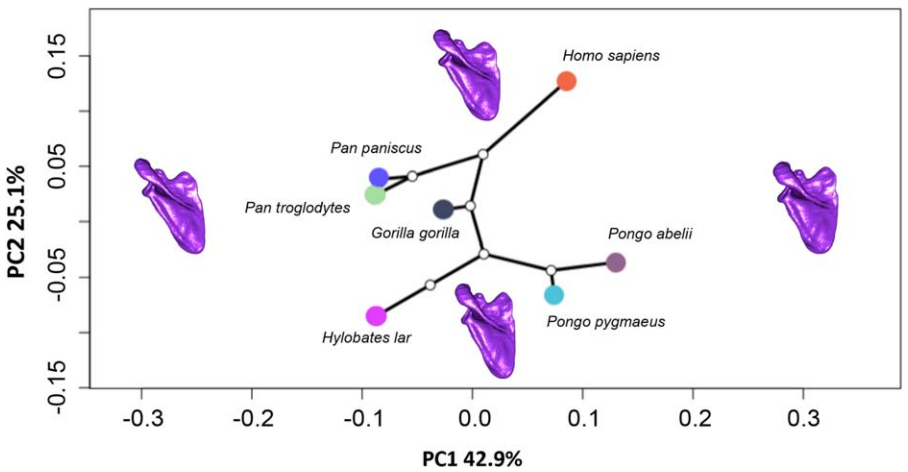

Fig. 5. Phylomorphospace of the hominoid scapular variation. The first two principal components (PCs) were used to display the majority of the morphological variation, while the projected phylogeny shows the evolutionary relationship between the analyzed taxa. The scapulae models were used to depict morphological variation along the PC axes. The model closest to the mean shape was warped to match the multivariate mean using the thin plate spline method (Bookstein, 1991). Then the obtained average model was warped to represent the variation along the two plotted PC axes. [Color figure can be viewed in the online issue, which is available at wileyonlinelibrary.com.]

hominoids. The multiple multivariate regressions of shape variables on the stress PC scores showed that there is significant relationship between scapular morphology and biomechanical performance (quadrupedal standing: adjusted-R^2: 0.79; F: 5.5918; P value: 0.022; bimanual suspension: adjusted-R^2: 0.63; F: 3.5333; P value: 0.006; 10,000 permutation rounds). However, only the PGLS regression of shape variables on the PC scores of the standing scenarios stress values was significant (quadrupedal standing: adjusted-R^2: 0.26; F: 1.4212; P value: 0.044; bimanual suspension: adjusted-R^2: 0.21; F: 1.4066; P value: 0.074; 10,000 permutation rounds). The low adjusted R^2 values are partially explained due to the reduced sample size, hence these results must be cautiously considered.

DISCUSSION

Previous studies have shown that primate scapular morphology is primarily related to positional behavior and/or movement needs (Oxnard, 1998). In fact, scapular morphological variation has been interpreted as being a reflection of the functional demands related to particular locomotion requirements (Inman et al., 1944; Oxnard, 1969; Radinsky, 1987; Larson, 1993; Hildebrand and Goslow, 1998). However, it is still not completely clear what the relationship is between scapular form and function. This question is relevant in order to address whether scapular shape reflects mostly functional or phylogenetic signals, because it has been frequently assumed that the postcranium is the product of stronger functional signals rather than containing phylogenetic information (Pilbeam, 1996, 2004; Ward, 1997; Lockwood, 1999; Collard et al., 2001). This assumption can lead to profoundly biased evolutionary reconstructions, in spite of the cumulative evidence that demonstrates the significant phylogenetic structure in mammalian postcrania (Sánchez-Villagra and Williams, 1998; Young, 2003, 2005). In spite of the widespread idea that the scapular morphology mainly reflects functional demands, our results showed that shape exhibited significant phylogenetic signal. This means that closely-related species tend to show similar trait values due to their common ancestry. This is consistent with more recent research that proposed within the functional structure of the scapula there is phylogenetic signal as well (Young, 2003, 2008). Although Young (2008) states that this phylogenetic signal is particularly noticeable at infant stages, we were able to clearly identify it in adult scapulae. The FEA results also showed significant phylogenetic signal, thus closest related species tended to show similar stress values in both loading scenarios, as broadly observed in the UPGMA clustering. However, as previously mentioned these results have to be carefully considered due to the reduced number of analyzed OTU's. It is necessary to increase the phylogenetic extent of this analysis including more anthropoid species so that the analysis can be more robust.

The FEA results showed that most species seem to behave relatively similarly under the two loading scenarios, with gibbons exhibiting the lowest stress levels, probably because their scapulae have to cope with the elevated stresses resulting from their highly demanding locomotion mode. Because of the fact that material properties were the same for all the models and that the same load was applied to all the specimens after scaling them to the same volume, it is possible to suggest that the particularly different scapular morphology of the gibbons could be the main factor reducing the experienced stress. Even though the locomotor morphology of gibbons is qualitatively similar to the anatomy of the other hominoids (Swindler and Wood, 1973), the highly suspensory locomotion mode of the gibbons has contributed to certain specialized anatomical features such as an axially elongated scapula (Takahashi, 1990). This could imply that their particular scapular morphology is adjusted to support their highly demanding locomotion habits. Interestingly, orangutans showed relatively higher stress values in the standing scenario but relatively lower values in the suspension case (similar to the gibbon values). Perhaps the slow climbing locomotion mode observed in these animals could explain this observation, because these species are noticeable slower and less acrobatic than the other hominoids. However, it is necessary to

include a broader sample of primate species in order to test this issue in a more comprehensive and robust manner.

The FEA results also showed that for the two analyzed loading scenarios, the stress was relatively distributed all over the scapular blade, although logically the higher localized areas were the locations where the forces were applied and where the constraints were positioned. This result is consistent with quantitative and qualitative studies that have shown that the scapula is relatively loaded all over its structure (van der Helm, 1994; Gupta and van der Helm, 2004). However in the suspension scenario higher loads were observed in the acromion. Epidemiological reports in human populations have shown that scapular fractures are extremely uncommon, showing the lowest incidence among all fractures, normally requiring exceptionally large amounts of energy to be affected (e.g., motor vehicle accidents) (van Staa et al., 2001). Of the different fractures that affect the bony components of the shoulder girdle, clavicle fractures are significant and notoriously more common (Armstrong and Van der Spuy, 1984; Nordqvist and Petersson, 1995). The scapula is wrapped by soft tissue and the clavicle tends to fracture more frequently, suggesting that when the scapula is loaded an important portion of the load is transmitted to the clavicle that seems to behave as a strut. The present FEA models are consistent with this possibility showing higher stress value at the scapular spine when they are "pulled" upwards such as in the suspension scenario.

The phylomorphospace (Fig. 5) showed that scapular shape seems to be consistent with the phylogenetic history of the group, thus morphological variation seems to relatively follow the evolutionary history. The absence of overlapping branches in the phylomorphospace suggests that scapular shape variation does not exhibit evident convergent evolution, however further analyses are required. Humans and orangutans showed the most divergent morphologies when compared to the rest of the hominoids (they were mostly distinguished by PC1, which accounted for 42.9% of the scapular shape variation). The morphological variation along this axis could be described as more slender shapes at the negative side (e.g., *Hylobates lar*; *Pan troglodytes*), while the scapular morphologies occupying the positive side were relatively wider (e.g., *Homo sapiens*, *Pongo abelii*). On the other hand, PC2 seems to separate between more arboreal species (i.e., orangutans and gibbons) and the rest of the hominoids. The morphological variation along this particular axis is associated with a scapular spine that points upwards in the negative portion of the axis, while the upper part exhibits morphologies that tend towards more horizontal spines. Additionally, the shapes occupying the negative side of the axis present different morphologies of the superior angles in comparison with those located on the positive side. This area provides the attachment site for some fibers of the levator scapulae muscle, thus suggesting different loading regimes of this muscle when elevating the scapula between arboreal and non-arboreal hominoid species.

There was a significant relationship between scapular shape and biomechanical performance both for the multiple multivariate regressions and when phylogenetic nonindependence was taken into account by performing the PGLS regression (excepting the suspension scenario, which was almost significant for this latter test). This means that there is relationship between scapular shape and its function, with at least part of the scapular shape variation due to non-phylogenetic factors, probably related to functional demands. This is logical, because the mechanical behavior of a structure depends on the combination of the geometry (i.e., shape) and the material properties that constitute the structure itself. Nonetheless, it is important to interpret all these results with caution, due to the small sample size used here. Further studies should increase the analyzed specimens to generate more robust statistical analyses. Interestingly, the most slender specimens (i.e., hylobatids) showed lower stress levels compared to the rest of the hominoids. In fact, hylobatids are clearly distinguished from other hominoids by a very angled spine and small infraspinous and supraspinous fossae. These specific differences might reflect gibbon adaptations to the highly specialized hylobatid locomotion (i.e., brachiation). Nonetheless, it is intriguing that gibbons and chimpanzees are distinguished along PC2, occupying almost the same position in PC1. Along this axis there is an overall similarity between panids and hylobatids. Both groups posses a narrow scapula from the vertebral border to the glenoid, with short and more acutely angled spine relative to the axillary border. The similarities suggest that these morphological traits could be an ancestral condition of apes, or could have arisen as convergent traits due to common function. Nevertheless, there are few specific locomotor similarities between panids and hylobatids, once the arboreal and suspensory adaptations shared also with *Pongo* and *Gorilla* are excluded. The analyses also revealed that *Homo* exhibit a derived morphology expressed in a relatively broader blade, probably associated with the fact that humans normally do not extensively use their arms during locomotion in comparison with the rest of the hominoids. Perhaps the biggest loads on human shoulders might relate to carrying, then being consequently tensile and complex. Human scapulae occupy the opposite morphological position of gibbons in the morphospace both in PC1 and PC2, suggesting a scapular shape possibly devoted to less demanding biomechanical regimens.

Interestingly, the scapula of *Pongo* seems to be distinct compared to the rest of hominoids (Young, 2003, 2008). The present study has also shown that this genera stands out when compared to the other hominoids due to its outlier position in the different analyses that were carried out. They have a scapular shape unique among the hominoids, which can be described as a combination of suspensory and quadrupedal characteristics. This trait combination is interesting; because orangutans are highly arboreal and suspensory, but these characters seem to suggest a closer morphological affinity to arboreal quadrupeds (Young, 2008). This distinctive morphology seems to combine both traits that have been traditionally associated with quadrupeds (e.g., glenoid greatest width caudally located and a scapular spine that extends to the vertebral border) and others that are typical of non-quadrupedal species (e.g., a cranially oriented glenoid cavity and long scapular shape blade that is also cranially oriented). The pongid scapular spine is comparatively robust, thus suggesting a larger trapezius attachment compared with the other hominoids. Nevertheless, its glenoid cavity seems to be more similar to the quadrupedal condition, although lacking the distinct lip that supposedly limits limb mobility during forelimb extension (Larson, 1993). A possible explanation for this singular morphology is that forelimb-dominated slow

climbing in orangutans could be related to these anatomical features, because they use more cautious pronograde suspensory behaviors compared to the rest of the African apes (Thorpe and Crompton, 2005, 2006). The particular shoulder morphology of orangutans could be related to suspensory postures and locomotion that imply placing the shoulder in orientations requiring special stabilization, especially while slowly moving through the canopy.

It has long been thought that hominoids are best defined by a common set of morpho-functional traits related to the trunk and upper limb, in which the scapula is characterized by being located on the back of the ribcage, while the glenohumeral joint would be adapted to allow extensive abduction (Keith, 1923; Rose, 1997; Larson, 1998). It has been suggested that these shared characteristics are related to forelimb-suspensory locomotion or brachiation. This idea has led us to consider hominoids as being relatively homogenous postcranially (Ward, 1997), despite evidence indicating that there is more variability than initially believed (Larson, 1998). For instance, locomotor ecology and recent analyses of the available fossil evidence indicate that suspensory locomotion may have been acquired independently by several hominoid lineages. In fact, it has been argued that Miocene apes characteristically lack many of the traits associated with suspensory behaviors that are present in their crown descendants (e.g., *Sivapithecus* and *Pongo*) (Begun and Kivell, 2011). The possible physical attributes of the last common ancestor of all hominoids have been discussed for a long time (Pilbeam, 2002). It has been traditionally thought that the majority of the postcranial resemblances of the crown hominoids correspond to shared-derived features (Schultz, 1930; Larson, 1998), however based on Miocene hominoid postcranial discoveries, this perspective has been recently re-examined (Begun and Kordos, 1997; Larson, 1998). These new fossils exhibit morphologies that differ with what would have been typically expected, thus raising the possibility that some of the extant ape postcranial similarities could be homoplasies (Begun, 1993). Furthermore, the inferences regarding Miocene hominoid positional behavior have shown that most of the fossil taxa seems to differ from the extant apes in that they seem to have been pronograde arboreal quadrupeds, although some exceptions have been proposed as well (Rose, 1997; Ward, 1997; Moyà-Solà et al., 2009). Although this research did not try to address this issue directly, the results show there is no generic and homogenous scapular morphology, but it noticeably varies in the different analyzed taxa. Hominoid scapular shape variation seems to be firstly distinguishing between "broad" versus "slender" scapulae, while secondly between arboreal and non-primarily arboreal hominoids. This morphological arrangement can be useful when discussing if the arboreal specializations observed in some of this species are in fact symplesiomorphies, as usually interpreted, or on the contrary represent evolutionary adaptations to novel environments. Hence it is important to consider this information when testing evolutionary models that explain the appearance of suspensory features gradually accreting in time (Moyà-Solà et al., 2004) or evolving as an integrated array (Pilbeam, 1996).

A limitation of the present study is that in reality shoulder soft tissues would mostly cope with strain and stress experienced by the shoulder (especially during the suspension scenario) but due to simplicity reasons, they were not modeled. In fact one of the main limitations of the proposed loading scenarios is that none of the muscular, ligamentous, capsular, fascia, or tendinous elements were considered, due to the absence of standardized data or because it was not possible to find information about their properties for all the analyzed species. Even though this is an unrealistic assumption, the objective of the present study was mostly comparative. Another limitation is that only relatively few stress values were analyzed (just 101 values in one slice of the models), which merely represents a localized part of the scapular biomechanical performance. Even though it was sufficient to carry out the presented analyses, following studies should include stress values more widely distributed on the scapula.

The present study has showed that the analysis of form and function using GM and FEA was able to cast some light regarding the functional and phylogenetic contributions in hominoid scapular morphology. Future studies should generate an integrative approach to analyze both shape and biomechanical data using more realistic loading scenarios derived from both observational and simulation data (e.g., multibody dynamics).

ACKNOWLEDGMENTS

The authors thank Charlotte Brassey and Viviana Toro-Ibacache for their useful suggestions about this work and help regarding FEA. They are also grateful to Ciara Stafford for her help during the preparation of this manuscript. This study benefited greatly from the constructive comments of two anonymous reviewers that clearly improved this manuscript.

LITERATURE CITED

Adams DC. 2014. A generalized K statistic for estimating phylogenetic signal from shape and other high-dimensional multivariate data. Syst Biol 63:685–697.

Adams DC, Otárola-Castillo E. 2013. geomorph: an R package for the collection and analysis of geometric morphometric shape data. Methods Ecol E 4:393–399.

Adams DC, Rohlf FJ, Slice DE. 2004. Geometric morphometrics: ten years of progress following the "revolution." Ital J Zool 71:5–16.

Adams DC, Rohlf FJ, Slice DE. 2013. A field comes of age: geometric morphometrics in the 21st century. Hystrix Ital J Mammal 21:7–14.

Aiello L, Dean C. 1990. An introduction to human evolutionary anatomy. London: Academic Press.

Alemseged Z, Spoor F, Kimbel WH, Bobe R, Geraads D, Reed D, Wynn JG. 2006. A juvenile early hominin skeleton from Dikika, Ethiopia. Nature 443:296–301.

Amadi HO, Hansen UN, Wallace AL, Bull AMJ. 2008. A scapular coordinate frame for clinical and kinematic analyses. J Biomech 41:2144–2149.

Armstrong CP, Van der Spuy J. 1984. The fractured scapula: importance and management based on a series of 62 patients. Injury 15:324–329.

Arnold C, Matthews LJ, Nunn CL. 2010. The 10kTrees website: a new online resource for primate phylogeny. Evol Anthropol Issues News Rev 19:114–118.

Ashton EH, Oxnard CE. 1963. The musculature of the primate shoulder. Trans Zool Soc Lond 29:553–650.

Ashton EH, Oxnard CE. 1964a. Functional adaptations in the primate shoulder girdle. Proc Zool Soc Lond 142:49–66.

Ashton EH, Oxnard CE. 1964b. Locomotor patterns in primates. Proc Zool Soc Lond 142:1–28.

Astúa D. 2009. Evolution of scapula size and shape in didelphid marsupials (didelphimorphia: didelphidae). Evolution 63: 2438–2456.

Badoux D. 1974. Structure and function of the primate scapula. In: Jenkins FAJ, editor. Primate locomotion. Elsevier, New York: Academic Press. p 171–200.

Bagg SD, Forrest WJ. 1986. Electromyographic study of the scapular rotators during arm abduction in the scapular plane. Am J Phys Med 65:111–124.
Bayraktar HH, Morgan EF, Niebur GL, Morris GE, Wong EK, Keaveny TM. 2004. Comparison of the elastic and yield properties of human femoral trabecular and cortical bone tissue. J Biomech 37:27–35.
Beaupré GS, Carter DR. 1992. Finite element analysis in biomechanics. In: Biewener AA, editor. Biomechanics-structures and systems: a practical approach. Oxford: RL Press at Oxford University Press.
Begun DR. 1993. New catarrhine phalanges from Rudabánya (Northeastern Hungary) and the problem of parallelism and convergence in hominoid postcranial morphology. J Hum E 24:373–402.
Begun DR, Kivell TL. 2011. Knuckle-walking in Sivapithecus? The combined effects of homology and homoplasy with possible implications for pongine dispersals. J Hum E 60:158–170.
Begun DR, Kordos L. 1997. Phyletic affinities and functional convergence in dryopithecus and other miocene and living hominids. In: Begun DR, Ward CV, Rose MD, editors. Function, phylogeny, and fossils. Advances in primatology. US: Springer. p 291–316.
Bello-Hellegouarch G, Potau JM, Arias-Martorell J, Pastor JF, Pérez-Pérez A. 2013. A comparison of qualitative and quantitative methodological approaches to characterizing the dorsal side of the scapula in hominoidea and its relationship to locomotion. Int J Primatol 34:315–336.
Berger LR, Ruiter DJ, de Churchill SE, Schmid P, Carlson KJ, Dirks PHGM, Kibii JM. 2010. Australopithecus sediba: a new species of *Homo*-like australopith from South Africa. Science 328:195–204.
Bhatti MA. 2005. Fundamental finite element analysis and applications: with mathematica and MatlabComputations, 1st ed. Hoboken, NJ: Wiley.
Blomberg SP, Garland T. 2002. Tempo and mode in evolution: phylogenetic inertia, adaptation and comparative methods. J Evol Biol 15:899–910.
Blomberg SP, Garland T, Ives AR. 2003. Testing for phylogenetic signal in comparative data: behavioral traits are more labile. Evolution 57:717–745.
Bookstein FL. 1991. Morphometric tools for landmark data: geometry and biology. Cambridge: Cambridge University Press.
Bookstein FL. 2013. Allometry for the twenty-first century. Biol Theor 7:10–25.
Bouckaert RR. 2010. DensiTree: making sense of sets of phylogenetic trees. Bioinformatics 26:1372–1373.
Brassey CA, Margetts L, Kitchener AC, Withers PJ, Manning PL, Sellers WI. 2013. Finite element modelling versus classic beam theory: comparing methods for stress estimation in a morphologically diverse sample of vertebrate long bones. J R Soc Interface R Soc 10:20120823.
Campoli G, Bolsterlee B, van der Helm F, Weinans H, Zadpoor AA. 2014. Effects of densitometry, material mapping and load estimation uncertainties on the accuracy of patient-specific finite-element models of the scapula. J R Soc Interface 11: 20131146.
Carlson KJ. 2006. Muscle architecture of the common chimpanzee (*Pan troglodytes*): perspectives for investigating chimpanzee behavior. Primates 47:218–229.
Chan LK. 2007. Scapular position in primates. Folia Primatol (Basel) 78:19–35.
Chen X, Povirk G. 1996. Assessing errors introduced by modeling the anisotropic human mandible isotropically with the finite element method. Am J Phys Anthropol Suppl 22:83.
Cheng EJ, Scott SH. 2000. Morphometry of *Macaca mulatta* forelimb. I. Shoulder and elbow muscles and segment inertial parameters. J Morphol 245:206–224.
Churchill SE, Holliday TW, Carlson KJ, Jashashvili T, Macias ME, Mathews S, Sparling TL, Schmid P, Ruiter DJ, de Berger LR. 2013. The upper limb of australopithecus sediba. Science 340:1233477.
Clabaut C, Bunje PME, Salzburger W, Meyer A. 2007. Geometric morphometric analyses provide evidence for the adaptive character of the tanganyikan cichlid fish radiations. Evolution 61:560–578.
Collard M, Gibbs S, Wood BA. 2001. Phylogenetic utility of higher primate postcranial morphology. Am J Phys Anthropol Suppl 32:52.
Corruccini RS, Ciochon RL. 1976. Morphometric affinities of the human shoulder. Am J Phys Anthropol 45:19–37.
Corruccini RS, Ciochon RL. 1978. Morphoclinal variation in the anthropoid shoulder. Am J Phys Anthropol 48:539–542.
Cox PG, Fagan MJ, Rayfield EJ, Jeffery N. 2011. Finite element modelling of squirrel, guinea pig and rat skulls: using geometric morphometrics to assess sensitivity. J Anat 219:696–709.
Currey JD. 1988. The effect of porosity and mineral content on the Young's modulus of elasticity of compact bone. J Biomech 21:131–139.
Currey JD. 2002. Bones: Structure and Mechanics, 1st ed. Princeton, NJ: Princeton University Press.
Currey JD, Butler G. 1975. The mechanical properties of bone tissue in children. J Bone Joint Surg Am 57:810–814.
Curtis N, Witzel U, Fitton L, O'higgins P, Fagan M. 2011. The mechanical significance of the temporal fasciae in *Macaca fascicularis*: an investigation using finite element analysis. Anat Rec Adv Integr Anat Evol Biol 294:1178–1190.
D'Août K, Vereecke EE. 2011. Primate locomotion linking field and laboratory research. New York: Springer.
Daegling DJ, Hotzman JL, McGraw WS, Rapoff AJ. 2009. Material property variation of mandibular symphyseal bone in colobine monkeys. J Morphol 270:194–204.
Davis D. 1949. The shoulder architecture of bears and other carnivores. Fieldiana: Zoology, Chicago Nat Hist Museum. 31: 285–305.
Dechow PC, Hylander WL. 2000. Elastic properties and masticatory bone stress in the Macaque mandible. Am J Phys Anthropol 112:553–574.
Dechow PC, Nail GA, Schwartz-Dabney CL, Ashman RB. 1993. Elastic properties of human supraorbital and mandibular bone. Am J Phys Anthropol 90:291–306.
Demes B, Larson SG, Stern JJT, Jungers WL, Biknevicius AR, Schmitt D. 1994. The kinetics of primate quadrupedalism: "hindlimb drive" reconsidered. J Hum E 26:353–374.
Ding M, Dalstra M, Linde F, Hvid I. 1998. Mechanical properties of the normal human tibial cartilage-bone complex in relation to age. Clin Biomech 13:351–358.
Diogo R, Potau JM, Pastor JF. 2013a. Photographic and descriptive musculoskeletal atlas of chimpanzees: with notes on the attachments, variations, innervation, function and synonymy and weight of the muscles, 1st ed. Boca Raton, FL: CRC Press.
Diogo R, Potau JM, Pastor JF, dePaz FJ, Ferrero EM, Bello G, Barbosa M, Aziz MA, Burrows AM, Arias-Martorell J, Wood BA. 2012. Photographic and descriptive musculoskeletal atlas of gibbons and siamangs, 1st ed. St. Helier: CRC Press.
Diogo R, Potau JM, Pastor JF, dePaz FJ, Ferrero EM, Bello G, Barbosa M, Wood BA. 2010. Photographic and descriptive musculoskeletal atlas of gorilla: with notes on the attachments, variations, innervation, synonymy and weight of the muscles, 1st ed. Enfield, NH: CRC Press.
Diogo R, Potau JM, Pastor JF, Paz FJ de, Barbosa M, Ferrero EM, Bello G, Aziz MA, Arias-Martorell J, Wood B. 2013b. Photographic and descriptive musculoskeletal atlas of orangutans: with notes on the attachments, variations, innervations, function and synonymy and weight of the muscles. Boca Raton: CRC Press.
Diogo R, Wood BA. 2012. Comparative anatomy and phylogeny of primate muscles and human evolution. Boca Raton, FL: CRC Press.
Dumont ER, Davis JL, Grosse IR, Burrows AM. 2011. Finite element analysis of performance in the skulls of marmosets and tamarins. J Anat 218:151–162.
Dumont ER, Grosse IR, Slater GJ. 2009. Requirements for comparing the performance of finite element models of biological structures. J Theor Biol 256:96–103.

Fayad F, Hoffmann G, Hanneton S, Yazbeck C, Lefevre-colau MM, Poiraudeau S, Revel M, Roby-Brami A. 2006. 3D scapular kinematics during arm elevation: effect of motion velocity. Clin Biomech 21:932–941.

Feldesman MR. 1976. The primate forelimb: a morphometric study of locomotor diversity. Eugene, Oregon: Department of Anthropology, University of Oregon.

Figueirido B, Serrano-Alarcón FJ, Slater GJ, Palmqvist P. 2010. Shape at the cross-roads: homoplasy and history in the evolution of the carnivoran skull towards herbivory. J Evol Biol 23: 2579–2594.

Fitton LC, Prôa M, Rowland C, Toro-Ibacache V, O'Higgins P. 2015. The impact of simplifications on the performance of a finite element model of a *Macaca fascicularis* cranium. Anat Rec Hoboken NJ 298:107–121.

Fitton LC, Shi JF, Fagan MJ, O'Higgins P. 2012. Masticatory loadings and cranial deformation in *Macaca fascicularis*: a finite element analysis sensitivity study. J Anat 221:55–68.

Fleagle JG. 1977. Locomotor behavior and muscular anatomy of sympatric Malaysian leaf-monkeys (*Presbytis obscura* and *Presbytis melalophos*). Am J Phys Anthropol 46:297–307.

Fleagle JG. 1998. Primate adaptation and evolution. London: Academic Press.

Friedman RJ, LaBerge M, Dooley RL, O'Hara AL. 1992. Finite element modeling of the glenoid component: effect of design parameters on stress distribution. J Shoulder Elbow Surg 1: 261–270.

Green DJ, Alemseged Z. 2012. Australopithecus afarensis scapular ontogeny, function, and the role of climbing in human evolution. Science 338:514–517.

Gröning F, Fagan MJ, O'Higgins P. 2011. The effects of the periodontal ligament on mandibular stiffness: a study combining finite element analysis and geometric morphometrics. J Biomech 44:1304–1312.

Gupta S, van der Helm FCT. 2004. Load transfer across the scapula during humeral abduction. J Biomech 37:1001–1009.

Gupta S, van der Helm FCT, Sterk JC, van Keulen F, Kaptein BL. 2004. Development and experimental validation of a three-dimensional finite element model of the human scapula. Proc Inst Mech Eng 218:127–142.

Haile-Selassie Y, Latimer BM, Alene M, Deino AL, Gibert L, Melillo SM, Saylor BZ, Scott GR, Lovejoy CO. 2010. An early Australopithecus afarensis postcranium from Woranso-Mille, Ethiopia. Proc Natl Acad Sci USA 107:12121–12126.

Harmon LJ, Kolbe JJ, Cheverud JM, Losos JB. 2005. Convergence and the multidimensional niche. Evol Int J Org E 59: 409–421.

Havill LM, Mahaney MC, Czerwinski SA, Carey KD, Rice K, Rogers J. 2003. Bone mineral density reference standards in adult baboons (*Papio hamadryas*) by sex and age. Bone 33: 877–888.

Hermida JC, Flores-Hernandez C, Hoenecke HR, D'Lima DD. 2014. Augmented wedge-shaped glenoid component for the correction of glenoid retroversion: a finite element analysis. J Shoulder Elbow Surg 23:347–354.

Hildebrand M, Goslow G. 1998. Analysis of vertebrate structure, 5th ed. New York: Wiley.

Hofmann T, Heyroth F, Meinhard H, Fränzel W, Raum K. 2006. Assessment of composition and anisotropic elastic properties of secondary osteon lamellae. J Biomech 39:2282–2294.

Hunt KD. 1991a. Positional behavior in the Hominoidea. Int J Primatol 12:95–118.

Hunt KD. 1991b. Mechanical implications of chimpanzee positional behavior. Am J Phys Anthropol 86:521–536.

Hunt KD. 1992. Positional behavior of Pan troglodytes in the Mahale Mountains and Gombe Stream National Parks, Tanzania. Am J Phys Anthropol 87:83–105.

Hunt KD. 2004. The special demands of great ape locomotion and posture. In: Russon AE, David RB, editors. The evolution of thought. Cambridge: Cambridge: University Press.

Inman VT, Saunders JB deC. M, Abbott LC. 1944. Observations on the function of the shoulder joint. J Bone Joint Surg Am 26:1–30.

Johnson GR, Spalding D, Nowitzke A, Bogduk N. 1996. Modelling the muscles of the scapula morphometric and coordinate data and functional implications. J Biomech 29:1039–1051.

Kaneko TS, Bell JS, Pejcic MR, Tehranzadeh J, Keyak JH. 2004. Mechanical properties, density and quantitative CT scan data of trabecular bone with and without metastases. J Biomech 37:523–530.

Keating JF, Waterworth P, Shaw-Dunn J, Crossan J. 1993. The relative strengths of the rotator cuff muscles: a cadaver study. J Bone Joint Surg Ser B 75:137–140.

Keith A. 1923. Hunterian Lectures on man's posture: its evolution and disorders. Br Med J 1:669–672.

Kibler WB, McMullen J. 2003. Scapular dyskinesis and its relation to shoulder pain. J Am Acad Orthop Surg 11:142–151.

Kimes KR, Siegel MI, Sadler DL. 1981. Musculoskeletal scapular correlates of plantigrade and acrobatic positional activities in *Papio cynocephalus* anubis and *Macaca fascicularis*. Am J Phys Anthropol 55:463–472.

Kimura T. 1992. Hindlimb dominance during primate high-speed locomotion. Primates 33:465–476.

Klingenberg CP, Ekau W. 1996. A combined morphometric and phylogenetic analysis of an ecomorphological trend: pelagization in Antarctic fishes (Perciformes: Nototheniidae). Biol J Linn Soc 59:143–177.

Kupczik K. 2008. Do it yourself virtual biomechanics: basic concepts and technical aspects of finite element analysis in vertebrate morphology. J Anthropol Sci 86:193–198.

Kupczik K, Dobson CA, Fagan MJ, Crompton RH, Oxnard CE, O'Higgins P. 2007. Assessing mechanical function of the zygomatic region in macaques: validation and sensitivity testing of finite element models. J Anat 210:41–53.

Kupczik K, Lev-Tov Chattah N. 2014. The adaptive significance of enamel loss in the mandibular incisors of cercopithecine primates (Mammalia: Cercopithecidae): a finite element modelling study. PLoS One 9:e97677.

Lacroix D, Murphy LA, Prendergast PJ. 2000. Three-dimensional finite element analysis of glenoid replacement prostheses: a comparison of keeled and pegged anchorage systems. J Biomech Eng 122:430–436.

Larson SG. 1993. Functional morphology of the shoulder in primates. In: Gebo DL, editor. Postcranial adaptations in nonhuman primates. Northern Illinois: University Press, DeKalb.

Larson SG. 1995. New characters for the functional interpretation of primate scapulae and proximal humeri. Am J Phys Anthropol 98:13–35.

Larson SG. 1998. Parallel evolution in the hominoid trunk and forelimb. Evol Anthropol Issues News Rev 6:87–99.

Larson SG. 2007. Evolutionary transformation of the hominin shoulder. Evol Anthropol Issues News Rev 16:172–187.

Larson SG, Stern JT. 1986. EMG of scapulohumeral muscles in the chimpanzee during reaching and "arboreal" locomotion. Am J Anat 176:171–190.

Larson SG, Stern JT Jr. 2013a. Rotator cuff muscle function and its relation to scapular morphology in apes. J Hum E 65: 391–403.

Larson SG, Stern JT, Jungers WL. 1991. EMG of serratus anterior and trapezius in the chimpanzee: scapular rotators revisited. Am J Phys Anthropol 85:71–84.

Li Y, Crompton RH, Wang W, Savage R, Günther MM. 2004. Hind limb drive, hind limb steering? Functional differences between fore and hind limbs in chimpanzee quadrupedalism. In: Shaping Primate Evolution. Cambridge Studies in Biological and Evolutionary Anthropology. Cambridge: Cambridge University Press.

Lockwood CA. 1999. Homoplasy and adaptation in the atelid postcranium. Am J Phys Anthropol 108:459–482.

Margulies SS, Thibault KL. 2000. Infant skull and suture properties: measurements and implications for mechanisms of pediatric brain injury. J Biomech Eng 122:364–371.

Meloro C, Raia P, Piras P, Barbera C, O'higgins P. 2008. The shape of the mandibular corpus in large fissiped carnivores: allometry, function and phylogeny. Zool J Linn Soc 154:832–845.

Michilsens F, Vereecke EE, D'Août K, Aerts P. 2009. Functional anatomy of the gibbon forelimb: adaptations to a brachiating lifestyle. J Anat 215:335–354.
Miller RA. 1932. Evolution of the pectoral girdle and fore limb in the primates. Am J Phys Anthropol 17:1–56.
Milne N, O'Higgins P. 2012. Scaling of form and function in the xenarthran femur: a 100-fold increase in body mass is mitigated by repositioning of the third trochanter. Proc R Soc B Biol Sci 279:3449–3456.
Monteiro LR, Nogueira MR. 2010. Adaptive radiations, ecological specialization, and the evolutionary integration of complex morphological structures. Evolution 64:724–744.
Moyà-Solà S, Köhler M, Alba DM, Casanovas-Vilar I, Galindo J. 2004. Pierolapithecus catalaunicus, a new middle miocene great ape from Spain. Science 306:1339–1344.
Moyà-Solà S, Alba DM, Almécija S, Casanovas-Vilar I, Köhler M, Esteban-Trivigno SD, Robles JM, Galindo J, Fortuny J. 2009. A unique middle miocene European hominoid and the origins of the great ape and human clade. Proc Natl Acad Sci USA 106:9601–9606.
Müller HJ. 1967. Form und Funktion der Scapula. Z Für Anat Entwicklungsgeschichte 126:205–263.
Myatt JP, Crompton RH, Payne-Davis RC, Vereecke EE, Isler K, Savage R, D'Août K, Günther MM, Thorpe SKS. 2012. Functional adaptations in the forelimb muscles of non-human great apes. J Anat 220:13–28.
Nogueira MR, Peracchi AL, Monteiro LR. 2009. Morphological correlates of bite force and diet in the skull and mandible of phyllostomid bats. Funct Ecol 23:715–723.
Nordqvist A, Petersson CJ. 1995. Incidence and causes of shoulder girdle injuries in an urban population. J Shoulder Elbow Surg 4:107–112.
Ogihara N, Aoi S, Sugimoto Y, Tsuchiya K, Nakatsukasa M. 2011. Forward dynamic simulation of bipedal walking in the Japanese macaque: investigation of causal relationships among limb kinematics, speed, and energetics of bipedal locomotion in a nonhuman primate. Am J Phys Anthropol 145:568–580.
Ogihara N, Yamanaka A, Ishida MNH. 2003. Functional morphology of primate scapula based on finite element analysis. Primate Res 19:203–215.
O'Higgins P. 2000. The study of morphological variation in the hominid fossil record: biology, landmarks and geometry. J Anat 197:103–120.
O'Higgins P, Cobb SN, Fitton LC, Gröning F, Phillips R, Liu J, Fagan MJ. 2011. Combining geometric morphometrics and functional simulation: an emerging toolkit for virtual functional analyses. J Anat 218:3–15.
O'Higgins P, Fitton LC, Phillips R, Shi J, Liu J, Gröning F, Cobb SN, Fagan MJ. 2012. Virtual functional morphology: novel approaches to the study of craniofacial form and function. Evol Biol 39:521–535.
O'Higgins P, Milne N. 2013. Applying geometric morphometrics to compare changes in size and shape arising from finite elements analyses. Hystrix Ital J Mammal 24:126–132.
Oishi M, Ogihara N, Endo H, Asari M. 2008. Muscle architecture of the upper limb in the orangutan. Primates 49:204–209.
Oishi M, Ogihara N, Endo H, Ichihara N, Asari M. 2009. Dimensions of forelimb muscles in orangutans and chimpanzees. J Anat 215:373–382.
Oxnard CE. 1967. The functional morphology of the primate shoulder as revealed by comparative anatomical, osteometric and discriminant function techniques. Am J Phys Anthropol 26:219–240.
Oxnard CE. 1968. The architecture of the shoulder in some mammals. J Morphol 126:249–290.
Oxnard CE. 1969. The descriptive use of neighborhood limited classification in functional morphology: an analysis of the shoulder in primates. J Morphol 129:127−148.
Oxnard CE. 1973. Functional inferences from morphometrics: problems posed by uniqueness and diversity among the primates. Syst Biol 22:409–424.
Oxnard CE. 1998. The information content of morphometric data in primates: function, development, and evolution. In: Strasser E, Fleagle JG, Rosenberger AL, McHenry H, editors. Primate locomotion: recent advances. Vol. Symposium on Primate Locomotion. New York: Plenum Press. p 255–275.
Oxnard CE, Ashton EH. 1962. Structure and function in bones and associated soft parts in primates. Birmingham: University of Birmingham.
Panagiotopoulou O, Kupczik K, Cobb SN. 2011. The mechanical function of the periodontal ligament in the macaque mandible: a validation and sensitivity study using finite element analysis. J Anat 218:75–86.
Parr WCH, Wroe S, Chamoli U, Richards HS, McCurry MR, Clausen PD, McHenry C. 2012. Toward integration of geometric morphometrics and computational biomechanics: new methods for 3D virtual reconstruction and quantitative analysis of finite element models. J Theor Biol 301:1–14.
Pearson OM, Lieberman DE. 2004. The aging of Wolff's "law": ontogeny and responses to mechanical loading in cortical bone. Am J Phys Anthropol 125:63–99.
Peres-Neto PR, Jackson DA. 2001. How well do multivariate data sets match? The advantages of a Procrustean superimposition approach over the Mantel test. Oecologia 129:169–178.
Peterson J, Dechow PC. 2003. Material properties of the human cranial vault and zygoma. Anat Rec Discov Mol Cell Evol Biol 274A:785–797.
Peterson SL, Rayan GM. 2011. Shoulder and upper arm muscle architecture. J Hand Surg 36:881–889.
Phelps JB, Hubbard GB, Wang X, Agrawal CM. 2000. Microstructural heterogeneity and the fracture toughness of bone. J Biomed Mater Res 51:735–741.
Pierce SE, Angielczyk KD, Rayfield EJ. 2008. Patterns of morphospace occupation and mechanical performance in extant crocodilian skulls: a combined geometric morphometric and finite element modeling approach. J Morphol 269:840–864.
Pilbeam D. 1996. Genetic and morphological records of the hominoidea and hominid origins: a synthesis. Mol Phylogenet E 5: 155–168.
Pilbeam D. 2002. Perspectives on the miocene hominoidea. In: Hartwig WC, editor. The primate fossil record. Cambridge: Cambridge University Press. p 303–310.
Pilbeam D. 2004. The anthropoid postcranial axial skeleton: comments on development, variation, and evolution. J Exp Zoolog B Mol Dev E 302:241–267.
Piras P, Maiorino L, Teresi L, Meloro C, Lucci F, Kotsakis T, Raia P. 2013. Bite of the cats: relationships between functional integration and mechanical performance as revealed by mandible geometry. Syst Biol 62:878–900.
Piras P, Sansalone G, Teresi L, Kotsakis T, Colangelo P, Loy A. 2012. Testing convergent and parallel adaptations in talpids humeral mechanical performance by means of geometric morphometrics and finite element analysis. J Morphol 273:696–711.
Preuschoft H. 1973. Functional anatomy of the upper extremity. In: Bourne G, editor. The chimpanzee, Vol. 6. Basel: Karger.
Preuschoft H. 2004. Mechanisms for the acquisition of habitual bipedality: are there biomechanical reasons for the acquisition of upright bipedal posture? J Anat 204:363–384.
Preuschoft H, Hohn B, Scherf H, Schmidt M, Krause C, Witzel U. 2010. Functional analysis of the primate shoulder. Int J Primatol 31:301–320.
Radinsky LB. 1987. The evolution of vertebrate design, 1st ed. Chicago: University of Chicago Press.
Raia P, Carotenuto F, Meloro C, Piras P, Pushkina D. 2010. The shape of contention: adaptation, history, and contingency in ungulate mandibles. Evolution 64:1489–1503.
Raichlen DA, Pontzer H, Shapiro LJ, Sockol MD. 2009. Understanding hind limb weight support in chimpanzees with implications for the evolution of primate locomotion. Am J Phys Anthropol 138:395–402.
Rayfield EJ. 2007. Finite element analysis and understanding the biomechanics and evolution of living and fossil organisms. Annu Rev Earth Planet Sci 35:541–576.
Rayfield EJ. 2011. Strain in the ostrich mandible during simulated pecking and validation of specimen-specific finite element models. J Anat 218:47–58.

Reynolds TR. 1985. Stresses on the limbs of quadrupedal primates. Am J Phys Anthropol 67:351–362.
Roberts D. 1974. Structure and function of the primate scapula. In: Jenkins FAJ, editor. Primate locomotion. Elsevier, New York: Academic Press. p 171–200.
Rodman P. 1984. Foraging and social systems of orangutans and chimpanzees. In: Rodman P, Cant JG, editors. Adaptations for foraging in nonhuman primates. New York: Columbia University Press. p 134–160.
Rose MD. 1974. Postural adaptations in new and old world monkeys. In: Jenkins FAJ, editor. Primate locomotion. New York: Academic Press. p 201–222.
Rose MD. 1979. Positional behaviour of natural populations: some quantitative results of a field study on *Colobus guereza* and *Cercopithecus aethiops*. In: Morbeck M, Preuschoft H, Gomberg N, editors. Environment, behavior and morphology: dynamic interactions in primates. New York: G. Fischer. p 75–94.
Rose MD. 1993. Functional anatomy of the elbow and forearm in primates. In: Gebo D, editor. Postcranial adaptation in nonhuman primates. DeKalb: Northern Illinois University Press. p 70–95.
Rose MD. 1997. Functional and phylogenetic features of the forelimb in miocene hominoids. In: Begun DR, Ward CV, Rose MD, editors. Function, phylogeny, and fossils. Advances in primatology. US: Springer. p 79–100.
Ross CF. 2005. Finite element analysis in vertebrate biomechanics. Anat Rec Discov Mol Cell Evol Biol 283A:253–258.
Ross CF, Patel BA, Slice DE, Strait DS, Dechow PC, Richmond BG, Spencer MA. 2005. Modeling masticatory muscle force in finite element analysis: sensitivity analysis using principal coordinates analysis. Anat Rec Discov Mol Cell Evol Biol 283A:288–299.
Rüber L, Adams DC. 2001. Evolutionary convergence of body shape and trophic morphology in cichlids from Lake Tanganyika. J Evol Biol 14:325–332.
Sánchez-Villagra MR, Williams BA. 1998. Levels of homoplasy in the evolution of the mammalian skeleton. J Mamm E 5: 113–126.
Schmidt M. 2005. Quadrupedal locomotion in squirrel monkeys (Cebidae: *Saimiri sciureus*): a cineradiographic study of limb kinematics and related substrate reaction forces. Am J Phys Anthropol 128:359–370.
Schmidt M. 2008. Forelimb proportions and kinematics: how are small primates different from other small mammals? J Exp Biol 211:3775–3789.
Schmidt M, Fischer MS. 2000. Cineradiographic study of forelimb movements during quadrupedal walking in the brown lemur (Eulemur fulvus, primates: Lemuridae). Am J Phys Anthropol 111:245–262.
Schmidt M, Krause C. 2011. Scapula movements and their contribution to three-dimensional forelimb excursions in quadrupedal primates. In: D'Août K, Vereecke EE, editors. Primate locomotion. Developments in primatology: progress and prospects. New York: Springer. p 83–108.
Schultz AH. 1930. The skeleton of the trunk of and limbs of the higher primates. Hum Biol 2:303–438.
Schultz AH. 1961. Vertebral column and thorax. Basel: S Karger Pub.
Sellers WI, Crompton RH. 2004. Using sensitivity analysis to validate the predictions of a biomechanical model of bite forces. Ann Anat Anat Anz 186:89–95.
Sellers WI, Pataky TC, Caravaggi P, Crompton RH. 2010. Evolutionary robotic approaches in primate gait analysis. Int J Primatol 31:321–338.
Shea BT. 1986. Scapula form and locomotion in chimpanzee evolution. Am J Phys Anthropol 70:475–488.
Slice DE. 2007. Geometric morphometrics. Annu Rev Anthropol 36:261–281.
Smith JM, Savage RJG. 1956. Some locomotory adaptations in mammals. J Linn Soc Lond Zool 42:603–622.
Stern JT, Oxnard CE. 1973. Primate locomotion: Some links with evolution and morphology. In: Hofer H, Schultz AH, editors. Primatologia 4. Basel: Karger.
Strait DS, Wang Q, Dechow PC, Ross CF, Richmond BG, Spencer MA, Patel BA. 2005. Modeling elastic properties in finite-element analysis: how much precision is needed to produce an accurate model? Anat Rec Discov Mol Cell Evol Biol 283A:275–287.
Strait DS, Weber GW, Neubauer S, Chalk J, Richmond BG, Lucas PW, Spencer MA, Schrein C, Dechow PC, Ross CF, Grosse IR, Wright BW, Constantino P, Wood BA, Lawn B, Hylander WL, Wang Q, Byron C, Slice DE, Smith AL. 2009. The feeding biomechanics and dietary ecology of *Australopithecus africanus*. Proc Natl Acad Sci 106:2124–2129.
Swindler DR, Wood B. 1973. An atlas of primate gross anatomy. Seattle: University of Washington Press.
Takahashi LK. 1990. Morphological basis of arm-swinging: multivariate analyses of the forelimbs of hylobates and ateles. Folia Primatol (Basel) 54:70–85.
Taylor AB. 1997. Scapula form and biomechanics in gorillas. J Hum E 33:529–553.
Thorpe SKS, Crompton RH. 2005. Locomotor ecology of wild orangutans (*Pongo pygmaeus* abelii) in the Gunung Leuser Ecosystem, Sumatra, Indonesia: a multivariate analysis using log-linear modelling. Am J Phys Anthropol 127:58–78.
Thorpe SKS, Crompton RH. 2006. Orangutan positional behavior and the nature of arboreal locomotion in Hominoidea. Am J Phys Anthropol 131:384–401.
Thorpe SKS, Crompton RH, Günther MM, Ker RF, McNeill Alexander R. 1999. Dimensions and moment arms of the hind- and forelimb muscles of common chimpanzees (*Pan troglodytes*). Am J Phys Anthropol 110:179–199.
Tseng ZJ. 2013. Testing adaptive hypotheses of convergence with functional landscapes: a case study of bone-cracking hypercarnivores. PLoS One 8:e65305.
Tuttle RH, Basmajian JV. 1978. Electromyography of pongid shoulder muscles. II. Deltoid, rhomboid and "rotator cuff." Am J Phys Anthropol 49:47–56.
van der Helm FCT. 1994. Analysis of the kinematic and dynamic behavior of the shoulder mechanism. J Biomech 27: 527–550.
van Eijden TMGJ, van der Helm PN, van Ruijven LJ, Mulder L. 2006. Structural and mechanical properties of mandibular condylar bone. J Dent Res 85:33–37.
van Staa TP, Dennison EM, Leufkens HGM, Cooper C. 2001. Epidemiology of fractures in England and Wales. Bone 29: 517–522.
Veeger HEJ, Van Der Helm FCT, Van Der Woude LHV, Pronk GM, Rozendal RH. 1991. Inertia and muscle contraction parameters for musculoskeletal modelling of the shoulder mechanism. J Biomech 24:615–629.
Wang Q, Strait DS, Dechow PC. 2006a. A comparison of cortical elastic properties in the craniofacial skeletons of three primate species and its relevance to the study of human evolution. J Hum E 51:375–382.
Wang Q, Strait DS, Dechow PC. 2006b. Fusion patterns of craniofacial sutures in rhesus monkey skulls of known age and sex from Cayo Santiago. Am J Phys Anthropol 131:469–485.
Ward CV. 1997. Functional anatomy and phyletic implications of the hominoid trunk and hindlimb. In: Begun DR, Ward CV, Rose MD, editors. Function, phylogeny, and fossils. Advances in primatology. US: Springer. p 101–130.
Weber GW, Bookstein F. 2011. Virtual anthropology: a guide to a new interdisciplinary field. Wien: Springer.
Whitehead PF, Larson SG. 1994. Shoulder motion during quadrupedal walking in *Cercopithecus aethiops*: integration of cineradiographic and electromyographic data. J Hum E 26:525–544.
Williams JL, Lewis JL. 1982. Properties and an anisotropic model of cancellous bone from the proximal tibial epiphysis. J Biomech Eng 104:50–56.
Wolff J. 1892. Das Gesetz der Transformation der Knochen. Berlin: Hirschwald.
Wroe S, Ferrara TL, McHenry CR, Curnoe D, Chamoli U. 2010. The craniomandibular mechanics of being human. Proc R Soc B Biol Sci 277:3579–3586.
Wroe S, Moreno K, Clausen P, Mchenry C, Curnoe D. 2007. High-resolution three-dimensional computer simulation of

hominid cranial mechanics. Anat Rec Adv Integr Anat Evol Biol 290:1248–1255.

Yongpravat C, Kim HM, Gardner TR, Bigliani LU, Levine WN, Ahmad CS. 2013. Glenoid implant orientation and cement failure in total shoulder arthroplasty: a finite element analysis. J Shoulder Elbow Surg 22:940–947.

Young NM. 2003. A reassessment of living hominoid postcranial variability: implications for ape evolution. J Hum E 45:441–464.

Young NM. 2004. Modularity and integration in the hominoid scapula. J Exp Zoolog B Mol Dev E 302B:226–240.

Young NM. 2005. Estimating hominoid phylogeny from morphological data: character choice, phylogenetic signal and postcranial data. In: Lieberman DE, Smith R, Kelley J, editors. Interpreting the Past: essays on human, primate and mammal evolution in honor of David Pilbeam. Interpret past Brill Acad Boston 19–31.

Young NM. 2006. Function, ontogeny and canalization of shape variance in the primate scapula. J Anat 209:623–636.

Young NM. 2008. A comparison of the ontogeny of shape variation in the anthropoid scapula: Functional and phylogenetic signal. Am J Phys Anthropol 136:247–264.

Young RL, Haselkorn TS, Badyaev AV. 2007. Functional equivalence of morphologies enables morphological and ecological diversity. Evol Int J Org E 61:2480–2492.

Zollikofer CP, Leon MPD. 2005. Virtual reconstruction: a primer in computer-assisted paleontology and biomedicine, 1st ed. Hoboken, NJ: Wiley-Liss.

Zysset PK, Edward Guo X, Edward Hoffler C, Moore KE, Goldstein SA. 1999. Elastic modulus and hardness of cortical and trabecular bone lamellae measured by nanoindentation in the human femur. J Biomech 32:1005–1012.

Quaternary Geochronology 5 (2010) 443–451

Contents lists available at ScienceDirect

Quaternary Geochronology

journal homepage: www.elsevier.com/locate/quageo

Research Paper

Earliest human remains in Eurasia: New $^{40}Ar/^{39}Ar$ dating of the Dmanisi hominid-bearing levels, Georgia

Tristan Garcia [a,*], Gilbert Féraud [b,1], Christophe Falguères [a], Henry de Lumley [c], Christian Perrenoud [d], David Lordkipanidze [e]

[a] Département de Préhistoire du Muséum National d'Histoire Naturelle, UMR 7194 du CNRS, 1, rue René Panhard, 75013 Paris, France
[b] Géosciences Azur, Université de Nice-Sophia Antipolis, UMR 6526 du CNRS, 06108 Nice Cedex 02, France
[c] Institut de Paléontologie Humaine, 1, rue René Panhard, 75013 Paris, France
[d] Département de Préhistoire du Muséum National d'Histoire Naturelle UMR 5198 du CNRS, Centre Européen de Recherches Préhistoriques, av. Léon-Jean-Grégory, 66720 Tautavel, France
[e] Georgian National Museum, 3, Rustaveli Avenue, 0105 Tbilisi, Georgia

ARTICLE INFO

Article history:
Received 27 February 2009
Received in revised form
24 August 2009
Accepted 29 September 2009
Available online 4 November 2009

Keywords:
Eurasia
Plio-Pleistocene
Dmanisi
Homo georgicus
Ar/Ar dating
Volcanic ashes

ABSTRACT

Several hominid remains have been discovered in the open-air site of Dmanisi (Georgia), the oldest prehistoric site in Eurasia. Two major arguments prove that this site is close in age to the Plio-Pleistocene boundary: a Villafranchian fauna and the morphological characteristics of hominid remains recently ascribed to *Homo georgicus*. Direct dating of the lower hominid-bearing level was carried out on volcanic glass and minerals using the $^{40}Ar/^{39}Ar$ method. The concordant results from two different sampled locations allow the determination of the age of the earliest human presence in Eurasia. This radioisotopic result strengthens the argument that the first dispersal of hominids outside Africa occurred at least 1.8 Ma ago.

1. Introduction

Hominid fossils from Dmanisi, Georgia, overturn theories of the first occupation of Eurasia. Hominid remains are associated with an archaic lithic industry, including chopping tools and choppers, which can be compared to the East-African Pre-oldowayan (Nioradze et al., 2000), and an Upper Villafranchian fauna with the coexistence of African and Eurasian species (Gabunia et al., 2000a). All these discoveries make Dmanisi the oldest prehistoric site outside Africa. The hominids bear morphological characteristics between those of *Homo habilis* and *Homo erectus* and have been ascribed to a new species: *Homo georgicus* (Gabunia et al., 2002).

The recently discovered D2700 skull has a small endocranial volume of 600 cm^3 and has been compared to *Homo habilis* (Vekua et al., 2002). These hominids thus substantiate the claim that the first humans to leave Africa were similar to *Homo habilis*. As this site is crucial for our understanding of the early occupation of Eurasia by hominids, it is essential to conduct precise dating of the fossil hominid-bearing levels. The fact that the human jaw D2600 was found in volcanic ash layers provides the opportunity to obtain a reliable and direct date for the fossil. Nevertheless, this site was previously dated by (1) the combination of $^{40}Ar/^{39}Ar$ dating of the underlying basaltic lava flow and paleomagnetism (Gabunia et al., 2000a,b) and (2) by preliminary $^{40}Ar/^{39}Ar$ data on the tephra itself. Based on both precise $^{40}Ar/^{39}Ar$ data obtained on various glass fractions and plagioclases from two locations in the site and a detailed examination of the ash deposits, we obtain an age of 1.81 ± 0.03 (2σ) Ma for the ash. As the latter appears to be contemporary with the human remains, it is reasonable to assume that this age represents the age of the hominid fossils.

* Corresponding author at: CEA, LIST, Laboratoire National Henri Becquerel (LNE-LNHB), F-91191 Gif-sur-Yvette, France. Tel.: +33 1 69 08 35 00.
E-mail addresses: tristan.garcia@cea.fr (T. Garcia), feraud@unice.fr (G. Féraud), falguere@mnhn.fr (C. Falguères), iph@mnhn.fr (H. de Lumley), perrenoud@mnhn.fr (C. Perrenoud), dlordkipanidze@hotmail.com (D. Lordkipanidze).
[1] Present address: Laboratoire de Radiochimie, Sciences Analytiques et Environnement, Institut de Chimie de Nice, FR CNRS 3037, Université de Nice-Sophia Antipolis, Parc Valrose, 06108 NICE Cedex 02, France.

1871-1014/$ – see front matter © 2009 Elsevier B.V. All rights reserved.
doi:10.1016/j.quageo.2009.09.012

2. Description of the site

The site is located about 80 km southwest of Tbilisi in Georgia (Fig. 1), on the northern slopes of the Little Caucasus, near the village of Patara Dmanisi, at an altitude of 915 m. This site lies on a basaltic spur formed by the confluence of the Pinezaouri and the Mashavera rivers that have carved valleys into the basalt flow. The fossiliferous Plio-Pleistocene levels were discovered in 1983 during the excavations of the medieval city, most of which was built during the 9th and 10th centuries. Since then, the State Museum of Georgia, directed by David Lordkipanidze, is in charge of excavations in the underlying layers. Several hominid remains, notably five skulls and four mandibles and a number of post-cranial remains, were found in the sedimentary sequence (Gabunia, 1992; Vekua et al., 2002; Gabunia et al., 2002; Lordkipanidze et al., 2006, 2007).

3. Site stratigraphy

The basaltic lava flow underlies the fossiliferous sedimentary sequence. The lava originates from volcanoes from the Dzavacheti mounts or Emliki mountains to the west (Gabunia et al., 2000b), and is characterized by a well-preserved, irregular, rough and fresh surface which suggests that no erosion occurred before the sediments were deposited. Six sedimentary units (layers VI to I), with a total thickness of around 3 m, were first defined by Bosinski et al., 1991 and completed by field observations (de Lumley et al., 2002). Other stratigraphies have since been elaborated (e.g. Gabunia et al., 2000a). More recently, two major units (A and B) have been identified following several steps (Lordkipanidze et al., 2006). A unit composed of A1 ash and A2 fluviatile colluvial and eolian deposits with many dispersed carbonated zones (which correspond to a secondary cementation of pedological and/or phreatic origin) was buried quickly, leading to the excellent preservation of human remains and associated fauna and artefacts. Pseudokarstic (piping) and gullies processes have affected the deposit of the first layer of B deposit, which is divided into B1 and B2 ensembles. B1 is formed by three episodes, the first and second containing bones, artefacts and human fossils. B2 deposit was followed by a calcareous soil formation which has sealed the archaeological sequence. In order to facilitate the understanding of our work versus our sampling we have decided here to adopt the first stratigraphy description. The sediments overlying layer VI are fluviatile (Fig. 2). Layer VI (A1 unit), which was sampled for dating, contains tools, faunal remains and human bones. It directly overlies the basalt lava flow. It is composed of black to grey volcanic ashes with a thickness varying from a few centimetres to several decimetres.

These studied ashes appear to be subcontemporaneous with the human bones for several reasons. Firstly, ash components are clearly not reworked (see the detailed description below). Similarly, bones do not generally present any weathering and, in some cases, they are well preserved and in anatomical connection (field observations). The associated fauna is coeval with this time range, ca 1.2 and 2.4 Ma (Fejfar et al., 1998).

For dating, we sampled the ash layer VI in two distinct locations (Fig. 3):

- Site A: Ashes come from the stratigraphic profile of the main excavated sector (sector II) described in Fig. 2. The dated materials were sampled directly beside the D2600 mandible (Fig. 4) discovered in 2000.
- Site B: Ashes were sampled in a pit dug through sediments down to the basalt lava flow about 15 m northwest of site A.

The ashes are homogeneous, compacted, without sedimentary structures, but are locally affected by small-diameter bioturbation (about 3–4 mm), some burrows and slight, localized secondary carbonatation. Furthermore, no aggregates of overlying sediments are included in this layer.

The granulometric study shows a uni-modal curve, with a median at 150 μm and a mode around 185 μm. This curve confirms that it is an eolian deposit of volcanic origin, with a very low clay percentage, even though clays are difficult to quantify in andosols.

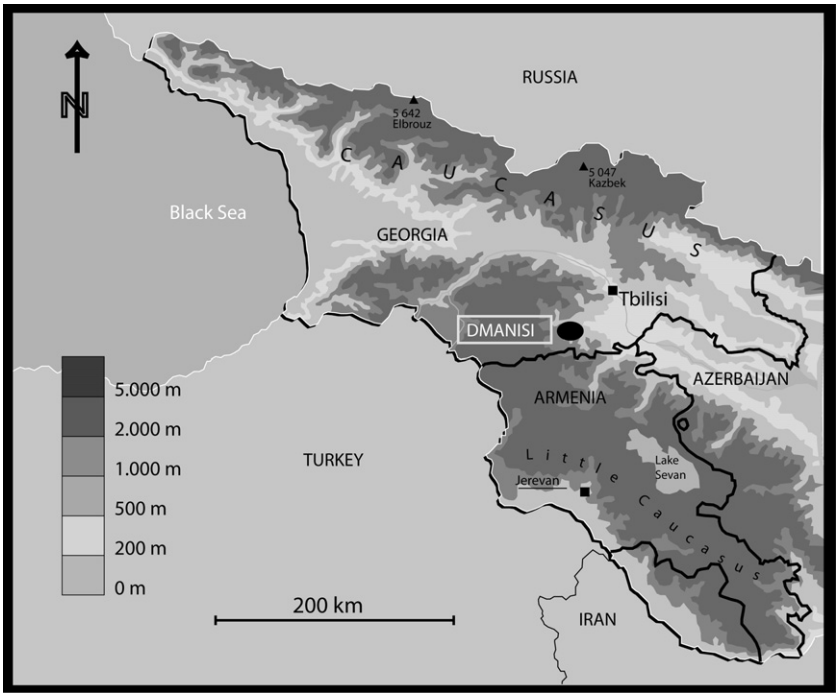

Fig. 1. Location of the Dmanisi prehistoric site.

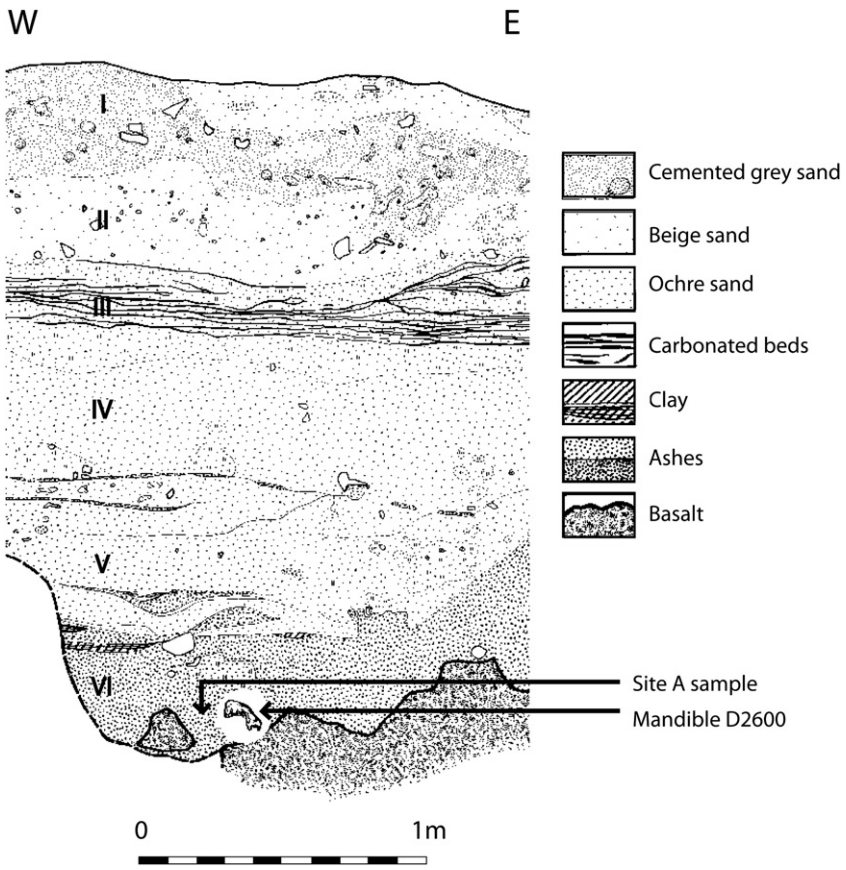

Fig. 2. Stratigraphic profile from sector II, W–E, (59/60) and site A location, showing the mandible D2600 and the sampled ash.

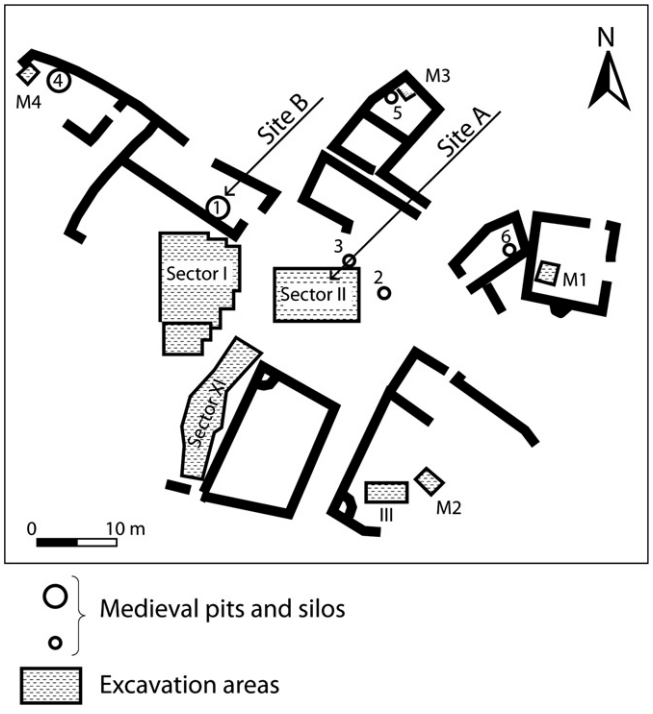

Fig. 3. Excavation areas showing sampled sites A and B (geographical coordinates: 41°20′16″ N and 44°20′54″ E).

The ashes from the two sites are entirely composed of volcanic materials. The same mineralogical assemblage is common to these two sites. Glass fragments are highly dominant (98%), and the remaining 2% consist of volcanic minerals which are olivine, feldspar, plagioclase, augite, a few hornblende and hypersthene.

There are three kinds of glasses: hyaline (transparent and colorless), brownish and black, 80% are sub-rounded (plates and grains),

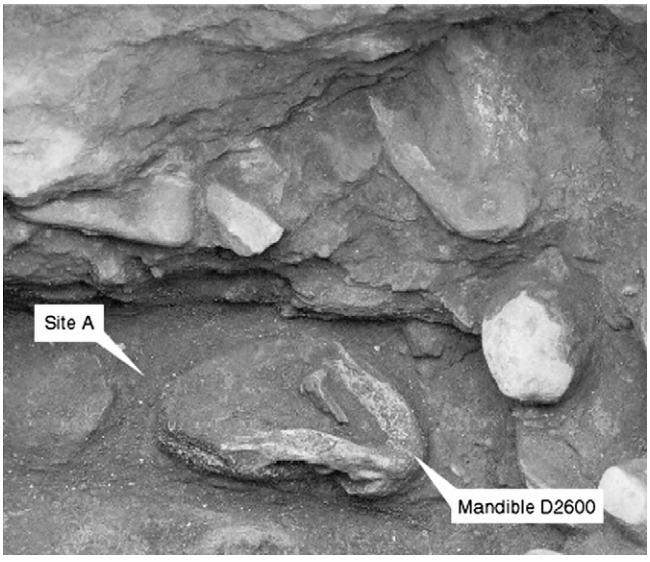

Fig. 4. Mandible D2600 and site A location.

and 20% are small sticks, prickles, very angular plates and grains. We noticed that more than 80% of the glasses include microlites, especially in brownish and always in black ones. These microlites may either derive from the same magma as the glassy fraction, or be extracted from older volcanic formations during explosive events. Therefore, the plagioclase and glass fractions (Fig. 5) selected for dating consist only of grains free of microlites.

4. Geochronology

4.1. Previous dating

Previous geochronological data on the site were initially obtained from the underlying basaltic lava flow, then more recently on the ashes from layer VI. The lava flow was successively dated (whole rock sample) to 0.53 ± 0.02 Ma (Rubinshtein et al., 1972), and to 1.8 ± 0.1 Ma (Majsuradze et al., 1989) by the K/Ar method, then to 2.0 ± 0.1 Ma with a $^{40}Ar/^{39}Ar$ isochron (Schmincke and Van den Bogaard, 1995) and finally to 1.85 ± 0.01 Ma by the $^{40}Ar/^{39}Ar$ method (Gabunia et al., 2000a). Nevertheless, with the help of paleomagnetic data, the latter authors assign an age younger than 1.77 Ma (that represents the age of the Olduvai–Matuyama boundary) to the hominid fossils, which differs from results obtained by Calvo-Rathert et al., 2008). This suggested age is the consequence of complex paleomagnetic data obtained on heterogeneous tuffaceous sands that were not present in our investigated sections (see below). (Note that all uncertainties in this paragraph are given at 2σ.)

Preliminary data were obtained on small clusters of feldspar and glass separated from ashes from site A, yielding a weighted mean age of 1.81 ± 0.05 Ma (de Lumley et al., 2002).

4.2. σAnalytical technique

The $^{40}Ar/^{39}Ar$ analyses were performed in the Geosciences Azur Nice laboratory on small clusters of grains (between 7 and 20) of about 200 μm in size from site B. They were irradiated for 2 h in the nuclear reactor at McMaster University in Hamilton, Canada, in position 5c, within cadmium shielding. The total neutron flux density during irradiation is 2.52×10^{17} n·cm^{-2}, with a maximum flux gradient estimated at ±0.2% in the volume where the samples were included. We used the Fish Canyon Sanidine (28.02 Ma; Renne et al., 1998) as monitor flux.

The gas extraction was carried out by a 50 W Synrad infrared continuous laser and the mass spectrometer was a VG 3600 working with a Daly detector system. The typical blank values of

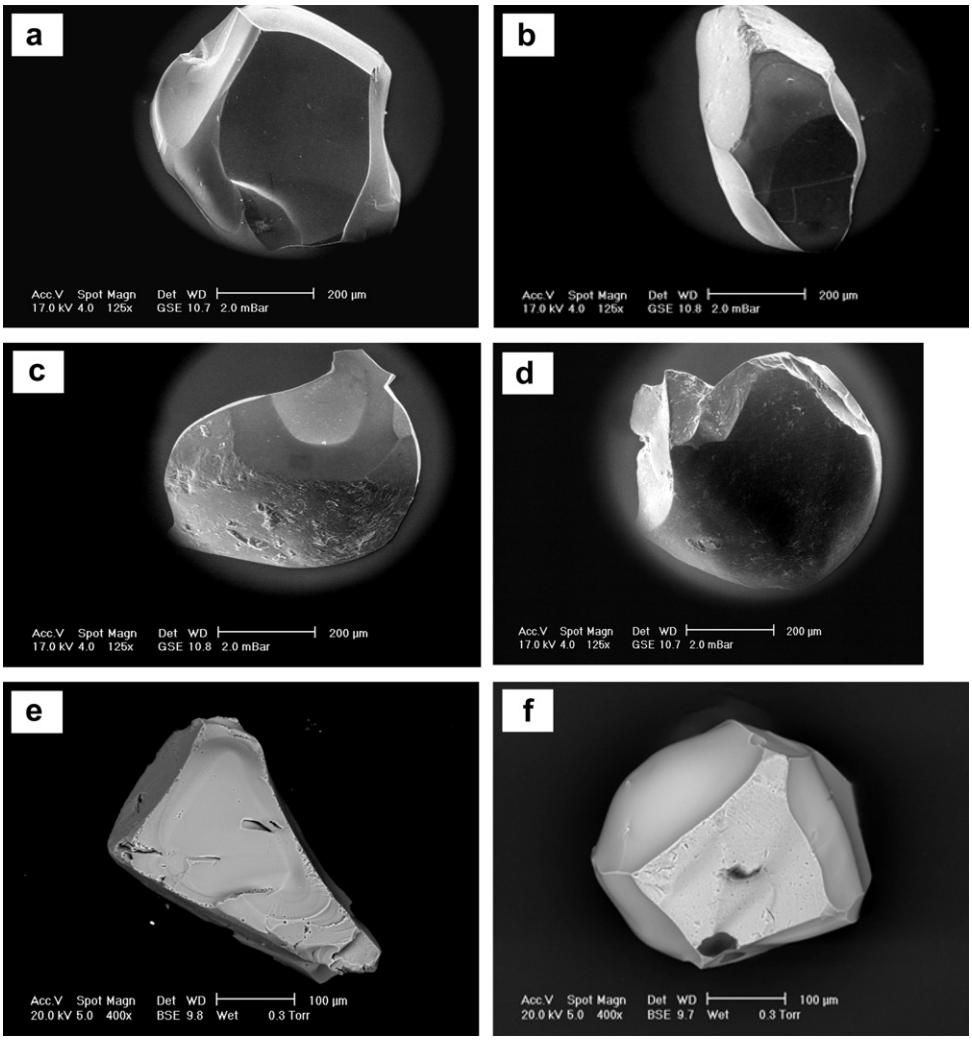

Fig. 5. Example of plagioclase (a,b), glass (c,d) at site A and glass (e,f) at site B from the dated layer VI.

Table 1
Detailed $^{40}Ar/^{39}Ar$ data obtained on glass from site B from Dmanisi site.

Step no.	Atmospheric contamination (%)	^{39}Ar (%)	$^{40}Ar/^{36}Ar$	$^{40}Ar/^{39}Ar$	$^{37}Ar_{Ca}/^{39}Ar_K$	$^{40}Ar^*/^{39}Ar_K$	Age (Ma)
G789 glass (J = 0.0004459 ± 0.0000009)							
1	75.6	22.1	391 ± 10	9.13 ± 0.05	0.078 ± 0.008	2.23 ± 0.20	1.79 ± 0.16
2	86.6	26.7	341.2 ± 4.3	16.67 ± 0.05	0.083 ± 0.007	2.24 ± 0.24	1.80 ± 0.19
3	59.7	17.7	494 ± 30	6.10 ± 0.03	0.075 ± 0.011	2.45 ± 0.23	1.97 ± 0.19
4	77.3	26.7	382.1 ± 4.7	9.92 ± 0.02	0.064 ± 0.007	2.25 ± 0.13	1.81 ± 0.10
Fusion	74.4	6.8	395 ± 26	9.41 ± 0.06	0.256 ± 0.031	2.40 ± 0.48	1.93 ± 0.39
							Integrated age = 1.84 ± 0.08
G790 glass (J = 0.0004459 ± 0.0000009)							
1	92.5	1.8	319 ± 12	30.83 ± 0.34	0.179 ± 0.048	2.32 ± 1.17	1.87 ± 0.94
2	84.9	6.3	347.9 ± 8.8	12.39 ± 0.10	0.032 ± 0.009	1.87 ± 0.30	1.50 ± 0.24
3	76.1	12.7	387.8 ± 9.3	8.36 ± 0.03	0.084 ± 0.008	1.99 ± 0.17	1.60 ± 0.14
4	90.7	19.1	325.7 ± 2.5	18.17 ± 0.05	0.088 ± 0.006	1.70 ± 0.21	1.36 ± 0.17
5	81.8	16.3	361.1 ± 4.9	12.63 ± 0.03	0.112 ± 0.008	2.30 ± 0.18	1.85 ± 0.15
6	87.4	21.0	337.8 ± 2.1	16.58 ± 0.04	0.062 ± 0.005	2.08 ± 0.18	1.67 ± 0.14
Fusion	89.8	22.7	328.8 ± 2.3	20.98 ± 0.02	0.117 ± 0.007	2.14 ± 0.24	1.72 ± 0.19
							Integrated age = 1.64 ± 0.07
G791 glass (J = 0.0004459 ± 0.0000009)							
1	79.6	1.0	373 ± 56	20.02 ± 0.47	0.000	4.15 ± 2.43	3.34 ± 1.95
2	71.5	26.6	412.9 ± 5.9	8.54 ± 0.02	0.054 ± 0.006	2.43 ± 0.11	1.95 ± 0.09
3	84.9	37.4	347.7 ± 2.4	14.55 ± 0.03	0.071 ± 0.005	2.19 ± 0.16	1.76 ± 0.13
Fusion	91.0	35.1	324.5 ± 1.9	24.14 ± 0.04	0.015 ± 0.005	2.17 ± 0.26	1.74 ± 0.21
							Integrated age = 1.82 ± 0.09
G792 glass (J = 0.0004459 ± 0.0000009)							
1	86.9	9.5	339 ± 12	17.75 ± 0.08	0.053 ± 0.011	2.32 ± 0.058	1.86 ± 0.46
2	93.1	26.7	317.4 ± 1.4	25.93 ± 0.05	0.113 ± 0.007	1.80 ± 0.27	1.45 ± 0.22
3	90.0	24.0	328.2 ± 2.5	19.46 ± 0.04	0.116 ± 0.008	1.95 ± 0.23	1.57 ± 0.18
Fusion	93.5	39.7	316.1 ± 1.1	29.09 ± 0.04	0.041 ± 0.004	1.91 ± 0.30	1.53 ± 0.24
							Integrated age = 1.55 ± 0.13
G794 glass (J = 0.0004459 ± 0.0000009)							
1	69.6	7.5	424 ± 13	8.46 ± 0.05	0.171 ± 0.015	2.57 ± 0.20	2.07 ± 0.16
2	70.9	13.3	415.0 ± 7.5	7.68 ± 0.02	0.270 ± 0.017	2.23 ± 0.12	1.80 ± 0.09
3	73.5	13.3	400.4 ± 9.9	8.01 ± 0.02	0.264 ± 0.016	2.12 ± 0.16	1.70 ± 0.13
4	81.4	14.6	362.3 ± 4.7	10.52 ± 0.02	0.234 ± 0.015	1.96 ± 0.14	1.58 ± 0.12
5	76.7	24.8	385.0 ± 3.8	9.80 ± 0.02	0.005 ± 0.003	2.28 ± 0.11	1.83 ± 0.09
6	22.9	8.8	1314 ± 168	3.25 ± 0.01	0.000	2.51 ± 0.10	2.02 ± 0.08
Fusion	50.3	17.7	590 ± 13	4.91 ± 0.01	0.000	2.44 ± 0.06	1.96 ± 0.05
							Integrated age = 1.83 ± 0.04
G795 glass (J = 0.0004459 ± 0.0000009)							
1	80.9	19.4	364.6 ± 3.8	11.09 ± 0.03	0.172 ± 0.010	2.11 ± 0.14	1.70 ± 0.11
2	65.5	13.8	449.5 ± 11.5	7.58 ± 0.03	0.191 ± 0.013	2.61 ± 0.14	2.10 ± 0.11
3	83.5	18.8	353.6 ± 3.6	16.06 ± 0.03	0.001 ± 0.001	2.64 ± 0.20	2.12 ± 0.16
4	78.8	16.6	374.6 ± 9.4	10.43 ± 0.03	0.085 ± 0.006	2.21 ± 0.23	1.78 ± 0.18
5	88.3	18.8	334.6 ± 3.6	16.99 ± 0.03	0.072 ± 0.005	2.00 ± 0.23	1.61 ± 0.18
6	84.2	5.9	350.7 ± 10.7	13.97 ± 0.06	0.075 ± 0.01	2.20 ± 0.39	1.77 ± 0.31
Fusion	71.5	6.7	413.5 ± 15.3	11.31 ± 0.05	0.000	3.23 ± 0.32	2.59 ± 0.26
							Integrated age = 1.89 ± 0.07
G796 glass (J = 0.0004459 ± 0.0000009)							
1	53.0	13.8	555 ± 39	5.96 ± 0.03	0.219 ± 0.014	2.80 ± 0.23	2.25 ± 0.18
2	35.6	21.3	826 ± 52	4.35 ± 0.02	0.101 ± 0.008	2.80 ± 0.10	2.25 ± 0.08
3	35.0	21.1	838 ± 78	3.71 ± 0.02	0.123 ± 0.010	2.41 ± 0.13	1.94 ± 0.10
4	74.3	5.1	397 ± 43	6.60 ± 0.03	0.135 ± 0.030	1.70 ± 0.54	1.36 ± 0.43
5	63.2	19.3	467 ± 26	6.11 ± 0.03	0.072 ± 0.009	2.25 ± 0.23	1.81 ± 0.18
6	75.2	11.4	391 ± 11	10.81 ± 0.04	0.366 ± 0.025	2.68 ± 0.25	2.15 ± 0.20
Fusion	62.7	7.8	464 ± 37	7.15 ± 0.04	0.982 ± 0.075	2.68 ± 0.37	2.15 ± 0.30
							Integrated age = 2.03 ± 0.07
G797 glass (J = 0.0004459 ± 0.0000009)							
1	15.8	41.5	1793 ± 180	2.88 ± 0.01	0.230 ± 0.015	2.42 ± 0.05	1.95 ± 0.04
2	13.8	28.3	2095 ± 543	2.71 ± 0.02	0.107 ± 0.009	2.34 ± 0.10	1.88 ± 0.08
3	19.9	11.63	1504 ± 564	3.09 ± 0.01	0.000	2.48 ± 0.23	1.99 ± 0.19
4	24.8	8.2	1188 ± 564	3.27 ± 0.02	0.048 ± 0.017	2.46 ± 0.39	1.98 ± 0.32
5	92.8	2.4	308 ± 85	5.13 ± 0.05	1.98 ± 0.20	0.37 ± 1.39	0.30 ± 1.12
Fusion	55.5	8.0	520 ± 94	4.38 ± 0.01	0.697 ± 0.043	1.95 ± 0.46	1.57 ± 0.37
							Integrated age = 1.87 ± 0.06
G798 glass (J = 0.0004459 ± 0.0000009)							
1	65.4	30.4	451 ± 15	6.85 ± 0.04	0.107 ± 0.008	2.36 ± 0.16	1.90 ± 0.13
2	82.9	30.8	356.1 ± 3.6	13.13 ± 0.04	0.187 ± 0.011	2.25 ± 0.16	1.81 ± 0.13
3	81.1	20.6	363.6 ± 6.3	10.89 ± 0.03	0.207 ± 0.012	2.06 ± 0.18	1.65 ± 0.15
4	95.4	11.2	309.4 ± 3.1	36.78 ± 0.09	0.316 ± 0.020	1.69 ± 0.51	1.36 ± 0.41
5	50.1	2.1	618 ± 449	4.60 ± 0.04	0	2.40 ± 1.63	1.93 ± 1.31
Fusion	74.0	4.9	399 ± 54	7.97 ± 0.05	0	2.07 ± 0.69	1.66 ± 0.55
							Integrated age = 1.75 ± 0.09

$^{40}Ar^*$ is radiogenic ^{40}Ar, subscripts Ca and K indicate produced by Ca and K neutron interference, respectively. All ratios are corrected for mass discrimination. All error bars are given at the 1σ level.

Table 2
Synthetic age data obtained on plagioclase and glass from two sites (A and B) from the Dmanisi site.

Site	Sample number	Material	Plateau age (Ma; ±2σ)	Steps number	Isochron age(Ma; ±2σ)	Initial $^{40}Ar/^{36}Ar$ ratio	MSWD	Weighted mean (Ma)	Weighted mean (Ma)
A[a]		Plagioclase	1.74 ± 0.29					1.81 ± 0.05	1.81 ± 0.03 (MSWD = 1.2, probability = 28%[b]
A[a]		Plagioclase	1.74 ± 0.18						
A[a]		Glass	1.82 ± 0.05						
B	G789	Glass	1.84 ± 0.16	1–5	1.9 ± 0.2	292 ± 7	0.2	1.80 ± 0.05	
B	G790	Glass	1.64 ± 0.15	1–7	1.7 ± 0.4	293 ± 12	2.0	(MSWD = 1.6,	
B	G791	Glass	1.82 ± 0.19	1–4	2.0 ± 0.2	290 ± 6	0.9	probability = 13%)[b]	
B	G792	Glass	1.55 ± 0.26	1–4	1.7 ± 0.4	293 ± 8	0.5		
B	G794	Glass	1.83 ± 0.08	1–7	2.1 ± 0.2	281 ± 5	1.5		
B	G795	Glass	1.84 ± 0.14	1–6	2.0 ± 0.6	290 ± 24	5.0		
B	G796	Glass	2.03 ± 0.13	1–7	2.1 ± 0.3	296 ± 32	2.4		
B	G797	Glass	1.87 ± 0.12	1–6	2.0 ± 0.1	235 ± 74	0.6		
B	G798	Glass	1.75 ± 0.18	1–6	1.9 ± 0.2	290 ± 5	0.4		

[a] Data from de Lumley et al. (2002).
[b] Weighted mean from plateau ages, one data (2.03 ± 0.13 Ma: experiment G796) excepted.

the extraction and purification laser system were in the ranges of 40–140, 3–14, 3–6 × 10^{-14} ccSTP for the mass 40, 39, 36, respectively, measured every third step, whereas argon isotopes measured on samples were typically to the order of 20–1000 and 100–900 times the blank level, for the ^{40}Ar and ^{39}Ar, respectively. In some cases, the ^{36}Ar was indistinguishable from the blank value. Corrections for neutron-induced reactions on ^{40}K and ^{40}Ca are: $[^{36}Ar/^{37}Ar]_{Ca} = 0.000279$, $[^{39}Ar/^{37}Ar]_{Ca} = 0.000706$, and $[^{40}Ar/^{39}Ar]_{K} = 0.001$ (with cadmium shielding). K decay constants are those of Steiger and Jaeger (1977). The criteria for defining plateau ages are as follows: (i) a plateau age should contain at least 70% of released ^{39}Ar; (ii) there should be at least three successive steps in the plateau; and (iii) the integrated age of the plateau should conform to each apparent age of the plateau within a 2σ error confidence interval. Plateau ages are calculated by weighting with ^{39}Ar, while errors on plateau ages are calculated by weighting with individual errors on apparent ages. All errors of apparent ages from each step are quoted at the 1σ level (Table 1), except the plateau ages that are given to the 2σ level, and do not include the errors on the $^{40}Ar^*/^{39}Ar_K$ ratio and age of the monitor. The error on the $^{40}Ar^*/^{39}Ar_K$ ratio of the monitor is included in the plateau age error bar calculation. Table 2 gives a summary of the data.

4.3. Geochronological results

The previous weighted mean calculated on the plateau ages obtained on the plagioclases and the glass from site A, is 1.81 ± 0.05 Ma (Table 2) (de Lumley et al., 2002).

At site B, nine fractions of 7–20 grains of glass displayed plateau ages ranging from 1.55 ± 0.26 to 2.03 ± 0.13 Ma (Fig. 6). Eight of these data (except G796 with an age of 2.03 ± 0.13 Ma, showing a slightly disturbed age spectrum characterized by a saddle shape) are internally concordant, with a weighted mean age of 1.80 ± 0.05 Ma (MSWD = 1.6), and are concordant with the plateau age weighted mean from site A. The reason for this saddle shaped age spectrum for G796 sample is unknown. Inverse isochron plots on each sample (Table 2) give ages concordant with plateau ages, and initial $^{40}Ar/^{36}Ar$ ratios are undistinguishable (sample G794 excepted) from the atmospheric composition.

The inverse isochron (not shown) calculated on all glass samples from site B, displays an age of 1.99 ± 0.06 Ma with an initial $^{40}Ar/^{36}Ar$ ratio of 289 ± 2, slightly lower than the atmospheric ratio, and a MSWD of 1.8. The dating of plagioclases was unsuccessful because they displayed variable integrated ages ranging from 3 to 19 Ma and variable ages versus temperature, (with very high apparent ages (up to 20–50 Ma) at low temperature (Fig. 7)). These high ages may be explained either by excess argon or by the existence of older minerals extracted from previous volcanic formations during the explosive volcanic eruption. The high variability of the Ca/K ratio (Fig. 7) may be the result of a heterogeneous population of plagioclases or the existence of variable amounts of glass surrounding the plagioclase grains, as observed with a binocular microscope. Another difference between the data obtained on the two sites is the general higher atmospheric contamination on glass fractions from site B, inducing larger error bars. Nevertheless, the Ca/K ratio of glass from the two sites is not significantly different.

When we plot the concordant plateau ages obtained on glass and plagioclase from the two sites (11 data, except glass G796 of site B) on a frequency diagram, the statistical distribution of ages shows a well-defined peak at 1.82 Ma, and an asymmetrical curve (Fig. 8). This asymmetry may be the result of alteration affecting some samples and producing ages that are too young despite the concordance of age data within error bars. This asymmetry is also visible on the statistical distribution of the eight concordant plateau ages of the glass from site B only, also giving a peak value at 1.82 Ma.

In conclusion, although the dated volcanic material from the two sites A and B does not yield exactly the same isotopic characteristics, and therefore may originate from distinct volcanic eruptions, the concordance of age data obtained from the two sites, as shown by both the weighted means and the probability distributions, allows us to consider the weighted mean age of 1.81 ± 0.03 Ma (calculated on 11 plateau ages, MSWD = 1.2) as the best estimate of the age of the hominid-bearing deposits. This age is in stratigraphic agreement with the $^{40}Ar/^{39}Ar$ age of 1.85 ± 0.01 Ma measured on the underlying basaltic lava flow (Gabunia et al, 2000a). In addition, this age is validated by our preliminary paleomagnetic analyses which yield a normal polarity for layer VI, which corresponds to the Olduvai subchron. Previous analyses are also in agreement with this result (Gabunia et al., 2000a,b; Sologasvili et al., 1995). However, these authors, who work on sector I (Fig. 3), which is a more complex stratigraphic zone, consider that fossil remains are intrusive in layer VI and belong to sediments yielding a reverse polarity. The clear stratigraphic position of the D2600 mandible in the ash layer (Fig. 2) and the 1.81 ± 0.03 Ma mean age imply that the hominids are contemporaneous with the Olduvai time range.

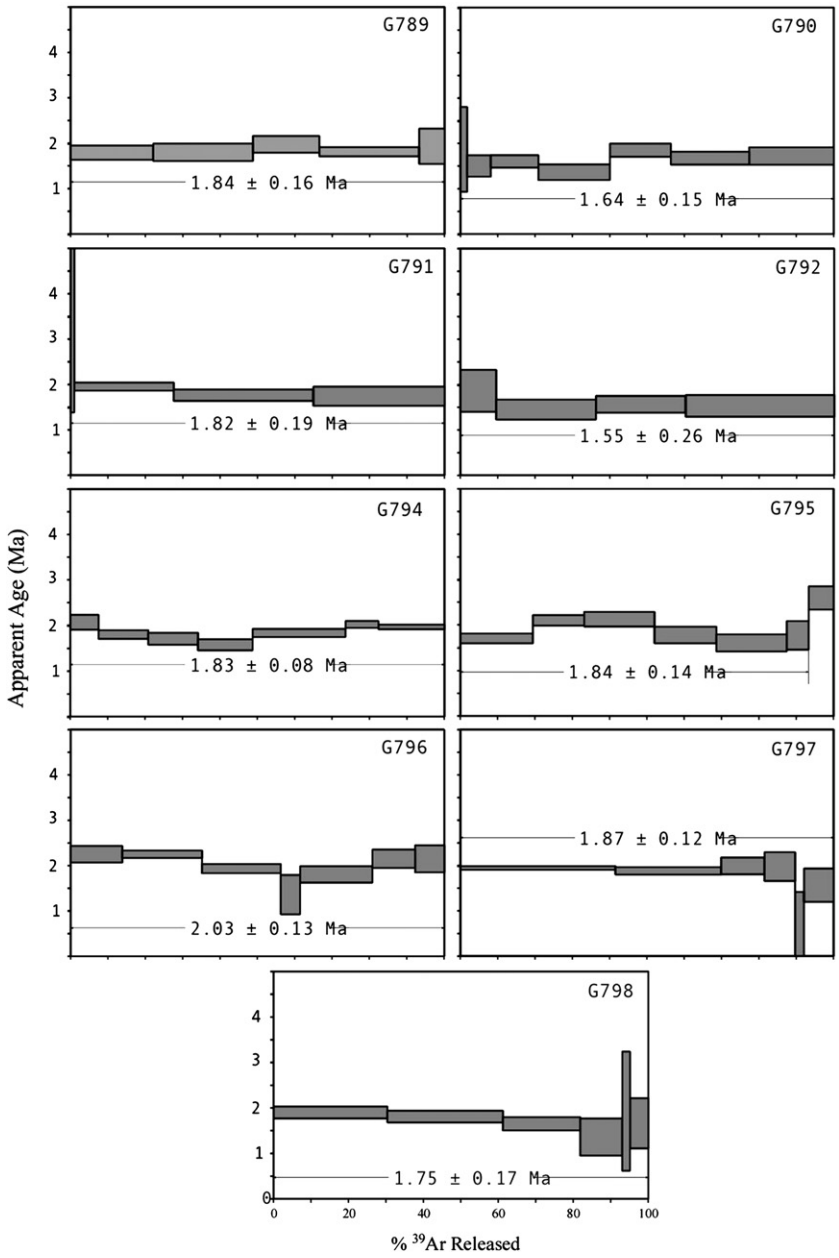

Fig. 6. Age spectra obtained on nine glass fractions from site B of the Dmanisi site. Plateau ages are given at the 2σ level. Apparent ages are given at the 1σ level, in order to be in agreement with Table 1 data.

5. Conclusion

The $^{40}Ar/^{39}Ar$ geochronological data obtained from 100% volcanic ashes, in which human remains were undoubtedly found (Gabunia et al., 2002; de Lumley et al., 2006; de Lumley and Lordkipanidze, 2006), from two distinct locations of the Dmanisi site, are concordant, and give a weighted mean age of 1.81 ± 0.03 Ma (calculated on 11 plateau ages).

This age is concordant with, or slightly younger than, the age of 1.85 ± 0.01 Ma measured on the underlying basaltic lava flow (Gabunia et al., 2000a). Its uncertainty shows that it belongs to the Olduvai subchron, which is not in agreement with the interpretation of those authors who attribute an age younger than 1.77 Ma (based on paleomagnetic data) to the hominid fossils.

Considering the stratigraphic position of the hominid fossil D2600 in the dated ash levels, we may now attribute an age of 1.81 ± 0.03 Ma to the Dmanisi hominids, which makes them the oldest Eurasians currently known. As D2600 is in a different stratigraphical layer (or unit) than the other human remains, and its morphological characteristics are different from theirs (Rightmire et al., 2006; Skinner et al., 2006), it is possible that the D2600 mandible is older than the other fossils, which could highlight two different populations. Moreover, for the other fossils, the upper stratigraphical position corresponds to a reverse polarity, and so a younger age than for the Olduvai ashes stratum. But, as we have no estimate of the sedimentation rate of the sedimentary deposits, there could just be a few millennia separating the different human remains and they could belong to the same paleodeme.

For the first time in Eurasia, a direct age can be assigned to the earliest known human remains, which were found in an established stratigraphical context at the Plio-Pleistocene limit.

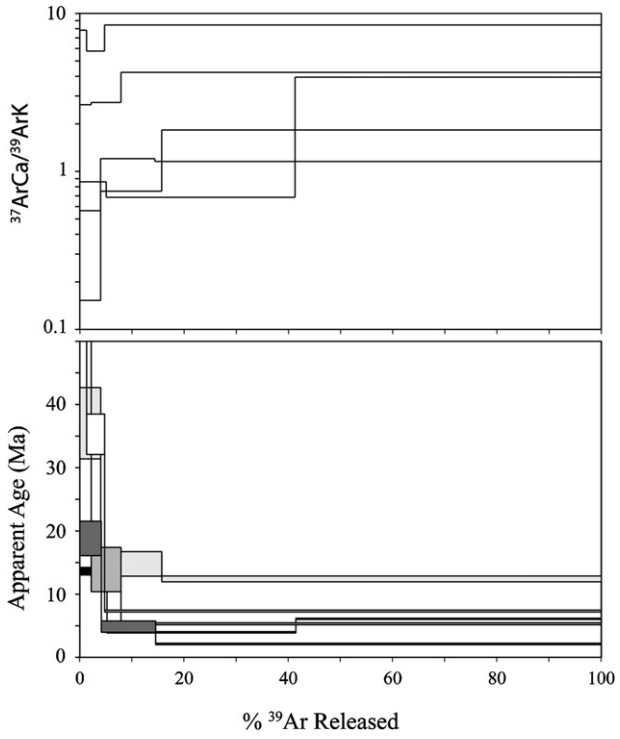

Fig. 7. Age and $^{37}Ar_{Ca}/^{39}Ar_K$ ratio spectra obtained on plagioclase from site B of the Dmanisi site.

The dating of Dmanisi is essential in order to understand the starting point of the dispersal of the *Homo* species. Indeed, the Dmanisi site appears to be a crossroads where hominids from Africa began to colonize the rest of the World.

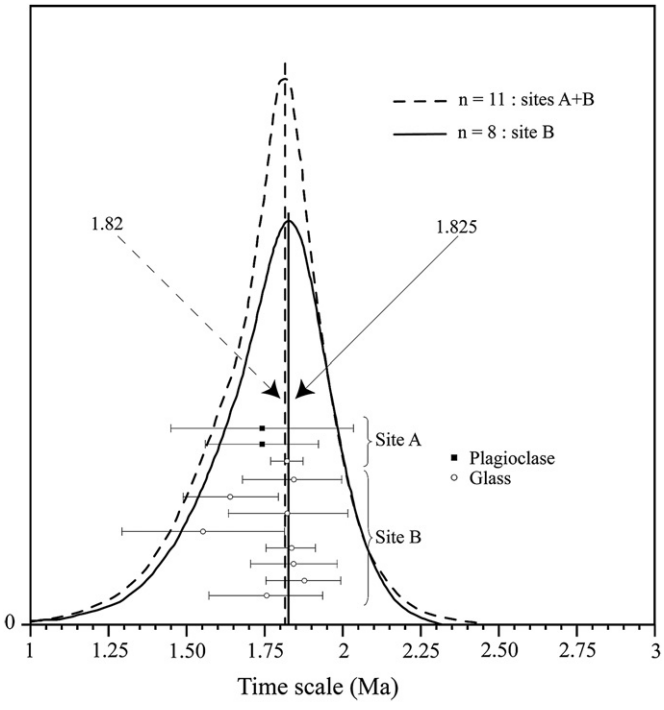

Fig. 8. Statistic distribution of 11 plateau ages from the two sites A and B (curve a) and eight plateau ages from glass fractions of site B (curve b).

Acknowledgements

We thank the Georgian State Museum team, particularly Gotcha Kiladze for the sampling. The glass and mineral separations were performed with the help of Michel Manetti (Geosciences Azur). We also thank Brigitte Deniaux (UMR 5590, CNRS) for some of the scanning microscope pictures, Jean Gagnepain for paleomagnetic samples and Louise Byrne for correcting the English translation. We extend our thanks to the international team who dig the Dmanisi site each year. We are grateful to Reid Ferring (University of North Texas) for useful comments on site geology.

Editorial handling by: P.R. Renne

References

Bosinski, G., Bugianisvili, T., Mgeladze, N., Nioradze, M., Tusabramisvili, D., 1991. Steinartefakte, in: Der altpaläolithische Fundplatz Dmanisi in Georgian (Kaukasus). Jahrbuch des Römisch-Germanischen Zentralmuseums, Mainz 36, 93–107.

Calvo-Rathert, M., Goguitchaichvili, A., Sologashvili, D., Villalaín, J.J., Bógalo, M.F., Carrancho, A., Maissuradze, G., 2008. New paleomagnetic data from the hominin bearing Dmanisi paleo-anthropologic site (Southern Georgia, Caucasus). Quaternary Research 69, 91–96 (doi:10.1016/j.yqres.2007.09.001).

de Lumley, H., Lordkipanidze, D., Féraud, G., Garcia, T., Perrenoud, C., Falguères, C., Gagnepain, J., Saos, T., Voinchet, P., 2002. Datation par la méthode $^{40}Ar/^{39}Ar$ de la couche de cendres volcaniques (couche VI) de Dmanissi (Géorgie) qui a livré des restes d'hominidés fossiles de 1,81 Ma. Comptes Rendus Palevol 1, 181–189.

de Lumley, M.-A., Lordkipanidze, D., 2006. L'Homme de Dmanissi (*Homo georgicus*), il y a 1 810 000 ans. Comptes Rendus Palevol 5, 273–281.

de Lumley, M.-A., Gabunia, L., Vekua, S., Lordkipanidze, D., 2006. Les restes humains du Pliocène final et du début du Pléistocène inférieur de Dmanissi en Géorgie. L'Anthropologie 110, 1–110.

Fejfar, O., Heinrich, W.-D., Lindsay, E.H., 1998. Updating the Neogene rodent biochronology in Europe. Medelingen Nederlands Inst. Toegepaste Geowetenschappen TNO 60, 533–539.

Gabunia, L., 1992. Der menschliche Unterkielfer von Dmanisi (Georgian, Kaukasus). Jahrbuch des Römisch-Germanischen Zentralmuseums Mainz 39, 185–208.

Gabunia, L., Vekua, A., Lordkipanidze, D., Swisher, C.C., Ferring, R., Justus, A., Nioradze, M., Tvalcrelidze, M., Anton, S.C., Bosinski, G., Jöris, O., de Lumley, M.-A., Majsuradze, G., Mouskhelishvili, A., 2000a. Earliest Pleistocene hominid cranial remains from Dmanisi, Republic of Georgia: taxonomy, geological setting, and age. Science 288 (5468), 1019–1025.

Gabunia, L., Vekua, A., Lordkipanidze, D., 2000b. The environmental contexts of early human occupation of Georgia (Transcaucasia). Journal of Human Evolution 38, 785–802.

Gabunia, L., de Lumley, M.-A., Vekua, A., Lordkipanidze, D., de Lumley, H., 2002. Découverte d'un nouvel hominidé à Dmanissi (Transcaucasie, Géorgie). Comptes Rendus Palevol 1, 1–11.

Lordkipanidze, D., Vekua, A., Ferring, R., Rightmire, G.P., Zollikofer, C.P.E., Ponce De Leon, M.S., Agusti, J., Kiladze, G., Mouskhelishvili, A., Nioradze, M., Tappen, M., 2006. A fourth hominid skull from Dmanisi, Georgia. The Anatomical Record Part A 288, 1–12.

Lordkipanidze, D., Jashashvili, T., Vekua, A., Ponce de León, M., Zollikofer, C., Rightmire, P., Pontzer, H., Ferring, R., Oms, O., Tappen, M., Bukhsianidze, M., Agusti, J., Kahlke, R., Kiladze, G., Martinez-Navarro, B., Mouskhelishvili, A., Nioradze, M., Rook, L., 2007. Postcranial evidence from early *Homo* from Dmanisi, Georgia. Nature 449, 305–310.

Majsuradze, G., Pavlenisvili, E., Schmincke, H.-U., Sologasvili, D., 1989. Paleomagnetik und datierung der Basaltlava, der altpaläolithische fundplatz Dmanisi in Georgian (Kaukasus). Jahrbuch des Römisch-Germanischen Zentralmuseums, Mainz 36, 74–83.

Nioradze, M., de Lumley, H., Barsky, D., Cauche, D., Celiberti, V., Notter, O., Biddittu, I., Kiladze, G., Zvania, D., 2000. Les industries lithiques archaïques du site de Dmanissi, Géorgie. Comparaisons avec les industries archaïques de l'Afrique de 1'Est et de 1'Europe méridionale. Volume des résumés des communications du Colloque international sur les premiers habitants de l'Europe, Tautavel, Lundi 10 au Samedi 15 Avril 2000, pp. 94–95.

Renne, P.R., Swisher, C.C., Deino, A.L., Karner, D.B., Owen, S.T., De Paolo, D.J., 1998. Intercalibration of standards. Absolute ages and uncertainties in 40 Ar/39 Ar dating. Chemical Geology: Isotope Geoscience section 145, 117–152.

Rightmire, G.P., Lordkipanidze, D., Vekua, A., 2006. Anatomical descriptions, comparative studies and evolutionary significance of the hominin skulls from Dmanisi, Republic of Georgia. Journal of Human Evolution 50, 115–141.

Rubinshtein, M., Adamia, S., Devnozashvili, D., Dobrinin, B., Pozentup L., 1972. Dating of some Neogene and Quaternary volcanics from Transcaucasus by geologic, radiometric and paleomagnetic data, in: Proceedings of the International Conference on the Problems of Neogene-Quaternary Boundary 162–167.

Schmincke, H.-U., Van Den Bogaard, P., 1995. Die datierung des Masavera-Basaltlavastrom. Jahrbuch des Römisch-Germanischen Zentralmuseums, Mainz 42, 75–76.

Skinner, M., Gordon, A., Collard, N., 2006. Mandibular size and shape variation in the hominins at Dmanisi, Republic of Georgia. Journal of Human Evolution 51, 36–49.

Sologasvili, D., Pavlenisvili, E., Gogicajsili, A., 1995. Zur frage der paläomagnestischen stratigraphie einiger junger vulkanite and sedimentgesteine im Masavera-Becken. Jahrbuch des Römisch-Germanischen Zentralmuseums, Mainz 42, 51–74.

Steiger, R.H., Jaeger, E., 1977. Subcommission on geochronology: convention of the use of decay constants in geo- and cosmochronology. Earth and Planetary Science Letters 36, 359–362.

Vekua, A., Lordkipanidze, D., Rightmire, G.P., Agusti, J., Ferring, R., Majsuradze, G., Mouskhelishvili, A., Nioradze, M., de Leon, M.P., Tappen, M., Tvalcrelidze, M., Zollikofer, C., 2002. A new skull of early *Homo* from Dmanisi, Georgia. Science 297, 85–89.

L'Anthropologie 105 (2001) 449-468

Évolution de la morphologie claviculaire au sein du genre *Homo*. Conséquences architecturales et fonctionnelles sur la ceinture scapulaire

Jean-Luc Voisin*

Résumé – La clavicule est un os qui a été peu étudié en anthropologie et paléoanthropologie malgré son importance fonctionnelle. Le travail présenté ici est une étude des courbures claviculaires chez les hominoïdea actuels et chez quelques hominidés fossiles (*Homo habilis, Homo ergaster, Homo antecessor* et néandertaliens). La morphologie claviculaire en vue supérieure traduit essentiellement les capacités d'élévation du bras de l'individu, alors que la morphologie claviculaire en vue postérieure informe sur la position de la scapula par rapport au thorax. Les clavicules fossiles, notamment les néandertaliennes, montrent, en vue supérieure, une morphologie proche de celle de l'homme moderne. Les capacités de mouvement du bras chez ces hominidés devaient donc être similaires à celles de l'homme actuel. En vue postérieure, les clavicules de ces fossiles présentent une double courbure. Ces caractéristiques traduisent chez ces hominidés une scapula plus haute par rapport au thorax que chez l'homme moderne. © 2001 Éditions scientifiques et médicales Elsevier SAS

clavicule / hominoïdea / Néandertal / *Homo erectus* / épaule

Abstract – Evolution of the Clavicular Morphology within the Genus *Homo*. Architectural and Functional Consequences on the Shoulder Girdle. The clavicle is the less studied shoulder bone from the point of view of comparative anatomy in spite of its importance for the movements of the upper limbs. In this study we have compared the clavicle curvature between extant hominoids and some fossils (*Homo habilis, Homo ergaster, Homo antecessor* and Neandertal). The curvature in superior view shows the capacity of arm elevation. In posterior view, the curves show the position of the scapula in regard to the thorax. In superior view, there is no real difference between fossils and modern man. This means that human fossils clavicles, in peculiar neandertal one, do not presented a more S shaped morphology than those of modern human. In posterior view, the clavicle of fossil men shows that their scapula was situated higher on the thorax than that of modern human. © 2001 Éditions scientifiques et médicales Elsevier SAS

clavicle / hominoidea / Neandertal / *Homo erectus* / shoulder

1. Introduction

L'épaule est un complexe anatomique particulier car elle est constituée de plusieurs articulations qui interviennent en synergie lors des mouvements du bras, en faisant une part très importante aux structures dites "molles" (muscles et ligaments) les mieux adaptées à supporter des forces de tension. En effet, l'épaule n'est constituée que de trois os : la scapula (omoplate), la clavicule et la partie proximale de l'humérus, et de plus de vingt muscles (le nombre exact dépendant de l'espèce de primate). Ainsi, pour comprendre l'architecture et la biomécanique de l'épaule chez les formes humaines fossiles, il est nécessaire d'étudier précisément chacune des structures osseuses et ses corrélations avec les parties molles chez les primates actuels.

Bien que l'épaule ne soit constituée que de trois os, on constate une disparité importante quant au nombre d'étude ayant porté sur chacun d'entre eux. La grande majorité des travaux porte sur la scapula, contrairement à la clavicule qui est le parent pauvre de la paléoanthropologie, de l'anthropologie et surtout de l'anatomie comparée.

* Correspondance et tirés à part. jeanlucv@mnhn.fr

Institut de paléontologie humaine, 1 rue R.-Panhard, 75013 Paris, France.

Tableau I. Effectifs de clavicules actuelles étudiées. Les pièces proviennent dans la mesure du possible d'individus sauvages.

Table I. Number of modern clavicle studied. Whenever possible they come from non captive specimen.

Espèces (abréviation)	Clavicule
Homo sapiens sapiens (Hm)	33
Pan troglodytes (Pt)	26
Pan paniscus (Pp)	19
Gorilla gorilla (Gor)	33
Pongo pygmaeus (Oo)	24
Hylobates sp. (Gb)	22
Papio hamadryas (Ba)	28

Tableau II. Pièces fossiles étudiées ; *pièces originales.

Table II. Fossil clavicles studied; *original remains.

Espèces	Individus	Clavicule
Neandertal	Régourdou	Droite et gauche
	Kebara	Droite et gauche
	La Ferrassie I*	Droite et gauche
	Krapina 4	Gauche
	Neanderthal	Droite
Homo antecessor	Gran Dolina ATD6-50	Droite
Homo ergaster	KNM-WT 15000	Droite et gauche
Homo habilis	OH 48	Gauche

Le travail présenté ici a pour but de comparer les clavicules des représentants fossiles du genre *Homo* avec celles de l'homme moderne. En fonction des résultats obtenus par comparaison avec différents primates, des interprétations architecturales et fonctionnelles seront proposées.

Les premières études sur la clavicule, bien que peu nombreuses, étaient essentiellement anthropologiques et avaient pour objectif de déterminer les différences et les similitudes entre les groupes humains (Parson, 1917 ; Kleiweg de Zwaan, 1931 ; Terry, 1932 ; Apostolakis, 1934 ; Olivier, 1951a, 1951b, 1954, 1955 ; Olivier et al., 1954 ; Olivier et Capliez, 1957 ; Ray, 1959 ; Jit et Kaur, 1986). Les travaux portant sur la fonction précise de cet os (Cave, 1961 ; Jenkins, 1974 ; Jenkins et al., 1978 ; Ljunggren, 1979 ; Harrington et al., 1993) ou ceux sur l'anatomie comparée, notamment au sein des primates (Schultz, 1930 ; Olivier, 1953 ; Voisin 2000a, 2000b) sont nettement moins nombreux. Cette lacune est d'autant plus étonnante que la clavicule présente un rôle fondamental dans les mouvements du bras. Elle permet, en effet, au membre supérieur de réaliser des mouvements de grande amplitude en dehors du plan parasagittal. En d'autres termes, elle permet la manipulation et l'arboricolisme. Ainsi, les transformations qui ont affecté la clavicule au cours de l'évolution humaine ont été accompagnées de modifications comportementales.

L'absence de données comparatives limite l'étude des pièces fossiles aux seules descriptions, exception faite de quelques travaux tels ceux de Heim (1974, 1982a, 1982b), Vandermeersch et Trinkaus (1995) et Sankhyan (1997).

2. Matériel et méthodes

2.1. Matériel

Le matériel étudié est composé de clavicules d'homme moderne, provenant de différentes

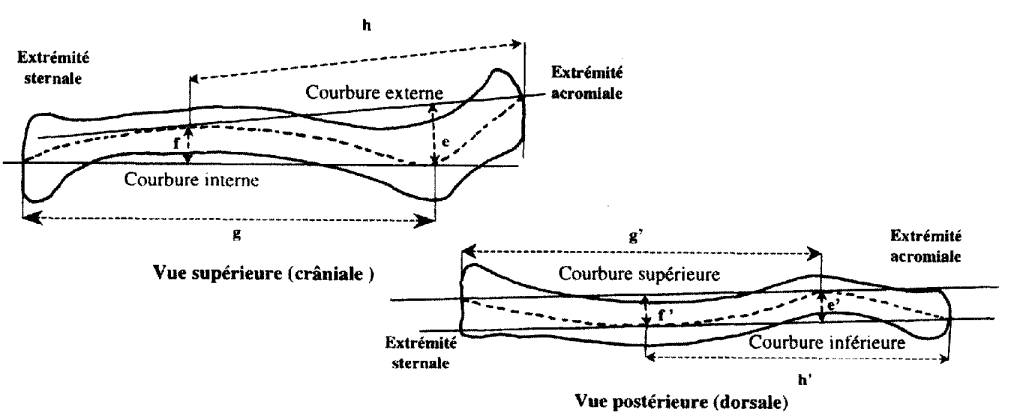

Figure 1. Détermination des arcs de courbures selon Olivier (1951a). Clavicule droite de *Pan troglodytes*.

Figure 1. Determination of the clavicle curves (Olivier, 1951a). Right clavicle of *Pan troglodytes*.

Tableau III. Caractéristiques des courbures interne et externe des espèces actuelles étudiées ici.

Table III. Characteristics of the clavicule curves in superior view (internal an external).

	Courbure interne			Courbure externe		
Espèce (nombre de pièces)	moyenne	écart-type	variance	moyenne	écart type	variance
Homo sapiens sapiens (33)	12,6	2,5	6,3	16,1	2,7	7,3
Pan troglodytes (26)	8,1	2,8	7,8	15,4	3,0	9,0
Pan paniscus (19)	7,5	2,0	4,0	14,8	2,6	6,8
Gorilla gorilla (33)	3,3	1,9	3,6	12,6	3,1	9,6
Pongo pygmaeus (24)	5,8	2,1	4,4	9,1	2,3	5,3
Hylobates sp. (22)	12,6	2,8	7,8	5,3	2,3	5,3
Papio hamadryas (28)	2,2	1,2	1,4	14,1	2,8	7,8

régions du monde, de gorille, de chimpanzé commun, de bonobo, d'orang-outan, de gibbon, de babouin (*tableau I*) et de fossiles (*tableau II*) contenant des pièces attribuées à *Homo habilis, Homo ergaster, Homo antecessor* et à des néandertaliens. Ce matériel provient des collections du Laboratoire d'Anthropologie Biologique du Musée de l'Homme, des Laboratoires d'Anatomie Comparée et des Mammifères et Oiseaux du Muséum National d'Histoire Naturelle, du Musée Royal d'Afrique Centrale de Tervuren (Belgique) et du *Mammals Group* du *Natural History Museum* de Londres (Royaume-Uni).

Les espèces de primates ont été choisies en fonction de leur mode locomoteur dominant et de leur place dans la phylogénie.

Le terme grand singe regroupe les chimpanzés communs, les bonobos, les gorilles et les orangs-outans, les trois premiers constituant les grands singes africains. Le terme hominoïde regroupe les hommes, les grands singes et les gibbons (Groves, 1993a). Sous l'appellation *Hylobates* sp., nous regroupons des clavicules appartenant aux sous-genres *Nomascus* et *Hylobates s. str.* En effet, ces deux sous-genres sont suffisamment proches pour que l'hybridation soit possible entre eux (Groves, 1993b).

2.2 Méthodes

Dans ce travail, seules les courbures claviculaires seront étudiées. Ces dernières, projetées dans deux plans perpendiculaires à l'aide d'un dioptographe, se décomposent en quatre courbures élémentaires, soit deux par plan (*figure 1*). Ces deux plans peuvent être assimilés, l'un à la vue supérieure, l'autre à la vue postérieure.

L'arc de courbure moyen est estimé, selon la méthode d'Olivier (1951a), en calculant le rapport entre la longueur de la corde et sa hauteur maximale (*figure 1*).

Vue supérieure

- La courbure acromiale correspond à la courbure externe : e / h.100.

- La courbure sternale correspond à la courbure interne : f / g.100.

Vue postérieure

- La courbure acromiale correspond à la courbure inférieure : e' / h'.100.

- La courbure sternale correspond à la courbure supérieure : f' / g'.100.

La description et la répartition des données ont été analysées à l'aide du logiciel Systaw5. La représentation graphique de l'amplitude de variation pour chaque variable est donnée par un diagramme représentant la valeur moyenne et +/- deux fois l'écart type.

3. Résultats

3.1. Les courbures en vue supérieure

3.1.1. Primates actuels

En vue supérieure, les courbures claviculaires permettent de différencier trois groupes (*figure 2*) :

- Les gorilles et les babouins qui présentent des clavicules caractérisées par un développement inégal des courbures. La courbure externe est très marquée contrairement à l'interne qui peut même être absente (*figure 3 et tableau III*).

- Les orangs-outans, les chimpanzés et les hommes qui sont caractérisés par des clavicules possédant simultanément une courbure externe

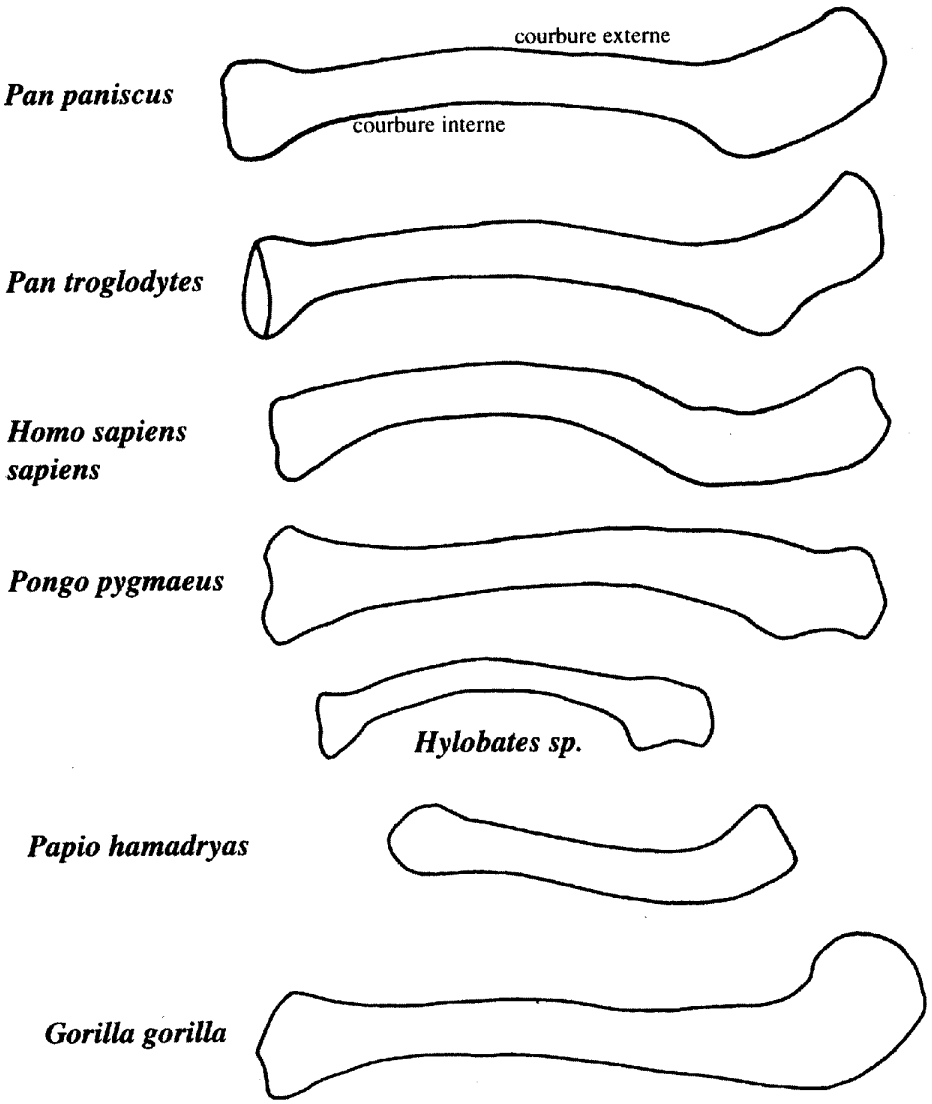

Figure 2. Clavicules droites en vue supérieure (les échelles ne sont pas respectées).

Figure 2. Right clavicles in superior view (scales are not respected).

et une interne (*figure 3 et tableau III*) qui sont en outre corrélées entre elles (*tableau IV*). Ces clavicules ne sont pas pour autant identiques. En effet, les clavicules des orangs-outans présentent les courbures les moins marquées, ce qui leurs confèrent un aspect presque rectiligne. Au contraire, les courbures sont beaucoup plus marquées chez les hommes et les chimpanzés, bien qu'il existe des dissemblances entre ces deux groupes. Autant la courbure externe ne présente pas de différence significative entre ces deux groupes (*tableau V*), autant la courbure interne est moins prononcée chez les chimpanzés que chez l'homme moderne (*tableau V*). La clavicule humaine est donc plus sinueuse que celle des chimpanzés contrairement à ce qui est classiquement décrit depuis Schultz (1930).

- Les gibbons sont caractérisés par des clavicules qui présentent une morphologie inversée par rapport à celle des gorilles et des babouins. En effet, les clavicules des gibbons présentent une courbure interne très prononcée contrairement à l'externe qui peut souvent manquer (*tableau III et figure 3*).

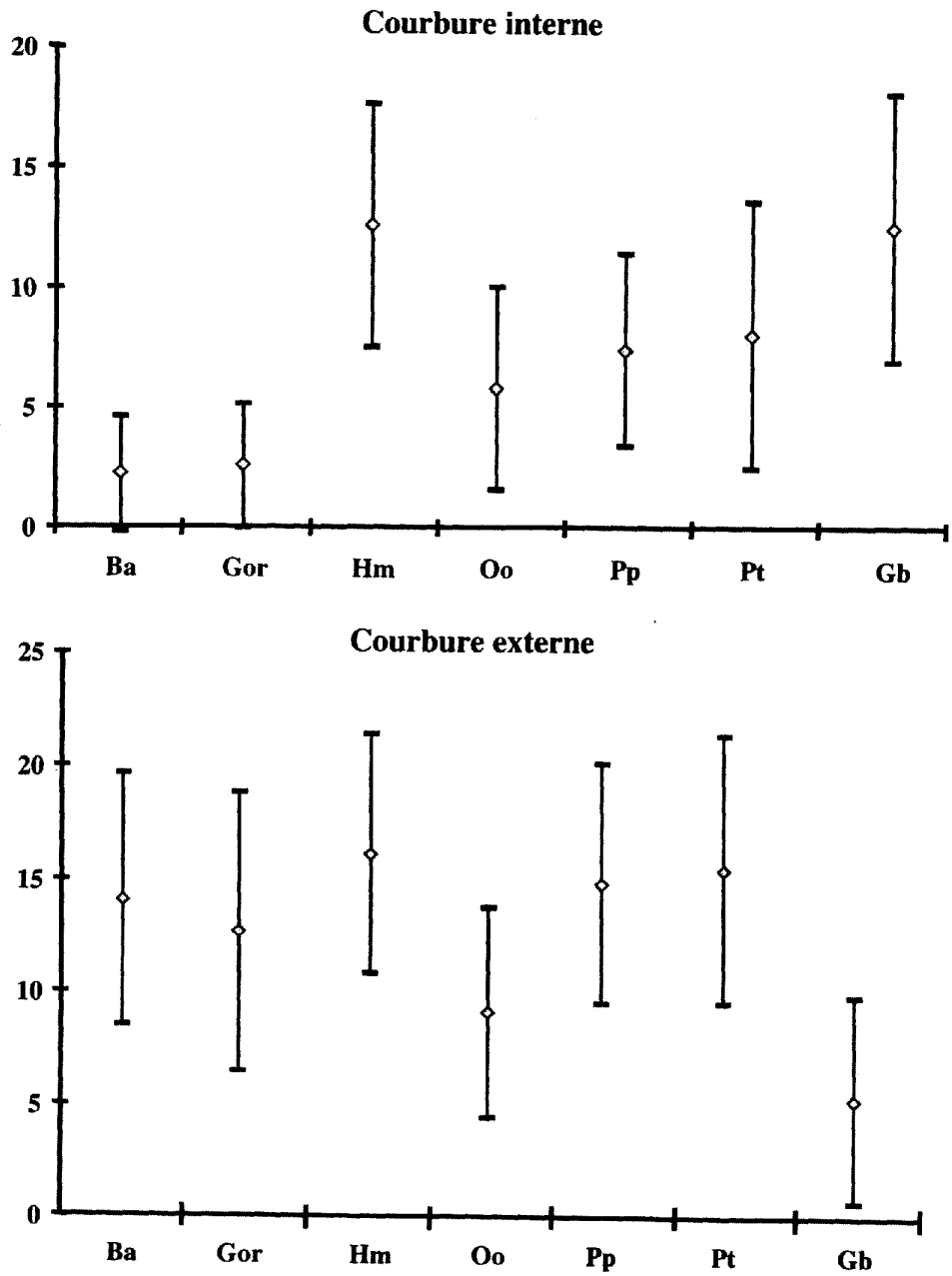

Figure 3. Valeurs moyennes et amplitudes de variation des courbures interne et externe chez les hominoïdes et les babouins.

Figure 3. Means and ranges of variation of the internal and external curves in hominoide and baboon.

3.1.2. Les représentants fossiles du genre Homo

En vue supérieure, les clavicules fossiles attribuées au genre *Homo* (*figures 4 et 5*) présentent des courbures comprises dans l'intervalle de valeurs de l'homme moderne (*tableau VI*), et cela même si l'on ne tient compte que des individus complets (clavicules gauches de la Ferrassie I et de Kebara, clavicules droites de

Tableau IV. Valeurs du coefficient de corrélation de Pearson r entre les courbures externe et interne chez l'homme, les chimpanzés et les orangs-outans

Table IV. Pearson coefficient of correlation r between the internal and the external curves in man, chimpanzees and orang-utan.

Espèce	r	r^2	p
Homo sapiens sapiens	0,6	0,4	0,00
Pan troglodytes	0,8	0,7	0,00
Pan paniscus	0,6	0,3	0,01
Orang-outan	0,7	0,5	0,00

Régourdou, d'ATD6-50 et de KNM-WT 15 000). Cependant, ces clavicules fossiles ne présentent pas toutes une morphologie identique à celle de l'homme moderne en vue supérieure. En effet, KNM-WT 15 000 (*Homo ergaster*) présente des valeurs très proches entre les courbures externe et interne. En d'autre termes, les deux courbures sont aussi marquées l'une que l'autre. Or, chez l'homme moderne la courbure externe est toujours plus prononcée que l'interne. Au contraire, la clavicule ATD6-50 (*Homo antecessor*) présente, en vue supérieure, une morphologie moderne avec une courbure externe plus prononcée que l'interne. Cependant, ces

Tableau V. Test-t entre les courbures interne et externe des clavicules de chimpanzé commun, de bonobo et d'homme moderne.

Table V. T-test between the internal and the external curves of common chimpanzee, pygmy chimpanze and man clavicles.

	Courbure interne				Courbure externe		
Group	n	mean	sd	Group	n	mean	sd
Pan troglodytes	26	8,1	2,8	*Pan troglodytes*	26	15,4	3,0
Pan paniscus	19	7,5	2,0	*Pan paniscus*	19	14,8	2,6
Separate variances	T = 0,9	DF = 43,0	Prob = 0,4	Separate variances	T = 0,7	DF = 41,2	Prob = 0,5
Pooled variances	T = 0,8	DF = 43,0	Prob = 0,4	Pooled variances	T = 0,7	DF = 43,0	Prob = 0,5
Group	n	mean	sd	Group	n	mean	sd
Pan troglodytes	26	8,1	2,8	*Pan troglodytes*	26	15,4	3,0
Homo sapiens sapiens	33	12,6	2,5	*Homo sapiens sapiens*	33	16,1	2,6
Separate variances	T = -6,5	DF = 51,1	Prob = 0,00	Separate variances	T = -0,9	DF = 50,7	Prob = 0,4
Pooled variances	T = -6,5	DF = 57,0	Prob = 0,00	Pooled variances	T = -0,9	DF = 57,0	Prob = 0,4

Tableau VI. Valeurs des courbures externe et interne chez les hommes de Néandertal, *Homo antecessor, Homo ergaster* et *Homo habilis.*

Table VI. Values of the internal and external curves in Neandertal, *Homo antecessor, Homo ergaster* and *Homo habilis.*

	Individu	Courbure interne	Courbure externe
Néandertaliens	Régourdou droite	10,0	14,5
	Régourdou gauche	11,9	13,2
	Kebara gauche	11,1	16,5
	Kebara droite	11,3	9,5
	La Ferrassie 1 droite	13,2	14,2
	La Ferrassie 1 gauche	12,3	17,7
	Krapina 4 gauche	8,3	11,1
	Neanderthal droite	13,2	16,7
	Moyenne	**11,4**	**14,2**
	Ecart-type	**1,7**	**2,8**
Homo ergaster	KNM-WT 15 000 droite	13,1	14,6
	KNM-WT 15 000 gauche	15,3	14,7
Homo antecessor	Gran Dolina droite	12,4	18,7
Homo habilis	OH48 gauche	14,3	13,8

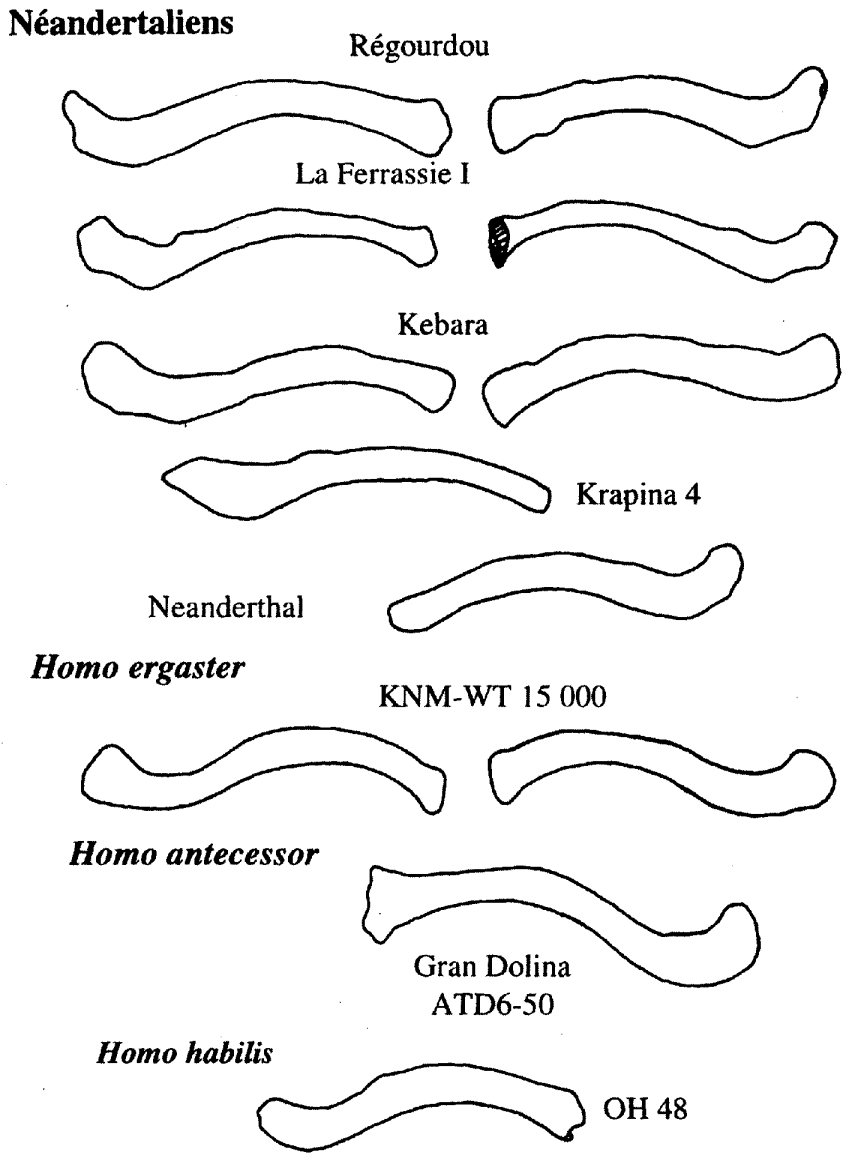

Figure 4. Clavicule de Néandertaliens, d'*Homo antecessor, Homo ergaster*, et *Homo habilis* en vue supérieure (les échelles ne sont pas respectées).

Figure 4. Neandertal, *Homo antecessor, Homo ergaster* and *Homo habilis* clavicles in superior view (scales are not respected).

valeurs ne seraient pas exceptionnelles chez l'homme moderne, contrairement aux affirmations de Carretero et al. (1999).

L'état fragmentaire de la clavicule OH48 (*Homo habilis*) fait que la courbure interne est plus prononcée que l'externe (*tableau VI*). En effet, l'extrémité sternale est pratiquement intacte alors qu'il manque une grande partie de l'extrémité acromiale (Napier, 1965). Ainsi, la courbure interne n'est que faiblement sous-estimée et se situe à la limite supérieure de l'intervalle de variation de l'homme moderne et pratiquement en dehors de celui du chimpanzé. Cet individu possédait donc des courbures très pro-

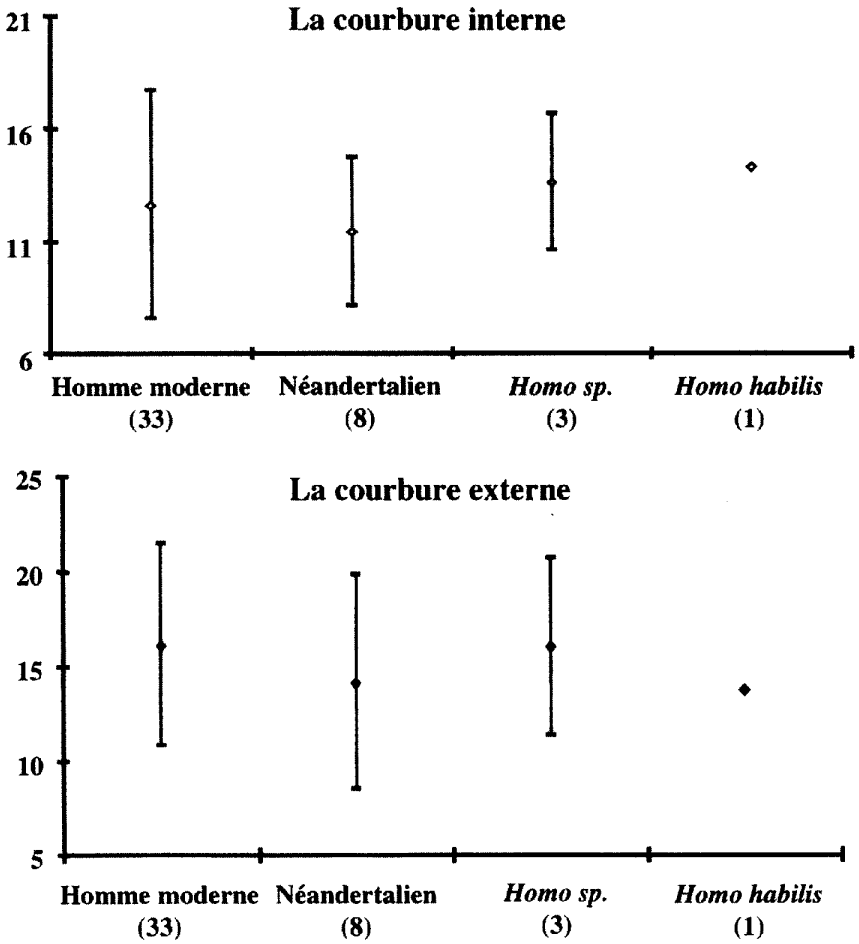

Figure 5. Valeurs moyennes et amplitudes de variation des courbures en vue supérieure chez l'homme moderne et différents groupes fossiles. *Homo* sp. regroupe *Homo ergaster* et *Homo antecessor.* Les chiffres entre parenthèse rappellent les effectifs.

Figure 5. Means and ranges of variation of clavicle curves in superior view in modern man and several human fossiles. *Homo* sp. means *Homo ergaster* plus *Homo antecessor*. Number in brackets indicates the number of specimens.

noncées en vue supérieure. Mais qu'en est-il exactement au sein de ce taxon ? Il faudrait plus de clavicules afin de conclure définitivement.

Ces résultats sont importants car ils montrent que :

- Les clavicules néandertaliennes ne sont pas plus sinueuses que celles de l'homme moderne contrairement à ce qui est fréquemment énoncé (Boule, 1912 ; Heim, 1974, 1982a, 1982b ; Vandermeersch et Trinkaus, 1995).

- Les clavicules d'*Homo antecessor* et d'*Homo ergaster* ne sont pas identiques. En effet, la morphologie claviculaire de KNM-WT 15 000 n'est pas semblable à celle de l'homme moderne, comme le considèrent Walker et Leakey (1993), contrairement à celle d'ATD6-50 qui s'en rapproche beaucoup plus.

- Les fortes courbures en vue supérieure sont apparues tôt dans l'histoire de l'humanité, sans pour autant être parfaitement identiques à la morphologie humaine moderne.

3.2 Les courbures en vue postérieure

3.2.1. Les grands singes et l'homme moderne

En vue postérieure les courbures claviculaires, constituant la déflexion (Matiegka, 1938), permettent de distinguer quatre groupes (*figures 6 et 7*) :

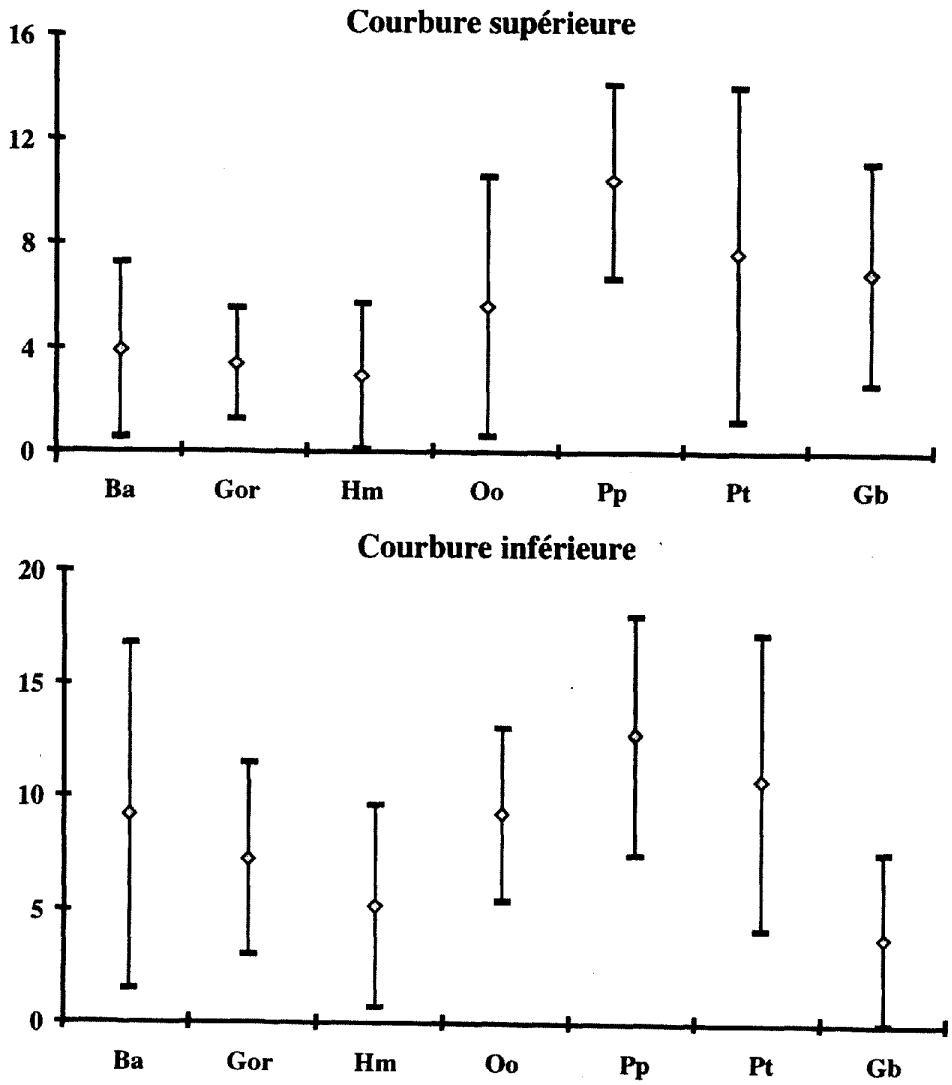

Figure 6. Valeurs moyennes et amplitudes de variation des courbures supérieure et inférieure chez les hominoïdes et les babouins.

Figure 6. Means and ranges of variation of the superior and inferior curves in hominoids and baboon.

- Les grands singes qui présentent toujours deux courbures en vue postérieure : une inférieure à l'extrémité latérale de la clavicule et une supérieure à l'extrémité médiale. Ces courbures sont plus ou moins développées selon les espèces, mais elles sont toujours présentes (*tableau VII*). Par ailleurs, la courbure inférieure est toujours plus prononcée que la supérieure pour une clavicule donnée (*tableau VII*).

- Les babouins qui présentent des clavicules dont la courbure inférieure est toujours présente alors que la supérieure est absente ou faiblement marquée.

- Les gibbons qui sont caractérisés par une seule courbure en vue postérieure, la courbure supérieure.

- L'homme moderne qui présente deux morphologies claviculaires distinctes. La première, et la plus fréquente (84,8%), correspond à une clavicule ne présentant qu'une courbure inférieure, qui de surcroît n'est pas très prononcée. Ce sont les clavicules de type I (Olivier, 1951b). Par ailleurs, certaines clavicules (24,2%) présentent en plus une courbure supérieure de l'extrémité acromiale. Ce sont les clavicules de type III (Olivier, 1951b). La seconde morphologie,

Tableau VII. Caractéristiques des courbures inférieure et supérieure des espèces actuelles étudiées ici.

Table VII. Characteristics of the clavicule curves in posterior view (inferior and superior).

	Courbure inférieure			Courbure supérieure		
Espèce (nombre de pièces)	moyenne	écart-type	variance	moyenne	écart type	variance
Homo sapiens sapiens (33)	5,1	2,3	5,3	1,1	1,7	2,9
Pan troglodytes (26)	10,7	3,3	10,9	7,6	3,2	10,2
Pan paniscus (19)	12,7	3,0	9,0	10,4	1,9	3,6
Gorilla gorilla (33)	7,2	2,2	4,8	3,4	1,1	1,2
Pongo pygmaeus (24)	9,2	1,9	3,6	5,6	2,5	6,3
Hylobates sp. (22)	3,8	1,9	3,6	6,9	2,1	4,4
Papio hamadryas (28)	9,2	3,8	14,4	0,8	1,8	3,2

Tableau VIII. Valeurs des courbures inférieure et supérieure chez les hommes de Néandertal, *Homo antecessor, Homo ergaster* et *Homo habilis.*

Table VIII. Values of the inferior and superior curves in Neandertal, *Homo antecessor, Homo ergaster* and *Homo habilis.*

	Individu	Courbure inférieure	Courbure supérieure
Néandertaliens	Régourdou droit	7,4	8,0
	Régourdou gauche	3,0	3,2
	Kebara gauche	4,9	0,0
	Kebara droite	3,4	0,0
	La Ferrassie 1 droite	5,4	5,8
	La Ferrassie 1 gauche	8,2	2,6
	Krapina 4 gauche	3,2	2,9
	Neanderthal droite	7,4	6,2
	Moyenne	**5,4**	**3,6**
	Ecart-type	**2,1**	**2,9**
Homo ergaster	KNM-WT 15 000 droite	5,0	7,4
	KNM-WT 15 000 gauche	5,3	8,1
Homo antecessor	Gran Dolina droite	8,8	5,4
Homo habilis	OH48 gauche	4,6	2,7

peu fréquente (15,2%), correspond à une clavicule ayant un morphotype grand singe. Ces clavicules, correspondant au type II, présentent des courbures supérieure et inférieure toujours faiblement développées par rapport à ce qui existe chez les grands singes (*figure 8*).

3.2.2. Les hommes fossiles

Les néandertaliens

A l'exception des clavicules de Kebara toutes les pièces néandertaliennes possèdent une courbure inférieure latérale et une courbure supérieure médiale (*figure 9*). Autrement dit, 75% des clavicules néandertaliennes étudiées présentent une morphologie de type II, alors que chez l'homme moderne cela représente 15% des clavicules.

Cependant, la morphologie des clavicules néandertaliennes, en vue postérieure, est particulière et ne correspond à aucun schéma actuel, ni à celui de l'homme moderne ni à celui des grands singes. En effet, la courbure supérieure chez l'homme moderne est nettement moins prononcée, quand elle existe, que chez les néandertaliens. L'amplitude et la moyenne de la courbure supérieure des clavicules néandertaliennes sont proches de celles des orangs-outans (*figure 10 et tableaux VII et VIII*) contrairement à l'inférieure qui est proche de celle de l'homme moderne (*tableaux VII et VIII*). En outre, certaines clavicules néandertaliennes (Régourdou droite et gauche ; la Ferrassie I droite) présentent une courbure supérieure plus prononcée que l'inférieure, ce qui ne se retrouve chez aucun autre primate.

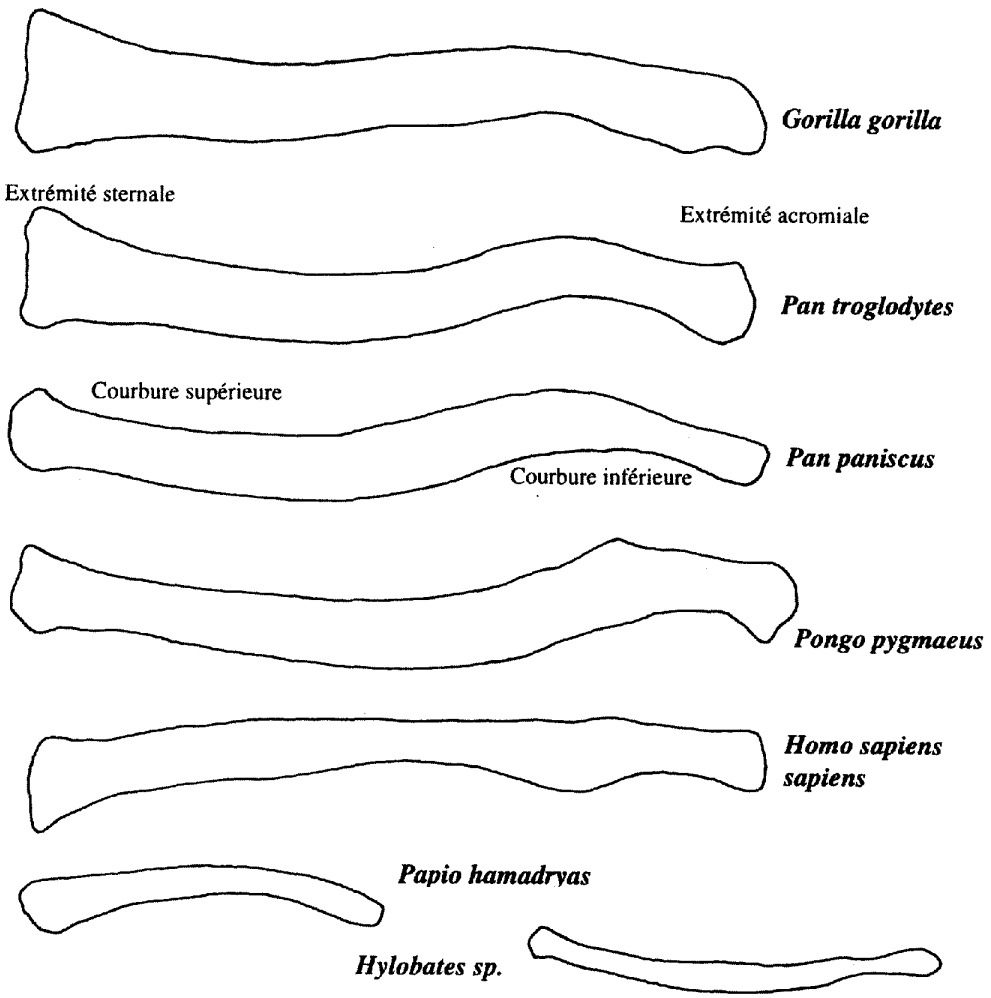

Figure 7. Clavicules droites en vue postérieure (les échelles ne sont pas respectées).

Figure 7. Right clavicles in posterior view (scales are not respected).

Homo ergaster et *Homo antecessor*

Les clavicules de Nariokotome (KNM-WT 15 000) et d'*Homo antecessor* (ATD6-50) présentent une double courbure en vue postérieure (*figure 11 et tableau VIII*). Autant les valeurs des courbures inférieures des clavicules de KNM-WT 15 000 et d'ATD6-50 sont comprises dans l'intervalle de valeurs de l'homme moderne (*tableau VIII*), autant les valeurs de la courbure supérieure de ces fossiles sont nettement au dessus de l'intervalle actuel (pour les clavicules modernes présentant cette courbure). De plus, les clavicules de Nariokotome ont une courbure supérieure plus prononcée que l'inférieure ce qui n'est pas le cas chez ATD6-50.

Ainsi, la morphologie claviculaire en vue postérieure des *Homo erectus* au sens large est différente de celle de l'homme moderne et se rapproche plutôt de celle des néandertaliens car :

- les deux courbures existent en vue supérieure et sont bien individualisées,

- la courbure supérieure peut être plus prononcée que l'inférieure, ce qui ne se retrouve que chez les néandertaliens.

Homo habilis

La clavicule d'OH 48, la seule clavicule d'*Homo habilis* connue, présente deux courbures en vue postérieure (*figure 11*), mais elles

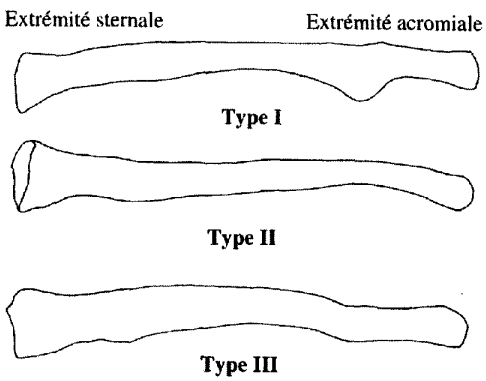

Figure 8. Les trois types de clavicules chez l'homme moderne.

Figure 8. The three types of modern man clavicle.

sont peu prononcées et entrent parfaitement dans l'intervalle de valeurs de l'homme moderne (*tableau VIII*). L'inférieure est la plus prononcée. Il est délicat d'affirmer que cette morphologie caractérise les *Homo habilis* car cette clavicule n'est pas complète (Napier, 1965). Cependant, cette déflexion avec une double courbure est plus fréquente chez les néandertaliens, *Homo ergaster* et *Homo antecessor* que chez l'homme moderne. Ainsi, la morphologie observée sur la clavicule OH 48 devrait être proche de celle des *Homo habilis* en général.

4. Discussion

4.1. Les courbures en vue supérieure

Le muscle grand pectoral a un rôle primordial lors des mouvements de flexion chez l'homme, notamment lors de leur initiation (Gagey, 1985). L'efficacité de ce muscle chez l'homme est due au développement de la courbure interne de la clavicule qui crée un effet de manivelle et ainsi aide à l'élévation du bras en facilitant le pivotement de la scapula pour orienter la cavité glénoïdale vers le haut (Voisin, 2000b). Chez les primates peu d'espèces présentent une insertion claviculaire du grand pectoral étendue. Ces espèces sont l'homme, les chimpanzés, les gorilles et les gibbons (Asthon et Oxnard, 1963). Au contraire, chez les orangs-outans cette insertion est très peu étendue et manque même fréquemment (Jouffroy, 1962 ; Sullivan et Osgood, 1927).

Les espèces présentant un développement important de l'insertion claviculaire du grand pectoral, ainsi qu'une courbure claviculaire interne marquée, sont les deux espèces de chimpanzés, l'homme et les gibbons. Le développement de la courbure interne est donc associé à une flexion puissante et rapide. Une telle disposition permet de développer la brachiation et / ou la manipulation.

Quelle que soit l'espèce d'Hominidae fossile, toutes les clavicules étudiées dans ce travail

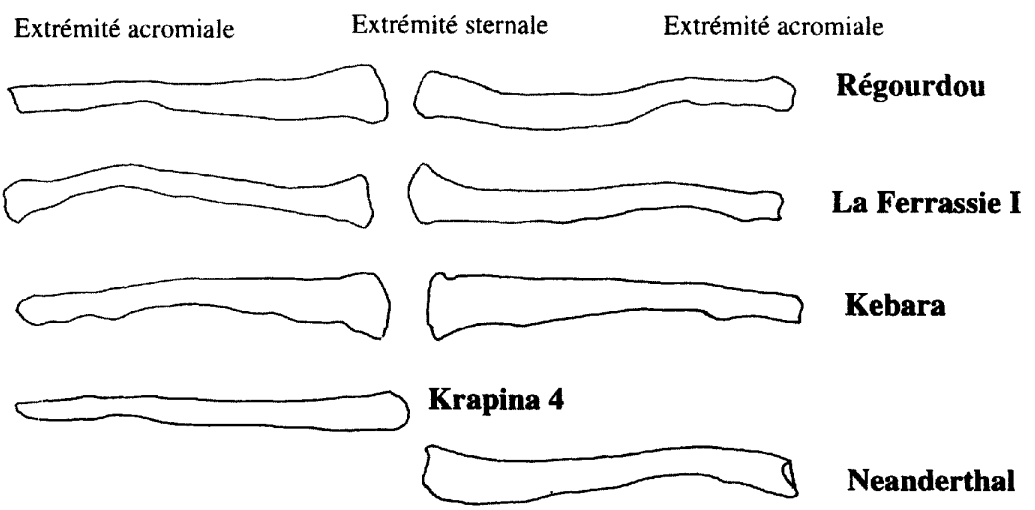

Figure 9. Clavicules néandertaliennes en vue postérieure (les échelles ne sont pas respectées).

Figure 9. Neandertal clavicles in posterior view (scales are not respected).

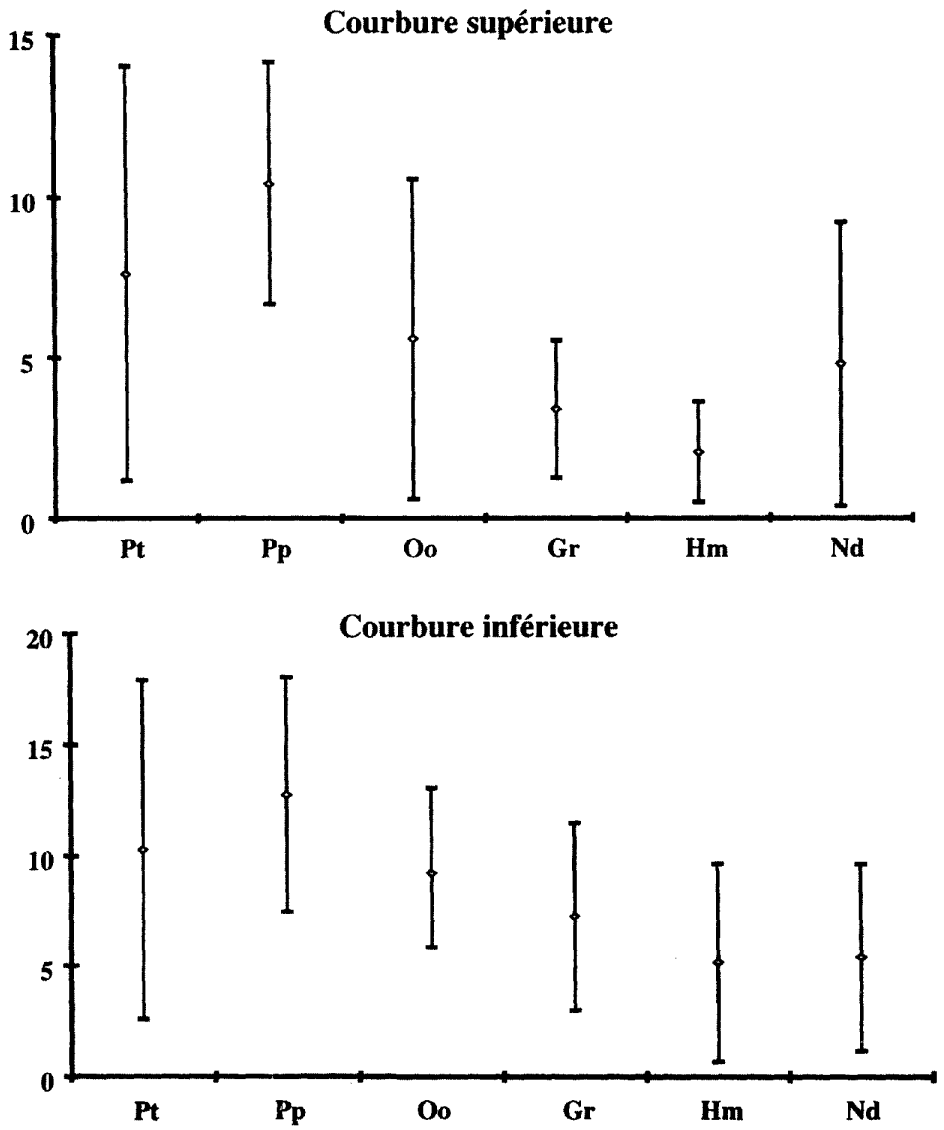

Figure 10. Comparaison des valeurs moyennes et des amplitudes de variation entre les Néandertaliens, les grands singes et l'homme moderne pour les courbures en vue postérieure.

Figure 10. Comparaison between means and ranges of variation of the Neandertal, great apes and modern man for the curves in posterior view.

présentent des courbures en vue supérieure identiques ou proches de celles de l'homme moderne (*figure 5*). Ainsi, la forte sinuosité décrite pour les clavicules néandertaliennes n'est pas une réalité physique, mais une impression due à leur extrême longueur. Bien que la clavicule OH 48 (*Homo habilis*) ne soit pas complète (Napier, 1965) les courbures devaient être proches de celles de l'homme moderne, notamment la courbure interne. Les capacités fonctionnelles d'élévation du bras des espèces humaines fossiles étaient donc identiques à celles de l'homme moderne. De plus, la morphologie claviculaire humaine en vue supérieure est une adaptation à la bipédie car elle permet le maintient mécanique de l'épaule en position érigée, c'est-à-dire avec un coût énergétique minimum (Voisin, 2000b). La morphologie claviculaire humaine moderne en vue supérieure est donc apparue rapidement dans l'histoire de

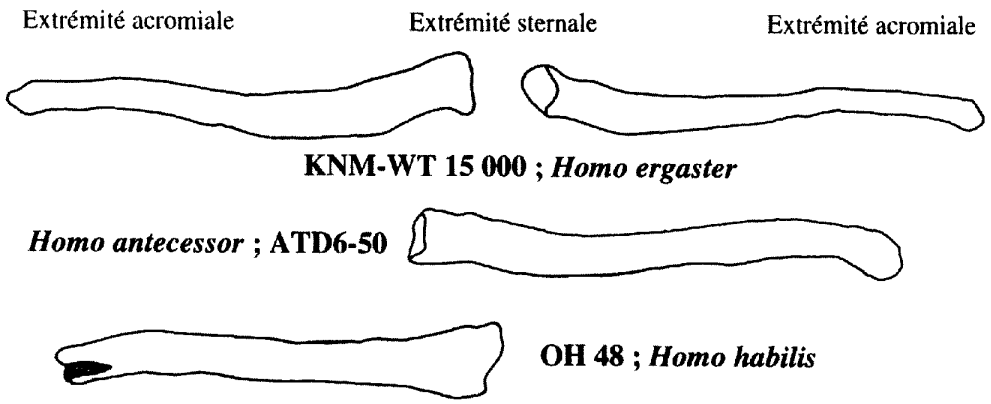

Figure 11. Clavicules d'*Homo antecessor, Homo ergaster*, et *Homo habilis* en vue postérieure (les échelles ne sont pas respectées).

Figure 11. *Homo antecessor, Homo ergaster* and *Homo habilis* clavicles in posterior view (scales are not respected).

l'homme, dès que la bipédie est devenue prépondérante et que la main s'est libérée des contraintes locomotrices.

Il existe peu de clavicules a peu près complètes attribuées aux *Homo erectus*. En dehors de celles étudiées dans ce travail, il existe deux autres restes, l'un africain et l'autre provenant de l'Inde. La clavicule africaine KNM-ER 1808 présente une morphologie et une sinuosité semblables à celles de l'homme moderne (Leakey et Walker, 1985). Au contraire, le reste découvert dans la vallée de la Narmada (Inde) et décrit comme une clavicule d'*Homo erectus* (Sankhyan, 1997), présente une morphologie particulière. En effet, les courbures sont très inégales (la méthode de mesure étant différente de la nôtre, toute comparaison métrique est impossible) et traduisent une forme plus proche de celle du gorille que de celle de l'homme moderne. Par ailleurs, cette clavicule est très courte, et ne rentre pas dans l'intervalle de valeurs actuelles (Voisin, 2000a). La morphologie particulière de la clavicule de la Narmada lui confère des fonctions plus proches de celle du gorille que de celle de l'homme moderne. Ainsi, cette clavicule ne semble pas appartenir au genre *Homo*.

4.2. Les courbures en vue postérieure

La clavicule travaille essentiellement en compression, transmettant la charge des membres supérieurs au squelette axial par l'intermédiaire de son grand axe (Jenkins, 1974 ; Fleagle, 1978 ; Mays et al., 1999). Ainsi la morphologie claviculaire influence sur la diffusion des forces et donc sur les modes de déplacement de l'individu.

La brachiation correspond à un déplacement suspendu par les membres supérieurs (*figure 12*), associé à un balancement alterné de ces derniers afin de saisir un nouveau support (Fleagle, 1974).

Afin que la brachiation soit efficace et peu coûteuse en énergie, certaines contraintes sont nécessaires. En particulier, le centre d'inertie de l'individu doit toujours rester dans un plan vertical passant par le centre de rotation du pendule (Fleagle, 1974). Pour contrôler ce facteur essentiel, l'individu peut uniquement jouer sur les articulations du poignet, du coude et de l'épaule.

Lorsque le bras arrière de l'animal lâche le support, le corps réalise un double mouvement (*figure 12*) :

- Un mouvement de pendule.

- Une rotation du corps sous le bras d'appui qui place le thorax dans le sens du mouvement du pendule.

Lors de la brachiation, la présence de la clavicule permet de réaliser le mouvement de rotation du thorax sous la main d'appui car, en maintenant constant la distance acromio-manubrium, elle empêche la scapula de s'écraser sur le thorax. De plus, l'efficacité du mouvement de pendule lors de ce mode de déplacement dépend

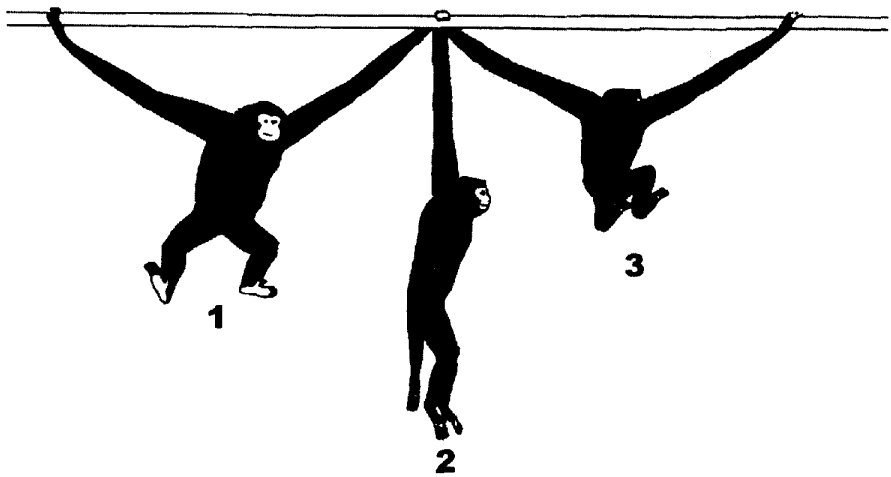

Figure 12. La brachiation chez le gibbon, la phase 1 correspond au départ du mouvement, la phase 3 à la fin du mouvement (d'après Fleagle, 1974).

Figure 12. Brachiation in the gibbon. Phase 1 is the start and phase 3 the end of the movement (redraw from Fleagle, 1974).

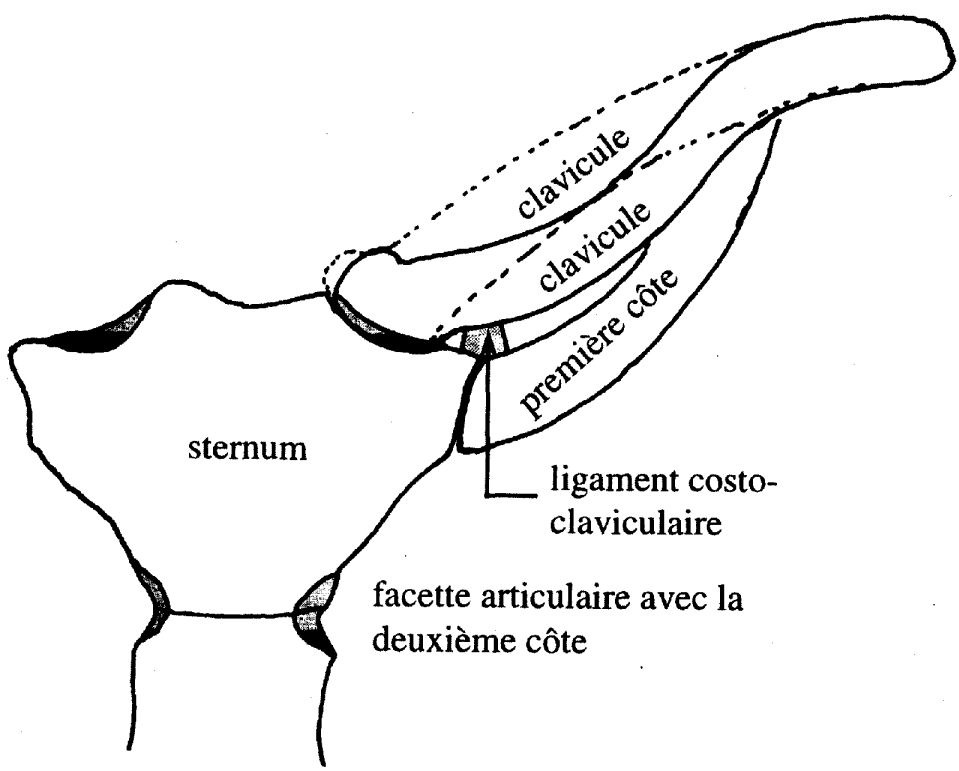

Figure 13. Clavicules associées à une scapula haute par rapport au thorax. En pointillés clavicule humaine (courbure inférieure unique). En traits pleins clavicule de grand singe (deux courbures). Noter la différence de hauteur par rapport au manubrium qui existe entre ces deux morphologies claviculaires (d'après Voisin, 2000c).

Figure 13. Clavicles associated with a high scapula in regard to the thorax. Dotted line: modern human clavicle (with a unique inferior curve), in full line the great apes clavicle (with two curves in posterior view). Note the difference in height in regard to the manubrium between the two clavicular morphology (from Voisin 2000c).

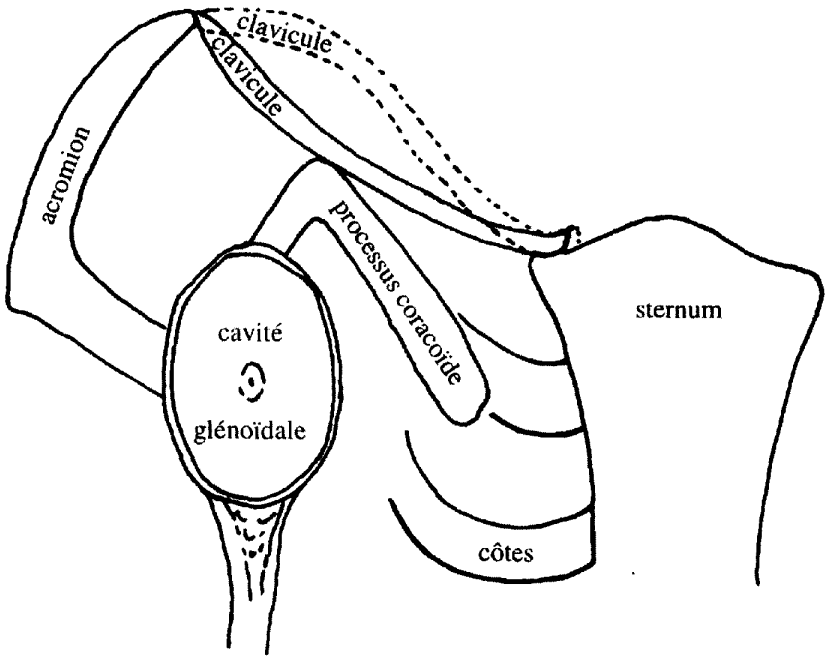

Figure 14. Relations entre la scapula, la clavicule et le sternum pour une clavicule de type gibbon (trait plein) et de type grand singe (trait pointillé) (d'après Voisin, 2000a).

Figure 14. Relations between scapula, clavicle and sternum for a gibbon clavicle (full line) and a great ape one (dotted line) (from Voisin, 2000a).

de la morphologie claviculaire en vue postérieure. Chez le gibbon, le mouvement de pendule est optimisé grâce à deux particularités claviculaires :

- La présence d'une courbure supérieure prononcée qui permet à l'extrémité sternale de la clavicule de rester parallèle au manubrium associée à une scapula haute par rapport au thorax (*figure 13*). Ainsi, le ligament costo-claviculaire et le muscle subclavier conservent leur fonction (Voisin, 2000a, 2000c) car ils ne subissent aucune élongation. Le ligament costo-claviculaire limite les mouvements verticaux et horizontaux de l'extrémité sternale de la clavicule (Kapandji, 1994). Un allongement de ce ligament augmenterait la mobilité de cette extrémité qui devrait alors être compensée par l'action de différents muscles tel que le subclavier. Cela entraînerait un coût énergétique plus élevé du mouvement, ainsi qu'un risque important de luxation de l'articulation sterno-claviculaire. Par ailleurs, chez les atèles, le muscle subclavier est très peu sollicité lors de la brachiation, alors qu'il l'est fortement lors du grimper sur structure verticale (Konstant et al., 1982), ce qui doit aussi être transposable aux *Hylobatidae*.

- L'absence de courbure inférieure, présente chez tous les autres primates, entraîne nécessairement une articulation entre le processus coracoïde et la clavicule (*figure 14*). Cette articulation, bien qu'étant la conséquence du développement particulier des courbures en vue postérieure, accroît la rigidité de l'ensemble clavicule/scapula en augmentant la cohésion entre ces deux os. En effet, chez les autres primates un ou deux ligaments réalisent cette liaison. L'ensemble clavicule/scapula est alors moins rigide. La forte liaison entre ces os chez les gibbons améliore la diffusion des forces et surtout permet de limiter les mouvements du centre d'inertie de l'individu en dehors du plan vertical passant par la main d'appui.

Chez les primates quadrupèdes, la présence de la clavicule permet aux membres supérieurs de réaliser des mouvements en dehors du plan parasagittal, mais elle ne doit pas non plus entraver les déplacements quadrupèdes. La présence d'une courbure inférieure prononcée permet à la scapula de réaliser des mouvements de bascule

importants lors de la marche, sans qu'elle aille buter contre la clavicule. Cependant, la faible cohésion de l'ensemble scapula / clavicule limite les capacités de brachiation et l'absence de courbure inférieure limite la remontée de la scapula le long du thorax lors des phases de suspension.

Chez les grands singes, la clavicule présente une déflexion caractéristique avec deux courbures. Ces espèces, caractérisées par une scapula haute et dorsale par rapport au thorax (Martin et O'Brien, 1939 ; Schultz, 1950 ; Sakka, 1985), pratiquent à la fois les déplacements suspendus et, au sol, le "knuckle-walking" (gorille & chimpanzé) ou le "fist-walking" (orang-outan) (Asthon & Oxnard, 1964). La morphologie claviculaire de ces primates, en vue postérieure, permet de répondre aux contraintes opposées que la locomotion suspendue et quadrupède imposent grâce à :

- L'existence d'une courbure supérieure médiale qui permet, nous l'avons vu chez le gibbon, de présenter une surface claviculaire à peu près parallèle au manubrium tout en associant une scapula haute par rapport au thorax.

- La courbure inférieure qui est toujours bien développée car elle est nécessaire au bon fonctionnement de l'épaule lors des déplacements quadrupèdes.

L'homme est caractérisé par l'émergence "cervico-céphalique" (Sakka, 1985), en regard des grands singes, car le cou se développe en hauteur entraînant la sortie de la tête hors des épaules. Selon Sakka (1985), ce phénomène est associé à une descente de la ceinture scapulaire le long du thorax. Par ailleurs, la clavicule est toujours orientée plus cranialement chez les grands singes que chez l'homme (Olivier, 1965 ; Sakka, 1985) et chez l'orang-outan elle réalise un angle de 30 à 50° par rapport au plan transversal (Vallois, 1928). La descente de la ceinture scapulaire chez l'homme, en regard de celle des grands singes, expliquerait la présence d'une unique courbure inférieure. En effet, une double courbure prononcée en vue postérieure n'est pas compatible avec une scapula basse par rapport au thorax, car une telle disposition entraînerait une dislocation de l'articulation sterno-claviculaire.

En dehors des clavicules de Kebara, toutes les clavicules néandertaliennes étudiées dans le cadre de ce travail présentent une double courbure dans le plan frontal. Les valeurs de ces courbures sont relativement importantes et leurs proportions relatives ne correspondent à aucun primate actuel. Ces particularités montrent une architecture du complexe scapulaire chez les néandertaliens différente de celle caractérisant les hommes modernes. En effet, la double courbure en vue postérieure montre que la scapula est plus haute par rapport au thorax chez les néandertaliens que chez l'homme actuel. Cette disposition entraîne, chez les néandertaliens, un cou court en comparaison du nôtre (Spoor & Wood, 1999 ; Voisin, 2000a, 2000c), bien que la hauteur de la colonne cervicale soit pratiquement identique à la nôtre (Heim, 1974, 1976 ; Vandermeersch, 1981). Ces différences d'architectures pourrait refléter la moindre "émergence cervico-céphalique" (Sakka, 1985) des néandertaliens en regard de l'homme moderne. En effet, chez les premiers, les insertions musculaires crâniennes sont plus hautes que chez l'homme moderne. Par ailleurs, ces différences d'architectures scapulaires entre ces deux groupes humains pourraient refléter des dissemblances fonctionnelles de certains muscles, notamment du trapèze. En effet, la partie crâniale de ce muscle est identique du point de vue anatomique entre l'homme et le chimpanzé, contrairement à sa fonction (Larson et al., 1991) et aux morphologies claviculaires en vue postérieure. Ainsi, la morphologie particulière de la clavicule néandertalienne ne refléterait-elle pas des fonctions différentes du trapèze par rapport à l'homme moderne ? La morphologie des canaux semi-circulaires des néandertaliens présente un argument dans ce sens puisqu'elle semble indiquer que le contrôle de l'équilibre ne nécessitait pas exactement les mêmes mouvements crâniens que chez l'homme moderne (Spoor & Wood, 1999).

Par ailleurs, cette position plus haute de la scapula néandertalienne par rapport au thorax entraîne une clavicule qui n'est pas orientée presque horizontalement comme chez l'homme moderne mais plus oblique. Or, pour un diamètre identique du thorax, plus la scapula est haute, plus la clavicule doit s'allonger. Ainsi, la très grande longueur des clavicules néandertaliennes ne serait due ni à une largeur d'épaule exceptionnelle comme cela est classiquement admis (Patte, 1955 ; Heim, 1974, 1982a ; Vandermeersch et Trinkaus, 1995), ni au développement important des insertions claviculaires du muscle sterno-cleido-mastoïdien et du trapèze (Nara, 1994). Quoi qu'il en soit, la très

grande longueur des clavicules néandertaliennes pourrait traduire une capacité au jet plus grande chez ces derniers que chez l'homme moderne (Voisin 2000a).

Les clavicules d'ATD6-50, de KNM-WT 15000 et d'OH 8 montrent la présence d'une double courbure en vue postérieure. Ainsi, ces individus devaient présenter une scapula haute par rapport au thorax, tout comme les néandertaliens. Cette architecture de l'épaule serait alors habituelle dans le genre *Homo*. Au contraire, celle de l'homme moderne, caractérisée par une scapula beaucoup plus basse par rapport thorax, serait une particularité dans l'histoire de notre genre. En d'autres termes, l'architecture de l'épaule néandertalienne serait héritée d'une morphologie ancestrale, contrairement à celle de l'homme moderne qui est une innovation. L'architecture de la ceinture scapulaire permet donc de définir deux groupes d'humains, qui peuvent aussi être déterminés d'après la morphologie de la ceinture pelvienne (Marchal, 2000a, 2000b).

Walker et Leakey (1993) considèrent que les clavicules de KNM-WT 15000 ne présentent que la courbure inférieure. Cette divergence d'interprétation s'explique par la morphologie particulière de cette clavicule qui rend difficile la détermination de la face inférieure par rapport au bord postérieur. La méthodologie employée dans cette étude lève cette difficulté.

5. Conclusion

Ce premier travail montre que l'étude de la clavicule est très riche en informations, et que cet os présente un intérêt particulier en anthropologie et paléoanthropologie. En vue supérieure sa morphologie donne des indications sur les capacités d'élévation du bras, alors qu'en vue postérieure elle participe à la description de l'architecture de l'épaule. Elle informe sur la position de la scapula par rapport au thorax (latérale ou dorsale, haute ou basse).

Par ailleurs, cette étude a permis de montrer que la scapula est plus haute par rapport au thorax chez *Homo habilis, Homo ergaster, Homo antecessor* et les néandertaliens que chez l'homme moderne. Cette descente du système scapulaire chez l'homme moderne est-il à mettre en relation avec le désenclavement musculaire de la tête ? En effet, au cours de l'évolution les insertions musculaires descendent de plus en plus bas le long du crâne, notamment le trapèze qui s'insère sur la base du crâne et la ceinture scapulaire.

Les courbures en vue supérieure, au contraire, ne montrent pas de différences (seules celles de KNM-WT 15 000 ne sont pas exactement identiques aux clavicules des hommes modernes) avec l'homme moderne. Ce résultat est important car il contredit les affirmations précédentes qui considéraient, notamment, que les clavicules néandertaliennes étaient plus sinueuses que les nôtres. Cette impression est due à la grande longueur des clavicules néandertaliennes.

Remerciement

Je tiens à remercier tout particulièrement Monsieur le Professeur Henry de Lumley qui m'a accepté au sein du Laboratoire de Préhistoire du Muséum National d'Histoire Naturelle ainsi qu'à Madame Marie-Antoinette de Lumley qui suit l'avancement de mes travaux. Mes remerciements vont aussi aux professeurs André Langaney, Daniel Robineau, Wim Van Neer, Paula Jenkins et Chris Stringer qui m'ont autorisé à consulter respectivement les collections des Laboratoires d'Anthropologie Biologique du Musée de l'Homme (Paris, France), d'Anatomie Comparée du Muséum National d'Histoire Naturelle (Paris, France), du Musée Royal d'Afrique Centrale (Tervuren, Belgique) et du *Natural History Museum, Zoological Group* et *Paleontological Group* (Londres, Grande Bretagne). Je remercie aussi toutes les personnes de l'Institut de Paléontologie Humaine qui m'ont apporté leur soutien.

Références

Apostolakis, G., 1934. La clavicule de l'Homme. Arch. Anat. Histol. Embryol. 18, 169-180.

Ashton, E.H., Oxnard, C.E., 1963. The musculature of the primate shoulder. Trans. Zool. Soc. Lond. 29, 553-650.

Ashton, E.H., Oxnard, C.E., 1964. Locomotor patterns in primates. Proc. Zool. Soc. Lond. 142, 1-28.

Boule, M., 1912. L'Homme fossile de la Chapelle-aux-Saints. Ann. Paleontol. 7, 21-192.

Carretero, J.M., Lorenzo, C., Arsuaga, J.L., 1999. Axial and appendicular skeleton of *Homo antecessor*. J. Hum. Evol. 37, 459-499.

Cave, A.J.E., 1961. Nature and morphology of the costoclavicular ligament. J. Anat. 95 (2), 170-179.

Fleagle, J.G., 1974. Dynamics of brachiating siamang *Hylobates (Symphalangus) syndactylus*. Nature 248, 259-260.

Fleagle, J.G., 1978. Mechanical function of primate clavicles (abstract). Am. J. Phys. Anthrop. 48, 394.

Gagey, O., 1985. Etude de l'élévation du membre supérieur. Rôle des ligaments articulaires et des muscles fléchisseurs de l'articulation scapulo-humérale. Mémoires du Laboratoire d'Anatomie de la Faculté de Médecine de Paris 76, 115 p.

Groves, C.P., 1993a. Primates. In: Wilson, D.E., Reeder, D.A. (Eds.), Mammal species of the World, a taxonomic and geographic reference, second edition. Smithsonian Institution Press, Washington and London, 1206 p.

Groves, C.P., 1993b. Speciation in living hominoid primates. In: Kimbel, W.H., Martin, L.B. (Eds.), Species, Species Concepts and Primate Evolution. Plenum Press, New York and London, 560 p.

Harrington, M.A., Keller, T.S., Seiler, J.G., Weikert, D.R., Moeljanto, E., Schwartz, H.S., 1993. Geometric properties and the predicted mechanical behavior of adult human clavicles. J. Biomechanics 26, 417-426.

Heim, J.L., 1974. Les Hommes fossiles de la Ferrassie (Dordogne) et le problème de la définition des Néandertaliens classiques, L'Anthropologie 78 (1), 81-112.

Heim, J.L., 1976. Les hommes fossiles de La Ferrassie I. Arch. Inst. Paléont. Hum. 35, 1-331.

Heim, J.L., 1982a. Les hommes fossiles de la Ferrassie II. Arch. Inst. Paléont. hum. 38, 1-272.

Heim, J.L., 1982b. Les enfants néandertaliens de la Ferrassie. Etude anthropologique et analyse ontogénique des hommes de néandertal. Masson, Paris, 169 p.

Jenkins, F.A. Jr., 1974. The movement of the shoulder in claviculate and aclaviculate Mammals. J. Morph. 144, 71-84.

Jenkins, F.A., Dumbrowski, P.J., Gordon, E.P., 1978. Analysis of the shoulder in brachiating spider monkeys (*Ateles geoffroyi*). Am. J. Phys. Anthrop. 48, 65-75.

Jit, I., Kaur, H., 1986. Rhomboid fossa in the clavicles of North Indians. Am. J. Phys. Anthrop. 70, 97-103.

Jouffroy, F.K., 1962. La musculature des membres chez les Lémuriens de Madagascar. Etude descriptive et comparative. Mammalia 26, suppl. 2, 322 p.

Kapandji, I.A., 1994. Physiologie articulaire. t1 Membre supérieur. 5ème édition, Maloine, Paris, 296 p.

Kleiweg de Zwaan, J.P., 1931. La clavicule des javanais de l'est de Java. L'Anthropologie 41, 273-287.

Konstant, W., Stern, J.T. Jr, Fleagle, J.G., Jungers, W.L., 1982. Function of the subclavius muscle in a nonhuman primate, the spider monkey (*Ateles*). Folia Primatol. (Basel) 38 (3-4), 170-182.

Larson, S.G., Stern, J.T. Jr., Jungers, W.L., 1991. EMG of serratus anterior and trapezius in the chimpanzee: scapular rotator revisited. Am. J. Phys. Anthrop. 85, 71-84.

Leakey, R.E.F., Walker, A.C., 1985. Further Hominids from the Plio-Pleistocene of Koobi Fora, Kenya. Am. J. Phys. Anthrop. 67, 135-163.

Ljunggren, A.E., 1979. Clavicular function, Acta. Orthop. Scand. 50, 261-268.

Marchal, F., 2000a. A new morphometric analysis of the hominid pelvic bone. J. Hum. Evol. 38, 347-365.

Marchal, F., 2000b. L'ischion et le pubis des néandertaliens : Morphologie particulière ou héritage ancestral ? Biom. Hum. et Anthropol. 18, 77-85.

Matiegka, J., 1938. La déflexion de la clavicule. L'Anthropologie 48, 596-597.

Martin, C.P., O'Brien, H.D., 1939. The coracoid process in the primate. J. Anat. and Physiol. 73, 630-642.

Mays, S., Steele, J., Ford, M., 1999. Directional asymmetry in the human clavicle. Int. J. Osteoarchaeol. 9, 18-28.

Napier, J.R., 1965. Réponse à Tobias, New discoveries in Tanganika, their bearing on hominid evolution. Curr. Anthrop. 6, 402-403.

Nara, T., 1994. Etude de la variabilité de certains caractères métriques et morphologiques des néandertaliens. Thèse de doctorat, Université de Bordeaux I, 212 p.

Olivier, G., 1951a. Technique de mesure des courbures de la clavicule. C.R. Ass. Anat., XXXIXème Réunion (Nancy) 69, 753-764.

Olivier, G., 1951b. Anthropologie de la clavicule. Bull. et Mém. de la Soc. Anthrop. Paris 2 (10), 67-99, 121-157.

Olivier, G., 1953. La clavicule du Semnopithèque. Mammalia XVII (3), 173-186.

Olivier, G., 1954. Anthropologie de la clavicule. Bull. et Mém. de la Soc. Anthrop. Paris V (10), 144-153.

Olivier, G., 1955. Anthropologie de la clavicule. Bull. et Mém. de la Soc. Anthrop. Paris VI (10), 282-302.

Olivier, G., 1965. Anatomie anthropologique. Vigot édition, Paris, 162 p.

Olivier, G., Capliez, S., 1957. Anthropologie de la clavicule. Bull. et Mém. de la Soc. Anthrop. Paris VIII (10), 225-261.

Olivier, G., Chabeuf, M., Laluque, P., 1954. Anthropologie de la clavicule. Bull. et Mém. de la Soc. Anthrop. Paris V (10), 35-46.

Parson, F.G., 1917. On the modern english clavicle. J. Anat. and Physiol. 51, 71-93.

Patte, E., 1955. Les Néandertaliens. Masson, Paris, 559 p.

Ray, L.J., 1959. Metrical and non-metrical features of the calvicle of the Australian Aboriginal. Am. J. Phys. Anthrop. 17, 217-226.

Sakka, M., 1985. Morphologie évolutive de la tête et du cou chez l'Homme et les Grands Singes. Application aux Hominidés fossiles, t.I ensembles anatomiques et cervicaux. Cahiers de Paléoanthropologie, CNRS, Paris, 168 p.

Sankhyan, A.R., 1997. Fossil clavicle of a Middle Pleistocene hominid from the central Narmada Valley, India. J. Hum. Evol. 32, 3-16.

Schultz, A.H., 1930. The skeleton of the trunk and limbs of higer primates. Hum. Biol. II (3), 303-438.

Schultz, A.H., 1950. The physical distinction of Man. Proc. Am. Phil. Soc. 94, 428-449.

Spoor, F., Wood, W., 1999. Neck proportion in modern humans and Neanderthals. Am. J. Phys. Anthrop., (abstract), suppl. 28, 256.

Sullivan, W.E., Osgood, C.W., 1927. The musculature of the superior extremity of the Orang-utan. Anat. Rec. 35, 193-239.

Terry, R.J., 1932. The clavicle of the American Negro. Am. J. Phys. Anthrop. 16, 351-379.

Vandermeersch, B., 1981. Les Hommes fossiles de Qafzeh (Israël). Cahiers de Paléoanthropologie, C.N.R.S, Paris, 308 p.

Vandermeersch, B., Trinkaus, E., 1995. The postcranial remains of the Regourdou 1 Neandertal: the shoulder and arm remains. J. Hum. Evol. 28, 439-476.

Vallois, H.V., 1928. L'omoplate humaine. Etude anatomique et anthropologique. Bull. et Mém. de la Soc. Anthrop. Paris, 7 (IX), 129-168.

Voisin, J.L., 2000a. L'épaule des hominidés. Aspects architecturaux et fonctionnels, références particulières à la clavicule. Thèse du Muséum National d'Histoire Naturelle, 442 p. 2 vols.

Voisin, J.L., 2000b. La clavicule humaine : adaptation à la station érigée ?, Biom. Hum. et Anthropol. 18, 15-22.

Voisin, J.L., 2000c. Les clavicules néandertaliennes : reflet d'un complexe scapulaire particulier ?, Acte du colloque : L'identité humaine en question, mai 1999 édition ARTCOM, Paris, 80-91.

Walker, A., Leakey, R., 1993. Clavicles In: Walker, A., Leakey, R. (Eds.), The Narikotome *Homo erectus* skeleton. Springer-Verlag (Berlin), 457 p.